Université de Paris

Doctoral School Bio Sorbonne Paris Cité (562)

Paris Cardiovascular Research Centre, INSERM U970

Mechanism of Action of Extracellular Vesicles Secreted by Cardiovascular Progenitor Cells in the Treatment of Heart Failure

By

Bruna Lima Correa

Doctoral Thesis in Cellular and Molecular Biology

Is submitted for the degree of

Doctor of Philosophy

Thesis Director(s)
Prof Philippe Menasché

Presented and defended publicly on the 26th March 2021

Jury Members:

President:	DR	Dr Maria Christina ZENNARO	Université de Paris, FR
Rapporteur:	PU-PH	Prof Christian JORGENSEN	Université de Montpellier, FR
Rapporteur:	DR	Dr Lucio BARILE	Università Svizzera Italiana, CH
Examiner:	DR	Dr Florence GAZEAU	Université de Paris, FR
Examiner:	MCU-PH	Dr Antoine MONSEL	Sorbonne Université, FR
Invited Member:	DR-HDR	Dr Chantal BOULANGER	Université de Paris, FR
Invited Member:	DR-HDR	Dr Jean-Sébastien SILVESTRE	Université de Paris, FR
Director :	PU-PH	Prof Philippe MENASCHÉ	Université de Paris, FR

Except where otherwise noted, this is work licensed under
https://creativecommons.org/licenses/by-nc-nd/3.0/fr/

Université de Paris

Ecole Doctorale Bio Sorbonne Paris Cité (562)

Paris Cardiovascular Research Centre, INSERM U970

Mechanism of Action of Extracellular Vesicles Secreted by Cardiovascular Progenitor Cells in the Treatment of Heart Failure

Par

Bruna Lima Correa

Thèse de doctorat de Biologie Cellulaire et Moléculaire

Pour obtenir le grade de
Docteur de l'Université de Paris

Dirigée par
Prof Philippe Menasché

Présentée et soutenue publiquement à Paris le 26 Mars 2021

Jury Members:

Président:	DR	Dr Maria Christina ZENNARO	Université de Paris, FR
Rapporteur:	PU-PH	Prof Christian JORGENSEN	Université de Montpellier, FR
Rapporteur:	DR	Dr Lucio BARILE	Università Svizzera Italiana, CH
Examinateur:	DR	Dr Florence GAZEAU	Université de Paris, FR
Examinateur:	MCU-PH	Dr Antoine MONSEL	Sorbonne Université, FR
Membre invité:	DR-HDR	Dr Chantal BOULANGER	Université de Paris, FR
Membre invité:	DR-HDR	Dr Jean-Sébastien SILVESTRE	Université de Paris, FR
Directeur:	PU-PH	Prof Philippe MENASCHÉ	Université de Paris, FR

Except where otherwise noted, this is work licensed under
https://creativecommons.org/licenses/by-nc-nd/3.0/fr/

A la mémoire de mon père.

Meu grande amor.

Acknowledgments

First of all, I would like to thank the members of the jury who agreed to evaluate my thesis work. I would like to thank Professor Lucio Barile and Professor Christian Jorgensen for accepting my invitation to be my rapporteurs and for making time in your busy schedule to evaluate this manuscript. I would also like to thank Dr Florence Gazeau, Dr Maria Christina Zennaro, and Dr Antoine Monsel for agreeing to participate in my thesis jury as examiners. And finally Dr. Chantal Boulanger for accepting the invitation to be President of the jury. It's an honor to have all of you in my jury.

Je souhaite adresser toute ma reconnaissance à mon directeur de thèse, le Professeur Philippe Menasché. Je vous remercie de m'avoir accepté au sein de votre équipe depuis mon Master et de m'avoir fait confiance pendant tout mon parcours, vous m'avez permis de vivre une expérience incroyable. Votre passion pour la recherche nous pousse à nous dépasser et représente une véritable inspiration. Merci de m'avoir toujours motivé, d'avoir été toujours aussi présent et pour votre soutien sans faille quand les choses devenaient difficiles, je me rends compte que j'ai eu beaucoup de chance de vous avoir comme directeur de thèse.
Je ne vous remercierai jamais assez pour tout ce que vous m'avez appris et confié, je ferai en sorte de ne pas l'oublier, et de mettre en pratique vos conseils. Je garderai toujours un affectueux souvenir de cette période et particulièrement de vous.

Un très grand merci à ma « Dream-Team », tout d'abord de m'avoir supporté au quotidien car je sais que je peux ne pas être quelqu'un de facile à vivre tous les jours (la faute à mon signe astrologique).
Merci tout d'abord à toi Nadia, de m'avoir encadré avec toute ton énergie, ton savoir-faire, ta rigueur scientifique et ton talent. Tu m'as fait devenir une scientifique (je l'espère un peu comme toi), tu es brillante. Merci pour toutes les confidences, les rires, les conversations et l'amitié que nous avons créées, je n'oublierai jamais nos journées éternelles de travail en ta compagnie, milles merci.

Merci à mes petites sœurs doctorantes Manon et Chloé Pezzana, que serait ma vie au laboratoire sans vous ? Travailler avec vous est un plaisir quotidien, nos conversations, nos rires, nos aventures, nos commérages. Vous avez des cœurs en or, et votre amitié m'a permis

de venir au labo avec le sourire tous les jours même quand ces derniers n'étaient pas les meilleurs car je savais que je pouvais trouver du réconfort à vos côtés. Vous avez rendu cette expérience fraternelle. Je vous attends avec hâte au Beach Club en Grèce une fois que vous aurez soutenu pour fêter ça.

Valérie et Laëtitia, j'ai beaucoup appris à vos côtés. Je vous remercie pour votre disponibilité, votre patience. Vous avez su me supporter avec beaucoup de compréhension et de professionnalisme dans les moments difficiles. Aujourd'hui je me rends compte que vous aviez raison sur beaucoup de choses. Merci pour tous les efforts que vous avez fourni pour me faire grandir.
Nisa, pour tout ce que tu m'as appris et pour tout ce que tu es, pour ta douceur et disponibilité. Ta rigueur et ton esprit critique font de toi une scientifique brillante. Merci d'avoir consacré autant d'efforts pour me les expliquer, tu es quelqu'un de merveilleux et ça me manque déjà toutes nos aventures lors des congrès.

Je tiens aussi à remercier ma chef stagiaire Maria. Pour ta gentillesse, ta bonne humeur, ton intelligence, j'ai adoré travailler avec toi, et tout le monde était jaloux car j'avais la meilleure stagiaire du monde, je suis très fière de ton parcours. Tu es devenue une amie et nos moments au labo resteront toujours un très bon souvenir dans ma mémoire.
Je vous remercie Keirth et Cloche pour votre bonne humeur, vos rires, votre esprit léger, votre soutien lors des manips et des fous rires qu'on a peut avoir lors des pauses déjeuners, vous êtes géniales.
Un grand merci, à tous les stagiaires, étudiants qui m'ont accompagné pendant cette thèse : Anaïs, Léa Thiebault, Gabriel Ifergan, Jeanne Gauthier, Emilie Barron, Sara Gouarderes, Flaminia Gyss, Thomas Hamada, Eirini, Line Legac, Marie Jungeling et Aline Derisio (minha companheira, amiga e compatriota maravilhosa, muito axé pra sua carreira).

Enfin encore une fois un grand merci à toute mon équipe, vraiment sans votre soutien et aide, ce travail n'aurait peut-être pas pu être accompli, notre laboratoire c'est comme une grande famille, et c'est génial de vous avoir, je vous aime.

Je remercie mon deuxième chef le Dr Jean-Sébastien Silvestre, co-directeur de l'équipe, pour tous tes conseils et ta bonne humeur (même quand tu arrives à pas de souris pour nous faire

peur délibérément). Jean-Sé ta rigueur et ton esprit critique font de toi un scientifique incroyable, je me sens privilégiée d'avoir pu travailler avec toi. Un grand merci.
Je tiens à remercier également tous les membres de l'équipe 6a. Mathilde, Angélique, Vincent, Stéphane et Ivana ça a toujours été un plaisir de vous croiser et de papoter avec vous. José Vilar, Monsieur Wikipédia, cómo encontrar las palabras para agradecerte. No he llamado a tu puerta ni una vez por una pregunta para la que no he encontrado una respuesta. Muchas gracias por todo el tiempo que le dedicas a todos los alumnos del edificio, eres increyble. Enfin, un grand merci à Ingrid et à Paul pour toutes les heures que nous avons passées ensemble en manip et votre bonne humeur.

Je remercie la Fondation Alain Carpentier, qui m'a accueillie au sein de ses locaux et Chantal Boulanger, directrice du PARCC. Enfin je remercie les membres du Laboratoire de Recherches Biochirurgicales de la Fondation Alain Carpentier : Claire Banissi, Stephania Cruzzo, Nermine Lila, Jeanne Rancic, Martine Rancic, Adrien Lalot, Chantal Mandet, Julie Piquet, Tiana Razakatiana et Dr. Sophie Carpentier. Merci pour votre accueil sympathique, votre convivialité et votre bonne humeur.

Je témoigne toute ma reconnaissance à nos nombreux collaborateurs pour ce projet : le Pr Onnik Agbulut, Pierre Johanne, Dr Alain Brisson, Dr Xavier Loyer, Dr Stephan Malzan, Michael Robillard, Marie-Cécile Périer, Thi Tran, Irmine Ferreira, Dr Bertrand Tavitien et son équipe. Je remercie également nos collaborateurs de Saint Louis : Dr Antonio Alberdi, Dr Jérôme Larghero, Camille Humbert, Dr Reem Al-Daccak, Pr Dominique Charron et Dr Hocine Rachid. Enfin, je remercie nos collaborateurs américains de Cellular Dynamic International.
J'adresse mes remerciements à tous les membres du PARCC : les chercheurs, les étudiants, les ingénieurs et les techniciens sans lesquels la vie au laboratoire n'aurait pas été aussi agréable. Merci à toute l'équipe administrative pour sa gentillesse et disponibilité : Muriel, Annette, Catherine, Martine, Julien, Bruno, Cyrille, Nicolas, Guillaume, Corinna, Gwen, Stéphanie et spécialement mon ange gardien Véronique. Merci à tous les sourires que j'ai eu la chance de croiser chaque matin et qui ont participé à rendre cette expérience agréable.

Merci à tous mes amis et ma famille, David (love of my life and BFF), Iris (minha melhor amiga mais ciumenta do mundo que amo tanto), Natacha et Aline (minhas parceiras e bagaceras de todas as horas), Andy et Fred (meus anjinhos), Taynara et Giulia (minhas

maridas e amantes pra sempre), Day, Bia, Jaque (minhas princesonas e Nicolys), Thaisa e Michele (minhas sis from another mother), Anna Claudia et Giana (minhas primas amadas), Lucas (meu melhor amigo desde sempre pra sempre), Fafa et Lubber (meus parceiros), Julio e Fabien (meus terapeutas maravilhosos que me ensinam tanto sobre mim mesma, vocês são uns tesouros) qui ont su me motiver, me donner du réconfort dans les moments le plus difficiles, et plein d'amour quand j'en avais le plus besoin, eu amo muito todos vocês.

Mes plus profonds remerciements vont à mes parents. Merci Mimi d'être le meilleur beau-père du monde, merci d'être à nos côtes, ta présence sereine nous équilibre, ta gentillesse, ta sagesse et ta générosité sont précieuses quotidiennement, je t'adore, et je suis ravie que tu fasses partie de notre famille.
Obrigada Mãe, d'être la mère merveilleuse que tu es, d'avoir traversé l'océan pour que je puisse avoir la chance que tu n'as pas eu et d'avoir mis de côté tellement de choses pour me permettre devenir la femme que je suis aujourd'hui, de m'avoir toujours acceptée, supportée et de m'aimer profondément. Merci d'être comme tu es, de m'avoir éduquée, écoutée, de me ter acolhido, escolhido, d'avoir consacré toute ta vie pour que je puisse être heureuse. Eu não conseguiria nem em um milhão de palavras expressar o quanto sou grata por ser sua filha.
Je t'aime à l'infini.
C'est tout simplement grâce à toi et papa que j'en suis là aujourd'hui. De tout mon cœur j'espère que vous trouverez, dans la réalisation de ce travail, un début d'aboutissement de vos efforts ainsi que l'expression de ma plus profonde gratitude.

Abbreviations

Extracellular vesicles (EV)

Induced pluripotent stem (iPS)

Heart failure (HF)

Left ventricle (LV)

New York Heart Association (NYHA)

Ejection Fraction (EF)

Myocardial infarction (MI)

Troponins I (TNI)

Troponins T (TnT)

B- type natriuretic peptide (BNP)

N- terminal pro B- type natriuretic peptide (NT- proBNP)

Angiotensin-converting-enzyme inhibitors (ACEIs)

Angiotensin receptor blockers (ARBs)

Hematopoietic stem cells (HSC)

Bone marrow (BM)

Dendritic cells (DC)

Toll-like receptors (TLR)

Lipopolysaccharides (LPS)

Antigen presenting cells (APC)

Major Histocompatibility Complex (MHC)

Antigen (Ag)

Natural Killer (NK)

ADCC (antibody-dependent cellular toxicity)

Antibody (Ab)

B Cell Receptor (BCR)

Antigen-binding fragment (Fab)

Immunoglobulins (Ig)

Complementarity Determining regions (CDR)

Activation Induced Cytidine Deaminase (AID)

Reactive oxygen species (ROS)

Interleukins (IL)

Damage associated molecular pattern (DAMP)

Pathogen associated molecular pattern (PAMP).

T helper (Th)

T regulator (Treg)

Human leukocyte antigens (HLA)

Embryonic stem cells (ESC)

Induced pluripotent stem cells (iPSC)

Bone marrow-derived cells (BMC)

Mesenchymal stem cells (MSC)

Cardiac stem cells (CSC)

Cardiovascular progenitors cells (CPC)

Embryonic stem cells (ESC)

Bone morphogenic proteins (BMPs)

micro-RNAs (miRNAs)

International Society of Extracellular Vesicles (ISEV)

Microvesicle (MV)

Intraluminal vesicles (ILV)

Multi-vesicular bodies (MVB)

Messenger RNA (mRNA)

Extracellular Vesicles derived from iPS-CPC (EV-CPC)

Magenetic Resonance Imaging (MRI)

Mosaic Analysis With Double Markers Model (MADM)

Advanced Therapy Medicinal Products (ATMP)

Exosomes (Exo)

Table of Figures

Figure 1: Ejection Fraction, HF and symptoms as described by the American Heart Association 2017. [2] 20
Figure 2: ESC Guidelines for the diagnosis and treatment of acute and chronic heart failure, 2016. 22
Figure 3: Types of heart disease and risk factors. From the site https://www.creative-diagnostics.com/Cardiac-Disease.htm 23
Figure 4 : Heart failure treatments metaphor. Arnold Katz, Heart Failure: pathophysiology, molecular biology and clinical management – 2nd ed, 2008. 24
Figure 5: Cellular actors of the immunity adapted from © Abbas, Cellular and Molecular Immunology, 6th edition by Elsevier. 28
Figure 6: Humoral and cell mediated immunity from © Abbas, Cellular and Molecular Immunology, 6th edition by Elsevier 31
Figure 7: a) The BCR receptor b) Composition of BCR receptor, light and heavy chain c) Different types of Ig 32
Figure 8: Activation of B cells from by T helper cells (CD4+) © Abbas, Cellular and Molecular Immunology, 6th edition by Elsevier. 33
Figure 9: a) Antibody secretion b) Opsonisation process from © Abbas, Cellular and Molecular Immunology, 6th edition by Elsevier. 35
Figure 10: Antigen presentation for T cells process from © Abbas, Cellular and Molecular Immunology, 6th edition by Elsevier. 35
Figure 11: Antigen presentation by dendritic cells on MHCI and II for CD4+ and CD8+ process from © Abbas, Cellular and Molecular Immunology, 6th edition by Elsevier. 36
Figure 12: Cross presentation process from © Abbas, Cellular and Molecular Immunology, 6th edition by Elsevier. 36
Figure 13: Overview of the adaptive immune response from © Abbas, Cellular and Molecular Immunology, 6th edition by Elsevier. 37
Figure 14: Diapedesis phenomenon from Advances in Immunology Volume 129, 2016, Pages 25-53 Elsevier, by Marie-Dominique Filippi. 39
Figure 15: Direct and indirect recognition from © Abbas, Cellular and Molecular Immunology, 6th edition by Elsevier. 42
Figure 16: Immune-inflammatory response during MI; from Zlatanova et al, Frontiers Cardiovascular Medicine 2016 43

Figure 17: Phases of inflammation after myocardial infarction from; Prabhu and Frangogiannis et al, 2017. 47
Figure 18: Evolution of cardiac regenerative therapies from Cambria et al, Translational Cardiac Cell, 2017. 50
Figure 19: Classification of different type of therapies in cell-based, cell-free or tissue engineering from Shamagian et al Circulation Research 2019. 53
Figure 20: Extracellular Vesicles types and biogenesis from Yáñez-Mó et al; Journal of Extracellular Vesicles 2015. 55
Figure 21: Exosome protein composition from Meckers et al; Journal of Virology 2011. 58
Figure 22: Targets of the cardiac regenerative process from Shamagian et al; Circulation Research 2019 60

Table of contents

Acknowledgments 7
Abbreviations 11
Table of Figures 14
Table of contents 16
Preface 18
I) Heart Failure 19
1) The pathology 19
3) Symptoms and diagnosis 21
4) Main Causes and risk factors 23
5) Current therapies for heart failure and future perspectives 24
II) Immune System 27
1) Properties and overview of the immune system 27
a) Innate immunity 28
b) Molecular components 29
c) Adaptive immunity 31
2) Inflammation 38
a) Inflammation and innate immunity 38
a) Inflammation and acquired immunity 40
3) Allo recognition, transplantation and immunosuppressive treatments 41
4) Inflammatory response after myocardial infarction 42
a) Cardiac remodeling 42
..... 43
b) The different cells of the inflammatory phase 43
c) Reparative phase and different cells 45
d) Late cardiac remodeling phase 46
..... 47
III) Cellular and acellular therapies 48
1) Cellular cardiac regenerative medicine 50
2) Acellular therapies or next generation 52
a) Extracellular vesicles 54
b) Biogenesis 55
c) Extracellular vesicle content 57

d) Therapeutic use of EV and cardiac repair 60
IV) Objective (ensemble of manuscripts) 61
V) Discussion 182
VI) Conclusions and perspectives 187
Drug formulation, storage and stability 188
a) Efficacy *in vitro and in vivo* 188
b) Route of administration, dosing and EV targeting 189
c) Scientific impact 191
Résumé 192
Abstract 197
References 199

Preface

The adult human heart exhibits a limited regenerative capacity after myocardial infarction. This can sometimes lead to the development of heart failure, a disease with epidemic proportions, burdened with a mortality rate that exceeds most cancers.

Despite considerable advances, available treatments for heart failure are only palliative. Once pharmacological therapies fail, invasive solutions like ventricular assist devices or heart transplantation are the only options. In such a context, a great deal of interest has been focused on cell therapy with the goal of healing the injured myocardium.

Nearly twenty years have passed since the quest for heart repair began. Nevertheless, it is still far from reaching the patients' bedside. However, some important advancements have been made: cell therapy was initially conceived to replace dead cells and boost cardiac function through the delivery of new, fresh, beating muscle cells. Nowadays, we know that this is typically not happening. In most cases, the transplanted cells, regardless of cell type, can quickly die off. Yet, even when all transplanted cells have gone, their beneficial effects are left behind. These effects have been ascribed to a paracrine action of the cells' secretome on the failing heart. Extracellular vesicles (EV) are a key component of the secretome, and are important mediators of cell signaling. Increasing evidence suggests EV convey many of the beneficial factors found to mediate the effects of cell therapy.

This thesis work is aimed at investigating the mechanism of action of EV secreted by human induced pluripotent stem (iPS) cell-derived cardiovascular progenitors.

The work hereinafter presented has been divided into 6 chapters. Chapter one describes the pathology of interest: heart failure. It elaborates on the biopathology of this disease, stressing its evolution as a continuum, and the pressing need for novel therapeutic options. Chapter two elaborates on the mechanism of heart repair with a focus on understanding the immunological system and its major role in the development of heart failure. Chapter three reports the scientific steps of biomedical research in cardiac cell therapy and heart regenerative medicine. The main biological concepts that have driven research progress are outlined, along with the key approaches that have been tested as well as a description of EV as a biological entity. This leads up to chapter four, which is an ensemble of peer-reviewed manuscripts resulting from my thesis work. Finally, in chapters five and six, a general discussion, conclusion and perspectives are presented.

I) Heart Failure

1) The pathology

Heart failure (HF) is a complex clinical syndrome, resulting in the alteration of cardiac function, leading to the incapacity of the heart to deliver a sufficient amount of blood to respond to the needs of the body. It is caused by functional and structural abnormalities of the myocardium which ultimately lead to the failure of cardiac pump and of heart chamber filling. The most common cause of heart failure is deficiency of the left ventricle (LV), however pericardium, cardiac valves or large vessel dysfunction within the myocardium or endocardium, alone or combined, can be at the origin of this complex syndrome. The main mechanisms resulting in HF are: dysfunction linked to ischemia, ventricle remodeling, excessive neuro-humoral stimulus, abnormal myocyte calcium cycle, excessive or insufficient extracellular matrix proliferation, intense hemolytic overload, and accelerated apoptosis.

The severity of HF is classified as a function of patient symptoms and ability to perform physical activity according to the classes established by the New York Heart Association (Table 1). [1]

Class I	No limitation of physical activity. Ordinary physical activity does not cause undue breathlessness, fatigue, or palpitations.
Class II	Slight limitation of physical activity. Comfortable at rest, but ordinary physical activity results in undue breathlessness, fatigue, or palpitations.
Class III	Marked limitation of physical activity. Comfortable at rest, but less than ordinary physical activity results in undue breathlessness, fatigue, or palpitations.
Class IV	Unable to carry on any physical activity without discomfort. Symptoms at rest can be present. If any physical activity is undertaken, discomfort is increased.

Table 1: Functional classification of HF by the New York Heart Association as a function of the gravity of symptoms and physical activity; NYHA classes.

Three principal forms exist: chronic, acute and transitory. These three forms involve an alteration of the heart Ejection Fraction (EF) that can be reduced (≤ 40 %), or preserved (≥ 41%), as described in Figure 1.[2]

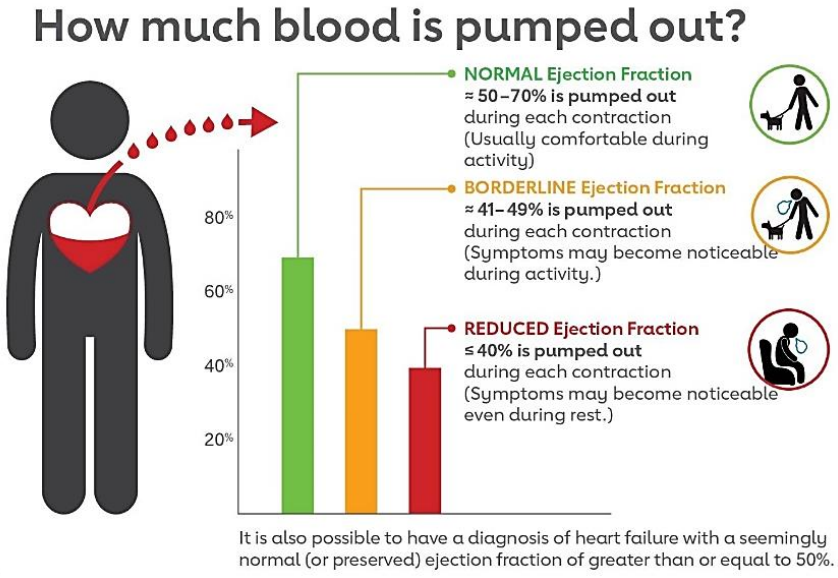

Figure 1: Ejection Fraction, HF and symptoms as described by the American Heart Association 2017. [2]

2) Epidemiology

According to the European Society of Cardiology, heart failure affects approximately 1- 2% of the adult population in developed countries, rising with age to as much as 10% in those older than 70 years of age.[3] In general, the overall prevalence of heart failure is increasing, probably fueled by current therapies for cardiovascular diseases, such as coronary artery disease, hypertension or valvular heart disease which allow patients to survive longer. In Europe and in the USA, a forty-year-old carries a risk of developing HF of 1 out of 5.

According to the latest American Heart Association report, more than 18 million Americans over the age of 20 have coronary artery disease, with males being more affected than females. The estimated incidence of myocardial infarction (MI) exceeds 800,000 attacks per year: approximately one every 40 seconds. In 2019, it is estimated that more than one million people in the United States alone will be hospitalized for an MI or coronary heart diseases. [4] In France, HF affects approximately 1 million people, [5] and despite therapeutic progresses, chronic heart failure remains a deadly disease and a major health problem.

3) Symptoms and diagnosis

The signs and symptoms commonly associated with HF are:

- Shortness of breath (dyspnea) during physical exercise
- Persistent tiredness and weakness
- Swelling of the legs, ankles and feet (edema)
- Irregular and accelerated cardiac rhythm (arrhythmia, and tachycardia, respectively)
- Reduced capacity to exercise
- Persistent cough or a wheeze
- Increased need to urinate overnight
- Abdomen swelling (ascites)
- Weight gain related to water retention
- Loss of appetite and persistent nausea

Serum markers

In normal conditions, the proteins contained in cardiomyocytes are absent or minimally represented in the systemic circulation. Upon injury, cardiomyocytes release several of these proteins that are normally intracellular: myoglobin, troponins, creatinine kinase and others. The appearance in blood of such molecules can be used to recognize myocardial necrosis. Cardiac troponins I (TnI) and T (TnT) [6] are part of the contractile apparatus of the heart muscle cells and are expressed almost only in the cardiac tissue: therefore, their rise in blood is rather specific of myocardial injury and for such reason, they are the preferred biomarkers for the evaluation of myocardial infarction nowadays a pathological level using cTn assay. Concerning HF the common markers are Natriuretic peptides know B- type natriuretic peptide (BNP) and N- terminal pro B- type natriuretic peptide (NT- proBNP) .[1] Levels are detailed here below:

Markers	**Pathological Level**	**Normal Levels**
TnI (Ultra assay)	Superior to 0.04 ng/mL	Inferior to 0.04 ng/mL
NT- proBNP	Superior to 100 pg/ml or 200 pg/ml (for patients with kidney failure)	Inferior to 100 -200 pg/ml
BNP	900 pg/ml in 50- to 75-year-olds 1,200 pg/ml in older patients	Inferior to 900 pg/ml in 50- to 75-year-olds or 1,200 pg/ml in older patients

Imaging

Using imaging techniques, HF can be confirmed by the algorithmic exams proposed by the European Society of Cardiology, described in Figure 2.[3]

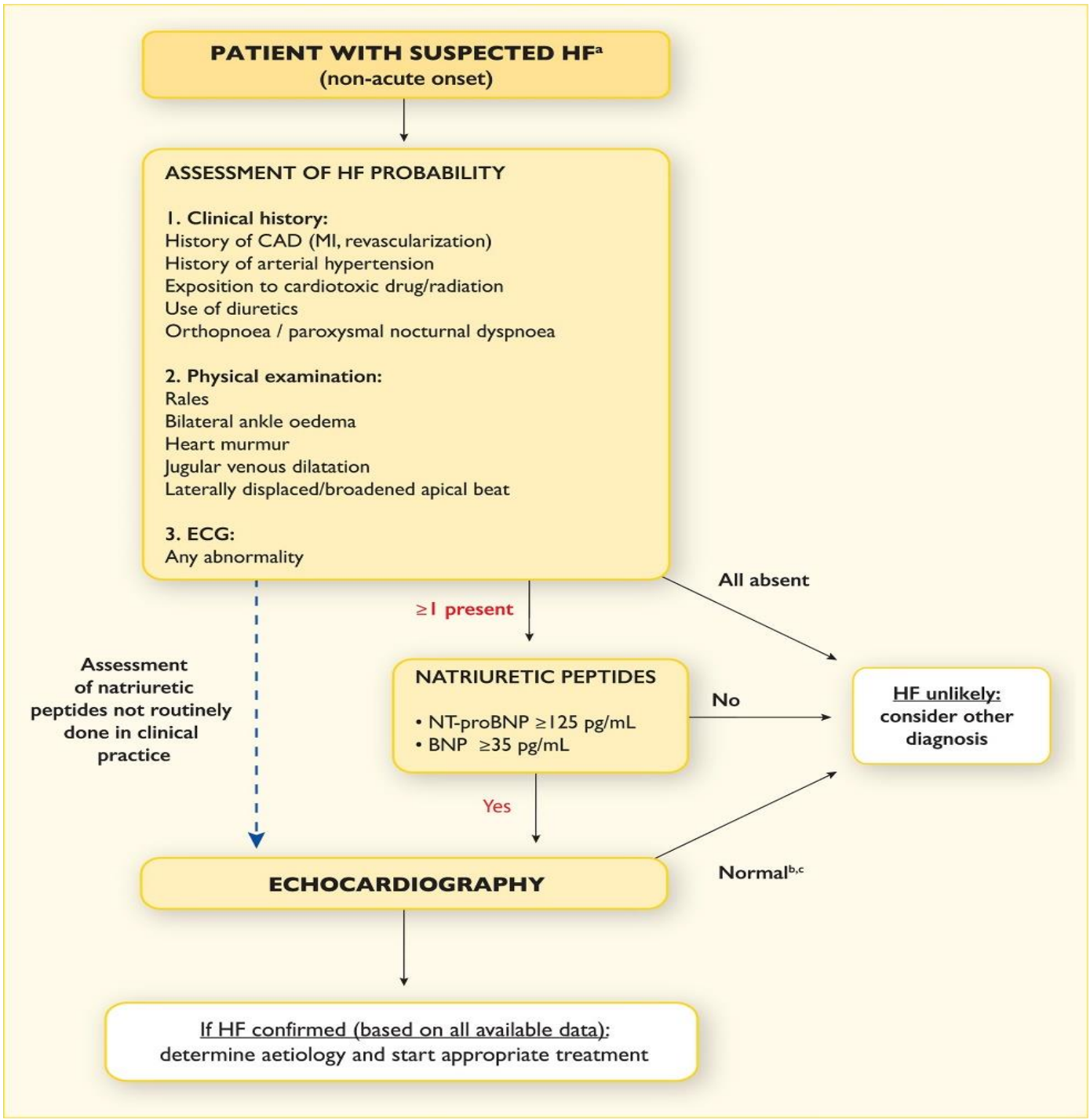

Figure 2: ESC Guidelines for the diagnosis and treatment of acute and chronic heart failure, 2016.

4) Main Causes and risk factors

The causes of HF can be varied: coronary disease, arterial hypertension, congenital malformation, valvulopathy, genetic mutations, infectious pathologies and rhythm disorders.

The occurrence of HF is strongly influenced by risk factors. While the presence of a single risk factor can be sufficient to provoke HF, the combination of many factors will increase the risk. Among the factors are notably: diabetes, alcohol and tobacco use, obesity and arterial hypertension, as illustrated in Figure 3. [7]

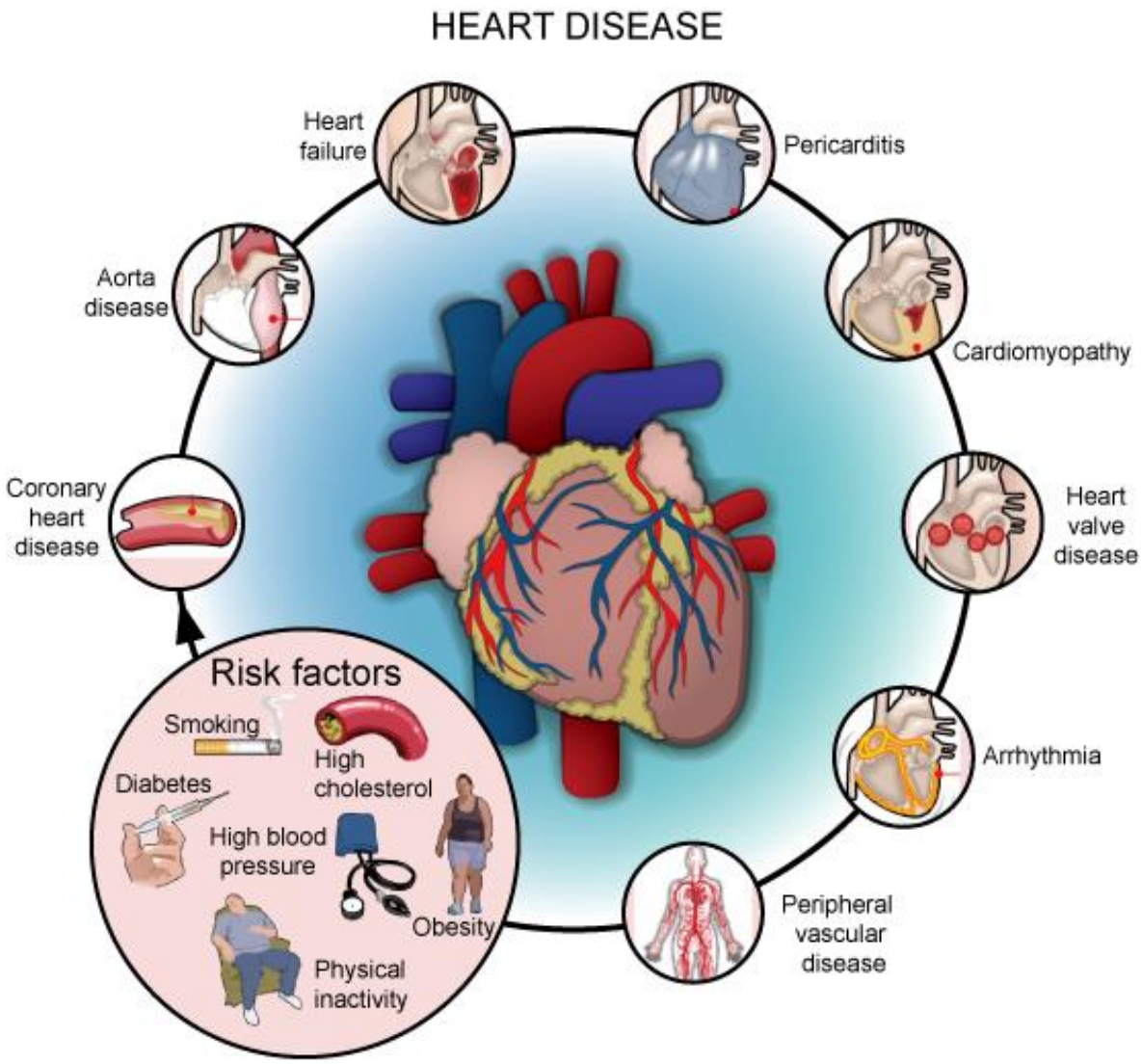

Figure 3: Types of heart disease and risk factors. From the site https://www.creative-diagnostics.com/Cardiac-Disease.htm .

5) Current therapies for heart failure and future perspectives

Treatments available for heart failure are nicely illustrated in a Figure by A. Katz in his book about HF. [8] Katz compares the failing heart to a tired work horse and treatments to the solutions that the farmer could adopt as reported in Figure 4.

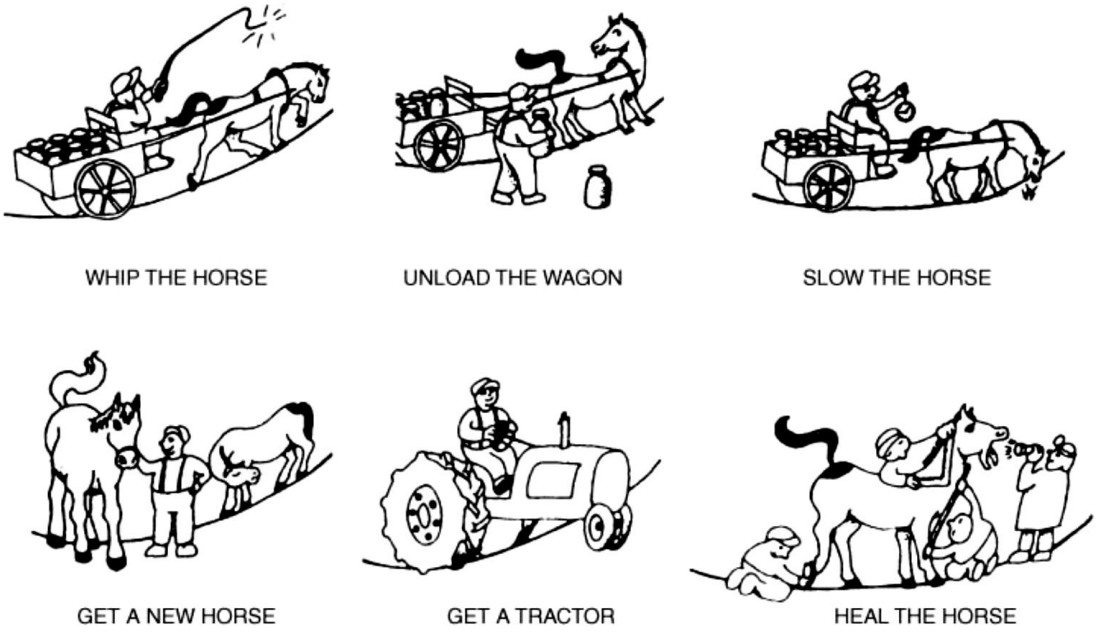

Figure 4 : Heart failure treatments metaphor. Arnold Katz, Heart Failure: pathophysiology, molecular biology and clinical management – 2nd ed, 2008.

Pharmacological treatments

By *whipping the horse* using inotropics, ß adrenergic agonists are currently used as a punctual treatment of acute heart failure. However, they worsen prognosis on the long term by adding a strain on the failing heart.

To *unload the wagon*, and reduce the charge by the inhibition of the renin –angiotensin II-aldosterone system. The inhibition is done using angiotensin-converting-enzyme inhibitors (ACEIs as enalapril, ramipril), antagonists of the mineralocorticoids receptors (as spironolactone) or antagonists of angiotensin II receptors (as valsartan, candesartan). These drugs have been shown to reduce morbidity and mortality [9] and are recommended in all

symptomatic patients, whichever the NYHA class. They reduce both pre and afterload on the heart (unloading the wagon) and they also counteract angiotensin-II-driven LV remodeling. Angiotensin receptor blockers (ARBs) are recommended as a second line in patients not tolerating ACEIs. Diuretic treatment is purely symptomatic and should not be abused, using the lowest efficacious dose. They do not change prognosis. Loop and thiazide diuretics are the most used classes.

Slow the horse: Slow the heart frequency to more homogeneous systoles and diastoles using beta blockers was considered deleterious in the past and has now become a cornerstone of treatment. They reduce the strain on the heart, decreasing blood pressure and slowing down the horse

Get a tractor or require device-assisted treatments such as a LV-assist devices or defibrillators. Approximately half of HF deaths are sudden and unexpected due to severe non-tolerated arrhythmias. Implantation of defibrillators reduces the incidence of such events.

All treatments mentioned up to here remain palliative and do not cure the disease itself.

Getting a new horse: Currently, surgery is the only therapy that is truly curative for HF. Cardiac transplantation is getting a new horse. Transplantation is limited by organ availability and by the strong lifelong immunosuppressive treatment it requires. Median waiting time for a heart transplant is 18 months in the Eurotransplant-covered region (a partnership covering 8 central Europe countries). Mortality while on the waiting list was 20% in 2017, with two times more patients entering the list than the actual number of transplants performed.[10]

Future perspectives for treatment of HF

Healing the horse: As more and more patients survive after MI or other sources causing heart damage, more and more patients develop HF through the loss of viable myocardium. Many therapies have focused on preventing the progressive process of cardiac remodeling but none addresses the underlying cause.
The discovery of stem cells has set a new path for cardiovascular research. Many studies seek to regenerate injured cardiac tissue and treat a pathology that, in spite of clinical advancements, still bears a high mortality burden. The overall capacity for regeneration of the

adult heart is limited, nonetheless these pathways do exist, and researchers are seeking methods to enhance and amplify them to achieve myocardial-cell replacement. A variety of cell substrates have been proposed for cardiac cell-based therapy and several therapeutic approaches have shown promising results in preclinical animal models. Therapeutic candidates remain to be firmly validated, and their efficacy and mechanisms well-established before their clinical use.

As defined by Kübler, cardioprotection includes "all mechanisms and means that contribute to the preservation of the heart by reducing or even preventing myocardial damage".[11] This broad definition encompasses what is commonly termed cardiac repair which attempts at "reducing… myocardial damage" by addressing some of its root causes (regardless of their etiology), i.e., loss of cardiomyocytes, impaired coronary artery macro- and micro-circulation and disorganization of the extracellular matrix.[12,13] Within this framework, cardiac regeneration is more focused on the generation of new cardiac contractile cells (regardless of their source) which could substitute for those which have been irreversibly damaged. Currently, however, there is compelling evidence that this mechanism is very limited in the adult mammalian heart.[14] Thus, while the main objective of this thesis was to assess whether extracellular vesicles could activate signaling pathways leading to re-boost cardiomyocyte proliferation, analysis of the final outcomes rather leads to consider that they improve heart function by alternate mechanisms and are thus better categorized as a cardio-reparative rather than a cardio-regenerating therapy.

.

II) Immune System

1) Properties and overview of the immune system

Immunity is the ability to respond to an attack in order to preserve the integrity of the body.[15] The immune system is composed of cells, molecules, tissues and organs, collectively acting to provide protection.

The immune reaction is a physiological phenomenon (not pathological) and has the role of fighting against the aggression. To this purpose, the body possesses several mechanisms to prevent the attack, starting with physiological barriers (ex. the skin, mucosa etc.), if these barriers are not sufficient and an immune reaction occurs, it acts to eradicate the attack and restore tissue homeostasis. An important role of the immune system is its capacity to distinguish between self & non-self, identify what is dangerous (ex: pathological signals, virus etc.) or not (ex: food). This is called the tolerance of the immune system .[15]

There are two types of immune mechanisms that work in collaboration with each other:
the innate immunity acts quickly, is short-lived (~hours to 2-3 days) and unspecific. The acquired immunity acts slowly, taking days to weeks. Acquired immunity is specific, adaptive, and results in the generation of a reservoir of memory cells.
The immunological memory is required in case of a second exposure to the aggressor to respond quicker. The immunity integrates two steps; the innate that halts the infection and the adaptive that clears it. This phenomenon takes place through a dialogue between both.

Innate immunity	Adaptive immunity
• Immediate protection, 1st line of defense • Blocks the entry and eliminates dangerous signals • Ready to act (components already present) • Recognizes patterns of molecules on antigens • No memory	• Late response, delayed development • Stimulated by innate immunity and the dangerous signals • Adapted response to invader via expansion of lymphocytes, specific to antigen • Immunological memory

The **cellular actors** of immunity are presented below in Figure 5 and further below.

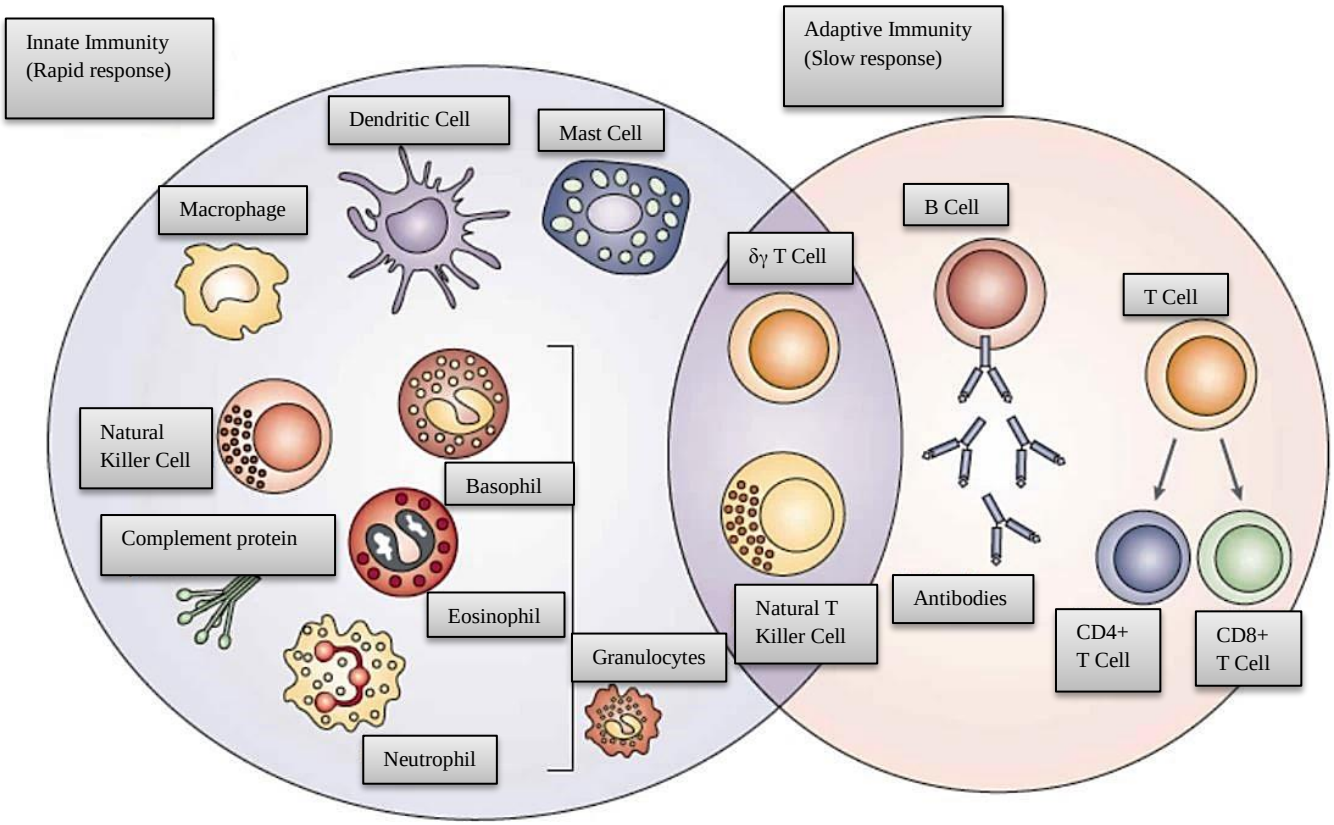

Figure 5: Cellular actors of the immunity adapted from © Abbas, Cellular and Molecular Immunology, 6th edition by Elsevier.

- **Dendritic cells (DC)** have a specific morphology. Born in the BM, they are resident in tissues. They recognize antigens by their toll-like receptors (TLR). As an example, TLR4 recognizes lipopolysaccharides (LPS) specific to bacteria. These cells are antigen presenting cells (APC) for CD4+ cells through the lymphatic system. The APC are responsible for: secretion of cytokines, release of inflammatory mediators, and phagocytosis (by endocytosis). The DC forms through the Major Histocompatibility Complex (MHC) a complex with the Antigen (Ag) which is responsible for lymphocytes activation.

- **Phagocytes** are cells which kill the danger signals non-specifically but can damage tissues if they stay too long on site. They live 1-2 days when activated. In this family eosinophils represent 1-3% of white blood cells. They act by defending the body against parasites. The resident monocytes/macrophages are also other members of this family. They can act by phagocyting the pathogenic signal directly or indirectly. They can also be

chemo-attractants for other immune cells. Macrophages can be divided into two different phenotypes: M1 = pro-inflammatory, M2 = anti-inflammatory.
The roles of phagocytes are: APC (recognition via TLR), secretion of cytokines and inflammatory mediators, phagocytosis (by endocytosis).
The antigen destruction by the phagocytes will occur via oxygen and nitric radicals.
Ultimately the combinatory of phagocytes + APC induces the massive secretion of cytokines *in situ*.

- **Mastocytes** are mainly implicated in the induction of inflammation because of their histamine content.

- **Natural Killer (NK)** cells kill injured, tumorous or infected cells by cytotoxic action (perforine/granzyme). NK cells can kill other cells by ADCC mechanism (antibody-dependent cellular toxicity).

b) Molecular components

Cytokines and chemokines are responsible for intercellular communication. They are secreted by activated cells, recognized by specific receptors, can act locally or distantly, by autocrine or paracrine stimulation and induce various cellular responses (activation, proliferation, apoptosis, mobility, secretion). Cytokines can be pro-inflammatory such as: TNFα, IL-1b, IL-8, IFNγ or anti-inflammatory such as: IL-10, TGFβ, IL-4. Another player is **the complement system** composed of proteins in the plasma. The system is inactive unless something occurs.

Summary of the innate immune response:

Presence of microorganism



Physical and chemical barrier



Complement activation

Phagocytosis by resident cells (PACMAN)

Degranulation of mastocytes



Local inflammatory reaction

(Cytokines, perforin & granzyme, C5a, C3a, histamine…)



Neutrophils, monocytes, NK recruitment.

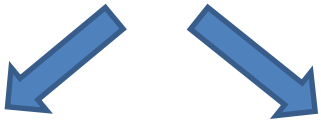

Success

Micro-organism elimination

Failure

Requirement for adaptive immune response

c) Adaptive immunity

Adaptive immunity is divided into two types: the humoral immunity responsible for defending against extracellular organisms, and the cell-mediated immunity defending against intracellular organisms, as illustrated in Figure 6. [15]

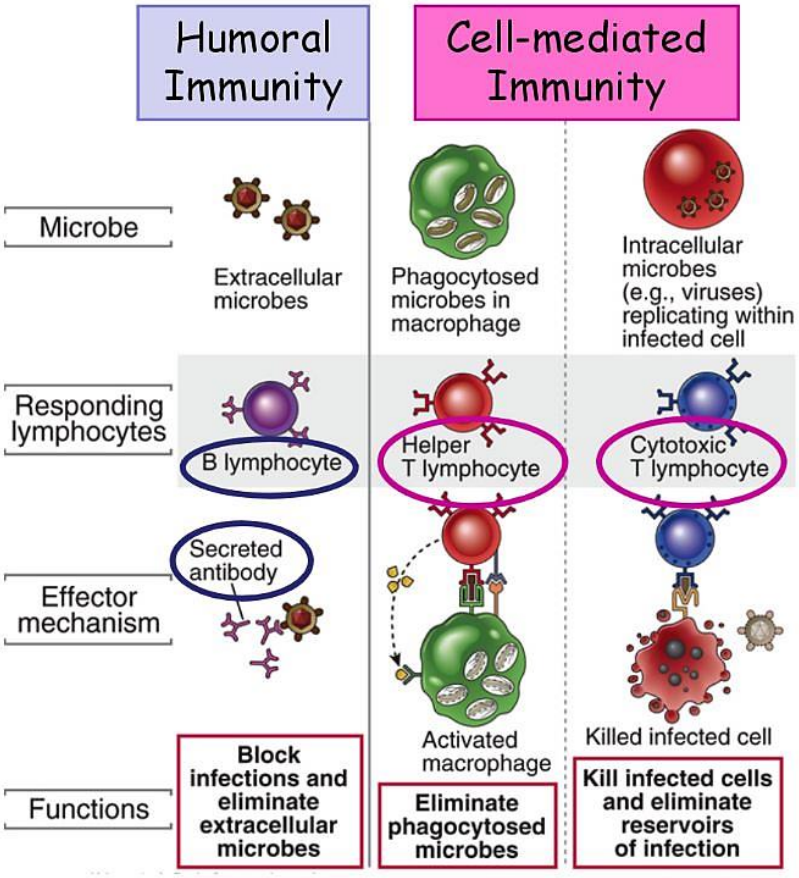

Figure 6: Humoral and cell mediated immunity from © Abbas, Cellular and Molecular Immunology, 6th edition by Elsevier

The adaptive immunity has three specific characteristics:

- Diversity – the expression of billions of T Cell Receptors (TCR) even before encountering an antigen.
- Specificity - only one TCR/peptide, with selection and proliferation of the proper clone when meeting with the Ag.
- Memory – is the property of remembering specific adaptive immune responses, and making a greater and more rapid response in the future if re-exposed to the same pathogen.

Adaptive immunity is mainly driven by lymphocytes. These are born in the BM and represent 30-40% of white blood cells. They are unique cells that express Ag-specific receptors. The B cells mature in the BM, whereas the T cells mature in the thymus. These two organs are the primary lymphoid organs. The meeting of APC and effector cells occurs in the secondary lymphoid organs, which are the lymph nodes and spleen.

i) B cells

The B lymphocytes express the B Cell Receptor (BCR) as illustrated in Figure 7a, which is a membrane form of immunoglobulin. The BCR is able to recognize Ag by the antigen-binding fragment (Fab) in 2 different forms: small peptides (presented by APC or soluble) or macromolecules. Naïve B lymphocytes differentiate in plasmocytes that secrete antibodies after activation. These antibodies are immunoglobulins (Ig). Immunoglobulins are composed of a light and a heavy chain. The light chain of an antibody can be classified as either kappa (κ) or lambda (λ) type based on small differences in the polypeptide sequence. The heavy chain makeup determines the overall class of each antibody; 5 types of heavy chains exist as a, d, e, g, m as illustrated in Figure 7c. IgA and IgM are secreted by naïve cells. IgM display affinity maturation and class-switching to IgE, IgG, and IgA (only one of these 3 isotypes are secreted per B cell). Their common characteristic is the Constant Fraction (Fc) allowing their recognition by other immune cells (Figure 7a) .[15]

There are three Complementarity Determining regions (CDR) in each variable domain.

a

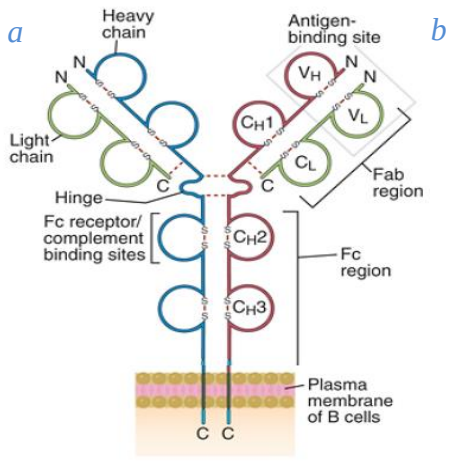

b

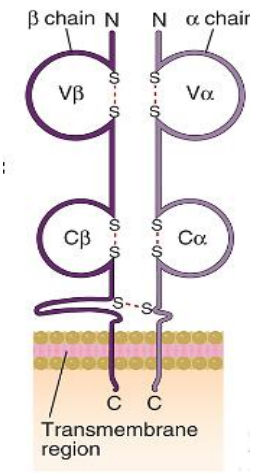

c

Isotype of antibody	Subtypes	H chain	Secreted form	Functions
IgA	IgA1,2	α (1 or 2)	Monomer, dimer IgA (dimer)	Mucosal immunity 2 binding sites
IgD	None	δ	None	Naive B cell antigen receptor
IgE	None	ε	Monomer IgE	Mast cell activation (immediate hypersensitivity) Defense against helminthic parasites
IgG	IgG1-4	γ(1,2,3 or 4)	Monomer IgG	Opsonization, complement activation, antibody-dependent cell-mediated cytotoxicity, neonatal immunity, feedback inhibition of B cells
IgM	None	μ	Pentamer IgM	Naive B cell antigen receptor, complement activation 5 binding sites

Figure 7: a) The BCR receptor b) Composition of BCR receptor, light and heavy chain c) Different types of Ig

ii) B cell activation and production of Ig

The B cells do not require any presentation to be activated and they all express CD19 as a pan marker. The T helper cells (CD4+) are in the paracortex and B cells are in the follicle of the lymph node. Their interaction occurs through the TCR-MHCII and CD40L-CD40 as illustrated in Figure 8.

The consequences of B cell activation are: proliferation, increase of cytokine receptor expression, preparation phase to interact with T cells, IgM secretion (soluble and pentameric form), class switching, and somatic hypermaturation.

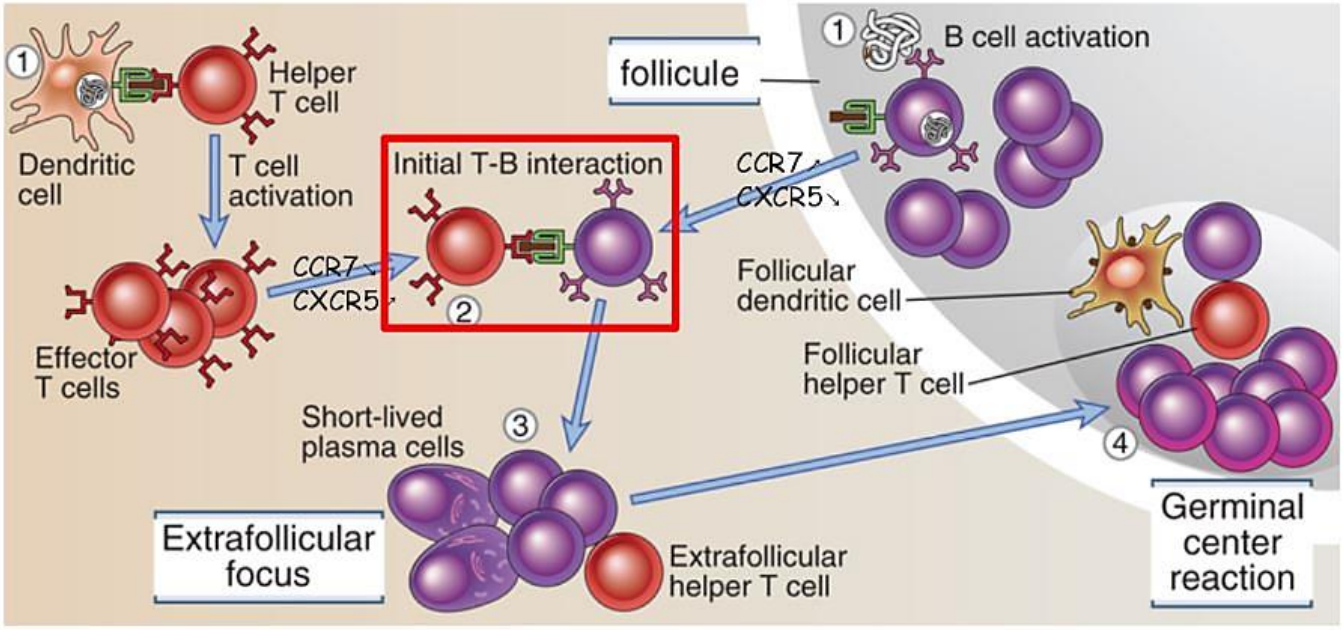

Figure 8: Activation of B cells from by T helper cells (CD4+) © Abbas, Cellular and Molecular Immunology, 6th edition by Elsevier.

Class-switching is the process by which the Fc region of the Ab heavy chain is changed, but the variable region of the heavy chain stays the same. Since the variable region does not change, class switching does not affect antigen specificity. Instead, the antibody retains affinity for the same antigens, but can interact with different effector molecules.

Somatic hypermutation is the process by which mutations occur in the variable region of the light and heavy chains. This phenomenon participates in the modulation of affinity to Ag. The B cell having a Ig with weak affinity to its epitope can increase its affinity by somatic hypermutation. This activity is done by the AID (Activation Induced Cytidine Deaminase) enzyme. [15]

Once Ig are produced, effector functions take place, including neutralization, opsonization, activation of complement, and production of mucosal immunity (Figure 9a and b). Concerning neutralization, the secreted Ab prevent the penetration of pathogens through epithelial barriers, they bind the organisms allowing their recognition by effectors cells and preventing the infection of adjacent cells.

The Ab production allows also opsonisation and phagocytosis (Figure 9b) through the recognition of the Fc by the macrophages, neutrophils and ADCC cells (ex: NK recognize IgG and secrete IFNγ and perforin/granzyme leading to the lysis of infected and cancerous cells only coated by the Ab).

The activation of complement triggers a cascade of actions, independent of the Ig, such as opsonization, osmotic lysis of microbes via the classical pathway and stimulation of inflammatory reactions.

Finally, the mucosal immunity takes place by the class-switching of Ig into IgA via TGFα secretion. Transport through epithelial cells can stop the microbe's entry. [15]

a)

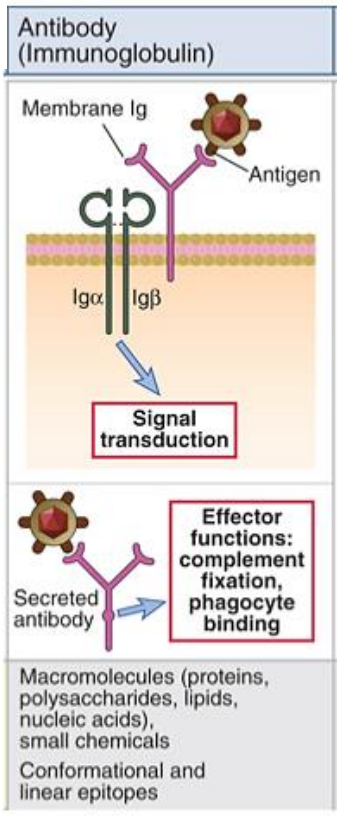

b)

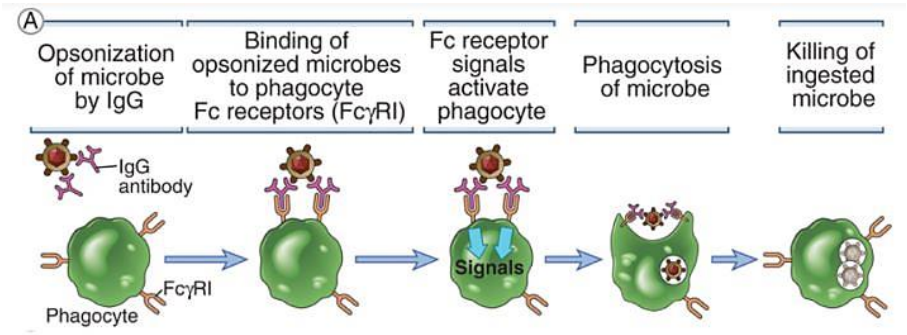

Figure 9: a) Antibody secretion b) Opsonisation process from © Abbas, Cellular and Molecular Immunology, 6th edition by Elsevier.

iii) T cell mediated immune response

T lymphocytes recognize only small peptides presented by MHC on APC. The T helper cells (CD4+) can activate other immune cells (macrophages, lymphocytes) and T cytotoxic cells (CD8+) can eliminate damaged cells using the granzyme and perforin lysis mechanism. Activation of T cells occurs in secondary lymph nodes. Naïve T cells can discriminate self from non-self and are mature, but T cells are not capable of meeting the Ag alone and need presentation (Figure 10). The APC for T cells are DC. The DC express both MHCI and MHCII. The T cytotoxic cells CD8+ meet MHCI and the T helper cells CD4+ meet MHCII only after activation (Figure 11).

The role of the T helper is leukocyte activation by cytokines, phagocytosis, and microbe killing. The role of the cytotoxic T-cell is to kill infected cells [15].

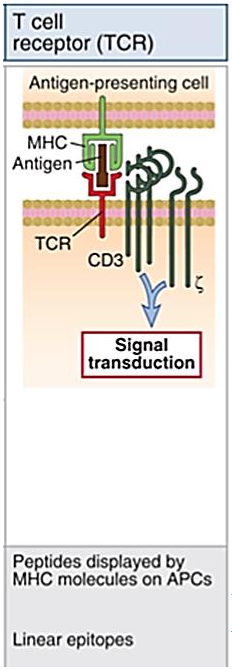

Figure 10: Antigen presentation for T cells process from © Abbas, Cellular and Molecular Immunology, 6th edition by Elsevier.

Differences between MHCI and MHCII loading presentation are described below (Figure 11):

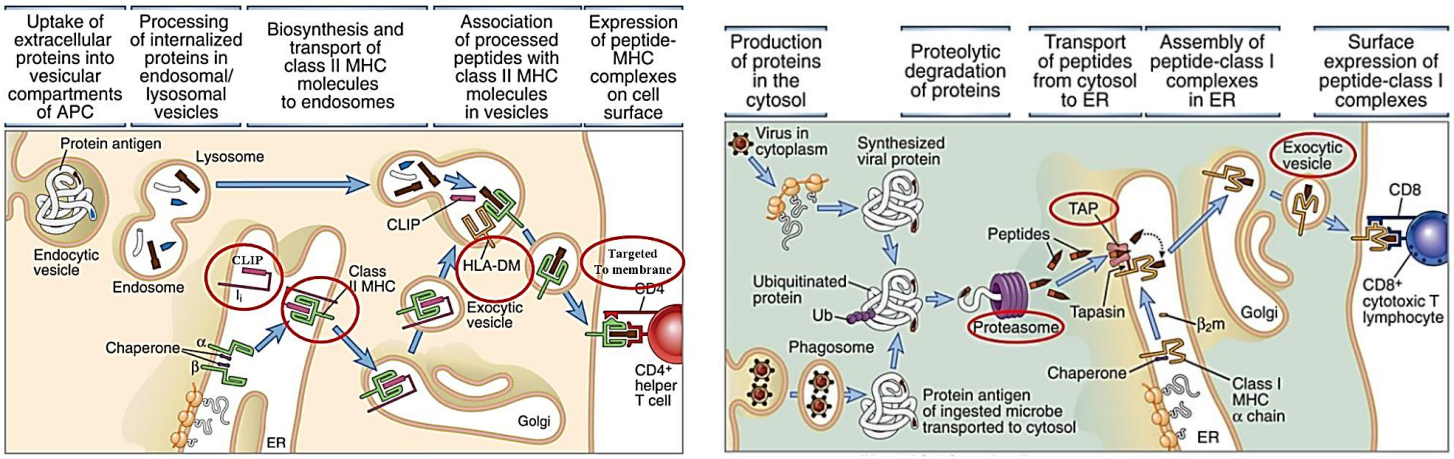

Exogenous Ag: Endocytosis → endosome → phagosome → phagolysosome → loading of peptide on MHCII (CLIP, 4LA-DM) → expression	Endogenous Ag: Proteasome→ Reticulum endoplasmic → loading of peptide on MHCI → expression

Figure 11: Antigen presentation by dendritic cells on MHCI and II for CD4+ and CD8+ process from © Abbas, Cellular and Molecular Immunology, 6th edition by Elsevier.

Cross presentation: In the phagolysosome, some proteins can be released in the cytoplasm, be taken as endogenous Ag, and presented by MHCI resulting in the activation of CD8+, this event is called cross presentation, as illustrated in Figure 12. The consequences of such event are clonal expansion and terminally contraction phase (90% of cell die, except for memory cells).

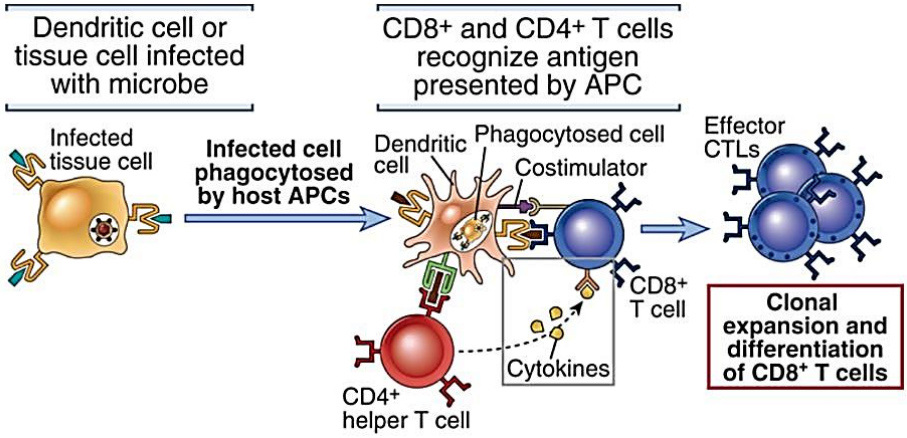

Figure 12: Cross presentation process from © Abbas, Cellular and Molecular Immunology, 6th edition by Elsevier.

The lymphocyte population is a major player of the acquired immune system memory. These cells behave in a physiological context by not reacting to self or non-dangerous substances (ex: food) and by reacting to dangerous signals or foreign bodies (ex: microbes).
In a pathological context they can be dysfunctional and not able to react against microbes, thus causing immunodeficiency, furthermore, they can react against the self, creating auto-immune diseases or also react against inoffensive substances, causing allergy.[15]

The Figure 13 recapitulates the late immune response process.

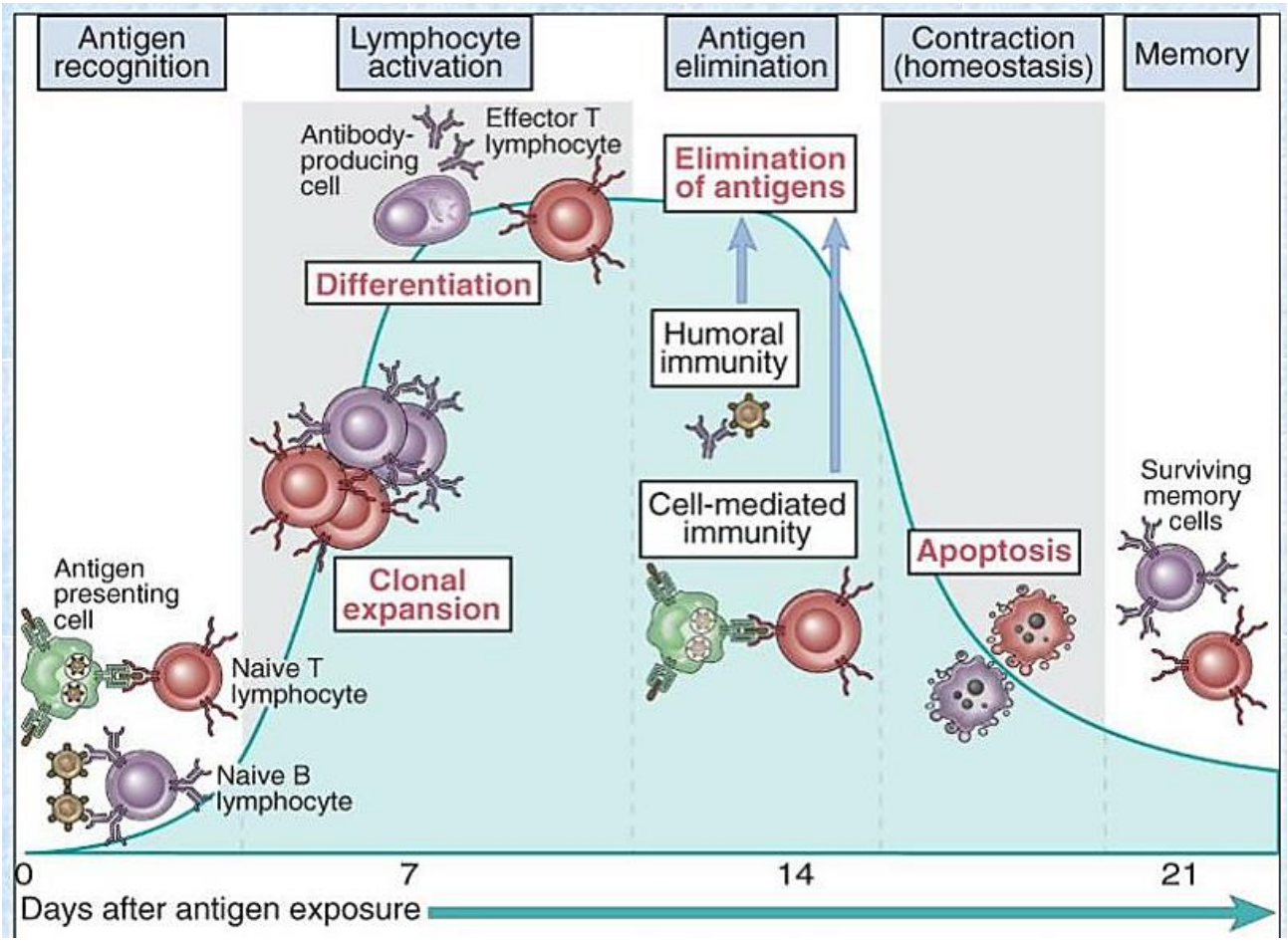

Figure 13: Overview of the adaptive immune response from © Abbas, Cellular and Molecular Immunology, 6th edition by Elsevier.

2) Inflammation

The inflammatory response is the physiological reaction built to fight against an aggression. Different potential events can be the cause such as traumas, infections, tumors and chemical poisoning among others. The cardinal signs are pain, redness, heat, swelling and malfunction. It is an immediate and local phenomenon that can become systemic (fever). The objective of this reaction is pathogen removal and tissue repair.

a) Inflammation and innate immunity

Composed by:

- Cells: macrophages, NK, DC, mastocytes (tissue) + leukocytes, platelets (blood).
- Vessels: endothelial cells.
- Chemical mediators: Cytokines, chemokines, growth factors, hormones.

Inflammation is organized in 3 steps: the initiation step involves vascularization and is the primary effector. It is due to the vasodilatation of small venules that increase the local blood flow causing redness and heat. The second step is the formation of inflammatory edema due to the increase of small vessels permeability. The third step is accompanied by exudate of water and plasma proteins (histamine, bradykinin, leukotriene), the accumulation of fluid causes pain and swelling.

Cells, plasma and lipid mediators are major players of the inflammatory response.
Cellular mediators are synthesized before inflammation and stored in granules, they are 1st to be secreted, and are known as vasoactive amines (released by activation of platelets and causing pain) and histamine (released by activation of mastocytes that degranulate thanks to pro-inflammatory cytokines secreted by macrophages).
Plasma mediators as the complement system have the ability to disrupt the membrane of the target pathogen, they stimulate phagocytosis by contact system (kinin) or coagulation system (fibrin).
Finally, the lipid mediators as prostaglandin (cyclooxygenase) and leukotrienes (lipoxygenase) derived from arachidonic acid and membrane phospholipid are involved in vasodilatation and chemotaxis.

The secondary effectors are neutrophils; they are recalled by pro-inflammatory mediators secreted in the tissue either by the endothelium (IL-8, PAF, LTB4), the resident macrophages (TNFα, IL-1β), complement (C3a, C5), bacteria (LPS, N-N-(N-formyl-L-methionyl)-L-leucyl (fMLP)) or prostaglandins and leukotrienes. They are chemo-attracted and recruited on the site of inflammation, and extravasation (diapedesis) of circulating neutrophils occurs in the 6-24h post injury.

The recruitment of the neutrophils to the inflammatory site and the crossing of the basement membrane by chemotaxis is described in Figure 14. To this goal the following steps are required: the neutrophil is capture by the vessel wall (P-selectin), it rolls (E-selectin), it adheres (integrins – ICAM-1) and lastly migrates (PECAM-1), to the injured tissue, this process is known as diapedesis (Figure 14).

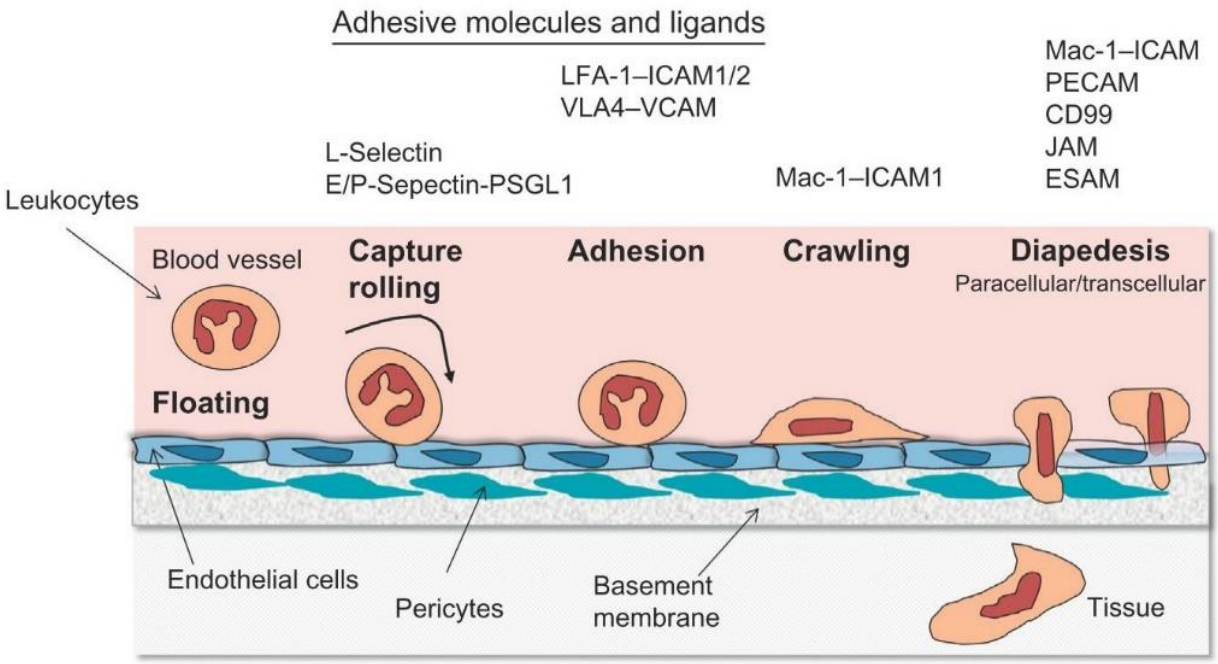

Figure 14: Diapedesis phenomenon from Advances in Immunology Volume 129, 2016, Pages 25-53 Elsevier, by Marie-Dominique Filippi.

Pathogen recognition is essential for the whole process. Pattern recognition receptors (PRR) bind on pathogen surfaces to proteins known as damage associated molecular pattern (DAMP) and pathogen associated molecular pattern (PAMP). Among many receptors are the mannose receptors, TLRs, scavenger receptors, Fc receptors, complement receptors.

The pathogen process of destruction can be done by intracellular lysis (degranulation of proteases or oxidative burst, phagocytosis) or extracellular lysis (degranulation of proteases or net DNA secreted by the neutrophil to trap the bacteria with proteases while dying).

The repair and resolution of inflammation, and ultimately the restoration of tissue integrity is an active phenomenon, not simply the deactivation of the inflammation process. Pro-resolutive mediators (arachidonic acid) are synthetized from lipoxin instead of prostaglandin and leukotriene. Synthesis of resolvins and protectins stimulates the elimination of microbes and apoptotic cells as well as the phagocytosis performed by pro-resolutive macrophages and the secretion of anti-inflammatory cytokines (ex: IL-10 and TGFb). [15] Leading to an elimination of inflammatory stimuli and generation of anti-inflammatory mediators. Then a stoppage of neutrophil infiltration, an increase of resolutive monocytes infiltration, a decreased of vascular permeability occurs gradually leading to homeostasis and elimination of apoptotic neutrophils.

If the scenario becomes pathological and no resolution of the inflammation occurs, chronic inflammation is installed, lasting for months or even years, becoming a systemic and uncontrolled process leading to tissue destruction and hyper-activation of inflammatory cells and strong secretion of pro-inflammatory mediators.
Inflammation is more generally associated with the innate immune response, however, increasing experimental and clinical evidence has highlighted its importance in antigen-driven adaptive immune responses.

a) Inflammation and acquired immunity

The components of adaptive immunity include memory cells which are probably also responsible for stimulating the chronic nature of inflammation. This new scenario supports that lymphocytes cooperate with innate immune cells and collectively orchestrate the inflammatory response .[16]

The interaction between adaptive immunity and the inflammatory process draws particular attention to the role of pro-inflammatory Th, Treg, T cell derived cytokines in autoimmune, cardiovascular and infectious diseases. [17–20] These studies highlight the importance of lymphocyte involvement during acute and chronic inflammation. [21–23]

3) Allo recognition, transplantation and immunosuppressive treatments

Many pathologies, such as auto-immune inflammatory diseases, degenerative diseases or heart failure can lead to organ, tissue or cell transplantation. Autograft is when a patient receives an organ, tissue or cells from itself, the allograft is the inverse, the patient and the donor are different individuals. The allorecognition is the term used to define immunological recognition of histoincompatible antigens between genetically disparate individuals within the same species.

One of the obstacles of transplantation is rejection, leading to graft destruction by the immune system. The recipient immune system recognizes Ag from the donor as non-self and triggers an immune rejection in the absence of immuno-suppression. There are three types of immune rejection. [24] The hyperacute, the humoral acute and cellular acute rejection.

The Hyperacute rejection occurs in less than 0.5% of cases. The use of suppressors preventive to the treatment (desensitization) as well as screening for cross match and ABO blood group compatibility can avoid this reaction. In the patient serum, antibodies recognize the endothelial cells of the graft causing coagulation.
The cross match test consists of the search for antibodies of the recipient against the MHC (or human leukocyte antigens (HLA)) of the donor (B and T cells) via flow cytometry for example. If there is fixation of the donor lymphocytes on the donor serum, the cross-match is positive and desensitization is necessary to enable the graft from an ABO incompatible donor.

Humoral acute rejection uses the same mechanism described above but there is time for cell adhesion before coagulation. It is the most frequent kind of acute rejection and occurs because of presensitization (previous acquired immunity by pregnancy, blood transfusion, previous transplantation) resulting in the production and stock of memory cells. The rejection can act for example by ADCC cells. The preventive treatment is desensitization removal of Ab by plasmapheresis.

Cellular acute rejection is divided into two arms; the direct one via donor APC with MHC+peptide engendering acute rejection, and indirect one via the recipient APC (recipient MHC, donor derived peptide) engendering chronic rejection (Figure 15).

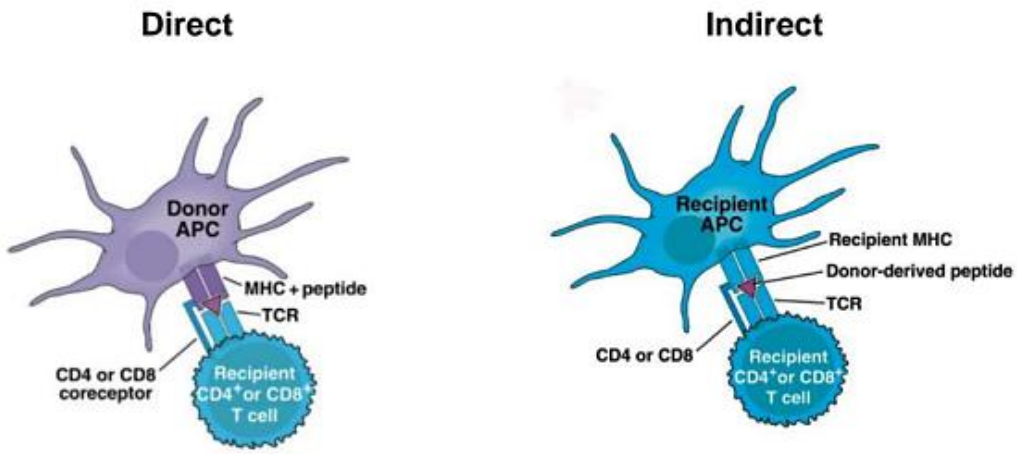

Figure 15: Direct and indirect recognition from © Abbas, Cellular and Molecular Immunology, 6th edition by Elsevier.

The nature of allo-antigen is the MHC (or HLA) system, which in humans is polymorphic and co-dominant. The immunosuppressive drugs target T cells: especially CD3 (signalization), signal (mTor inhibitor), blockers of the cell cycle or calcineurine inhibitors (tacrolimus for example). We addressed this point here because the use of cellular therapy or acellular therapy for heart failure demand the investigation of the potential immunogenicity of the administrated biological product.

4) Inflammatory response after myocardial infarction

a) Cardiac remodeling

In mammals, the sudden loss of cardiomyocytes after MI exceeds the limited regenerative capacity of the myocardium and a fibrotic scar is formed. The necrotic cells provoke the release of dangerous signals activating immune pathways and initiate an intense inflammatory response. The induction of cardiac remodeling proceeds through cellular and molecular changes in size, shape and function. [25,26] It is primed by an intense sterile inflammation followed by an infiltration of immune cells to eliminate the necrotic cardiomyocytes and the extracellular matrix. Thus, during this period, the neutrophil, monocyte/macrophage, DC and lymphocyte populations significantly increase in the myocardium. This first phase lasts ~ 3 to 4 days in mice, and is followed by a reparative phase during which the inflammation is attenuated. This attenuation is caused by the polarization of immune cells towards an immunomodulatory profile, the proliferation of fibroblasts and a neo-vascularization which facilitates scarring.

The number, type and activation state of different types of immune cells dictate their impact on cardiac repair after MI (figure 16) .[20] In this section we will address the inflammatory phase in the murine heart.

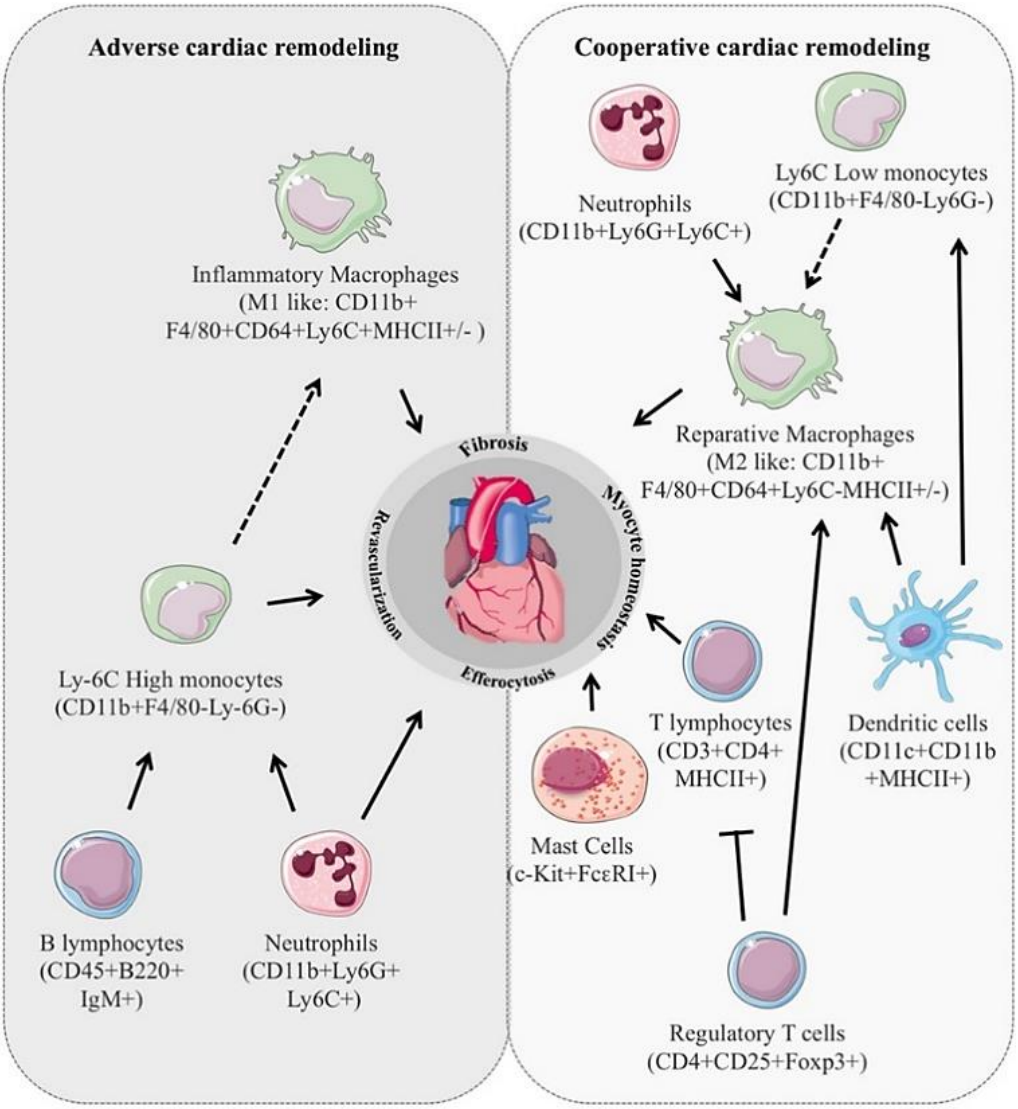

Figure 16: Immune-inflammatory response during MI; from Zlatanova et al, Frontiers Cardiovascular Medicine 2016.

b) The different cells of the inflammatory phase

Cardiomyocytes

The necrosis of CM constitutes the principal stimulus of inflammatory reaction after the MI through the generation of DAMPs in the infarcted area. The DAMPs motifs trigger an immune inflammatory reaction. The presence of ROS and healthy CM in the peri-infarcted area bring on the secretion of cytokines. Nevertheless, the contribution of CM in the inflammatory post –infarct response is still poorly understood.

Endothelial cells

Endothelial cells are the second most abundant population [27] in the heart. Leucocyte infiltration in the injured tissue requires the endothelial activation via expression of selectins (P and E selectins). The selectins bind to neutrophils and monocytes. This capture is followed by rolling through the endothelium and the trans-vascular diapedesis occurs. [28]

Neutrophils

Neutrophils are the first immune cells to infiltrate the myocardium after MI in response to the inflammatory mediators such as cytokines, chemokines and components of the complement.[28,29] This infiltration depends on the interaction of adherent molecules present on the leucocyte and the endothelium, as mentioned previously, and continues until the junction of endothelial cells pass through the basal membrane. [30] Once in the infarcted area, neutrophils release proteolytic enzymes and contribute to the elimination of dead cells and matrix debris. This neutrophil penetration drives the amplification of the immune response. [31]

Monocytes

Cardiac remodeling is separated in two waves with regard to the recruitment of monocytes. [32] First, a recruitment of Ly6C^{high} pro-inflammatory monocytes occurs via IL-1 [33] and anti-inflammatory monocytes Ly6C^{low} are then mobilized during the reparative phase to minimize the inflammatory response. These two populations of monocytes migrate to the heart from the BM and the spleen. [34]

Lymphocytes

Experimental studies in a rat model suggest activation of cytotoxic T lymphocytes after infarction. [29] The CD4+ and CD3+ T cells rapidly colonize the infarcted heart, whereas B cell upregulation peaks in the 6th day. The lymphocyte activation occurs after recognition of autologous antigens in the myocardium through the BCR and TCR receptors. *In vitro* data have shown that lymphocytes can likely exert cytotoxic effects on healthy CM. [35] Likewise, the B lymphocytes can stimulate the recruitment of Ly6C^{high} pro-inflammatory monocytes.

Fibroblasts

The adult myocardium comprises an abundance of fibroblasts. Under physiological conditions, these cells play a role in the maintenance and renewal of the extracellular matrix.[36] After an MI, fibroblasts acquire a pro-inflammatory phenotype in response to DAMP and ROS stimuli and secrete important amounts of pro-inflammatory cytokines .[37] [38] Fibroblast inflammatory activation inhibits the expression of alpha-actin of smooth muscle cells and the myo-fibroblast conversion. The inhibition will be lifted only after removal of dead cells and matrix debris.

Resident mastocyte and macrophages

As many organs, the heart has its own reserve of resident macrophages the origin of which remains uncertain.[27,39] When a MI occurs, resident macrophages die and are replaced by new macrophages derived from pro-inflammatory monocytes. Thereafter, the number of macrophages increases along with cardiac remodeling. After neutrophils, monocytes-macrophage are the most abundant cell population in the infarcted myocardium

The extracellular matrix

All cardiac cells are implicated in the maintenance of the extracellular matrix network.
In addition to its mechanistic role of support, this matrix permits the transfer of molecular signals and actively participates in the regulation of inflammatory responses during the two phases of cardiac repair.[40] Its fragmentation constitutes an essential stimulus for the activation of the inflammatory cascade via the release of collagen and fibrin fragments.[41]

c) Reparative phase and different cells

The transition towards a reparative phase after MI is caused by the microenvironment changes.

Monocytes, macrophages and dendritic cells

The second phase (~ 7 days post-MI) is the tissue repair characterized by the enrollment of anti- inflammatory cells such as $Ly6C^{low}$ monocytes and M2-type macrophages. The enrollment goes with the high expression of anti-inflammatory, pro-fibrotic and angiogenic

factors (IL-10, TGF-β and VEGF) [42] and the rise of DC which play a key role in the resolution phase, healing and angiogenesis. [43,44]

T lymphocytes

The T (CD4 + and CD8+) lymphocytes are essential for the pro-angiogenic macrophage recruitment and collateral arteries formation [45] contributing to the suppression of the inflammatory response. [45] The role of Treg accumulation has also been highlighted with a switch from a pro-inflammatory to a pro-regenerative state. These muscle Treg cells express the growth factor as example the amphiregulin, which acts directly on muscle satellite cells in vitro and improves muscle repair in vivo. [44]

Endothelial and vascular cells

After MI, a pro-angiogenic robust response arises subsequent to the increased expression of the endothelial- vascular growth factor VEGF. This augmentation occurs in the healthy tissue containing the peri-infarcted CM and endothelial cells. [28,46] The vessel maturation involving pericytes and myocytes during the reparative phase results in the reduction of vessel permeability and infiltration of immune cells. [47] Another study has shown that engraftment of pericytes in the infarcted border zone attenuated vascular permeability, reduced leucocyte infiltration and increased angiogenesis thereby attenuating myocardium remodeling. [48]

d) Late cardiac remodeling phase

The murine cardiac remodeling described above is composed of two distinct phases: an acute inflammation and a massive cellular infiltration lasting 0 to 4 days post MI, followed by a resolution of the inflammatory phase aimed at tissue repair and lasting until the 14th day post MI. After both events, a progressive dilation can occur and lead to a chronic heart failure. This evolution can cause a new inflammatory phase. [49]

This third phase is dependent on several conditions among which the infarct size and the initial immune response characterized by the rise in macrophages and T lymphocytes and the expression of adherent molecules on endothelial cells. [50] The late cardiac remodeling may be partly explained by the incomplete or altered inflammatory resolution of the myocardial inflammation and extensive lesions amplified over time. An overview of these different phases is described in Figure 17.

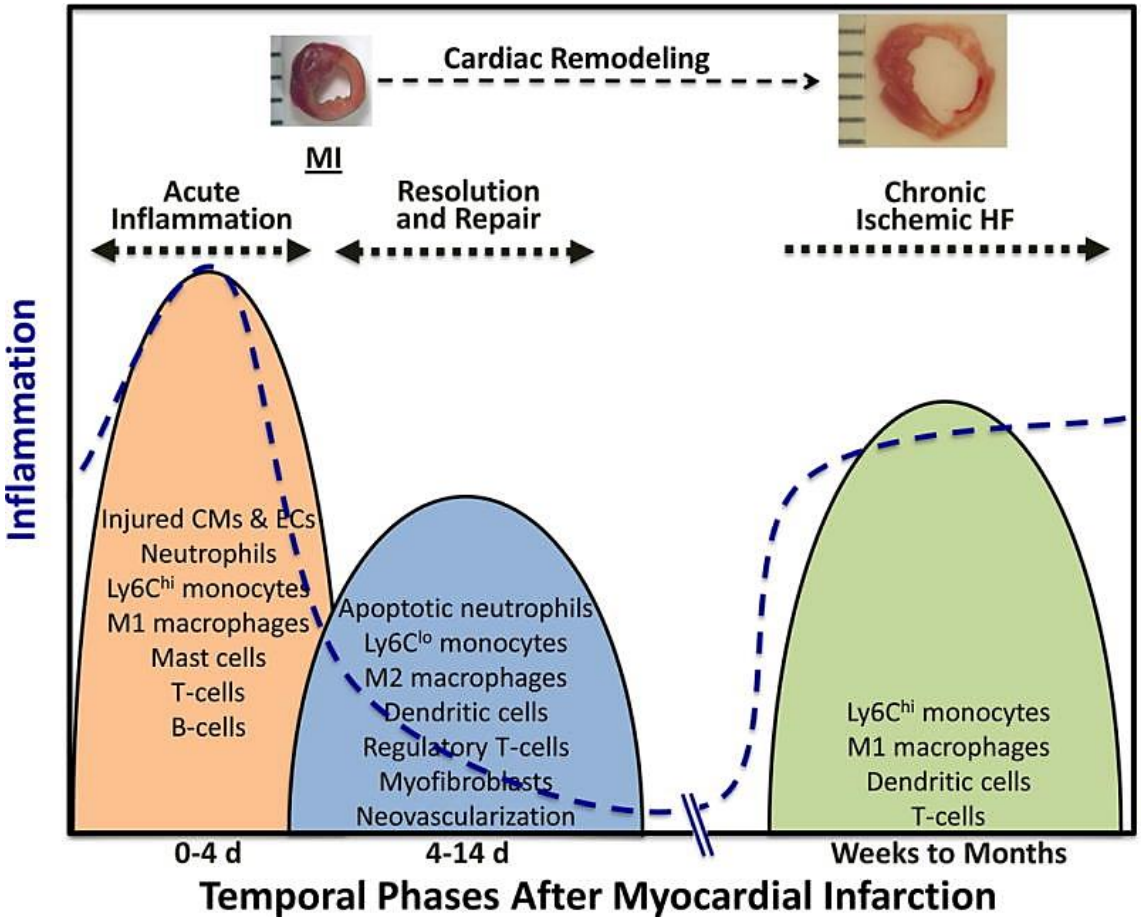

Figure 17: Phases of inflammation after myocardial infarction from; Prabhu and Frangogiannis et al, 2017.

III) Cellular and acellular therapies

The regenerative capacity of organs is an essential feature to maintain tissue homeostasis throughout life. Regeneration has been a major topic of research in the attempt to better understand why some organisms and not others are able to regenerate, and which factors enable them to do so. Vertebrates such as zebrafish are able to regenerate many structures, including the heart muscle.[51,52] When it comes to mammals and in particular to humans, it is known that some organs and tissues are capable of regeneration, such as epidermis or the liver, while others are allegedly not, such as the brain, because the organ is terminally differentiated. The heart is one of these differentiated organs, meaning that the number of cardiac cells is determined at birth.

Over the past two decades when the scientific era of stem cell biology emerged, studies were published that challenged this biological assumption of a post-mitotic heart, and it is now recognized that the heart harbors a pool of stem cells and is to some extent capable of regeneration.[53–56] Such concepts encouraged major advances in cardiac developmental biology but mostly they gave hope for cardiac regenerative medicine. Although cardiac proliferation has been described [57] and there is evidence for heart regeneration early after birth,[58] the regenerative potential of the adult heart is modest and only serves homeostatic purposes but it cannot repair the extensive damage resulting from the loss of contractile myocytes post infarction (approximately 1 billion) that will evolve to scar formation and heart failure. Because cardiomyocyte renewal of the adult heart is very limited, the appropriate therapy would be the one which would successfully replace lost cardiac tissue.

This is why many researchers have been working to find efficient alternatives to current therapies through repopulation of damaged areas either by replacing tissue loss with the delivery of exogenous stem cells to replace dead myocytes or rather by enhancing the endogenous reparative process of the heart.

In this context, cell therapy appears as a promising strategy. Among all the cell types that have been tested, stem cells are the most attractive due to their differentiation potential and scalability.

Stem cells are undifferentiated cells capable of both generating differentiated cells and self-renewing through asymmetric division. They can be:

- Totipotent: they have the potential to give rise to all specialized cell types of the body (i.e. the zygote).

- Pluripotent: they can generate almost all cell types, excluding extra-embryonic tissues such as the placenta. They include embryonic stem cells (ESC) and induced pluripotent stem cells (iPSC).

- Multipotent: adult stem cells able to generate a diverse set of differentiated cell types originating from the same embryonic layer.

- Unipotent: precursor stem cells that can only differentiate to one cell type. (i.e., satellite cells)

Several clinical trials have now tested cell therapy in a variety of diseases including spinal cord injury, [59] age-related macular degeneration, [60] Parkinson's disease,[61] joint damage [62] or diabetes. [63] Regarding heart diseases, a myriad of studies have shown that various stem cell populations (e.g.: skeletal myoblasts, bone marrow mononuclear cells, bone marrow-, umbilical cord- and adipose-derived mesenchymal cells, putative c-kit+ cardiac stem cells, cardiospheres) have the potential to improve cardiac function or to attenuate cardiovascular pathologies.[64]

1) Cellular cardiac regenerative medicine

Cardiac regenerative pre-clinical and clinical studies can be divided in three generations [65] as illustrated in Figure 18.

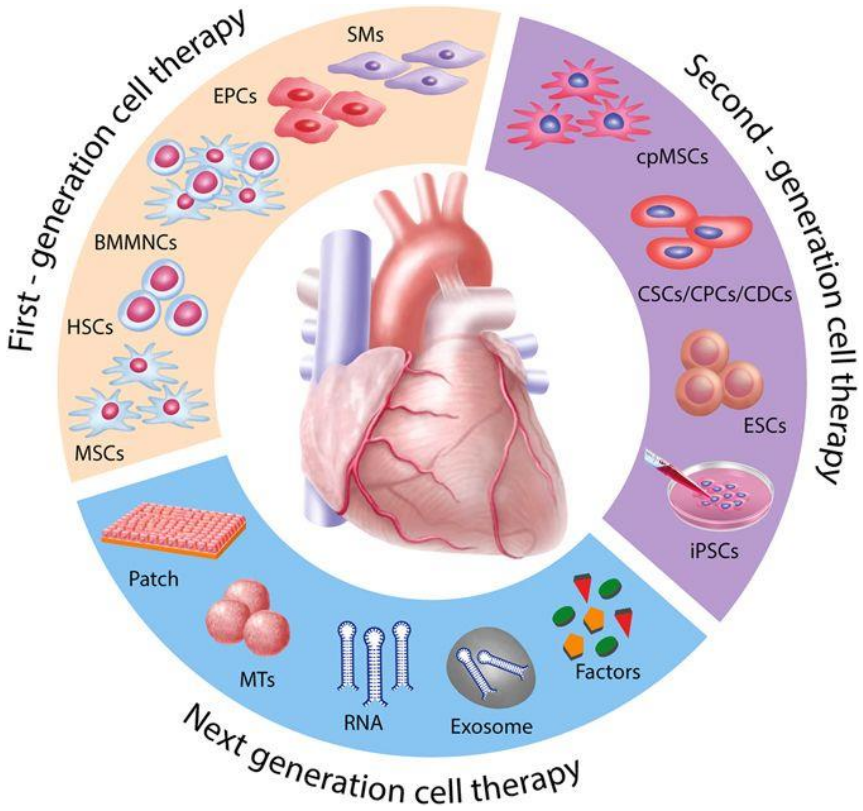

Figure 18: Evolution of cardiac regenerative therapies from Cambria et al, Translational Cardiac Cell, 2017.

The first generation was launched in the 90s aimed at remuscularizing heart tissue with differentiated mature cells. [66] Many cellular sources were used. The first to be tested were skeletal myoblasts, selected because of their muscular phenotype, ability to contract, easy availability (muscular biopsy) and *in vitro* expansion potential. Researchers tried to integrate these cells into the myocardium expecting they would acquire a cardiac phenotype and ameliorate heart contractibility. Pre-clinical studies demonstrated such an improvement [67] and the ability of myoblast to form myotubes but without evidence for an electro-mechanical integration. Encouraging data from a phase I study then led to the multicenter MAGIC phase 2 trial which, however, failed to meet its primary efficacy end point and raised some concerns related to the occurrence of arrythmias.[68] Overall, the lack of evidence for myoblast differentiation into fully functional and electromechanically coupled cardiomyocytes has led to the progressive abandonment of the technique.

Another cell type tested to promote cardiac repair were bone marrow-derived cells (BMC) based on the theoretical plasticity of adult stem cells capable of transdifferentiating into cells types of other lineages. This cell type was particularly attractive because of its accessibility, simplicity of use and a long-standing safety record of hematopoietic stem cell transplantation in hematological diseases. At the beginning of the 2010s, different pre-clinical studies reported successful trans-differentiation and repopulation of the ischemic myocardium by bone marrow-derived mononuclear cells or unfractioned cells.[69,70] These seemingly promising studies led to multiple clinical trials but most of them have failed to show clinically meaningful improvements in patient outcomes and it is now recognized that BMC do not transdifferentiate into new cardiomyocytes and that their beneficial effects, when present (and usually at a limited extent), are probably due to their angiogenic properties. In general, also this cell type is now being discarded due to the lack of a solid body of evidence.

Finally, mesenchymal stem cells (MSC) are adult stromal stem cells capable of differentiating towards both mesoderm and non-mesoderm derived cells [71,72] and which feature attractive angiogeneic, anti-inflammatory and immune-evasive properties. Regardless of the tissue source (bone marrow, adipose tissue, umbilical cord primarily), they have shown benefits in ischemic heart preclinical models. [73,74] Clinical trials like POSEIDON have likewise reported improved patient outcomes including when cells were of allogenic origin (a major practical advantage) which supports the ability of these cells to transiently escape the immune system but these results still need to be further confirmed by larger placebo-controlled trials. [75] In *Desgres et al,* a summarized study for completed or ongoing trials concerning pluripotent stem cells discusses their potential mechanisms of action, and considers how to address the challenges required for them to become a major therapy, using heart repair as a case study.[76]

Overall, preclinical and clinical studies have demonstrated safety and feasibility of cell transplantation while drawing attention to the fact that in contrast to the initial expectations, grafted cells do not seem to generate new cardiac muscle but rather seem to improve heart function “trough non-cardiogenic mechanisms”. [66]

The second generation of cell therapies has then attempted to repair the heart with cells committed to a cardiac lineage with the hope that such a phenotype was more likely to promote regeneration of the injured tissue.

The use and discovery of cardiac stem cells (CSC) or cardiovascular progenitors cells (CPC) expressing stem cells markers like c-kit, Sca-1, MDR-1and ISL1, [77] capable of differentiation

into new cardiomyocytes [78] and endothelial cells were then the main hopes for cardiac repair. These cells could be harvested from the heart itself, expanded in culture and reinjected to repopulate necrotic areas but only two clinical trials (SCIPIO and CADUCEUS) using c-kit+ and cardiospheres derived cells, respectively, have been carried out and their results are non-conclusive. Regardless of the results, a common characteristic of all trials is that even these cells are not able to differentiate into well-characterized adult cardiomyocytes. This has led scientists to look for a way of generating functional cardiomyocytes and the first source for this approach has been represented by embryonic stem cells (ESC). ESC are pluripotent cells derived from the blastocyst's inner mass. They were first isolated in 1998 by Thomson et al. [79] ESC can be guided to cardiac differentiation through the *in vitro* replication of the conditions that normally drive mesodermal and cardiac development in the embryo. There are three main pathways involved to differentiate ESC: the bone morphogenic proteins (BMPs), the WNT pathway proteins and fibroblast growth factors. [80] Various pre-clinical trials have demonstrated the efficacy of ESC leading to the ESCORT clinical trial [81] that tested ESC-derived cardiac progenitors and proved feasibility and safety of the procedure with no tumor formation and patients' symptomatic improvement. Unfortunately, the use of ESC is hindered by various concerns including their possible teratogenicy, risk of rejection, and ethics. To circumvent these concerns, in 2006 Yamanaka's team discovery that mature somatic cells could be reprogrammed to pluripotency by four retrovirally transduced transcription factors (Oct4, Sox2, Klf4, Myc2) thus creating induced Pluripotent Stem Cells (iPSC) .[82] The iPSC behave as ESC and do not need the destruction of the blastocyst to generate new cells but can rather be collected from skin fibroblasts for example. Moreover, the differentiation towards a cardiac lineage from iPSC is possible.

Retrospectively, it is worth mentioning that pluripotent stem cells, embryonic or induced, are the only cells that can be truly defined as stem cells in that they fully embody all parameters of stemness definition. First generation cells as well as the so-called cardiac stem cells did not prove able to transdifferentiate into cardiomyocytes except under rare and exceptional circumstances as well as they did not appear to be able to do so routinely *in vivo*.

2) Acellular therapies or next generation

Interestingly, numerous studies have accumulated over the last years showing that the therapeutic benefits of many stem cell-based therapies cannot be attributed to stem cell

survival and/or differentiation, and are, rather, due to factors released by the transplanted cells that may stimulate endogenous injury repair [83]. This so-called 'paracrine hypothesis' of cell therapy is primarily based on the consistent finding that the functional benefits of cell therapy can be observed at a time where cells have been cleared from the grafted tissue. [84] This hypothesis was first formulated in 2005 after studies on mesenchymal stem cells (MSC) as a potential therapy for acute myocardial infarction and it is based on the fact that cells, MSC in particular, are able to produce and release several soluble factors that exert a cardioprotective effect [85] (Figure 19) .[12] Researchers found that administering to ischemic cardiomyocytes *in vitro* the conditioned culture medium in which mesenchymal cells had been grown, recapitulated the same beneficial effects that had been seen with direct MSC transplantation. Results have been replicated *in vivo*. [86]

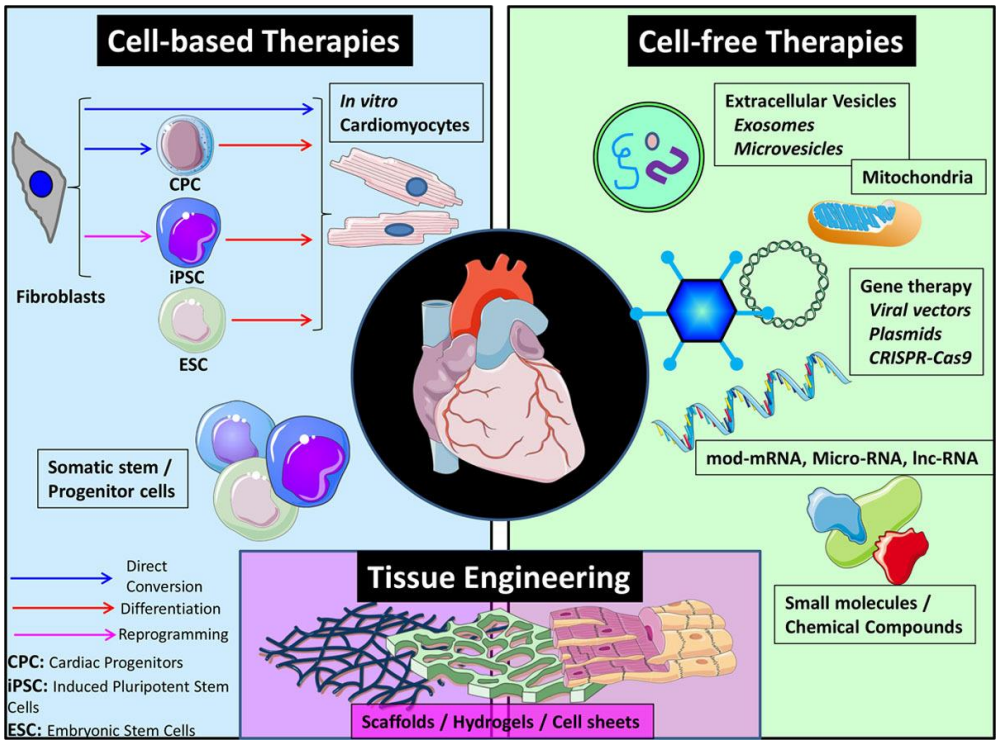

Figure 19: Classification of different type of therapies in cell-based, cell-free or tissue engineering from Shamagian et al Circulation Research 2019.

These paracrine mediators include various proteins, chemokines, cytokines, growth factors, exosomes (Exo) and other extracellular vesicles (EV) themselves packed with other factors, like microRNAs. All these molecules play an important role in myocardial protection, by acting on cardiac metabolism, inflammatory related pathways and possibly also stimulation of endogenous regeneration by activating resident cardiac cells. They also trigger

neovascularization and can mitigate the cardiac remodeling process. The concept of paracrine signaling gave also more importance to the microenvironment in which stem cells thrive. The paracrine hypothesis marked a juncture toward next generation cell-free approaches to deliver only the supposedly beneficial paracrine factors. These therapies, being cell free, have the advantages of being much safer and easier to formulate and to deliver, being much closer to a pharmacological compound than cells.

Among acellular therapies, different factors have been tested. Growth factors like G-CSF or VEGF have been investigated, but showed no improvements compared to controls. [87,88] Also implicated in paracrine signaling are micro-RNAs (miRNAs). Hundreds of micro-RNAs have been studied for their role in cardiovascular development and disease [89] and some have been implicated in cardiac repair with several preclinical studies proving their beneficial potential. [90,91] While paracrine factors keep on being studied and characterized and new ones are yet to be discovered, there is growing evidence and scientific belief that many are contained in EV that would deliver them from one cell to another. Not only EV would be a concentrate of beneficial factors, but they would also constitute a perfect cell-to cell delivery system because their lipid bilayer protects their cargo from degradation. In addition, an advantage of EV is that they do not seem to be immunogenic, at least depending on their mother cells. By virtue of their rich cargo and their limited constraints in terms of production and delivery, EV constitute a very interesting biotherapeutic entity. Various studies have shown how EV recapitulate the effects of their parent cells in pre-clinical models of ischemic heart injury [92–94] and the therapeutic potential of these particles has also been tested with success in many other areas including retinal damage,[95] neurodegenerative diseases [96] and cancer immunotherapy.[97,98]

a) Extracellular vesicles

The EV are small spherical particles delimited by a lipid bilayer containing cytoplasmic components that shuttle from cell to cell to transfer their content and allow inter-cellular communication, Pan and Johnstone were the first to describe EV in 1983. [99] Initially the role of EV role was thought to be cellular waste elimination; then studies have shown their importance for cell to cell communication in physiological and pathological contexts [100–102,102–104]. The EV are present in the prokaryote kingdom as in the eukaryote and in all biological fluids (blood, urine, tears, saliva, maternal milk, bile and seminal liquid) as well in conditioned cellular medium. [105,106]

There are several types of EV and each one has its own structural and biochemical properties depending on their size and biogenesis that affect probably their function. They are classified in three categories: the microvesicle (MV) originating from the plasma membrane sprouting, [107] the Exo derived from multi-vesicular bodies that then fuse with the plasma membrane [108,109] and the apoptotic bodies released by the fragmentation of apoptotic cells. Besides the release mode, EV size is use for their classification. In general, MV are in the range of 100-1000nm and are more recently referred now as large vesicles, while Exo are in the range of 30-150nm and referred as small particles. [110] For many years the nomenclature and size of EV have been subject to controversies. [111,112] Nevertheless, basic requirements are now stablished by the International Society of Extracellular Vesicles (ISEV) which has drafted guidelines to help normalizing their characterization.[113] In that respect identification only by their size is not sufficient as sizes overlap. The biogenesis and EV content are essential criteria for EV characterization.

b) Biogenesis

The biogenesis of Exo, MV and apoptotic bodies is illustrated in the Figure 20 and will be detailed below [114].

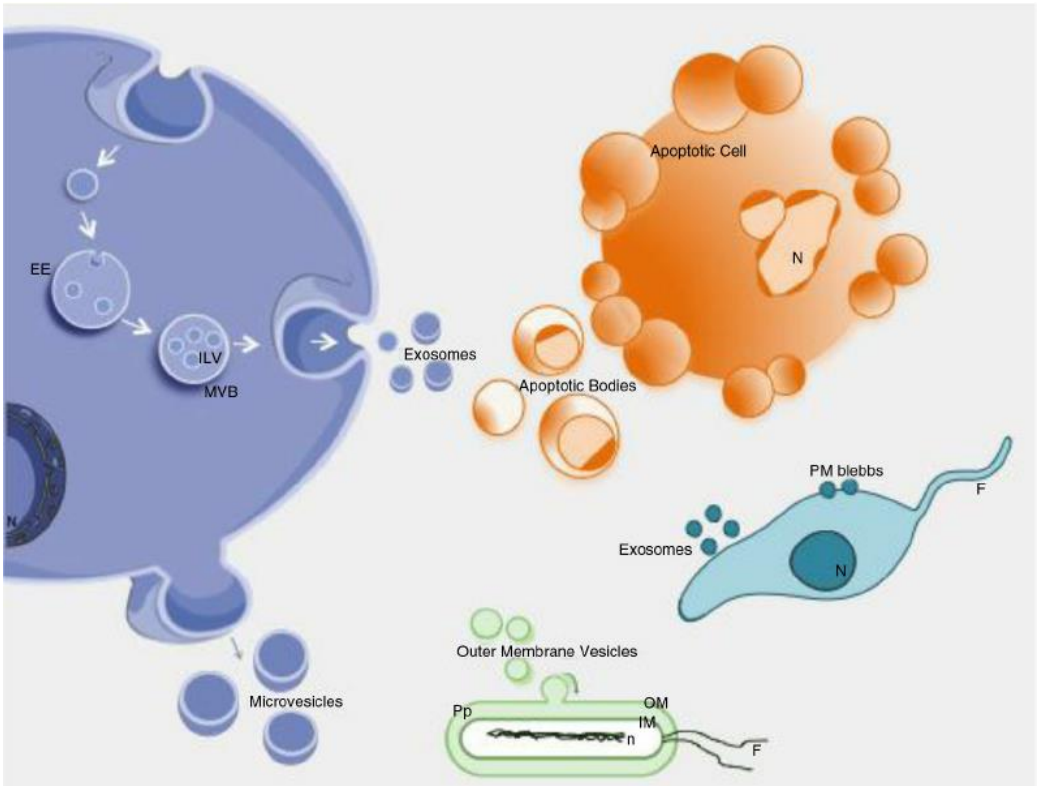

Figure 20: Extracellular Vesicles types and biogenesis from Yáñez-Mó et al; Journal of Extracellular Vesicles 2015.

Exosomes

Derived from the endosomal system and synthetized as intraluminal vesicles (ILV) in the multi-vesicular bodies (MVB). The endosomes sprout from the invagination of the plasma membrane and are divided in distinct compartments: early, late and recyclable endosomes. [115] Throughout the formation of early endosomes, ILV incorporate specifically proteins, lipids, nucleic acids and the cytosol. This content is designated to degradation, recycling or exocytosis. [116] The remaining early endosomes become late endosomes through a series of transformations [117] and accumulate in the ILV by the sprouting of the endosomal membrane. Over the process, cytosolic proteins, nucleic acids and lipids are sorted out in small vesicles. The late endosomes containing these variety of vesicles are known as MVB. If the content is destined to degradation, the MVB merge with the lysosome; if its designated to release, the MVB merge with the plasma membrane releasing the ILV as Exo in the extracellular space.[115] The ILV formation into MVB is the beginning of Exo biogenesis and requires two distinct processes. The endosome membrane is reorganized as being highly enriched in CD9, CD63 and or CD81. [118]

Then, endosomal sorting complexes required for transport (ESCRT) are requisitioned in the formation site of ILV. [119] Four ESCRT complexes exist; ESCRT 0,I,II,III .[120]

The ESCRT0 recognizes ubiquitous proteins in the exterior of endosomal membranes, [121] ESCRT I, II are the initiators of intra-luminal membrane sprouting via the stimulation of endosomal cytosolic recruitment whereas ESCRT III completes this whole process. [122]

The ESCRT machinery complex is associated with proteins such as Alix and TGS101, both requisitioned for the vesicle sprouting to the luminal endosome. Although the ESCRT pathway is considered the main driver of Exo biogenesis, other studies have shown the existence of an independent pathway via the sphingolipid ceramide. Lastly, fusion mechanisms of MVB to the plasma membrane are far from being completely elucidated but GTPases and the Rab protein family have been implicated in the regulation of the endosomal traffic and the secretory pathway leading to Exo release.

Microvesicles

The MV are generated by the sprouting and fission of the plasma membrane via the combinatory redistribution of phospholipids and the actin-myosin contractile machinery. [105] They are described as specifically charged with proteins like ARF6, MHC-I, B1 integrin,

VAMP3 and MT1MMP. [123] The release of MV may also be possible via the TSG101/ESCRT-I complex but this signalization cascade does not modify significantly the MV secretion, confirming the biogenesis distinction between Exo and MV. A study demonstrate that MV release is influenced by the calcium influx; if an increment of calcium occurs, a redistribution of phospholipids results in an intensified MV release. [124,125] Similarly, hypoxia can stimulate MV release via the expression of RAB22A under the dependence of the hypoxic inductor factor (HIF). [126]

Apoptotic Bodies

Apoptosis is a major physiological process necessary to survival, conducting to cell death of normal and abnormal (cancerous, infected) cells. Apoptosis progression is organized in several stages, initiated by the condensation of nuclear chromatin, followed by the membrane sprouting and disintegration of the cellular content to vesicles called apoptotic bodies .[127] Contrary to Exo and MV secreted during normal cellular processes, apoptotic bodies are secreted during programmed cellular death. Apoptotic bodies are in the range size of 500-4000nm. [128,129] During apoptosis, specific modifications take place, the cellular membrane undergoes a translocation of phosphatidylserine to the exterior of the lipid bilayer and binds to Annexin V. [130,131] Other membrane alterations occur via oxidation, creating sites of liaison to thrombospondine [132] or the complement protein C3b. [130]

c) Extracellular vesicle content

Proteins

The EV content is widely described in the literature,[133–135] however depending on the cellular source and isolation method, vesicular proteins vary but some seem to be highly conserved as those associated to biogenesis via ESCRT machinery like ALIX, TSG101; the Annexins; cyto-squeskeletal proteins (actin, tubulin); and EV release-related protein (PAB27A, ARF6). The EV are also enriched in tetraspanins (CD9, CD81, CD63), integrins, heat shock proteins (Hsp family), transmembrane proteins (LAMP1, TfR) and histocompatibility major complexes (MHC I and II). Some proteins are more abundant in Exo than in MV or apoptotic bodies and vice-versa. [118,136] For example, tetraspanins and endosomal protein are more abundant in Exo while for MV the protein composition is closer to that of their parent cell.

Transcriptional factors like Notch and Wnt are also found in EV [137] and have brought to light EV's ability to regulate some important pathways. Finally, some intercellular mediators like TNTα, IL-β or the TGF-β can also be present in EV. [138] An illustration of the most conserved proteins in Exo is represented in Figure 21. [139]

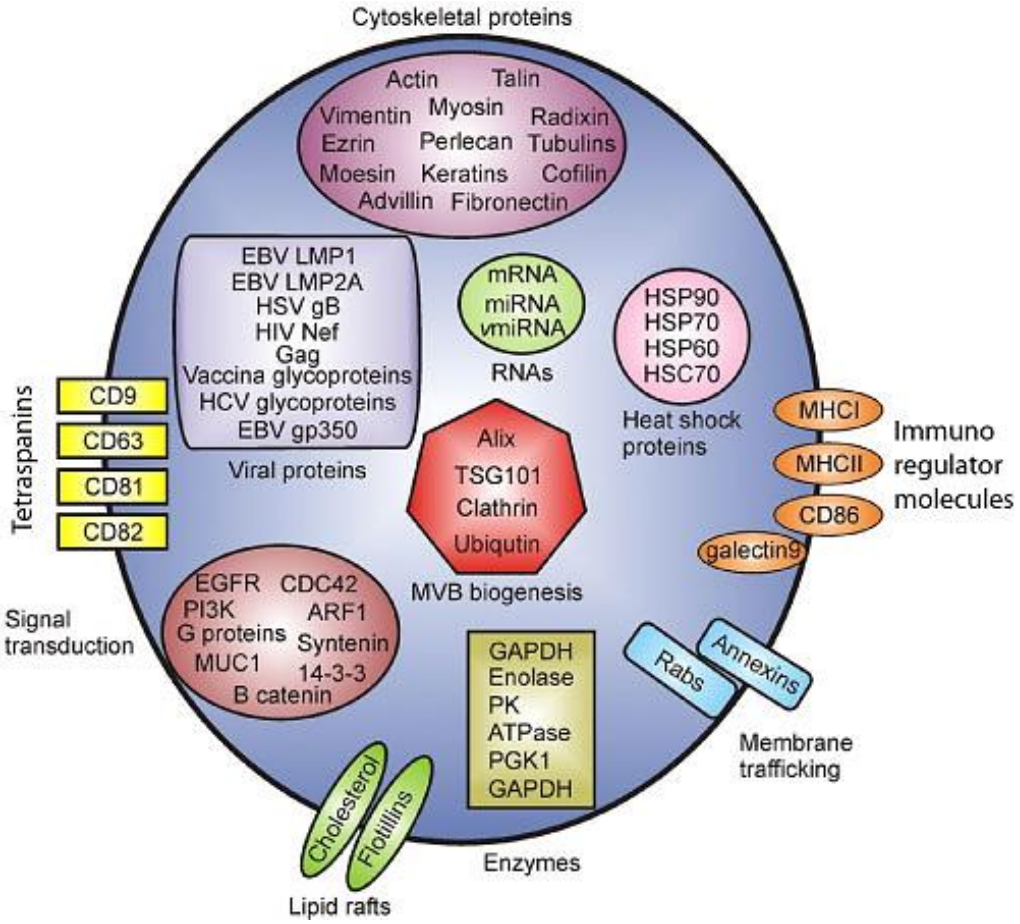

Figure 21: Exosome protein composition from Meckers et al; Journal of Virology 2011.

Lipids

Lipid composition has been studied in several contexts. [137,140,141] In general, common characteristics are shared between the mother cell and the EV type. The most abundant lipids are sphingomyelin, phosphatidylserine, cholesterol, ganglioside GM3, unsaturated lipids and ceramides. [140] For example, Exo are richer in phosphatidylserine, facilitating their internalization into recipient cells, [142,143] while MV are enriched in glycerophosphoserin and phosphatidylserine polyunsaturated. [144,145] As a whole, the lipid composition reflects their biogenesis and parental cell.

Nucleic Acids

The EV nucleic acid composition is variable and includes almost all classes of nucleic acids, such as DNA and coding and non-coding RNAs. Some studies have shown that EV could contain genomic and mitochondrial DNA, [146–148] but EV are mainly enriched in small RNAs: ribosomal RNA, transfer RNA, messenger RNA (mRNA), miRNA and non-coding RNAs. [149–151] Many studies *in vitro* and *in vivo* have reported that the RNA-EV content can be transferred to recipient cells and induce functional effects or epigenetic reprograming. [151–154] These effects are for the main part attributed to miRNA because of their capacity to modulate gene expression. [152,153] These data altogether suggest that EV enrichment is done selectively, and is also dependent of EV biogenesis, the cell source and the physiologic state of the cell. [153,154]

EV interaction with target cells

When EV reach their target cell, they can interact with it in various ways and affect fundamental biological processes. The EV can exert an action on stem cell maintenance, tissue repair and immune surveillance among others. [154] Likewise, EV are also thought to be key mediators in pathological processes. [155] The specificity of EV targeting towards particular recipient cells is probably conferred by the surface ligands present on both. [106] Three main mechanisms of EV to target cell interaction have been described:

1) Direct interaction: A ligand-receptor binding induces a signaling cascade downstream the receptor of the target cell. Proteins allowing this type of interaction are located on the external membrane of the EV and include among others integrins, the above mentioned tetraspanins, heat shock proteins and intercellular adhesion molecules.

2) Endocytosis of the extracellular vesicles. It follows the ligand-receptor binding mentioned above, but instead of directly triggering the activation of intracellular signaling pathways, the vesicle is uptaken by endocytosis to eventually fuse with the endosome.

3) Membrane fusion: Once recognized by receptors, the vesicular membrane fuses with the plasmic membrane so that its membrane proteins will remain embedded in it and the cargo of the vesicle will be released in the cytoplasm.

d) Therapeutic use of EV and cardiac repair

Strategically, the therapeutic use of EV can be classified in two main categories: the first considers EV as a pharmaceutical-biological entity acting though the active molecules that they secrete; the second entails the use of EV as vectors by leveraging their capacity to target the recipient cells via their specific receptors. [154] Leading to an instinctive development of 'artificial' EV known as liposomes and the engineering of active molecules in the membrane to target the recipient cell, and deliver their cargo containing the appropriate messengers to either activated or inactivate specific pathways. [156]

The use of these biological entities has now reached the bedside with many clinical trials already completed or ongoing for several diseases. They are registered on ClinicalTrials.gov. (49 EV studies, 163 for Exo but these figures are constantly evolving).

Given the recognition of the importance of paracrine events, the use of EV is generating a great deal of interest for cardiac repair because of the several potential targets they might hit such as endogenous cardiomyocytes, inflammatory and immune cells, fibroblasts, the extracellular matrix, vessels (including those of the lymphatic system) and nerves (Figure 22). [12]

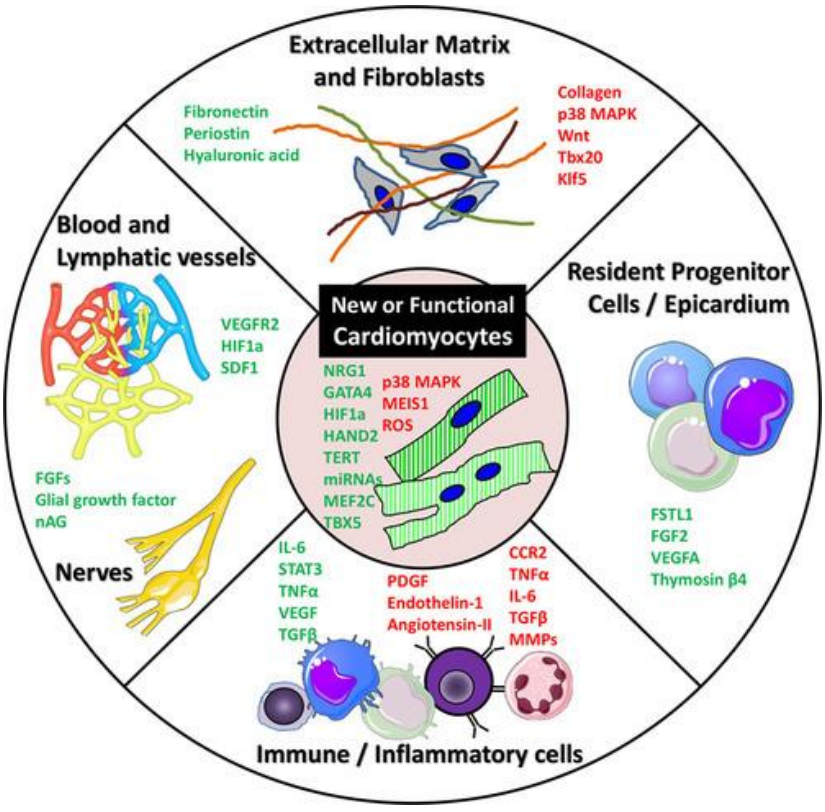

Figure 22: Targets of the cardiac regenerative process from Shamagian et al; Circulation Research 2019

IV) Objective (ensemble of manuscripts)

Previous studies of our team [84,157] have tested, experimentally and clinically (the ESCORT trial) the use of cardiovascular progenitor cells secreted by human ESC. The progressive shift from remuscularization by exogenously transplanted cells to paracrine harnessing of endogenous repair pathways has then led us to focus on the secretome exclusively. For practicality reasons, we have next switched to iPS cells as the pluripotent stem cell source of these progenitors, reasoning that the potential safety issues raised by iPSC if they were directly transplanted in patients were no longer relevant if they were exclusively used as *ex vivo* biofactories.

The general purpose of my thesis has been to provide some additional insights into the mechanism of action of the secretome enriched-EV of iPS- cardiovascular progenitors cells (CPC) with 3 specific objectives:

1) To investigate if iPS-CPC are as efficient as ESC and if their secreted EV are equally functional.

2) To test in an allogenic context, EV derived from iPS-CPC (EV-CPC) for their immunogenicity *in vitro and in vivo* and assess the effects of the induced immune response on cardiac repair;

3) To evaluate EV-CPC capacity to stimulate the production of new cardiomyocytes *in vivo*.

These research axes were deemed necessary to shed more light on the mechanism of action of EV and thus contribute to improve the chances of success of their therapeutic use.

Abstract - Scientific Work

This chapter summarizes the overall scientific work done during my thesis.

The first article explored the hypothesis that EV-CPC from iPS-CPC were as effective as their mother cells and as efficient as ESC. To this purpose, an immunodeficient mouse model of chronic heart failure was generated and the results have actually confirmed the functional equivalence between the cells and their EV which were shown to have in common an increased transcription of cardio-protective genes in heart tissue.

The second article looked at the immunological effects of EV-CPC. At this stage, we turned to iPSC as the source of the CPC (otherwise very similar to those from ESC previously tested) and switched to an immune-competent mouse model in both acute and chronic myocardial ischemia settings. The data showed that these EV-CPC do not trigger an immune response (at least in this xenogenic context) either *in vitro* or in the animal models and at the same time they unraveled the capacity of EV to fine-tune the response of monocyte/macrophages towards a resolution of inflammation that likely bolsters their therapeutic potential.

The third paper was designed to assess whether EV-CPC could trigger cardiomyocyte proliferation and, if so, which was the source of these newly generated cardiomyocytes. To this end, we used two lineage-tracing models and have shown that while EV actually failed to induce cardiogenesis, their cardio-protective effects could still be confirmed and likely accounted for, at least in part, to a modulation of cardiac fibrosis.

Overall, these data are thus consistent with the currently prevailing hypothesis that the regulation of immune-inflammatory responses by transplanted cells or, in our case, their EV-enriched secretome is a major mechanism whereby these biologics improve heart function.

ESC European Society of Cardiology

European Heart Journal (2018) **39**, 1835–1847
doi:10.1093/eurheartj/ehy012

BASIC SCIENCE
Heart failure/cardiomyopathy

Acellular therapeutic approach for heart failure: *in vitro* production of extracellular vesicles from human cardiovascular progenitors

Nadia El Harane[1,2‡], Anaïs Kervadec[1,2‡], Valérie Bellamy[1,2], Laetitia Pidial[1,2], Hany J. Neametalla[3], Marie-Cécile Perier[1,2], Bruna Lima Correa[1,2], Léa Thiébault[1,2], Nicolas Cagnard[4], Angéline Duché[5,6], Camille Brunaud[2], Mathilde Lemitre[1,2], Jeanne Gauthier[1,2,7], Alexandra T. Bourdillon[8], Marc P. Renault[9†], Yeranuhi Hovhannisyan[10], Solenne Paiva[10], Alexandre R. Colas[11], Onnik Agbulut[10], Albert Hagège[1,2,3], Jean-Sébastien Silvestre[1,2], Philippe Menasché[1,2,12*], and Nisa K.E. Renault[1,2*]

[1]Institut National de la Santé et de la Recherche Médicale (INSERM), UMRS-970, Paris Centre de Recherche Cardiovasculaire, 56, rue Leblanc, 75015 Paris, France; [2]Université Paris Descartes, Sorbonne Paris Cité, Paris, France; [3]Department of Cardiology, Assistance Publique-Hôpitaux de Paris, Hôpital Européen Georges Pompidou, 20, rue Leblanc, 75015 Paris, France; [4]Université Paris Descartes, US 024 SFR Necker, 24 Boulevard du Montparnasse, 75015 Paris, France; [5]Institut National de la Santé et de la Recherche Médicale (INSERM), U 1016, Institut Cochin, Université Paris Descartes, Sorbonne Paris Cité, 22 rue Mechain, 75014 Paris, France; [6]CNRS, Université Paris Descartes, UMR-8104, Paris, France; [7]Ecole normale supérieure, PSL Research University Paris, 45 rue d'Ulm, 75005 Paris, France; [8]Department of Engineering, Stanford University, 475 Via Ortega, Stanford, 94305 CA, USA; [9]IRIF, Université Paris Diderot-Paris 7, UMR 8243, Bâtiment Sophie Germain, 8 place Aurélie Nemours, 75013 Paris, France; [10]Sorbonne Universités, UPMC Université de Paris-6, Institut de Biologie Paris-Seine (IBPS), UMR CNRS 8256, Biological Adaptation and Ageing, 4 Place Jussieu, 75005 Paris, France; [11]Sanford Burnham Prebys Medical Discovery Institute, Development, Aging and Regeneration Program, 10901 N Torrey Pines Rd, La Jolla, 92037 CA, USA; and [12]Department of Cardiovascular Surgery, Assistance Publique-Hôpitaux de Paris, Hôpital Européen Georges Pompidou, 20, rue Leblanc, 75015 Paris, France

Received 17 January 2017; revised 3 May 2017; editorial decision 8 January 2018; accepted 9 January 2018; online publish-ahead-of-print 6 February 2018

See page 1848 for the editorial comment on this article (doi: 10.1093/eurheartj/ehy097)

Aims We have shown that extracellular vesicles (EVs) secreted by embryonic stem cell-derived cardiovascular progenitor cells (Pg) recapitulate the therapeutic effects of their parent cells in a mouse model of chronic heart failure (CHF). Our objectives are to investigate whether EV released by more readily available cell sources are therapeutic, whether their effectiveness is influenced by the differentiation state of the secreting cell, and through which mechanisms they act.

Methods and results The total EV secreted by human induced pluripotent stem cell-derived cardiovascular progenitors (iPSC-Pg) and human induced pluripotent stem cell-derived cardiomyocytes (iPSC-CM) were isolated by ultracentrifugation and characterized by Nanoparticle Tracking Analysis, western blot, and cryo-electron microscopy. *In vitro* bioactivity assays were used to evaluate their cellular effects. Cell and EV microRNA (miRNA) content were assessed by miRNA array. Myocardial infarction was induced in 199 nude mice. Three weeks later, mice with left ventricular ejection fraction (LVEF) $\leq 45\%$ received transcutaneous echo-guided injections of iPSC-CM (1.4×10^6, $n = 19$), iPSC-Pg (1.4×10^6, $n = 17$), total EV secreted by 1.4×10^6 iPSC-Pg ($n = 19$), or phosphate-buffered saline (control, $n = 17$) into the peri-infarct myocardium. Seven weeks later, hearts were evaluated by echocardiography, histology, and gene expression profiling, blinded to treatment group. *In vitro*, EV were internalized by target cells, increased cell survival, cell proliferation, and endothelial cell migration in a dose-dependent manner and stimulated tube formation. Extracellular vesicles were rich in miRNAs and most of the 16 highly abundant, evolutionarily conserved

* Corresponding author. Tel: +33 (0)1 56 09 59 09, Fax: +33 (0)1 53 98 79 52, Email: nisa.renault@gmail.com; Tel: +33 (0)1 56 09 59 09, Fax: +33 (0)1 53 98 79 52, Email: philippe.menasche@aphp.fr

† Present address. Computer Sciences Department, University of Wisconsin – Madison, 1210 West Dayton Street, Madison, WI 53706-1685, USA.

‡ The first two authors are co-first authors.

Published on behalf of the European Society of Cardiology. All rights reserved. © The Author(s) 2018. For permissions, please email: journals.permissions@oup.com.

Downloaded from https://academic.oup.com/eurheartj/article-abstract/39/20/1835/4840711 by brunacorrea@hotmail.fr on 13 April 2020

miRNAs are associated with tissue-repair pathways. *In vivo*, EV outperformed cell injections, significantly improving cardiac function through decreased left ventricular volumes (left ventricular end systolic volume: -11%, $P < 0.001$; left ventricular end diastolic volume: -4%, $P = 0.002$), and increased LVEF (+14%, $P < 0.0001$) relative to baseline values. Gene profiling revealed that EV-treated hearts were enriched for tissue reparative pathways.

Conclusion Extracellular vesicles secreted by iPSC-Pg are effective in the treatment of CHF, possibly, in part, through their specific miRNA signature and the associated stimulation of distinct cardioprotective pathways. The processing and regulatory advantages of EV could make them effective substitutes for cell transplantation.

Keywords Heart failure • Extracellular vesicles • miRNA • Regenerative medicine • Acellular therapy

Downloaded from https://academic.oup.com/eurheartj/article-abstract/39/20/1835/4840711 by brunacorrea@hotmail.fr on 13 April 2020

Translational perspectives

Induced pluripotent stem cells (iPSC) are currently used for drug screening and disease modelling and, to a lesser extent, for experimental cell therapy. Here, we show that iPSC-derived cardiovascular progenitors release extracellular vesicles (EVs) that are effective therapeutics for mice in chronic heart failure. *In vitro* analyses suggest that EV may promote cell survival, proliferation of resident cardiac cells, and angiogenesis thereby improving left ventricular function. These effects, combined with the logistic, safety, and regulatory advantages of a cell-free approach, make EV a potentially viable option for the treatment of heart failure and reveal a new role for iPSC as *in vitro* 'biofactories'.

Introduction

Cardiovascular disease remains the leading cause of death in the developed world, with chronic heart failure (CHF) among the top causes of cardiovascular morbidity. While the evidence-based guidelines mandated by the European Society of Cardiology[1] have contributed to the improved management of patients with heart failure, some of them remain refractory to treatment. When exploring alternatives to conventional therapies, cell transplantation remains an attractive option. However, while there is some indication of the potential for efficacy, this approach still fails to demonstrate clinically meaningful improvements in outcomes.[2] Data generated by this research have led to a major shift in our understanding of the mechanism of action of transplanted cells; while the original hypothesis was that implanted cells could directly replace damaged tissue, it has become increasingly apparent that the therapeutic effects of transplanted cells are largely mediated by the release of factors which stimulate endogenous regeneration or repair pathways.[3,4] There is mounting evidence that most of these paracrine factors are found in extracellular vesicles (EVs), which are membrane-bound vesicles containing proteins, bioactive lipids, messenger RNA (mRNA), microRNA (miRNA) and other macromolecules.[5]

Given their ability to target specific cell types, possibly through the presence of distinctive surface markers, and deliver bio-active macromolecules, EV have now been successfully tested in preclinical models of stroke,[6] acute kidney injury,[7] myocardial infarction,[8–11] myocardial infarction/reperfusion injury,[12,13] and hind limb ischaemia,[14] among others. Clinical trials in this field are in their infancy, but antitumour therapies based on EV derived from dendritic cells have already entered phase II human clinical trials.[15]

We have previously demonstrated that the EV secreted by human embryonic stem cell (hESC)-derived cardiovascular progenitor cells could replicate the therapeutic effects of their parent cells in a mouse model of CHF.[8] While these results open new clinical perspectives for cell-free therapies for CHF, there are ethical, logistic, and practical concerns that may limit the implementation of therapies dependent on hESC sources. In this study, we have thus considered an alternative source of pluripotent stem cells, namely human induced pluripotent stem cells and used both *in vitro* and *in vivo* approaches to investigate whether the EV released by human induced pluripotent stem cell-derived cardiovascular progenitors (iPSC-Pg) and human induced pluripotent stem cell-derived cardiomyocytes (iPSC-CM) are therapeutic, whether their effectiveness is influenced by the differentiation state of the secreting cell, and through which mechanisms they may act.

Methods

Detailed materials and methods are given in the Supplementary material online.

Extracellular vesicle preparation

Human iPSC-Pg and iPSC-CM were purchased from Cellular Dynamics International (Madison, WI, USA). Conditioned media were collected and ultracentrifuged for 16 h at 100 000 g to pellet all EV. At the end of the culture period, cells were harvested and characterized by quantitative PCR (qPCR) and immunofluorescence to confirm their differentiation state. Extracellular vesicles were characterized by Nanoparticle Tracking Analysis (NTA3.2, Malvern, Malvern, UK) and cryo-transmission electron microscopy (cryo-TEM), and the presence of exosomes was confirmed by western blot. The miRNA contents of iPSC-Pg and their EV were examined by Affymetrix miRNA Array (ArrayExpress accession number E-MTAB-5165).

In vitro bioactivity assays

To determine the pro-survival effects of iPSC-Pg-EV, serum deprived H9c2 cardiac myoblasts were incubated with iPSC-Pg-EV and the number

of viable cells at the end of 27 h was determined. The potential for these EV to be internalized by target cells was examined by observing the fluorescence of H9c2 cells after 20 h of incubation with calcein-AM-labelled iPSC-Pg-EV by imaging flow cytometry, confocal microscopy and by fluorescence video microscopy (spinning disk). The pro-angiogenic potential of iPSC-Pg-EV was determined using human umbilical vein endothelial cell (HUVEC) wound healing and Matrigel tube formation assays. Human embryonic stem cell derived-cardiomyocytes (hESC-CM) were used to study the pro-proliferative effect of iPSC-Pg-EV.

Animal experiments

Myocardial infarction was induced in 199 nude mice by permanent left anterior coronary artery occlusion. Three weeks later, mice were assessed echocardiographically and assigned to receive transcutaneous echo-guided peri-infarct injections of phosphate-buffered saline (PBS), iPSC-CM cells, iPSC-Pg cells, or iPSC-Pg-EV. Functional improvement was assessed again by echocardiography (blinded to treatment groups) 7 weeks after treatment. After sacrifice, approximately half of the animals were evaluated for infarct size, percent fibrosis, and vascular density by histology on cryo-sections. The remaining hearts were evaluated for differentially expressed genes when compared with PBS controls by Affymetrix mouse mRNA array (ArrayExpress accession E-MTAB-5164).

Statistical analyses

Data are summarized using mean (standard deviation) or median (q1–q3) for continuous variables when appropriate and *n* (%) for categorical variables. Comparisons of LV function variables across groups were performed using analysis of variance; multiple comparisons were done using pairwise comparison with Tukey correction for *post hoc* tests. For multiple comparisons with a control group, Dunnett correction was used. Across groups, the change of LV function variables between baseline and 7 weeks post-treatment were compared using a Student test. The reliability of measurements of heart function by the same echocardiographer was assessed using the intra class correlation coefficient (ICC). Comparisons of histological parameters between groups were performed using a mixed model analysis of variance-covariance taking into account the intraheart correlation. For all analyses, a two-tailed *P*-value <0.05 was considered statistically significant. Analyses were conducted using SAS 9.4 (Statistical Analysis System, Cary, NC, USA).

Results

Characterization of induced pluripotent stem cell-derived cardiovascular progenitors and cardiomyocytes

Thawed human iPSC-Pg were cultured for 4 days in serum-free media supplemented with bFGF. At this time point, their cardiovascular progenitor identity was confirmed by both qPCR and immunostaining which showed the reduced expression of the pluripotency markers NANOG, SOX2, OCT3/4, the expression of the early cardiovascular lineage markers ISL-1, MEF2C, NKX2.5 and GATA4, and the absence of mature cardiomyocyte markers such as TBX20, TNNT2, PLN, MYH6, MYH7, MYL2 (see Supplementary material online, *Figures S1* and *S2*, *Tables S1* and *S2*). Thawed human iPSC-CM were plated and cultured 7 days, at the end of which time they expressed markers of mature cardiomyocytes (see Supplementary material online, *Figures S1* and *S3*).

Extracellular vesicle isolation and characterization

Extracellular vesicle were isolated from iPSC-Pg conditioned media on Day 2 (for *in vitro* experiments only) and on Day 4 (for *in vitro* and *in vivo* experiments) of culture. Both time points yielded consistently large quantities of iPSC-Pg-EV (*Figure 1A*). This was in contrast to iPSC-CM, which produced no detectable EV in any of the six culture conditions tested, including three different media types under normoxic and hypoxic (3% O_2) conditions (see Supplementary material online, *Figure S4*). Nanoparticle tracking analysis of iPSC-Pg-EV preparations detected a poly-disperse population of particles ranging primarily from approximately 50–550 nm, with a small population at around 1000 nm. The majority of particles in our preparations (approximately 68% of detected particles) were in the size range of exosomes (approximately 50–150 nm). These results were consistent with cryo-TEM, which identified primarily particles of the size of exosomes, many microparticles and a few apoptotic bodies (*Figure 1B–D*). This mixed population of particles was expected since our isolation protocol (ultracentrifugation at 100 000 g for 16 hours) pellets total EV, and does not distinguish between EV sub-types. The presence of exosomes was confirmed by western blot, which identified both CD81 and CD63 exosomal markers in our iPSC-Pg-EV Day 4 preparations (two independent EV preparations, Supplementary material online, *Figure S5*).

In vitro bio-activity of extracellular vesicles

Induced pluripotent stem cell-derived cardiovascular progenitor-extracellular vesicles promote survival of stressed cardiac cells

Serum deprivation of H9c2 rat cardiac myoblasts for 27 h led to a dramatic decrease in the number of viable cells. Conversely, iPSC-Pg-EV increased viability in a seemingly dose-dependent fashion (*Figure 2*). This effect was highly reproducible for numerous independent iPSC-Pg-EV preparations. While the virgin media contains no detectable particles of the size of EV, other components, such as growth factors or proteins, in the media could have accounted for some of the effect of the EV preparations. To control for this possibility, virgin complete media, was incubated 48 h in coated culture flasks in the CO_2 incubator (without cells) and ultracentrifuged; the bottom of the tube was then thoroughly rinsed with PBS in a volume equivalent to the one used in our iPSC-Pg-EV preparations and tested in an H9c2 survival assay. This preparation had no positive effect on cell survival (see Supplementary material online, *Figure S6*).

Induced pluripotent stem cell-derived cardiovascular progenitor–extracellular vesicles induce angiogenic responses

Scratch wound assay: The percent wound invasion was determined at numerous time points, with the 18-h time point showing clear and consistent differences between positive and negative controls (97% and 10% healing, respectively). Human umbilical vein

Downloaded from https://academic.oup.com/eurheartj/article-abstract/39/20/1835/4840711 by brunacorrea@hotmail.fr on 13 April 2020

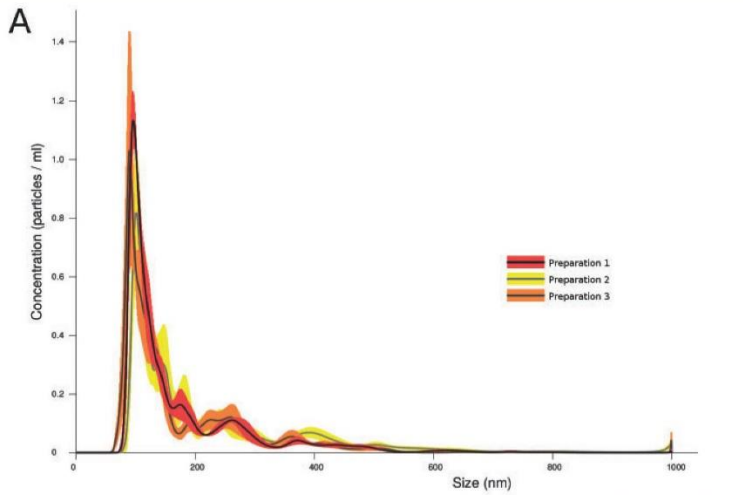

Preparation	Total concentration	Yield (particles/cell)	Mode size (nm)	% particles 50-150 nm	% particles 151-500 nm	% particles 501-1000 nm
1	6.2 X 10^8 p/µL	16 702	97.2	63.4%	34.1%	2.2%
2	5,9 X 10^8 p/µL	18 961	101	48.7%	44,0%	6.3%
3	6.0 X 10^8 p/µL	16 378	97.4	64.2%	33.8%	1.6%

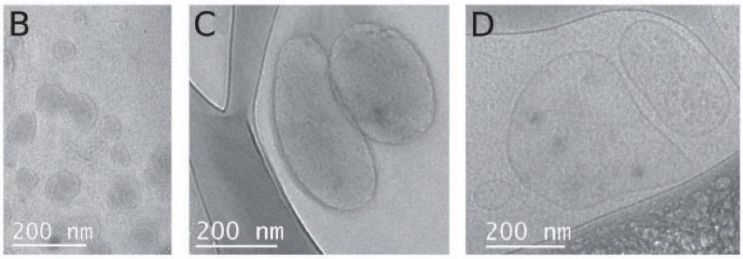

Figure 1 Characterization of induced pluripotent stem cell-derived cardiovascular progenitor–extracellular vesicle preparations. (*A*) Similar overall concentrations and yields of particles per cell were found in three separate preparations of induced pluripotent stem cell-derived cardiovascular progenitor–extracellular vesicles by Nanoparticle Tracking Analysis. Cryo-transmission electron microscopy of these extracellular vesicles identified membrane-bound vesicles of the size of (*B*) exosomes, (*C*) microparticles, and (*D*) large vesicular bodies that may be apoptotic bodies.

endothelial cell invasion was increased by iPSC-Pg-EV incubation, even at the lowest concentration tested, with a seemingly dose-dependent effect (*Figure 3*). *Tube formation assay:* Tube formation, as measured by total segment length and number of nodes after 24 h, was also increased by iPSC-Pg-EV, though in contrast to the scratch wound assay, this effect was without a clear dose-dependent response (see Supplementary material online, *Figure S7*, *Results*).

Induced pluripotent stem cell-derived cardiovascular progenitor–extracellular vesicles increase cardiomyocyte proliferation

The number of proliferating cells was determined by EdU incorporation. After 3 days of iPSC-Pg-EV incubation, the percentage of proliferating hESC-CM cells increased in a dose-dependent manner from 15% (basal rate) up to 35% (*Figure 4*, Supplementary material online, *Results*).

Induced pluripotent stem cell-derived cardiovascular progenitor–extracellular vesicles are internalized by cardiac cells

In order to determine whether EV were taken up by H9c2 target cells, EV were first labelled with calcein-AM green fluorescent dye. Extracellular vesicle labelling was confirmed by ImageStream (see Supplementary material online, *Figure S8*A-B). Labelled EV were incubated with serum-deprived H9c2 cells which, after 20 h of incubation, were themselves analysed by ImageStream. H9c2 cells incubated with

Downloaded from https://academic.oup.com/eurheartj/article-abstract/39/20/1835/4840711 by brunacorrea@hotmail.fr on 13 April 2020

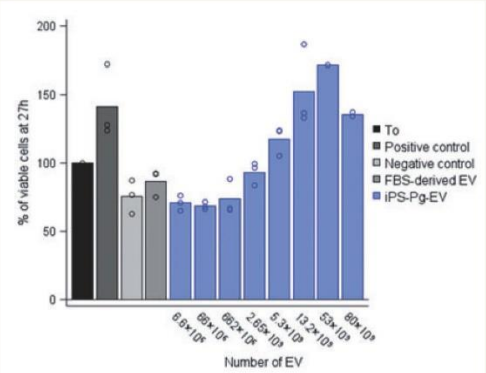

Figure 2 Induced pluripotent stem cell-derived cardiovascular progenitor–extracellular vesicles improve cardiac cell survival of immortalized H9c2 rat cardiac myoblasts. At T_0, media was refreshed with complete media (positive control, dark grey bar), stressful serum free media (Dulbecco's Modified Eagle Medium glutamax, +1% penicillin/streptomycin/Amphotericin B) (negative control, bright grey bar), or serum free media plus 5.3×10^9 foetal bovine serum-derived extracellular vesicles (medium grey bar) or induced pluripotent stem cell-derived cardiovascular progenitor–extracellular vesicles at Day 4 of culture at increasing concentrations (blue bars). At $T = 27$ h, the number of viable cells from each condition was determined and normalized to the number of cells at the start of the stress ($T_0 = 100\%$). Results are the average of 1–3 independent experiments, each in duplicate. Extracellular vesicle concentrations were determined by Nanoparticle Tracking Analysis at high camera sensitivity (camera level 15).

labelled EV were more fluorescent than any of the negative controls [see Supplementary material online, *Figure S8*E and F 1-complete medium; 2-poor medium; 3-poor medium + unlabelled foetal bovine serum (FBS)-EV; 5-poor medium + unlabelled-iPSC-Pg-EV; 6-poor medium + wash], with fluorescence not reaching the level of intensity as high as cells directly labelled with calcein dye (see Supplementary material online, *Figure S8*E and F: 7-cells incubated in poor medium with unlabelled-FBS-EV and directly labelled with 1 μM calcein AM from T_{19h}-T_{20h}; 8-cells incubated in poor medium with unlabelled-FBS-EV and directly labelled with 1 μM calcein AM from T_0-T_{20h}). These data suggest that labelled iPSC-Pg-EV were internalized by or closely associated with H9c2 cells. In order to distinguish between these two possibilities, cells were imaged by confocal microscopy. Punctate green signals were detected in cells incubated with labelled iPSC-Pg-EV (see Supplementary material online, *Figure S8*G). Z-stack analysis confirmed that the green fluorescence was indeed within the cell body and not on the surface of the cells. Green fluorescence was not detected in the negative controls (see Supplementary material online, *Figure S8*H: H9c2 and non-labelled iPSC-Pg-EV; Supplementary material online, *Figure S8*I: H9c2 and wash to control for possible contaminating free calcein-AM). The internalisation of calcein-labeled iPS-Pg-EV by H9c2 cells was also captured by fluorescence video microscopy (see Supplementary material online, *Video S1*).

Induced pluripotent stem cell-derived cardiovascular progenitor–extracellular vesicles contain microRNAs associated with a cardioprotective potential

Bioanalyser analyses of small RNAs showed that iPSC-Pg-EV were enriched in miRNAs when compared with their parent cells, with an average of 53% of small RNAs of the size of miRNAs in EV and 17% in iPSC-Pg cells (average of three independent iPSC-Pg cultures and their corresponding EV preparations). Furthermore, Affymetrix array showed that at the highest detection thresholds, the number of miRNAs in EV exceeded that in their parent cells, thereby suggesting that certain miRNAs are specifically targeted to EV, which are not simply a random sampling of cytosolic content (see Supplementary material online, *Figure S9*, *Results*).

In order to identify miRNAs potentially relevant to the therapeutic effects of the iPSC-Pg-EV, we first considered only the most highly abundant miRNAs (log intensity threshold 9). Next, since the human derived iPSC-Pg-EV had an effect on rat and human cells *in vitro* and on mouse hearts *in vivo*, we selected only miRNAs broadly conserved across species as annotated in Target Scan (v 7.1, released June 2016). Sixteen miRNAs were then identified that met these criteria (*Table 1*, Supplementary material online, *Results*), of which 11 have previously been reported to be stably present in the heart or cardiovascular cells and have predicted biological functions expected to benefit the failing heart (cell differentiation, proliferation, survival, development, and angiogenesis).

Functional assessment in the chronic heart failure model

At the final 7-week time point, the study group included 72 mice: PBS (vehicle control, $n = 17$); iPSC-CM cells (1.4×10^6 cells per mouse, $n = 19$); iPSC-Pg cells (1.4×10^6 cells per mouse, $n = 17$); and the iPSC-Pg-EV secreted by the same batch of iPSC-Pg cells over 48 h (Day 2–4 of culture; $n = 19$) (see Supplementary material online, *Results*). ANOVA showed no baseline differences between groups for left ventricular end systolic volume (LVESV) (PBS: 48.94 ± 6.61 μL; iPSC-CM cells: 47.92 ± 7.30 μL; iPSC-Pg cells: 50.87 ± 8.16; iPSC-Pg-EV: 50.71 ± 7.07 μL), left ventricular end diastolic volume (LVEDV) (PBS: 78.84 ± 6.62 μL; iPSC-CM cells: 76.31 ± 8.20 μL; iPSC-Pg cells: 79.28 ± 8.52 μL; iPSC-Pg-EV: 79.55 ± 7.57 μL), or ejection fraction (EF) (PBS: 38.08 ± 4.09%; iPSC-CM cells: 37.36 ± 5.23%; iPSC-Pg cells: 36.06 ± 4.70%; iPSC-Pg-EV: 36.43 ± 4.13%).

After 7 weeks, the best preservation of LV function was found in the EV-injected hearts with LVESV significantly decreased (by 11%) compared with baseline values (change: -5.75 μL, $P < 0.0001$) (*Figure 5A–C*) along with a decrease of 4% in LVEDV (-3.25 μL vs. baseline, $P = 0.001$). Because of these parallel reductions in LV volumes, EV treatment resulted in the highest post-treatment EF with an increase of 14% over baseline (+4.85%, $P < 0.0001$), with no difference between animals treated with fresh or frozen EV ($P = 0.34$). A randomly selected subset of echocardiographic data were re-assessed, blinded to previous results, to confirm these results and a high ICC was found for all functional parameters (ICC range: 0.97–0.99).

Downloaded from https://academic.oup.com/eurheartj/article-abstract/39/20/1835/4840711 by brunacorrea@hotmail.fr on 13 April 2020

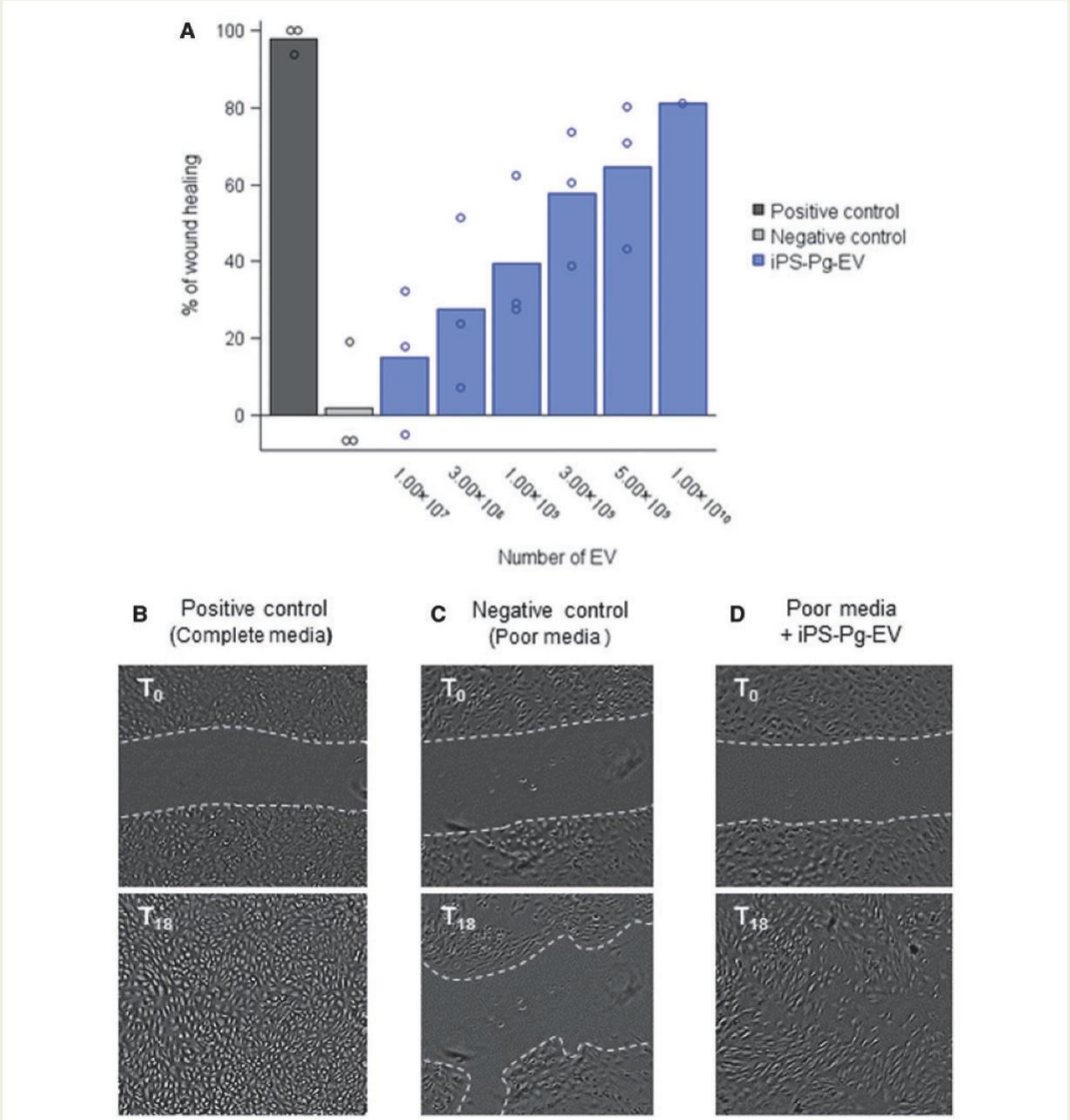

Figure 3 Induced pluripotent stem cell-derived cardiovascular progenitor–extracellular vesicles exhibit pro-angiogenic effects in a scratch wound assay. The potential for induced pluripotent stem cell-derived cardiovascular progenitor–extracellular vesicles to affect human umbilical vein endothelial cell migration was evaluated by the scratch wound assay. A scratch was induced in a human umbilical vein endothelial cell monolayer. (*A*) The percent wound invasion was determined at numerous time points, with the 18-h time point showing clear and consistent differences between (*B*) positive control (complete media = endothelial cell growth medium plus endothelial cell growth medium supplement pack; dark grey bar), and (*C*) negative control (poor media = endothelial cell growth medium; bright grey bar) with 97% and 10% healing, respectively. (*D*) Human umbilical vein endothelial cell invasion was increased by extracellular vesicle incubation (poor media + extracellular vesicles), even at the lowest concentration tested, with a seemingly dose-dependent increase in cell migration, reaching 80% invasion with 1×10^{10} extracellular vesicles per 15 000 human umbilical vein endothelial cells.

Downloaded from https://academic.oup.com/eurheartj/article-abstract/39/20/1835/4840711 by brunacorrea@hotmail.fr on 13 April 2020

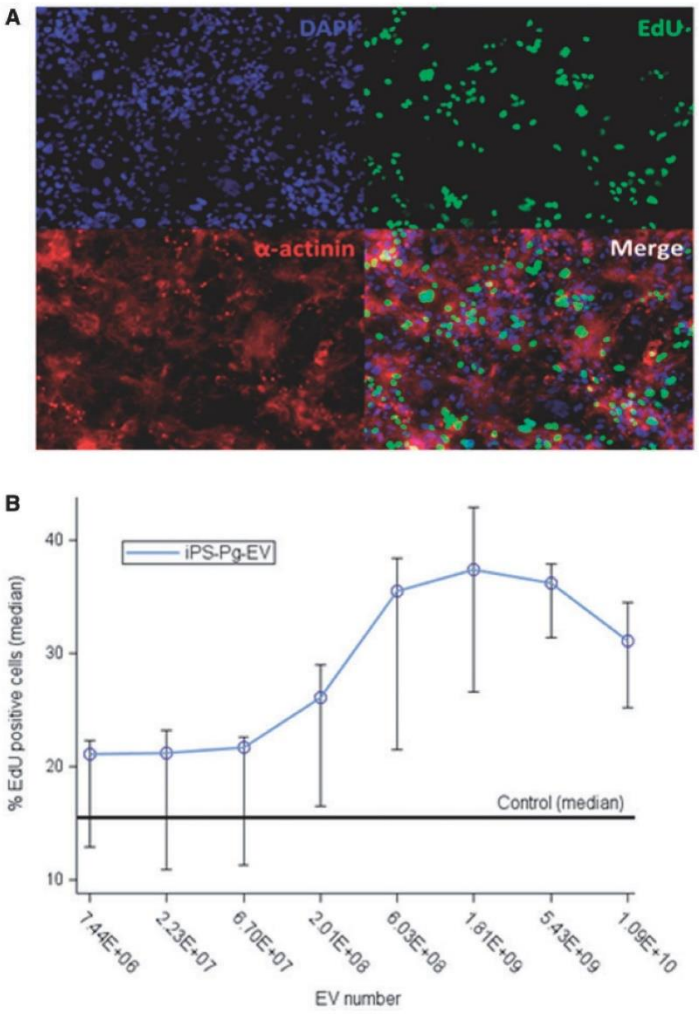

Figure 4 Induced pluripotent stem cell-derived cardiovascular progenitor–extracellular vesicles stimulate human embryonic stem cell derived-cardiomyocyte proliferation. EdU incorporation was used to assess the potential for extracellular vesicles to stimulate cardiomyocyte proliferation. After 48 h of extracellular vesicle incubation, human embryonic stem cell derived-cardiomyocytes were incubated with EdU for an additional 24 h. (*A*) An α-actinin staining confirmed the cell phenotype. (*B*) The basal rate of proliferative cells was 15% which increased in a seemingly dose-dependent manner up to 35% of cells at 1.81×10^9 extracellular vesicles per 10 000 human embryonic stem cell derived-cardiomyocyte.

Of note, significantly more mice in the EV group responded positively to treatment (LVESV improvements greater than 5%) compared with the other groups ($P = 0.04$, χ^2 test) (*Figure 5D*). Furthermore, while individual functional improvements were well clustered in the EV group, they were more variable in the iPSC-Pg group. Likewise, analysis of variance found that the iPSC-CM group also had significantly greater variances in the distributions of LVESV changes than the EV group ($P = 0.02$).

Gross macroscopic and histological analyses of heart tissue

No significant differences were detected between groups for any of the histological or gross macroscopic analyses of heart tissue. This is illustrated in Supplementary material online, *Figure S10*, where the box plots indicate that there are no differences in the distribution of the parameters between groups.

Downloaded from https://academic.oup.com/eurheartj/article-abstract/39/20/1835/4840711 by brunacorrea@hotmail.fr on 13 April 2020

Table 1 Top 16 conserved miRNA and their respective families

miRNA	Intensities (log)				Family
	S1	S2	S3	Avg	
hsa-miR-6088	12.4	12.6	13.0	12.7	miR-143-3p
hsa-miR-92a-3p	11.8	12.1	12.0	12.0	miR-25-3p/32-5p/92-3p/363-3p/367-3p
hsa-miR-17-5p	10.6	11.7	11.4	11.3	miR-17-5p/20-5p/93-5p/106-5p/519-3p
hsa-miR-106a-5p	10.6	11.6	11.3	11.2	
hsa-miR-20a-5p	9.7	11.3	10.8	10.7	
hsa-miR-93-5p	9.8	10.8	10.0	10.3	
hsa-miR-20b-5p	8.7	10.0	9.7	9.6	
hsa-miR-302d-3p	9.6	10.4	10.7	10.3	miR-302-3p/372-3p/373-3p/520-3p
hsa-miR-103a-3p	10.1	10.1	10.5	10.3	miR-103-3p/107
hsa-miR-107	8.7	9.5	10.0	9.5	
hsa-miR-24-3p	9.8	10.8	9.6	10.2	miR-24-3p
hsa-miR-191-5p	9.0	10.0	10.2	9.8	miR-191-5p
hsa-miR-26a-5p	6.4	9.7	10.6	9.7	miR-26-5p
hsa-miR-23a-3p	8.2	10.4	9.8	9.7	miR-23-3p
hsa-miR-16-5p	7.8	9.9	9.4	9.2	miR-15-5p/16-5p/195-5p/424-5p/497-5p
hsa-miR-130b-3p	8.8	9.8	8.4	9.1	miR-130-3p/301-3p/454-3p

Avg, log of the average of the intensities; S1, EV sample 1; S2, EV sample 2; S3, EV sample 3.

Transcriptomic analysis of heart tissue

Differential gene expression analysis comparing each treatment group to the PBS vehicle controls revealed distinct gene expression profiles following each treatment (*Figure 6*).

The differentially expressed genes were then analysed by Ingenuity Pathway Analysis (IPA, Qiagen, https://www.qiagenbioinformatics.com/). The three treatments were found to be associated with distinct gene expression patterns with the iPSC-Pg-EV group being more enriched for pathways thought to be beneficial to hearts in chronic failure, such as increased growth, proliferation, survival, metabolism, angiogenesis, vasculogenesis, and decreased organismal morbidity and mortality (*Figure 7*, Supplementary material online, *Figure S11*, *Results*).

Discussion

Rationale

In parallel to conducting our current clinical trial testing the epicardial delivery of SSEA-1$^+$ ISL-1$^+$ cardiovascular progenitors embedded into a fibrin gel,[16] we investigated the mode of action of these cells and have data supporting a paracrine signalling mechanism; in a mouse model of CHF, the functional benefits of these cardiovascular progenitors could be duplicated by the sole administration of the EV that they had released under stress conditions.[8] This study builds on these previous data by further assessing the effects of EV released by cardiac progenitors, but with an important switch in the cell source from ESC to iPSC for clinically relevant practical reasons: unlimited availability of iPSC, better suitability for industrial, robust, reproducible and scalable cell culture, limited ethical issues and, importantly, reduced safety issues as long as the cells are now intended to be exclusively used for producing the EV and not for being transplanted to patients. The switch to these cells, with the necessary evaluation of the therapeutic potential of their EV was, in our view, a crucial step, necessary for the development of a therapeutic with the potential for widespread clinical use.

Functional data

The main result of this study is that EV released by iPSC-Pg yielded the best functional outcomes 7 weeks after treatment. These data support the protective effects of EV previously documented in reperfused[12,13] and non-reperfused[8–11] myocardial infarctions. In our experiments, the EV-related preservation of LV function was best illustrated by the significant decrease in LVESV from baseline values, which is clinically relevant in view of the correlation between changes in LVESV and patient outcomes.[17] Extracellular vesicle treatment was also the only one to cause a highly significant decline in LVEDV, thereby reflecting an attenuation of adverse LV remodelling. Of note, the benefits of EV were similar in the fresh and cryo-frozen subsets, consistent with the idea that exosomes are stable across a wide range of temperatures,[5,9,18] which reinforces their attractiveness as an off-the-shelf product readily available for clinical use.

An unexpected finding of our study was that the EV globally outperformed their iPSC-Pg parent cells, largely because the latter was associated with a greater scattering of cardiac functional changes. Possible explanations for this heterogeneous pattern include different rates of cell death during injections, different rates of post-injection retention depending on the locally present inflammatory cues, or large variation in the number of cells delivered to each mouse due to clumping or settling out of cells within the syringe during the injection process (contrasting with a highly homogeneous EV suspension which does not settle out at all during the injection

Downloaded from https://academic.oup.com/eurheartj/article-abstract/39/20/1835/4840711 by brunacorrea@hotmail.fr on 13 April 2020

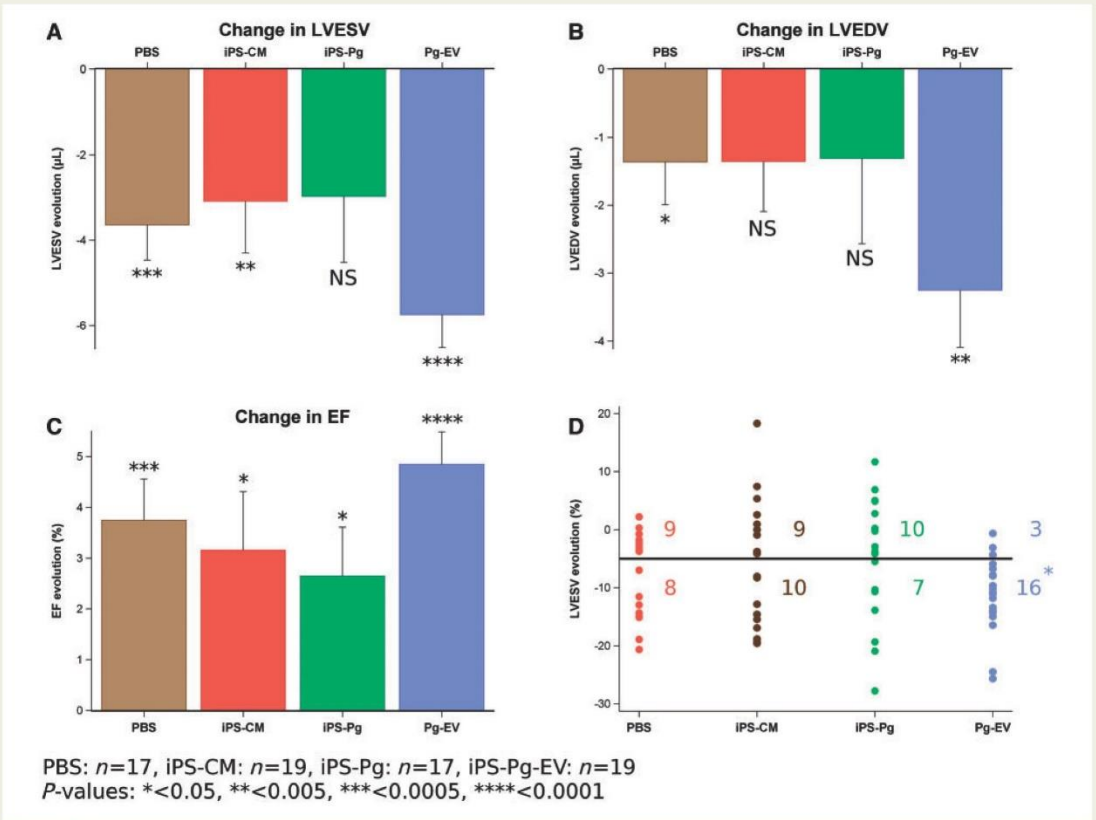

Figure 5 Induced pluripotent stem cell-derived cardiovascular progenitor–extracellular vesicle treatment significantly improves cardiac function. Left ventricular end systolic volume, left ventricular end diastolic volume, and ejection fraction were determined 3 weeks after myocardial infarction (baseline) and 7 weeks after treatment. All groups showed some decrease in ventricular volumes and increase in ejection fraction. For the extracellular vesicle group, there is a clear and highly significant improvement in all three functional parameters, representing a decrease in (*A*) left ventricular end systolic volume and (*B*) left ventricular end diastolic volume of 11% and 4% relative to baseline, respectively, and an increase in (*C*) ejection fraction of 14% relative to baseline. (*D*) Considering left ventricular end systolic volume changes of individual mice in each group, significantly more mice responded to treatment (>5% decrease, 'responders', below the line) in the extracellular vesicle group than in any other group ($P = 0.04$, χ^2 test). Analysis of variance indicates that the evolution of individual mice in the extracellular vesicle group is significantly more homogeneous than the evolution of mice in the induced pluripotent stem cell-derived cardiomyocytes and progenitor cell groups.

process). Another possible explanation for the apparent superiority of EV therapy over cell injection could be related to a dose-effect. Since these cells are only transiently present in the host tissue,[19] the number of EV released by the dwindling numbers of iPSC-Pg cells *in situ* could be dramatically reduced from the number they had released after 48 h of healthy culture *in vitro*. Indeed, our *in vitro* results are consistent with the possibility of a dose effect. One potential corollary to this could be that multiple injections over time could increase therapeutic effectiveness of EV and provide better long-term effects.

We also found that hearts injected with iPSC-CM failed to recover cardiac function to a greater extent than PBS-injected controls. Although it would be over simplistic to relate therapeutic effectiveness to EV release, it is noteworthy that we only found a minimal release of EV from our mature CM, a finding also reported by Malik *et al.*[20]

Mechanistic insights

The protective effects of EV are generally attributed to the transfer of their content to target cells and the subsequent intracellular activation of repair pathways.[21,22] This idea is supported in this study by three main lines of evidence. First, EV were shown to be internalized into cultured cardiac cells. Second, most of the miRNAs identified in the iPSC-Pg-EV were associated with tissue repair pathways. These miRNAs were preferentially packaged in EV when compared with their parent cells, indicating a selective enrichment of the transcripts as has been described previously in the literature.[5,23,24] The predicted targets of these miRNA are consistent with the improved viability of stressed cardiomyocytes, the vascular repair of the scratch-induced wound and the increased proliferation of hESC-CM seen in our *in vitro* bioassays. These effects are also consistent with the strong

Downloaded from https://academic.oup.com/eurheartj/article-abstract/39/20/1835/4840711 by brunacorrea@hotmail.fr on 13 April 2020

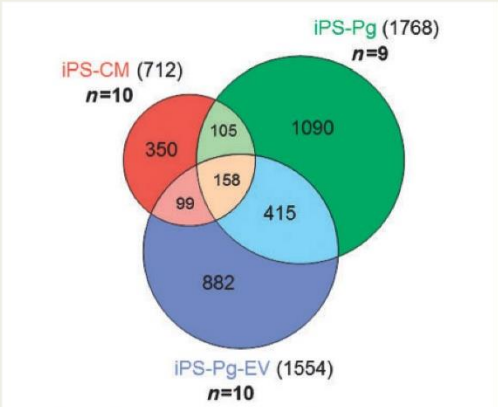

Figure 6 Induced pluripotent stem cell-derived cardiomyocytes, induced pluripotent stem cell-derived cardiovascular progenitors, and induced pluripotent stem cell-derived cardiovascular progenitor–extracellular vesicle treatments lead to distinct gene expression patterns 7 weeks after treatment. Gene expression patterns in mouse hearts 7 weeks after treatment were analysed via mRNA array. Genes differentially expressed in each group when compared with the control phosphate-buffered saline group were identified and gene lists were compared with one another to identify common and specific differentially expressed genes. One-hundred and fifty-eight genes were common to all three treatments, whereas induced pluripotent stem cell-derived cardiomyocytes, induced pluripotent stem cell-derived cardiovascular progenitors, and induced pluripotent stem cell-derived cardiovascular progenitor–extracellular vesicles differentially expressed 350, 1090, and 882 genes, respectively.

pro-survival, pro-angiogenic and pro-proliferative roles of EV derived from diverse cellular sources, including undifferentiated ESC.[11] Third, gene transcription profiles in hearts treated by cells or EV suggest that both interventions affect myocardial cell gene expression but that EV treatment induced the greatest transcriptional changes associated with cardiac functional improvement. These changes primarily consisted of an up-regulation of signalling pathways known to be possible targets of the EV miRNA content, such as cell proliferation/growth, cardiogenesis, and vessel formation.

We have not explored here the relative therapeutic importance of each of the 16 promising miRNA identified in our study. While others have indeed found links between EV therapeutic effectiveness and a single miRNA,[10,25] at this juncture, we feel that it could be counterproductive to deconstruct the EV cargo into single components as it is likely that it is a combination of molecules acting synergistically which account for the biological effects of EV. Furthermore, even the identification of particularly effective miRNAs would only give a truncated picture of the overall mechanism of action of EV because of the likely additional involvement of proteins and lipid rafts.[23,25] Finally, it should be emphasized that one of the great advantages of EV as a therapeutic is their inherent ability to deliver cargo much more efficiently than if the individual components of that cargo were to simply encounter the target cells in a 'naked' form.[26] Indeed this capacity of EV for shuttling a full cargo directly to the recipient cell in which it is internalized is increasingly exploited for targeted delivery of drugs or other therapeutics.[27]

Limitations

We acknowledge that this study has several limitations. Firstly, we have only investigated cardiovascular progenitor-derived EV on the premise that cardiac repair is best served by cardiac-committed cells.[28] However, we cannot exclude that another source of parent cells, particularly mesenchymal stem cells,[29] could yield equally effective EV. Secondly, we used total EV preparations, partly because of a lack of consensus regarding the selective isolation of EV sub-populations and lack of consistent markers to determine sub-fraction purity, and also because it is unknown which sub-population is endowed with the greatest cardioprotective potential. Future studies are warranted to identify the most effective EV fraction, characterize specific biomarkers allowing its isolation,[30] and develop more discriminatory purification methods. Third, the uptake of EV by target cells was demonstrated *in vitro* and remains to be demonstrated *in vivo*. However, as we have previously documented the efficacy of our transcutaneous echo-guided injections for delivering EV in infarcted hearts using fluorescent dye injection,[8] it is reasonable to speculate that the improved functional recovery yielded by EV injections is a consequence of their actual presence in the target sites. Future work is nevertheless warranted to identify the specific cell-type(s) which internalizes the EV. Lastly, we used here an animal model prone to a high rate of spontaneous recovery and a late study Endpoint of 7 weeks after treatment, which may have resulted in missing some early histological or transcriptomic changes in the treated hearts. Indeed, the lack of histological evidence for an increase in vessel density at the 7-week post-treatment time point contrasts with the *in vitro* findings that EV stimulate endothelial cell migration and tube formation. The explanation might be the rapid rate of spontaneous collateral revascularisation of the mouse species[31] which could then make it difficult to show a benefit in the EV treatment group at a late time point because of the 'catch-up' of angiogenesis in controls.

Translation of extracellular vesicle-therapies to clinical use

Currently, iPSC-derived differentiated cells have been used for drug screening and disease modelling while 'regenerative' therapy remains a more lofty goal. This is largely due to the fact that potential genetic and epigenetic changes incurred by these cells during the reprogramming process raise safety issues that may hamper approval from regulatory agencies. Our results open the way for possibly reconciling the advantages of iPSC-based therapies and patient safety by assigning a new role to these cells, i.e. that of an *in vitro* factory of therapeutically effective EV acting as cell surrogates. In addition to circumventing the safety issues that might be associated with direct transplantation of iPSC-derived cells in patients, this strategy features multiple clinically relevant advantages: greater standardization and reproducibility of manufacturing, scalability, more accurate product characterization, greater suitability for regulation-compliant quality controls and therefore better alignment with a pharmaceutical production model. Consequently, pharmaceutical companies may be stimulated to invest in the development of this field facilitating the translation of

Downloaded from https://academic.oup.com/eurheartj/article-abstract/39/20/1835/4840711 by brunacorrea@hotmail.fr on 13 April 2020

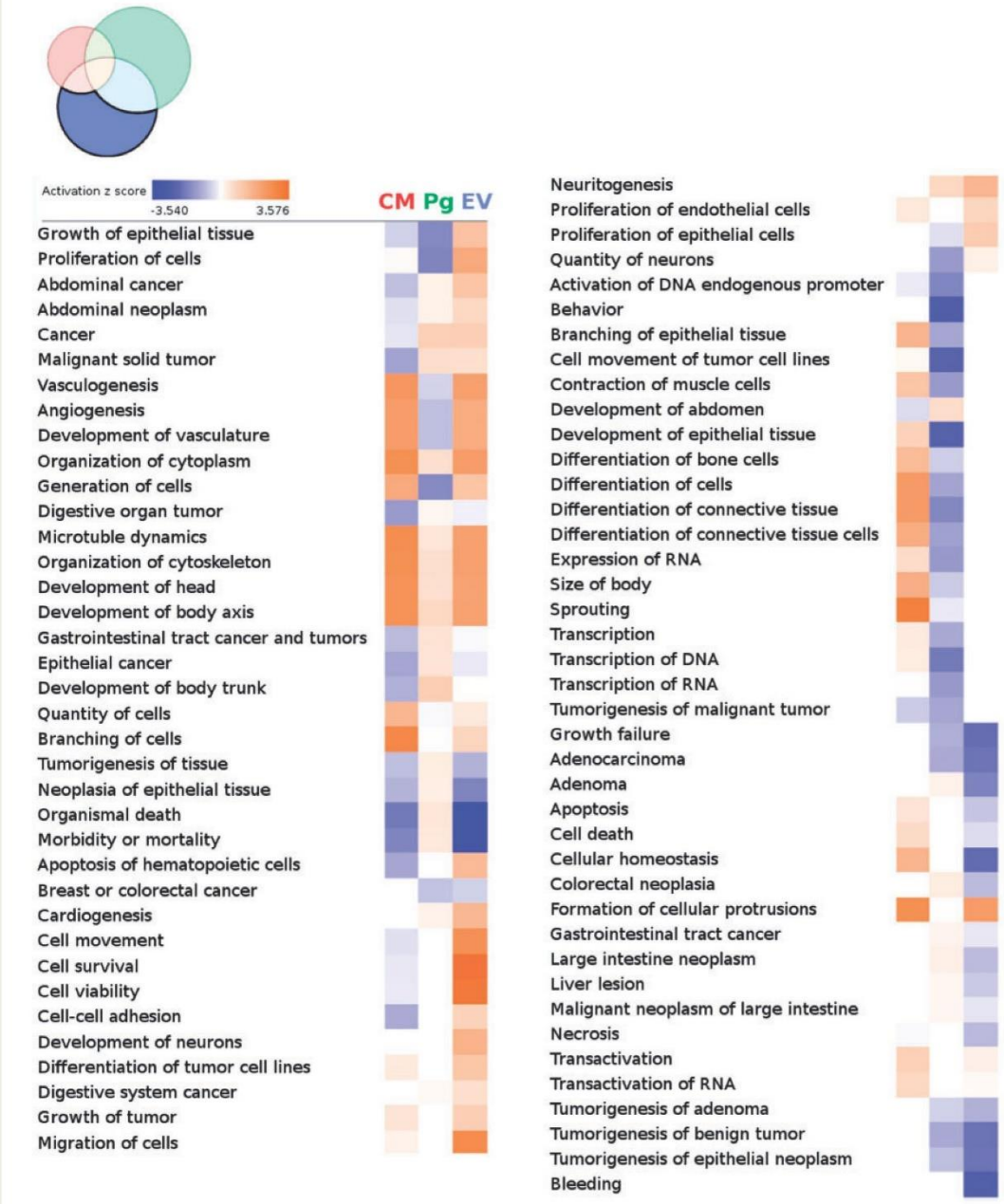

Figure 7 Heat map of differential functions by group—specific gene lists. Differentially expressed genes from each treatment group were assessed by Ingenuity to predict upregulated (warm colours) and downregulated (cool colours) diseases and biological functions when compared with phosphate-buffered saline controls. Each column examines differentially expressed genes uniquely present in the indicated treatment group (left—induced pluripotent stem cell-derived cardiomyocytes; middle—induced pluripotent stem cell-derived cardiovascular progenitors; right—induced pluripotent stem cell-derived cardiovascular progenitor–extracellular vesicles). Induced pluripotent stem cell-derived cardiovascular progenitor–extracellular vesicle treated hearts were the most enriched for functions consistent with increased cell proliferation/growth, cardiogenesis, and vessel formation. The list is sorted to have the greatest difference in enrichment between the extracellular vesicle group and the other groups at the top of the list. This list was truncated after the 78th line.

Downloaded from https://academic.oup.com/eurheartj/article-abstract/39/20/1835/4840711 by brunacorrea@hotmail.fr on 13 April 2020

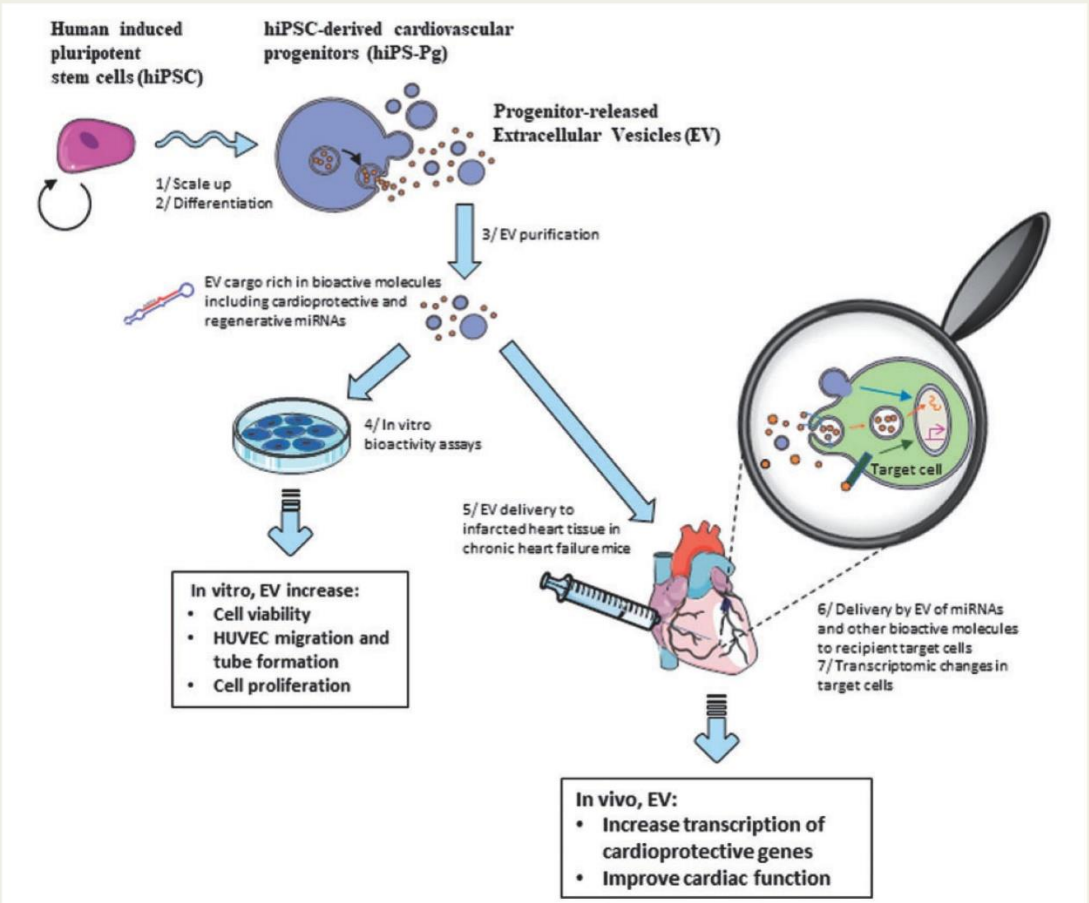

Take home figure Human induced pluripotent stem cell-derived cardiovascular progenitor cell 'biofactories' produce therapeutic extracellular vesicles that benefit cells and tissues, improving outcomes. Human induced pluripotent stem cells are 1-expanded and 2-differentiated to cardiovascular progenitors. Under the appropriate culture conditions, the latter release extracellular vesicles which can be 3-concentrated and purified, eliminating the secretory cells. The human induced pluripotent stem cell-derived cardiovascular progenitor cell–extracellular vesicles contain a unique miRNA signature, including miRNAs associated with cardio protective and reparative pathways. *In vitro*, 4-these extracellular vesicles are internalized by target cells leading to cellular effects consistent with cardio-protection or repair. When 5-extracellular vesicles are delivered to the infarcted heart tissue of mice in chronic heart failure, human induced pluripotent stem cell-derived cardiovascular progenitor–extracellular vesicles appear to stimulate transcriptomic changes leading to improved cardiac function.

EV-therapies to the clinic. The obvious pre-requisite for such a development is to validate the safety of the final EV formulation to ensure a lack of arrhythmias, immune reaction (particularly if time-release formulations or multiple EV injections are considered) and tumourigenesis. This last point is particularly important considering that some of the miRNA identified in the iPSC-Pg-EV are associated both with regeneration and cancer pathways.

Overall, we have found that iPSC-Pg-derived EV are effective in the treatment of CHF, possibly, in part, through their specific miRNA signature and the associated stimulation of cardioprotective pathways (*Take home figure*). The production and regulatory advantages of EV could make them appealing alternatives to cell transplantation.

Supplementary material

Supplementary material is available at *European Heart Journal* online.

Acknowledgements

The authors thank the Plateforme Génomique of the Institut Cochin (INSERM U1016-CNRS UMR8104-Université Paris Descartes, Paris, France) for performing all the microarray experiments and Ghislaine Frébourg and the Electron Microscopy Facility (FR 3631-CNRS-UPMC) for performing cryo-electron microscopy. We would like to thank Daniel Balvay (Plateforme d'Imagerie du Vivant de Paris Descartes) for his help with the macroscopic image preparation and the assessment of

Downloaded from https://academic.oup.com/eurheartj/article-abstract/39/20/1835/4840711 by brunacorrea@hotmail.fr on 13 April 2020

infarct size using his physio3D3 software, Sean Spiering for the preparation of human embryonic stem cell-derived cardiomyocytes and Thomas Mathivet (INSERM U970 PARCC, Paris, France) for his help with the confocal microscopy.

Funding

Institut National de la Santé et de la Recherche Médicale (INSERM); Université Paris Descartes; the LabEx REVIVE (ANR-10-LABX-73); the Fondation pour la Recherche Médicale (DEQ20160334910); the Fondation de France (FDF/2014 00047970); and the LeDucq Foundation (SHAPEHEART network). PhD students were supported by fellowships from the Ecole Doctorale, Université Paris Descartes (NE), the LabEX REVIVE (AK), the Université Pierre et Marie Curie (SP), and the AFM-Téléthon (YH).

Conflict of interest: none declared.

References

1. Ponikowski P, Voors AA, Anker SD, Bueno H, Cleland JGF, Coats AJS, Falk V, González-Juanatey JR, Harjola V-P, Jankowska EA, Jessup M, Linde C, Nihoyannopoulos P, Parissis JT, Pieske B, Riley JP, Rosano GMC, Ruilope LM, Ruschitzka F, Rutten FH, van der Meer P; Authors/Task Force Members. 2016 ESC Guidelines for the diagnosis and treatment of acute and chronic heart failure: the Task Force for the diagnosis and treatment of acute and chronic heart failure of the European Society of Cardiology (ESC)Developed with the special contribution of the Heart Failure Association (HFA) of the ESC. *Eur Heart J* 2016;**37**:2129–2200.
2. Fisher SA, Doree C, Mathur A, Taggart DP, Martin-Rendon E. Stem cell therapy for chronic ischaemic heart disease and congestive heart failure. *Cochrane Database Syst Rev* 2016;**12**:CD007888.
3. Timmers L, Lim SK, Arslan F, Armstrong JS, Hoefer IE, Doevendans PA, Piek JJ, El Oakley RM, Choo A, Lee CN, Pasterkamp G, de Kleijn DPV. Reduction of myocardial infarct size by human mesenchymal stem cell conditioned medium. *Stem Cell Res* 2008;**1**:129–137.
4. Timmers L, Lim SK, Hoefer IE, Arslan F, Lai RC, van Oorschot AAM, Goumans MJ, Strijder C, Sze SK, Choo A, Piek JJ, Doevendans PA, Pasterkamp G, de Kleijn DPV. Human mesenchymal stem cell-conditioned medium improves cardiac function following myocardial infarction. *Stem Cell Res* 2011;**6**:206–214.
5. Vlassov AV, Magdaleno S, Setterquist R, Conrad R. Exosomes: current knowledge of their composition, biological functions, and diagnostic and therapeutic potentials. *Biochim Biophys Acta* 2012;**1820**:940–948.
6. Xin H, Li Y, Cui Y, Yang JJ, Zhang ZG, Chopp M. Systemic administration of exosomes released from mesenchymal stromal cells promote functional recovery and neurovascular plasticity after stroke in rats. *J Cereb Blood Flow Metab* 2013; **33**:1711–1715.
7. Bruno S, Porta S, Bussolati B. Extracellular vesicles in renal tissue damage and regeneration. *Eur J Pharmacol* 2016;**790**:83–91.
8. Kervadec A, Bellamy V, El Harane N, Arakélian L, Vanneaux V, Cacciapuoti I, Nemetalla H, Périer M-C, Toeg HD, Richart A, Lemitre M, Yin M, Loyer X, Larghero J, Hagège A, Ruel M, Boulanger CM, Silvestre J-S, Menasché P, Renault NKE. Cardiovascular progenitor-derived extracellular vesicles recapitulate the beneficial effects of their parent cells in the treatment of chronic heart failure. *J Heart Lung Transplant* 2016;**35**:795–807.
9. Barile L, Lionetti V, Cervio E, Matteucci M, Gherghiceanu M, Popescu LM, Torre T, Siclari F, Moccetti T, Vassalli G. Extracellular vesicles from human cardiac progenitor cells inhibit cardiomyocyte apoptosis and improve cardiac function after myocardial infarction. *Cardiovasc Res* 2014;**103**:530–541.
10. Ibrahim AG-E, Cheng K, Marbán E. Exosomes as critical agents of cardiac regeneration triggered by cell therapy. *Stem Cell Rep* 2014;**2**:606–619.
11. Khan M, Nickoloff E, Abramova T, Johnson J, Verma SK, Krishnamurthy P, Mackie AR, Vaughan E, Garikipati VNS, Benedict C, Ramirez V, Lambers E, Ito A, Gao E, Misener S, Luongo T, Elrod J, Qin G, Houser SR, Koch WJ, Kishore R. Embryonic stem cell-derived exosomes promote endogenous repair mechanisms and enhance cardiac function following myocardial infarction. *Circ Res* 2015;**117**:52–64.
12. Gallet R, Dawkins J, Valle J, Simsolo E, de Couto G, Middleton R, Tseliou E, Luthringer D, Kreke M, Smith RR, Marbán L, Ghaleb B, Marbán E. Exosomes secreted by cardiosphere-derived cells reduce scarring, attenuate adverse remodelling, and improve function in acute and chronic porcine myocardial infarction. *Eur Heart J* 2016;**38**:201–211.
13. Lai RC, Arslan F, Lee MM, Sze NSK, Choo A, Chen TS, Salto-Tellez M, Timmers L, Lee CN, El Oakley RM, Pasterkamp G, de Kleijn DPV, Lim SK. Exosome secreted by MSC reduces myocardial ischemia/reperfusion injury. *Stem Cell Res* 2010;**4**:214–222.
14. Leroyer AS, Ebrahimian TG, Cochain C, Récalde A, Blanc-Brude O, Mees B, Vilar J, Tedgui A, Levy BI, Chimini G, Boulanger CM, Silvestre J-S. Microparticles from ischemic muscle promotes postnatal vasculogenesis. *Circulation* 2009;**119**:2808–2817.
15. Lener T, Gimona M, Aigner L, Börger V, Buzas E, Camussi G, Chaput N, Chatterjee D, Court FA, Del Portillo HA, O'Driscoll L, Fais S, Falcon-Perez JM, Felderhoff-Mueser U, Fraile L, Gho YS, Görgens A, Gupta RC, Hendrix A, Hermann DM, Hill AF, Hochberg F, Horn PA, Kleijn D. D, Kordelas L, Kramer BW, Krämer-Albers E-M, Laner-Plamberger S, Laitinen S, Leonardi T, Lorenowicz MJ, Lim SK, Lötvall J, Maguire CA, Marcilla A, Nazarenko I, Ochiya T, Patel T, Pedersen S, Pocsfalvi G, Pluchino S, Quesenberry P, Reischl IG, Rivera FJ, Sanzenbacher R, Schallmoser K, Slaper-Cortenbach I, Strunk D, Tonn T, Vader P, Balkom B. W M V, Wauben M, Andaloussi SE, Théry C, Rohde E, Giebel B. Applying extracellular vesicles based therapeutics in clinical trials—an ISEV position paper. *J Extracell Vesicles* 2015;**4**:30087.
16. Menasché P, Vanneaux V, Hagège A, Bel A, Cholley B, Parouchev A, Cacciapuoti I, Al-Daccak R, Benhamouda N, Blons H, Agbulut O, Tosca L, Trouvin J-H, Fabreguettes J-R, Bellamy V, Charron D, Tartour E, Tachdjian G, Desnos M, Larghero J. Transplantation of human embryonic stem cell-derived cardiovascular progenitors for severe ischemic left ventricular dysfunction. *JACC* 2018;**71**: 429–438.
17. McManus DD, Shah SJ, Fabi MR, Rosen A, Whooley MA, Schiller NB. Prognostic value of left ventricular end-systolic volume index as a predictor of heart failure hospitalization in stable coronary artery disease: data from the Heart and Soul Study. *J Am Soc Echocardiogr* 2009;**22**:190–197.
18. Ge Q, Zhou Y, Lu J, Bai Y, Xie X, Lu Z. miRNA in plasma exosome is stable under different storage conditions. *Mol Basel Switz* 2014;**19**:1568–1575.
19. Bellamy V, Vanneaux V, Bel A, Nemetalla H, Emmanuelle Boitard S, Farouz Y, Joanne P, Perier M-C, Robidel E, Mandet C, Hagège A, Bruneval P, Larghero J, Agbulut O, Menasché P. Long-term functional benefits of human embryonic stem cell-derived cardiac progenitors embedded into a fibrin scaffold. *J Heart Lung Transplant* 2015;**34**:1198–1207.
20. Malik ZA, Kott KS, Poe AJ, Kuo T, Chen L, Ferrara KW, Knowlton AA. Cardiac myocyte exosomes: stability, HSP60, and proteomics. *Am J Physiol Heart Circ Physiol* 2013;**304**:H954–H965.
21. Yuan A, Farber EL, Rapoport AL, Tejada D, Deniskin R, Akhmedov NB, Farber DB. Transfer of microRNAs by embryonic stem cell microvesicles. *PloS One* 2009;**4**:e4722.
22. Waldenström A, Gennebäck N, Hellman U, Ronquist G, Qin G. Cardiomyocyte microvesicles contain DNA/RNA and convey biological messages to target cells. *PloS One* 2012;**7**:e34653.
23. Bobis-Wozowicz S, Kmiotek K, Sekula M, Kedracka-Krok S, Kamycka E, Adamiak M, Jankowska U, Madetko-Talowska A, Sarna M, Bik-Multanowski M, Kolcz J, Boruczkowski D, Madeja Z, Dawn B, Zuba-Surma EK. Human induced pluripotent stem cell-derived microvesicles transmit RNAs and proteins to recipient mature heart cells modulating cell fate and behavior. *Stem Cells* 2015;**33**: 2748–2761.
24. Ogawa Y, Taketomi Y, Murakami M, Tsujimoto M, Yanoshita R. Small RNA transcriptomes of two types of exosomes in human whole saliva determined by next generation sequencing. *Biol Pharm Bull* 2013;**36**:66–75.
25. Cervio E, Barile L, Moccetti T, Vassalli G. Exosomes for intramyocardial intercellular communication. *Stem Cells Int* 2015;**2015**:482171.
26. Deregibus MC, Cantaluppi V, Calogero R, Lo Iacono M, Tetta C, Biancone L, Bruno S, Bussolati B, Camussi G. Endothelial progenitor cell derived microvesicles activate an angiogenic program in endothelial cells by a horizontal transfer of mRNA. *Blood* 2007;**110**:2440–2448.
27. Ohno S-I, Drummen GPC, Kuroda M. Focus on extracellular vesicles: development of extracellular vesicle-based therapeutic systems. *Int J Mol Sci* 2016;**17**:172.
28. Fernandes S, Chong JJH, Paige SL, Iwata M, Torok-Storb B, Keller G, Reinecke H, Murry CE. Comparison of human embryonic stem cell-derived cardiomyocytes, cardiovascular progenitors, and bone marrow mononuclear cells for cardiac repair. *Stem Cell Rep* 2015;**5**:753–762.
29. Lai RC, Yeo RWY, Lim SK. Mesenchymal stem cell exosomes. *Semin Cell Dev Biol* 2015;**40**:82–88.
30. Kowal J, Arras G, Colombo M, Jouve M, Morath JP, Primdal-Bengtson B, Dingli F, Loew D, Tkach M, Théry C. Proteomic comparison defines novel markers to characterize heterogeneous populations of extracellular vesicle subtypes. *Proc Natl Acad Sci USA* 2016;**113**:E968–E977.
31. Zhang H, Faber JE. De-novo collateral formation following acute myocardial infarction: dependence on $CCR2^+$ bone marrow cells. *J Mol Cell Cardiol* 2015;**87**: 4–16.

Downloaded from https://academic.oup.com/eurheartj/article-abstract/39/20/1835/4840711 by brunacorrea@hotmail.fr on 13 April 2020

Acellular therapeutic approach for heart failure: *in vitro* production of extracellular vesicles from human cardiovascular progenitors

Nadia El Harane MSc* (1,2), Anaïs Kervadec PhD* (1,2), Valérie Bellamy BSc (1,2), Laetitia Pidial MSc (1,2), Hany J Neametalla MD, PhD (3), Marie-Cécile Perier MSc (1,2), Bruna Lima Correa MSc (1,2), Léa Thiébault MSc (1, 2), Nicolas Cagnard MSc (4), Angéline Duché (5,6) Camille Brunaud MSc (2), Mathilde Lemitre BSc (1,2), Jeanne Gauthier (1,2,7), Alexandra T Bourdillon (8), Marc P Renault PhD (9), Yeranuhi Hovhannisyan MSc (10), Solenne Paiva MSc (10), Alexandre R Colas PhD (11), Onnik Agbulut PhD (10), Albert Hagège MD, PhD (1,2,3), Jean-Sébastien Silvestre PhD (1,2), Philippe Menasché MD, PhD (1,2,12), Nisa KE Renault PhD (1,2) *co-first authors

1. Institut National de la Santé et de la Recherche Médicale (INSERM), UMRS-970, Paris Centre de Recherche Cardiovasculaire, 56, rue Leblanc, 75015 Paris, France.
2. Université Paris Descartes, Sorbonne Paris Cité, Paris, France.
3. Assistance Publique-Hôpitaux de Paris, Hôpital Européen Georges Pompidou, Department of Cardiology, 20, rue Leblanc, 75015 Paris, France.
4. Université Paris Descartes, US 024 SFR Necker, 24 Boulevard du Montparnasse, 75015 Paris, France.
5. Institut National de la Santé et de la Recherche Médicale (INSERM), U 1016, Institut Cochin, Université Paris Descartes, Sorbonne Paris Cité, 22 rue Mechain, 75014 Paris, France.
6. CNRS, Université Paris Descartes, UMR-8104, Paris, France.
7. Ecole normale supérieure, PSL Research University Paris, 45 rue d'Ulm 75005 Paris, France.
8. Department of Engineering, Stanford University, 475 Via Ortega, Stanford, Ca 94305, USA.
9. IRIF, Université Paris Diderot-Paris 7, UMR 8243, Bâtiment Sophie Germain, 8 place Aurélie Nemours, 75013 Paris, France. Current affiliation: Computer Sciences Department, University of Wisconsin – Madison, 1210 West Dayton Street, Madison, WI 53706-1685, USA.

10. Sorbonne Universités, UPMC Université de Paris- 6, Institut de Biologie Paris-Seine (IBPS), UMR CNRS 8256, Biological Adaptation and Ageing, 4 place Jussieu, 75005 Paris, France.
11. Sanford Burnham Prebys Medical Discovery Institute, Development, Aging and Regeneration Program, 10901 N Torrey Pines Rd, La Jolla, CA 92037, USA.
12. Assistance Publique-Hôpitaux de Paris, Hôpital Européen Georges Pompidou, Department of Cardiovascular Surgery, 20, rue Leblanc, 75015 Paris, France.

Supplemental Material

Supplemental Material and Methods

Cell culture and characterization

Cell culture: iPSC-derived cardiovascular progenitors (iPSC-Pg: iCell Cardiac Progenitor Cells, ref.: CPC-301-020-001-PT) and cardiomyocytes (iPSC-CM; iCell Cardiomyocytes, ref.: CMC-100-010-005) were purchased from Cellular Dynamics International (CDI, Madison, WI, USA). Both the iPSC-Pg and iPSC-CM have been previously characterised[1;2]. Cryopreserved iPSC-Pg were thawed and plated at a density of 78,000 cells/cm^2 on fibronectin-coated flasks (ref.: 11051407001, Roche Applied Sciences, Indianapolis, IN, USA) and cultured 4 days at 7% CO_2 and 37°C in serum-free media according to the proliferation protocol recommended by the manufacturer: William's E medium (ref.: A12176-01, Life Technologies, Saint Aubin, France) with Cocktail B from hepatocyte maintenance supplement pack (ref.: CM4000, Life Technologies), 25µg/mL Gentamicin (ref.: 15750, Life Technologies) and 1µg/ml of zebrafish FGF-2 (ref.: GFZ1 Cell Guidance System, Cambridge, UK). Media were refreshed on day 2 of culture, and day 4 conditioned media (containing the EV secreted over the previous 48 hours) was collected for EV isolation. For iPSC-CM, all media were provided by CDI, and culture conditions were performed according to the manufacturer's instructions. Briefly, iPSC-CM were plated at a density of 53,000 cells/cm^2 on 0.1% gelatin-coated flasks (ref.: G1890, Sigma-Aldrich, Saint-Quentin-Fallavier, France) and cultured in 7% CO_2 at 37°C in iCell Cardiomyocytes Plating Medium (ref.: CMM-100-110-001, CDI) for 48 hours. On day 2, media was fully changed to iCell Cardiomyocyte Maintenance Medium (ref.: CMC-100-120-005, CDI) and cells were maintained in this media, until day 7 at which time they were consistently beating. Media was refreshed every dy. Conditioned media, containing the EV secreted over a 24 hours period were collected on day 7 for subsequent EV isolation.

Cell characterisation: Aliquots of harvested cells were cytospun (Cytospin 4, Fisher Scientific, Illkirch, France) onto glass slides with 5,000 cells per spot at 2,000 rpm for 5 min. Cells were fixed in 4% paraformaldehyde and stained for early cardiovascular progenitors (MEF2C, ISL1, NKX2.5) and mature cardiomyocytes (TNNI3, ACTN2, MHCαβ). Dilutions and references for each antibody are given in Supplemental Table 1. RNA was extracted from iPSC-Pg and iPSC-CM cell pellets by RNeasy Mini kit (ref.: 74104, Qiagen, Hilden, Germany) according to the

manufacturer's instructions. The expression of genes associated with pluripotency (*NANOG, SOX2, OCT3/4*), cardiac progenitor fate (*ISL1, MEF2C, NKX2.5, GATA4*) and mature cardiomyocytes (*TBX20, TNNT2, PLN, MYH6, MYH7, MYL2*) were evaluated by qPCR. Primer sequences are found in the Supplemental Table 2.

EV *in vitro* bioactivity

Pro-survival potential: Immortalized H9c2 rat cardiac myoblasts were plated on 0.2% gelatin-coated 6-well plates at 25,000 cells/cm^2 and cultured at 5% CO_2 and 37°C in complete medium (Dulbecco's Modified Eagle Medium (DMEM) + glutamax (ref.: 10566-016, GIBCO, Waltham, MA, USA)), supplemented with 10% foetal bovine serum (FBS; ref.: S1810, Biowest, Nuaille, France) and 1% Penicillin / Streptomycin / Amphotericine (PSA; ref.: A5955, Sigma Aldrich). After 48 hours, cells were counted (T_0) by the Muse™ cell analyser (ref.: 0500-3115, Merck Millipore, Guyancourt, France) with the Muse count and viability kit (ref.: MCH100102, Merck Millipore) according to the manufacturer's directions. The media in the remaining wells were replaced with complete media (positive control), serum-free media (negative control: DMEM glutamax + 1% PSA), serum-free media supplemented with EV isolated from pure FBS (FBS-EV, taken as an additional control), or serum-free media supplemented with iPSC-Pg-EV at various concentrations. Twenty-seven hours later (T_{27}), viable cells from each condition were counted by the cell analyser. Each condition was evaluated in duplicate (technical replicates) and the yielded values were averaged. The percent viability was calculated as: 100% x (T_{27} cell count-T_0 cell count)/T_0 cell count. The pro-survival assay was used as a quality control measure for all iPSC-Pg-EV preparations at 5x10^9 EV for 250,000 plated H9c2 cells. The dose-response analysis was repeated three times using 3 separate iPSC-Pg-EV preparations (biological replicates).

Endothelial cell activation: The potential for iPSC-Pg-EV to activate endothelial cells was evaluated by two assays: 1) scratch wound assay and 2) tube formation.

1) Scratch wound assay: Human Umbilical Vein Endothelial cells (HUVEC single donor, ref.: C-12200, PromoCell, Heidelberg, Germany) were seeded at a density of 41,667cells/cm^2 on uncoated 96-well plates and cultured in 'complete endothelial cell media' (Endothelial Cell Growth Medium, ref.: C-22210, PromoCell, plus Endothelial Cell Growth Medium Supplement Pack, ref: C-39210, PromoCell) at 37°C and 5% CO_2 until confluence (overnight). A gap in the confluent monolayer was induced at T_0 by scratching with a 10µl pipette tip and the wound was located by real-time inverted research microscope (Nikon-ECLIPSE Ti, Nikon Corporation, Tokyo, Japan). Cells were cultured for 24 hours in complete endothelial cell media (positive control), 'poor endothelial cell media' without supplement (negative control; Endothelial Cell Growth Medium alone), poor endothelial cell media plus EV isolated from pure FBS, or poor endothelial cell media plus iPSC-Pg-EV. Images of each well were taken every 6 hours for 24 hours. The surface area of the scratch was determined at each time point by image analysis (ImageJ v.1.50i). The wound healing process was calculated as: % wound healing = 100% x (T_0 surface area- $T_{time\ point}$ surface area-)/ T_0 surface area. Each condition was averaged over three technical replicates. The scratch wound assay dose-response experiment was repeated three times using 3 independent preparations of iPS-Pg-EV (biological replicates).

2) Tube formation assay: HUVEC were seeded at a density of 41,667cells/cm^2 on Matrigel Growth Factor Reduced (ref.: 354230, BD Biosciences, Erembodegem, Belgium) and cultured at 37°C and 5% CO_2 in complete endothelial cell media (positive control), poor endothelial cell media (negative control), or poor endothelial cell media supplemented with EV isolated from pure FBS (additional positive control) or various doses of iPSC-Pg-EV. Cells were cultured for 24 hours. Images were taken at 18 and 24 hours. Endothelial cell tube formation was evaluated by image analysis (ImageJ v.1.50i; using the Angiogenesis Analyzer) to extract characteristic information on the tube formation network, such as number of nodes, segment length and branch length. Each condition was tested in triplicate (technical replicates). The tube formation dose-response experiment was repeated three times using 3 independent iPSC-Pg-EV preparations (biological replicates).

Pro-proliferative potential: CM were differentiated from H9 human embryonic stem cell (hESC) line (WA09) supplied by WiCell Research Institute. H9 cells were cultured in mTeSR1 (Stem Cell Technologies, 05850) on growth factor-reduced Matrigel at 9µg/cm² (Corning, 356231). After at least 5 passages using ReLeSR (Stem Cell Technologies, 05872), H9 cells were first differentiated into cardiogenic mesoderm progenitors (CMP) using basal differentiation medium (BDM: RPMI 1640 medium [Life Technologies, 11875-093] and B27 supplement minus insulin [Life Technologies, A1895601]) supplemented with recombinant human Activin A (R&D Systems, 338-AC-050) and puromycin (Acros, 227420100) until day 5 of differentiation, as previously described [3]. Cardiogenic mesoderm progenitors are then differentiated into beating cardiomyocytes on Matrigel-coated 384-well plates (Greiner Bio-One) at a cell density of 25,000 cells per well using BDM and hESC recovery supplement (Stemgent). The BDM was replaced every other day until day 23. At day 23 of maturation, iPSC-Pg-EV (isolated from day 2 iPSC-Pg culture media) were incubated with hESC-CM at different doses. Each condition was evaluated in triplicate and the yielded values were averaged. After 48 hours of incubation, CM proliferation was assessed using the Click-iT EdU Alexa Fluor 488 Imaging Kit (Ref.: C10337, Life Technologies, Eugene, OR, USA). EdU was incubated for 24 hours at a concentration of 10µM and cells were fixed with 4% PFA. The EdU reaction was performed, and cells were stained with α-actinin (ref.: A7811, 1/800, Sigma Aldrich, Saint-Louis, MO, USA) and counterstained with DAPI (ref.: D9542-5MG; 1/1000, Sigma-Aldrich, Saint-Louis, MO, USA) before imaging (ImageXpress Micro XLS Widefield High-Content Analysis System, Molecular Devices, Sunnyvale, CA, USA) with the CyteSeer scanner software and analysed with CyteSeer 2.8.0.11. The proliferative potential experiment was repeated using 3 independent iPS-Pg-EV preparations.

EV internalization

Calcein-AM labelling: Calcein-AM is a hydrophobic, non-fluorescent molecule, which passes through lipid bilayers of cells and EV. In the presence of functional esterases, the precursor is cleaved, rendering it fluorescent and hydrophilic, trapping the signal inside the cell/EV. Calcein-AM (ref.: C3100MP, Life Technologies) was dissolved in dimethyl sulfoxide (DMSO; ref.: P60-36720100, Dominique Dutscher, Brumath, France) to a final concentration of 1mM. Conditioned media from iPSC-Pg culture (day 2 of culture) were incubated with 2µM calcein-

AM at 37°C for 1 hour. Media were ultracentrifuged for 16h at 100,000 g, as described above. The labelled EV pellet was resuspended in PBS, then 17 mL of fresh PBS were added, and this suspension was again ultracentrifuged for 3 hrs at 100,000 g to pellet the washed EV (wash). The washed EV pellet was resuspended in a minimal volume of fresh PBS for internalization experiments. The supernatant from the wash was used to control for a possible contamination by free calcein-AM which could potentially label target cells directly. Calcein-AM labelling of iPSC-Pg-EV was confirmed by imaging flow cytometry (ImageStream^X MkII imaging cytometer, Merck Millipore) as described below.

Internalization assay: The pro-survival assay was used to determine if fluorescent EV were internalized by their target cells. For this assay, the H9c2 cell line was cultured as described above. At T_0, the media in each well was replaced with complete media, poor media, poor media supplemented with 5 x 10^9 FBS-EV, poor media supplemented with 5 x 10^9 unlabelled iPSC-Pg-EV, poor media supplemented with 5 x 10^9 calcein-AM-labelled iPSC-Pg-EV, or poor media supplemented with 'wash' (same volume as the volume of calcein-AM labelled iPSC-Pg-EV used in the assay). Control cells in poor media supplemented with FBS-EV were also directly labelled with 2 µM calcein-AM during the entire 20-hour assay period or for the final 1-hour before the end of the assay. Cells were harvested after 20 hours of incubation and directly analysed by imaging flow cytometry to determine if the H9c2 cells had become fluorescently labelled. Green fluorescence in the H9c2 cells would indicate EV internalization and/or fusion. Harvested cells were also visualized by confocal microscopy.

Imaging Flow Cytometry: Calcein-AM fluorescence was determined by imaging flow cytometry as described in the literature –Reviewed in *Scientific Reports*[4]. Briefly, an ImageStream^X MkII imaging cytometer (Merck Millipore) was used to image EV or cells and to quantify the fluorescence intensity of each event. Settings were as follows: 60X optical magnification for EV and 40X for cells; low flow/high sensitivity acquisition using the INSPIRE software (Merck Millipore); upper collection event gate was of 15,000 events; channel 01 = bright field; channel 06 = SSC (side scatter, 785nm); channel 02 = laser 488 nm. For EV acquisition, EV were gated first as SSC negative (to eliminate speed beads), and then evaluated by channel 02 fluorescence with the laser set to 80mW. Cells were gated first by morphology, then by focus, and then evaluated by channel 02 fluorescence with the laser set to 10mW (most conditions) or 0.25 mW (only for conditions with strongly fluorescent cells that were directly labelled with calcein-AM). Results were analysed by IDEAS software (Merck Millipore).

Confocal microscopy: H9c2 cells were cultured on 12-well glass slide chambers (ref: 81201, Biovalley, Nanterre, France). Cells were fixed with PFA 1% and stained with wheat germ agglutinin-TRITC (WGA; diluted 1/5000 in DMEM; Lectin from Triticum vulgaris (wheat) TRITC, CliniScience) for 1 hour at room temperature and counter-stained with the nuclear marker 4',6-diamidino-2-phenylindole (DAPI, ref.: 268298, Calbiochem, Fontenay-sous-Bois, France), and mounted with Dako Fluorescence Mounting Medium (Ref.: Dako Cytomation, Glostrup, Denmark). Slides were visualized by a confocal microscope SP8 (Leica TCS SP8, LAS software, Leica microsystems, Wetzlar, Germany), with a 63X optical objective.

Fluorescence video microscopy: We tracked the internalization of green-labelled extracellular vesicles by stressed rat cardiomyocytes (modelling infarcted myocardium) and non-stressed cells (modelling healthy myocardium) following the protocol used in the pro-survival assay. For this experiment, the progenitor-derived EVs labelled with calcein AM were purified by ultracentrifugation for 16h and, to remove any free dye, two additional 90-minute wash steps were added. H9c2 rat cardiac myoblasts were plated in a 12-well Chamber Slide System (Ibidi), with 30,000 cells/well and after 24 hours, the membrane was labelled with lectin WGA conjugated to Texas Red. To determine whether EV half-life differs between stressed and non-stressed cardiomyocytes, H9c2 in complete media or poor media were treated with labelled iPS-Pg-EVs. For 45 hours, z-stacks of each well were taken every 5 minutes with a fluorescence video microscope (Spinning disk). A video reconstruction was subsequently performed using image analysis (Fiji) for each condition from each image sequence obtained (ie 540 images for each of the three channels: GFP, RFP and white light).

EV microRNAs

MicroRNAs (miRNAs) were isolated from iPSC-Pg cells and iPSC-Pg-EV by *mir*Vana miRNA Isolation Kit (Ref.: AM1560, Thermo Fisher Scientific Inc., Waltham, MA, USA) following the manufacturer's instructions for 'Total RNA isolation', eluting RNA with 95°C RNAse/DNAse-free water. The percentage of miRNAs present among small RNAs was assessed by Bioanalyser. The miRNA contents of iPSC-Pg and iPSC-Pg-EV were assessed by miRNA microarray (miR 4.0, Affymetrix, Santa Clara, California, USA) for 3 independent iPSC-Pg cultures and their 3 corresponding independent iPSC-Pg-EV preparations. Array data were normalized as for the transcriptomic analyses below. After removal of control probes, the frequency and identity of miRNAs present in iPSC-Pg and iPSC-Pg-EV above a sliding threshold were determined and compared to generate Venns and a sliding Venn. To detect potentially important EV-miRNAs, miRNAs with an average intensity > 2^9 (log threshold 9) or average intensity >2^{10} (log threshold 10) from 3 separate cell cultures and EV preparations were identified and listed, and those miRNAs denoted as broadly conserved in target scan (TargetScanHuman, release 7.1, targetscan.org) were flagged as potentially important in mediating the effects of iPSC-Pg-EV. These microarray analyses have been submitted to, and validated by ArrayExpress (accession E-MTAB-5165).

Functional assessment in the CHF model

Myocardial infarction was induced in 199 male nude mice (Rj/NMRI-Foxn1nu/Foxn1nu, Janvier Labs, Le Genest-Saint-Isle, France) aged from 64 to 71 days by permanent ligation of the left anterior descending coronary artery as previously described[5]. Between 21 and 27 days after infarction, echocardiographic assessment of left ventricular function was performed as described previously[5] by a cardiologist blinded to the treatment groups. Only mice with ejection fraction (EF) equal to or less than 45% were included in the study. They were then sorted into four treatment groups such that baseline cardiac functional parameters [left ventricular end systolic volume (LVESV, primary functional end point), left ventricular end diastolic volume (LVEDV), and ejection fraction (EF)] were matched among groups in order to ensure that differences in heart failure outcomes could not be confounded by extraneous factors. Within one week of baseline measurements, animals received 3 closed-chest, echo-guided, transcutaneous injections (40-60 µL total) into the peri-infarcted myocardium of iPSC-CM (1.4

x 10^6 cells; 24 mice injected), iPSC-Pg (1.4 x 10^6; 21 mice), iPSC-Pg-EV secreted by the same batch of iPSC-Pg over 48 hrs (approximately 3 x 10^{10} EV per mouse; 22 mice) or PBS (vehicle control, 20 mice). Extracellular vesicles were either injected immediately after preparation (fresh, 11 mice) or were thawed from frozen stocks (11 mice). From 49 to 52 days after treatment, cardiac function of the 72 surviving mice (iPSC-CM: n=19; iPSC-Pg: n=17; iPSC-Pg-EV: n=19; PBS: n=17) was re-evaluated by the same cardiologist. Echographic cine-loops at baseline and at the end of the study were re-assessed for 10 randomly selected animals by the same ultrasonographer, blinded to treatment groups and to the results of the first analyses, in order to calculate intra-observer variability (Intraclass Correlation Coefficients, ICC).

All procedures were approved by our institutional ethics committee (project #04073.01) and complied with European legislation (European Commission Directive 86/609/ EEC) on animal care. All animals received humane care in compliance with the "Principles of Laboratory Animal Care" formulated by the National Society for Medical Research and the "Guide for the Care and Use of Laboratory Animals" prepared by the Institute of Laboratory Animal Resources and published by the National Institutes of Health (NIH Publication No. 86-23, revised 1996).

Gross macroscopic and histological analyses of heart tissue

End of study analyses: At the end of the study period, animals were sacrificed and hearts harvested. Approximately half of the hearts from each treatment group were designated for gross macroscopic assessment and RNA extraction and half for histological assessment. Care was taken to distribute the animals such that baseline cardiac functional parameters were balanced between sacrifice sub-groups for all treatment groups.

Macroscopic analyses: Hearts were removed, cleaned and radially dissected from apex to base to flatten the sphere of the left ventricle. Photographs were taken macroscopically in order to determine infarct size by image analysis (custom software physioD3D[6]). Tissues were then rapidly flash-frozen in liquid nitrogen for total RNA extraction. Infarct size was calculated from macroscopic images as the surface area of white tissue, normalized to a ruler. Heart size was calculated as the surface area of the total tissue, normalized to a ruler. Percent infarct size was calculated as the surface area of the white tissue / total tissue surface area.

Histological analyses: After removing atria, hearts were bisected to separate apex and base, and each tissue block was submerged in Optimal Cutting Temperature compound (O.C.T.; ref.: KMA-0100-00A, Cell Path, Newtown, UK), frozen in liquid nitrogen and stored at -80°C until sectioning. Hearts were cryo-sectioned into 8-µm thin-sections and analysed for infarct size (Hematoxylin and Eosin staining), cardiomyocyte size, number of vessels per cardiomyocyte (WGA; ref: FL-1021-5, Cliniscience; Griffonia Simplicifolia Lectin-IsolectinB, diluted 1/20, ref: DL-1207, Clinisciences) and density of large vessels (Smooth Muscle Actin (SMA), diluted 1/400, ref: A5228, Sigma).

Transcriptomic analysis of heart tissue

To identify pathways that could have been activated by the transplanted cells or their secreted EV, total RNA was extracted from flash-frozen hearts (atria and outflow tracks removed). RNA was isolated by phenol-chloroform extraction using TRI REAGENT (ref.: T9424, Sigma-Aldrich, St. Louis, MO, USA) according to the manufacturer's instructions. Microarray experiments were performed on Affymetrix GeneChip® Mouse Transcriptome Array 1.0 (Affymetrix, Santa Clara, California, USA), a genome wide array with 25,336 probe sets. Raw data CEL files were imported in R/Bioconductor using the Oligo package (Reference: The R project for Statistical Computing [http://www.r-project.org/]). Expression levels were normalized using the RMA algorithm from the Affymetrix package and background noise was computed using a custom algorithm within R as follows:

Assuming that a maximum of 80% of genes are expressed on any given microarray, we considered the 20% of probes with the lowest intensity for each microarray as our initial background. A new background threshold was fixed at 2 standard deviations over the mean of these 20%. All probes on the microarray for which normalised intensities were lower than the computed threshold were designated as background for each array.

When comparing gene expression levels between two groups, a probe was included in the analysis if its intensity exceeded the background threshold in at least 80% of the animals from at least 1 group. To identify differentially expressed genes, we used the absolute difference in mean probe intensities. We also added a statistical significance in the amplitude filtering that was appropriate for this kind of comparison. We therefore examined the probes designated as background in both groups, calculated the absolute difference in intensities between groups and determined the standard deviation (SD) of the distribution of those differences. A threshold of the average plus 3 SD was established as the minimum intensity difference for significant differential gene expression. Group comparisons were done using Student's *t* test and lists were filtered at p <= 5%.

These experiments were performed on approximately half of the hearts of each group (PBS, n=9; iPSC-CM, n=10; iPSC-Pg, n=9, iPSC-Pg-EV n=10), selected such that baseline cardiac functional parameters were balanced between groups. Functional analyses were then carried out using Ingenuity Pathway Analysis (IPA, Qiagen, http://www.ingenuity.com).

Microarray experiments were performed by the *Plateforme Génomique* at the *Institut Cochin*, (INSERM U1016-CNRS UMR8104-Université Paris Descartes, Paris, France). Data were analysed at the *Plate-forme Bioinformatique* at *Imagine Institute, Hôpital Necker-Enfants Malades* (Paris Descartes University, US 024 SFR Necker). Microarray analyses have been submitted to, and validated by ArrayExpress (accession E-MTAB-5164).

Supplemental Results

Bioassay experiments

iPSC-Pg-EV promote survival of stressed cardiac cells

Extracellular vesicles derived from cardiovascular progenitors markedly increased the viability of rat cardiomyoblasts stressed by serum deprivation with survival increase trending towards significance at 5.3 x 10^9 EV for 250,000 seeded H9c2 cells (21,200 EV per target cell). To control for the possible confounding effects of contaminants coming from the culture media itself, such as residual bFGF, virgin complete media, was incubated 48 hours in coated culture flasks in the CO_2 incubator and ultracentrifuged; the bottom of the tube was then thoroughly rinsed with PBS in a volume equivalent to our iPSC-Pg-EV preparations and tested in an H9c2 survival assay. This preparation had no positive effect on cell survival (data not shown).

iPSC-Pg-EV have proangiogenic effects

Extracellular vesicles derived from cardiovascular progenitors increased migration of HUVEC in the scratch wound assay and this effect seemed again dose-dependent, trending towards significance at 1.00 x 10^9 EV per 15,000 plated HUVEC (67,000 EV per target cell) while a 80% invasion was reached at 1 x 10^{10} iPSC-Pg-EV per 15,000 seeded HUVEC cells (Figure 3). This response was highly reproducible over 3 three independent preparations of iPSC-Pg-EV. Likewise, iPSC-Pg EV increased tube formation in the Matrigel assay with total segment length reaching 750 pixels at a dose of 1 x 10^9 iPSC-Pg-EV per 15,000 seeded HUVEC, and number of nodes reaching 27 nodes at the same dose. Unlike for the scratch wound assay, this response did not appear to be dose-dependent.

iPSC-Pg-EV increase cardiomyocyte proliferation

Extracellular vesicles derived from cardiovascular progenitors isolated at day 2 of culture increased the rate of proliferating hESC-CM. Once again, the EV seemed to act through a dose-dependent mechanism reaching 35% of proliferative CM at 1.81 x 10^9 EV for 10,000 seeded cells (181,000 EV per target cell) whereas the basal proliferative rate was 15%. Above this EV dose, the pro-proliferative effect of EV seemed to decrease. Similar results were obtained with EV derived from hESC-CM at day 4 of iPS-Pg cell culture (data not shown).

Internalization experiments

Imaging flow cytometry showed internalization of calcein-AM-labelled EV into target cells and was also used to analyse cells directly labelled with calcein-AM. Fluorescence intensity for directly labelled cells was much greater; despite the laser intensity needing to be greatly reduced for this analysis, the fluorescence intensity remained superior to the other samples (Supplemental Figure 8-e7, 8-f7, 8-e8 and 8-f8). Visually, the aspect of these directly labelled cells also differs from the cells incubated with labelled EV. In the former, the fluorescence is present throughout the cell (Supplemental Figure 8-f7 and 8-f8), whereas for the latter, the fluorescence appears as strong punctate staining (Supplemental Figure 8-f4), suggesting the presence of fluorescently labelled bodies within or attached to the cell. This pattern of fluorescence was seen in 3 separate experiments using 3 independent preparations of iPSC-Pg-EV.

Confocal microscopy was utilised to determine whether EV were internalized in the cells or attached to the cell surface. Z-stack images were taken from the surface attached to the plate to the uppermost membrane. Scrolling through these images, it is apparent that the fluorescent staining is indeed within the cell body, including in slices traversing the nucleus, and is not associated with the cell surface. The image presented in Supplemental Fig 8 consists of a collapsed z-stack.

The internalization of labelled EV into their target cells was further tracked by fluorescence video microscopy. Analyses of video series finds that it takes approximately 10 min for a vesicle to be internalized that is, between the moment the EV is facing the cell and the moment when it crosses the cell membrane. Then, by tracking several labeled vesicles and by taking the average of the amount of time that they are seen inside the cell, we determined that vesicles remain inside the cell for approximately 12 to 14 hours. Interestingly, we observed that the vesicles move to the nucleus and we can see their disappearance inside of the nucleus. This is consistent with reports in the literature [7]. A representative fluorescence video is available in the Supplemental material online, Video S1. There was no observable difference in the number of internalized vesicles between stressed and unstressed cells.

MicroRNA content of EV

A comparison of the lists of miRNAs present in iPSC-Pg cells and their secreted iPSC-Pg-EV as determined by Affymetrix array, found that iPSC-Pg cells had a greater variety of miRNA species. This can be seen in the Venn diagram comparing the miRNAs in iPSC-Pg cells and iPSC-Pg-EV at or above an intensity threshold of 6 (Supplemental Figure 9) and on the left part of the sliding Venn diagram, where the number of miRNAs specifically found in iPSC-Pg and not in their EV (green line) exceeds the number specifically found in the iPSC-Pg-EV (blue line). The fact that there are any miRNAs present in the EV at these low thresholds that are not found in iPSC-Pg cells above the background suggests that some miRNAs are disproportionately packaged into EV. This assumption is also supported by the observation that at intensity thresholds between approximately 7.5 and 12.5, there is a greater number of miRNAs above the threshold in iPSC-Pg-EV than in their parent cells.

Among the 16 miRNAs which were broadly conserved across species, 11 have previously been reported to be stably present in the heart or cardiovascular cells (hsa-miR-17-5p, 20a-5p, 103a-3p, 107, 26a-5p, 23a-3p, 16-5p) or muscle cells (106a-5p, 93-5p, 24-3p, 191-5p)[8] and one, hsa-miR-103a-3p, was also reported as being stably present in EV[9].

Functional outcomes

Out of the 199 nude mice, 112 mice survived until the 3-week baseline echocardiographic assessment. Sixteen mice with EF>45% or with a posterior infarct were excluded (one mouse, who had an ejection fraction of 45.6% but had a large left ventricle (LVESV 39.8 µL) was included in the study). Of the included mice, 6 died between baseline examination and injection and 3 were excluded due to cachexia or excessive fibrosis impeding transcutaneous injections. One mouse died during intramyocardial injections and a further 14 died between injection and the end-of-study examinations. Thus, the study group included 72 mice at the final 7-week study time point: PBS (vehicle control, n=17); iPSC-CM cells ($1.4x10^6$ cells per mouse, n=19); iPSC-Pg cells ($1.4x10^6$ cells per mouse, n=17); and the iPSC-Pg-EV secreted by the same batch of iPSC-Pg cells over 48 hours (day 2-4 of culture; n=19). For this last group, each mouse received the equivalent number of EV as secreted by $1.4x10^6$ cells (approximately 2.4×10^{10} EV per mouse). For this iPSC-Pg-EV group, nine received freshly prepared EV, and the remaining ten received EV that had been frozen and stored at -80°C for several days. From the onset, mice were equitably allocated to four treatment groups such that baseline cardiac functional parameters were balanced between groups. Considering

only those animals surviving to the end of the study, ANOVA showed no baseline differences between groups (global p-values were not significant, with p = 0.55, 0.56 and 0.56 for baseline LVESV, LVEV and EF, respectively).

Transcriptomics of heart tissue

Gene expression profiles differed between groups. iPSC-Pg-EV-treated animals had slightly more genes in common with iPSC-Pg treated mice (37% of the iPSC-Pg-EV differential gene set) than with the iPSC-CM-treated mice (17% of the iPSC-Pg-EV differential gene set), perhaps reflecting the fact that iPSC-Pg-EV are directly derived from these cells. Few differentially expressed genes were common to all three groups (10% of the iPSC-Pg-EV differential gene set).

The Ingenuity Pathway Analysis program was first used to identify pathways specifically associated with the EV group (excluding any genes common to other treatment groups) and found them to predict overall cardioprotective effects. A second analysis including all differentially expressed genes within each group, including those common to two or more groups, was then performed and showed very similar results (Supplemental Figure 11).

Since we had some indication that the mice injected with iPSC-CM or iPSC-Pg cells had a variable response to treatment, we investigated whether there might be common differentially expressed genes between the iPSC-Pg and iPSC-Pg-EV 'responders' as compared to the PBS 'non-responders'. For this analysis, 'responders' were considered to be animals with LVESV improved by more than 5%, and 'non-responders' those with 5% or less improvement. These comparisons generated two new lists of genes: 856 differentially expressed genes in the iPSC-Pg-EV responders as compared to PBS non-responders, and 328 genes differentially expressed in the iPSC-Pg responders as compared to PBS non-responders. A list of 80 differentially expressed genes common to both lists was identified; however, these genes were not related to cardioprotective pathways.

Supplemental Tables

Supplemental Table 1. Antibodies for the characterisation of cultured cells

Antibodies	Dilution	Reference	Supplier	City	Country
MEF2C	1/50	ab79436	Abcam	Cambridge	UK
NKX2.5	1/50	ab35842	Abcam	Cambridge	UK
ISL1	1/500	ab20670	Abcam	Cambridge	UK
MHCαβ, clone: F26.2D11	1/10	MAB1552	Merck Millipore	Darmstadt	Germany
TNNI3	1/200	ab52862	Abcam	Cambridge	UK
ACTN2	1/500	A7811	Sigma Aldrich	Saint-Louis	MO, USA

Supplemental Table 2. qPCR primers for the characterisation of cultured cells

Gene	Forward (5'-3')	Reverse (5'-3')
NANOG	CTCAGCTACAAACAGGTGAAGA	GAGTAAAGGCTGGGGTAGGT
SOX2	AGGAGTTGTCAAGGCAGAGAA	TCCTAGTCTTAAAGAGGCAGCA
OCT3/4	ATCAAGCAGCGACTATGCAC	CCAGAGGAAAGGACACTGGT
ISL1	CCAGTCCAGAGAGACACGAC	AATTGACCAGTTGCTGAAAAGC
MEF2C	ATACCAGTGGGTGGGAAAGG	GTTGCTGAGGCAAATTGCAG
NKX2.5	ATGGTATCCGAGCCTGGTAG	ATGCAAAATCCAGGGGACTC
GATA4	GACACCCCAATCTCGATATGTT	GTTGCACAGATAGTGACCCG
TBX20	GCAGGAGGATGTTTCCAACC	GGACGATGTCCATCAGGACT
TNNT2	AATAGAGCCTGGCCTCCTTC	CCCCATTTCCAAACAGGAGC
PLN	CAGCTGCCAAGGCTACCTAA	CAGCAGGACAGGAAGTCTGA
h/MYH6	TGACATTGGTGCCAAGCAAA	GTTGGCAAGAGTGAGGTTCC
h/MYH7	AAAGGTCAAGGCCTACAAGC	TGTGGCAAAGCTACTCCTCAT
MYL2	GGGTGCTGAAGGCTGATTAC	GGTCAACCTCCTCCTTGGAA

Supplemental Figures and Legends

Supplemental Figure 1: **Characterisation of the differentiation state of iPSC-Pg and iPSC-CM at the end of the culture period.** qPCR analysis of iPSC-Pg confirm a gene expression pattern consistent with cardiovascular progenitors. iPSC-CM show a more fully differentiated gene expression profile. iPSC: n= 2; iPSC-Pg: n= 4; iPSC-CM: n = 2.

Supplemental Figure 2: **Characterisation by immunofluorescence of the differentiation state of iPSC-Pg at the end of the culture period.** At the end of the 4-day culture period, cells were harvested by trypsin treatment, cytospun onto glass slides, fixed and analysed by immunofluorescence for the presence of proteins consistent with cardiovascular progenitors. Microscopy confirms a protein expression pattern consistent with cardiovascular progenitors. Images taken with a 20X optical zoom. Scale bar = 50 μm

Supplemental Figure 3: **Characterisation by immunofluorescence of the differentiation state of iPSC-CM at the end of the culture period.** At the end of the 7-day culture period, cells were harvested by trypsin treatment, cytospun onto glass slides, fixed and analysed by immunofluorescence for the presence of proteins consistent with CM. Microscopy confirms a protein expression pattern consistent with CM. Images taken with a 20X optical zoom. Scale bar = 50 μm

Supplemental Figure 4: iPS-CM do not produce significant numbers of EV. iPS-CM were cultured for 24 hours in 1 - their standard media (iCell CM Maintenance Medium), 2 - in William's E supplemented with cocktail B, 3 - in Nutristem, and 4 - in DMEM + 0.5% BSA. Each condition was tested under both normoxic and hypoxic conditions (eight conditions in total). iPS-Pg were also cultured under normoxic and hypoxic conditions in their standard media, William's E + cocktail B. Conditioned media were harvested and ultracentrifuged, and the number of EV collected were quantified by NanoSight. None of the culture conditions led to significant production of EV by iPS-CM. By comparison, the production of EV by progenitors over the same duration of culture was three times fold higher than that of mature cardiomyocytes.

Supplemental Figure 5: Exosomal markers CD63 and CD81 are present in iPS-Pg-EV preparations. A total of $1x10^9$ EV from two different preparations were loaded onto a gel (EV1, EV2) as well as an equivalent volume of ultracentrifuged virgin media (VM) for Western blot analysis. (a) Anti-CD63 and (b) CD81 antibodies confirm the presence of these two exosome markers in the EV preparations and their absence from the virgin media control, confirming the presence of exosomes in our EV preparations.

Supplemental Figure 6: The effect of EV on H9c2 viability is independent of virgin media components. In order to determine whether any of the effect of the EV seen in the H9c2 pro-survival assay could be due to contaminating components in the media itself, virgin media was ultracentrifuged in parallel to conditioned media, resuspended and loaded into the H9c2 pro-survival assay. While the EV secreted by iPS-Pg show a strong effect on H9c2 survival, the virgin media preparation did not increase cell survival above the basal level of the negative control. This confirms that the effects of the EV preparations are due to factors secreted by the cells and not due to the media components such as growth factors.

Supplemental Figure 7: iPSC-Pg-EV stimulate endothelial cell tube formation. The potential for iPSC-Pg-EV to trigger HUVEC activation was evaluated by a tube formation assay. At T = 24 hours, the positive control (complete media) led to extensive tube formation (dark grey bars in a and b, panel c), whereas no tubes were formed in the negative control (poor media; light grey bars in a and b, panel d). Tube formation was detected when HUVEC were cultured in poor media + iPSC-Pg-EV with an increased total segment length and number of nodes (blue bars in a and b; panel e) as compared to the negative control. Each condition was evaluated in triplicate and in 3 independent experiments, using 3 independent EV preparations. Only the maximum dose was evaluated in triplicate in a single experiment. Unlike for the scratch wound assay, the effects of EV on tube formation do not appear to be dose-dependent

Supplemental Figure 8: Internalisation of calcein-AM-labelled iPSC-Pg-EV. (a-b) iPSC-Pg-EV were labelled with calcein-AM for 1h at a final concentration of 2µM and visualised by ImageStream imaging flow cytometry. (a) The histogram showing the frequency of fluorescence intensities of calcein-labelled EV confirms that a large proportion of these EV are fluorescent. (b) Three representative ImageStream images illustrate that green fluorescence intensity varies among individual labelled EV. EV smaller than 300 nm (such as exosomes) are not visible in the brightfield (limit of detection) but can still be detected in channel 02 if they are fluorescently labelled, as in the second EV illustrated. (c-f) ImageStream analysis determined that serum deprived H9c2 cells, incubated for 20 hours with calcein-labelled iPSC-Pg-EV (condition 4), were more fluorescent than any of the negative controls. (c) ImageStream selection of cell population. (d) Gating by focus. (e) Over-layed histograms of the frequency of green fluorescence intensities for control and test conditions. (f) Representative ImageStream images of individual cells from each control and test condition. (e-f) *Negative controls:* 1- complete medium; 2- poor medium; 3- poor medium + unlabelled-FBS-EV; 5- poor medium + unlabelled-iPSC-Pg-EV; 6- poor medium + wash. *Positive controls:* 7- cells incubated in poor medium with unlabelled-FBS-EV and directly labelled with 1µM calcein AM from T_{19h}-T_{20h}; 8- cells incubated in poor medium with unlabelled-FBS-EV and directly labelled with 1µM calcein AM from T_0-T_{20h}. *Test condition:* 4- H9c2 cells incubated with poor medium + calcein AM-labelled-iPSC-Pg-EV. (g-i) Internalization of calcein AM labelled-iPSC-Pg-EV in H9c2 cells was then confirmed by confocal microscopy. iPSC-Pg-EV were labelled with 2µM calcein AM for 1h and incubated with H9c2 cells for 20 hours. Cells were cultured on glass slides, stained with WGA and counterstained with DAPI and visualized by confocal microscopy (63X). Green fluorescence-labelled-iPSC-Pg-EV were located within the cytoplasm of many cells, suggesting that they are indeed internalized by these target cells. (g) H9c2 and labelled iPSC-Pg-EV, (h) H9c2 and non-labelled iPSC-Pg-EV, (i) H9c2 and wash to control for possible contaminating free calcein-AM.

Supplemental Figure 9: Evidence that miRNA are specifically packaged into EV. In 3 separate experiments, the percentage of miRNAs among the small RNAs in a) iPSC-Pg cells was much less than in b) their secreted EV as shown by bioanalyser. c) The expression level of individual miRNAs was then analysed by miRNA array. Here, the number of miRNAs

expressed as a function of intensity threshold present only in iPSC-Pg (SpePg, green line), only iPSC-Pg-EV (SpeEV, blue line), or in both iPSC-Pg cells and iPSC-Pg-EV (Common, orange line) is tracked from a low intensity threshold to a high intensity threshold. Venn diagrams at two distinct thresholds, 6 and 9, are pictured where green areas represent the number of miRNAs specifically found in iPSC-Pg cells at intensities above the threshold. Similarly, blue areas represent the number of miRNAs specifically in the iPSC-Pg-EV. The orange areas represent the miRNAS present in both cells and EV.

Supplemental Figure 10: Gross macroscopic and histological analyses of hearts explanted seven weeks after treatment revealed no significant difference between groups. Gross macroscopic examination: a) Total surface area of the left ventricle normalised to a ruler (arbitrary units) and b) relative infarct size (% surface area). Immunofluorescence staining: c) capillary density expressed as number of capillaries per CM, d) arteriolar density (x 10^{-6} arteriols per mm^2, and e) cardiomyocyte size in the peri-infarcted zone (x 10^{-4} mm^2).

Supplemental Figure 11: Heat map of differential functions by group – full gene lists. Differentially expressed genes from each treatment group were assessed by Ingenuity to predict upregulated (warm colours) and downregulated (cool colours) diseases and biological functions as compared to PBS controls. Each column examines all genes differentially expressed in the indicated treatment group when compared to the control PBS group (left - iPSC-CM, middle – iPSC-Pg, right – iPSC-Pg-EV). iPSC-Pg-EV-treated hearts were the most enriched for functions consistent with increased cell proliferation/growth, cardiogenesis and vessel formation. The list is sorted to have the greatest difference in enrichment between the EV group and the other groups at the top of the list. This list was truncated after the 93rd line.

Supplemental References

1. Drowley L, Koonce C, Peel S, Jonebring A, Plowright AT, Kattman SJ, Andersson H, Anson B, Swanson BJ, Wang Q-D, Brolen G. Human Induced Pluripotent Stem Cell-Derived Cardiac Progenitor Cells in Phenotypic Screening: A Transforming Growth Factor-β Type 1 Receptor Kinase Inhibitor Induces Efficient Cardiac Differentiation. *Stem Cells Transl Med* 2016;**5**:164–174.

2. Drawnel FM, Boccardo S, Prummer M, Delobel F, Graff A, Weber M, Gérard R, Badi L, Kam-Thong T, Bu L, Jiang X, Hoflack J-C, Kiialainen A, Jeworutzki E, Aoyama N, Carlson C, Burcin M, Gromo G, Boehringer M, Stahlberg H, Hall BJ, Magnone MC, Kolaja K, Chien KR, Bailly J, Iacone R. Disease modeling and phenotypic drug screening for diabetic cardiomyopathy using human induced pluripotent stem cells. *Cell Rep* 2014;**9**:810–821.

3. Cunningham TJ, Yu MS, McKeithan WL, Spiering S, Carrette F, Huang C-T, Bushway PJ, Tierney M, Albini S, Giacca M, Mano M, Puri PL, Sacco A, Ruiz-Lozano P,

Riou J-F, Umbhauer M, Duester G, Mercola M, Colas AR. Id genes are essential for early heart formation. *Genes Dev* 2017; Aug 9. doi: 10.1101/gad.300400.117. [Epub ahead of print]

4. Headland SE, Jones HR, D'Sa ASV, Perretti M, Norling LV. Cutting-edge analysis of extracellular microparticles using ImageStream(X) imaging flow cytometry. *Sci Rep* 2014;**4**:5237.

5. Kervadec A, Bellamy V, El Harane N, Arakélian L, Vanneaux V, Cacciapuoti I, Nemetalla H, Périer M-C, Toeg HD, Richart A, Lemitre M, Yin M, Loyer X, Larghero J, Hagège A, Ruel M, Boulanger CM, Silvestre J-S, Menasché P, Renault NKE. Cardiovascular progenitor-derived extracellular vesicles recapitulate the beneficial effects of their parent cells in the treatment of chronic heart failure. *J Heart Lung Transplant* 2016;**35**:795–807.

6. Balvay D, Troprès I, Billet R, Joubert A, Péoc'h M, Cuenod CA, Le Duc G. Mapping the zonal organization of tumor perfusion and permeability in a rat glioma model by using dynamic contrast-enhanced synchrotron radiation CT. *Radiology* 2009;**250**:692–702.

7. Vanacova S, Stefl R. The exosome and RNA quality control in the nucleus. *EMBO Rep* 2007;**8**:651–657.

8. Mentzel CMJ, Skovgaard K, Córdoba S, Herrera Uribe J, Busk PK, Cirera S. Wet-lab tested microRNA assays for qPCR studies with SYBR® Green and DNA primers in pig tissues. *MicroRNA* 2014;**3**:174–188.

9. Akers JC, Ramakrishnan V, Kim R, Skog J, Nakano I, Pingle S, Kalinina J, Hua W, Kesari S, Mao Y, Breakefield XO, Hochberg FH, Van Meir EG, Carter BS, Chen CC. MiR-21 in the extracellular vesicles (EVs) of cerebrospinal fluid (CSF): a platform for glioblastoma biomarker development. *PloS One* 2013;**8**:e78115.

Supplemental Figure 1

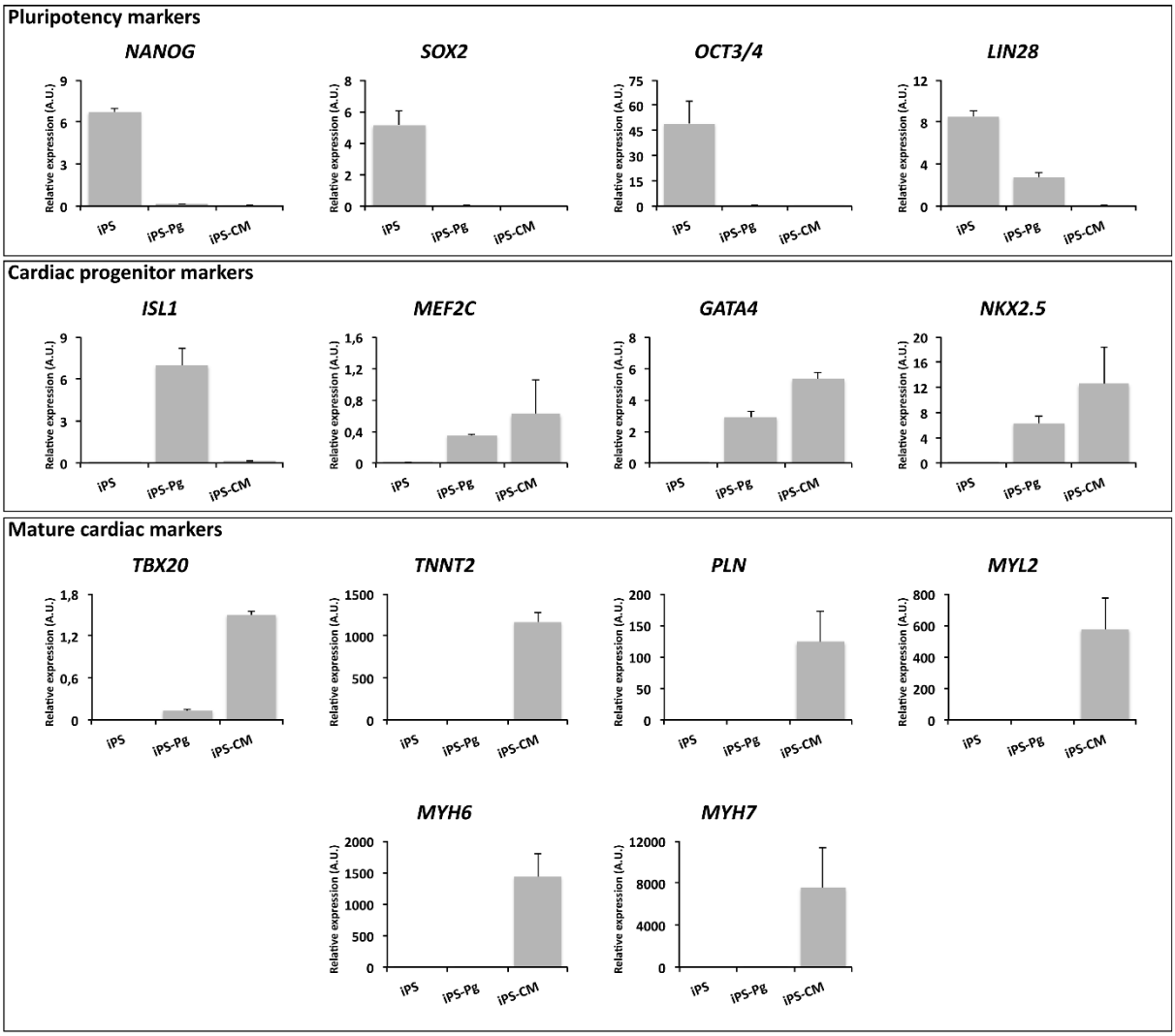

Supplemental Figure 2

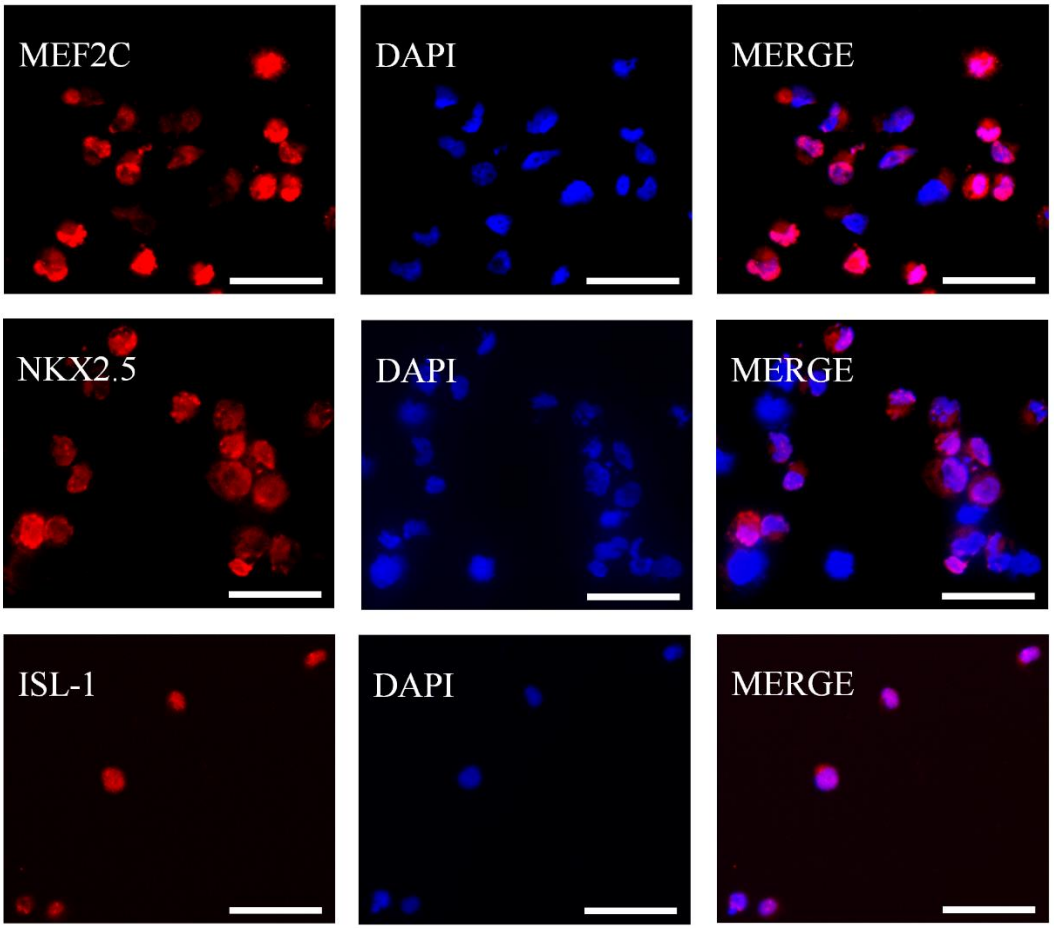

Supplemental Figure 3

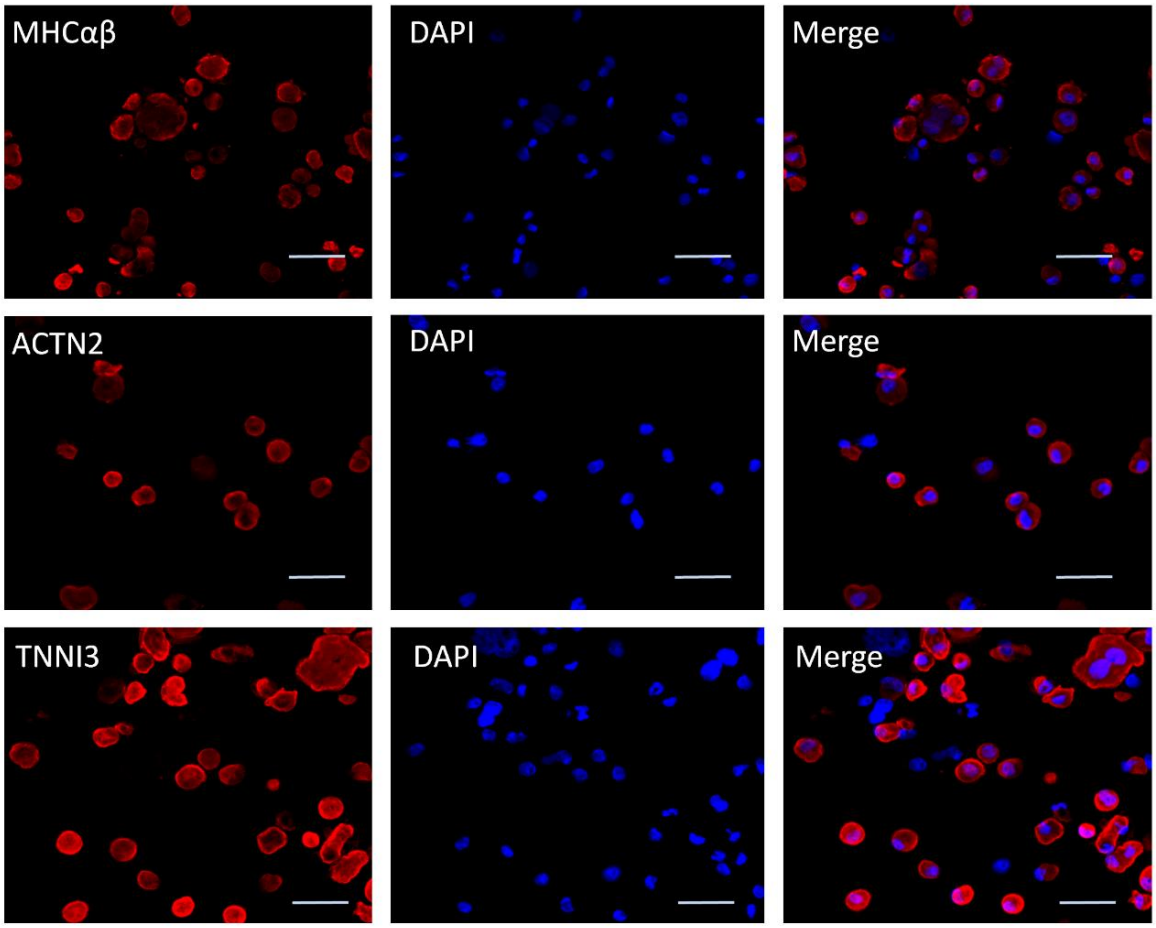

Supplemental Figure 4

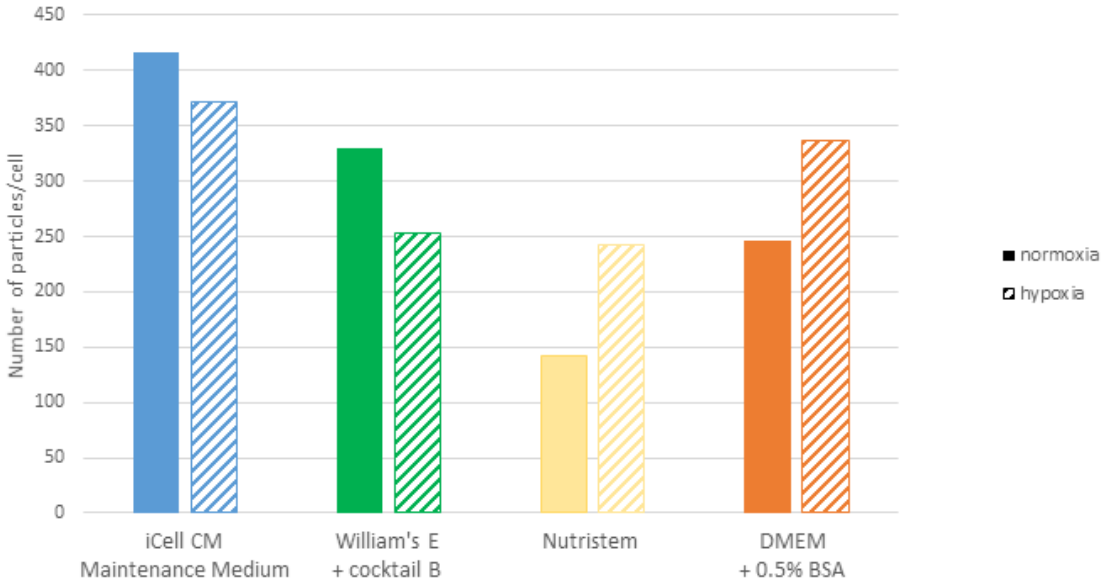

Supplemental Figure 5

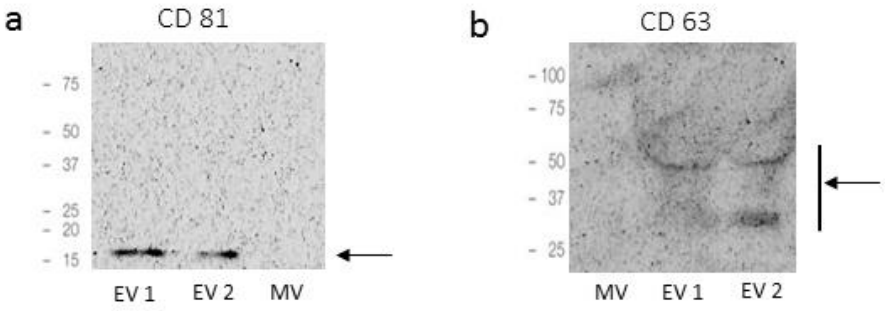

Supplemental Figure 6

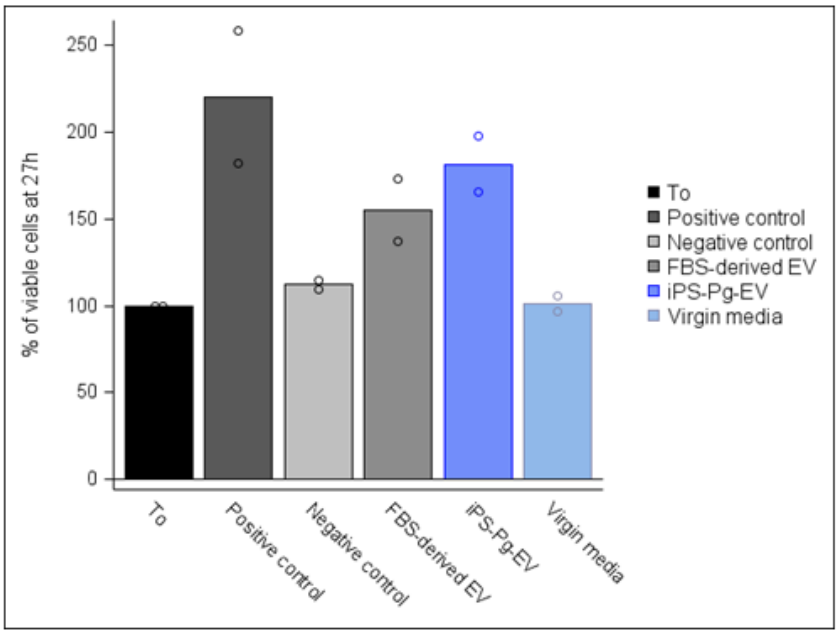

Supplemental Figure 7

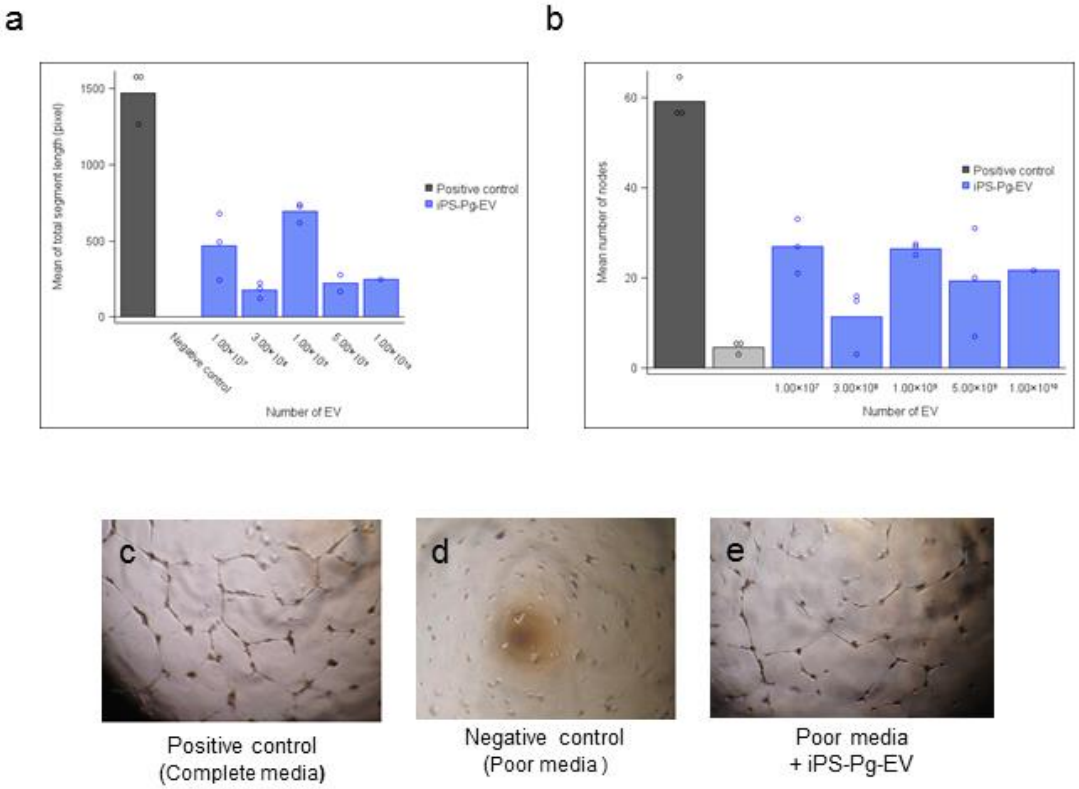

Supplemental Figure 8

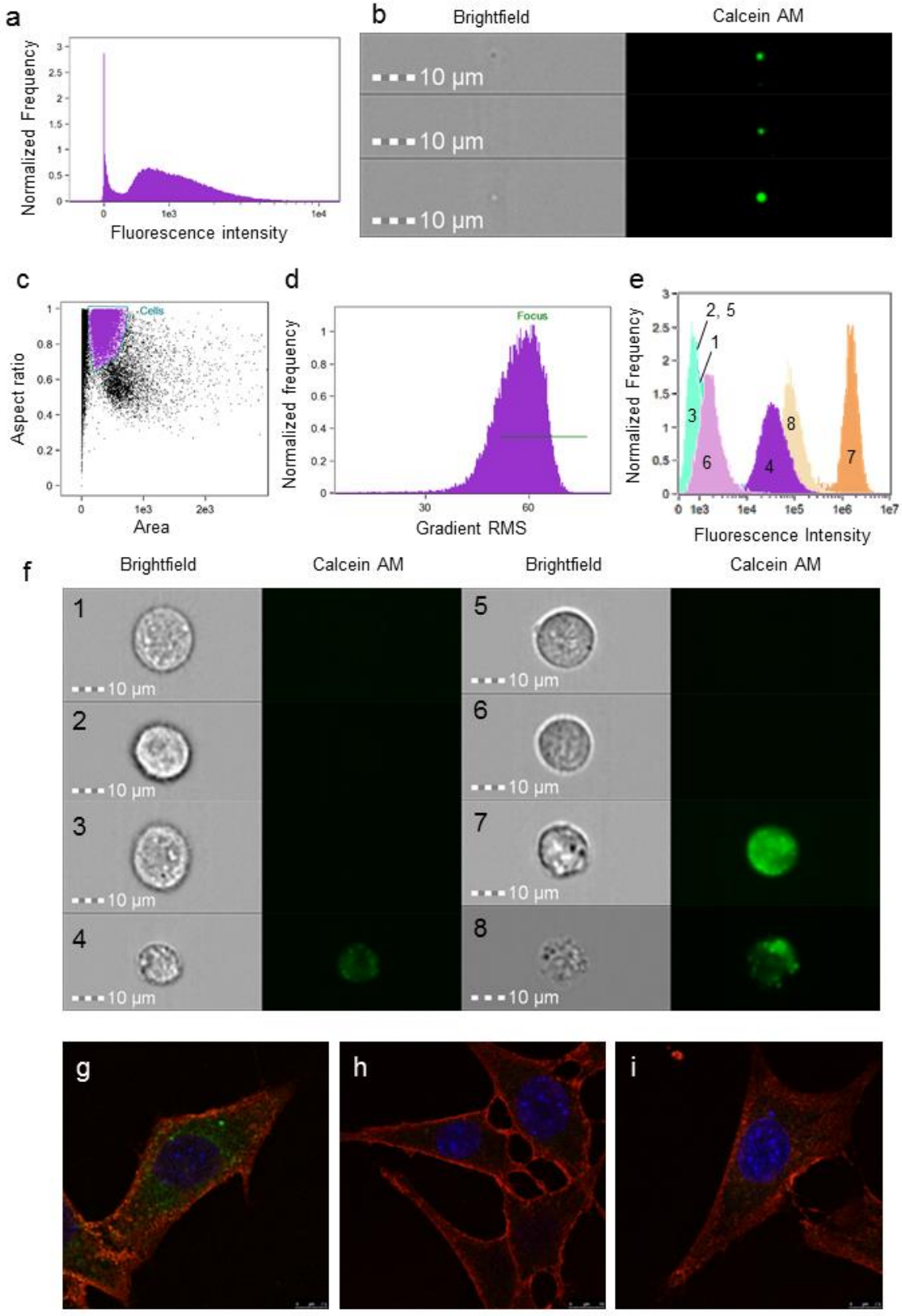

Supplemental Figure 9

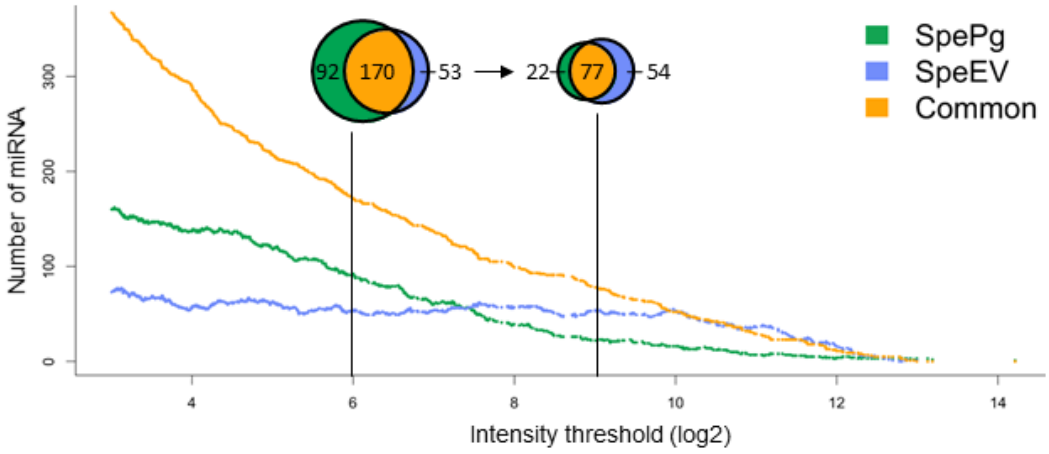

Supplemental Figure 10

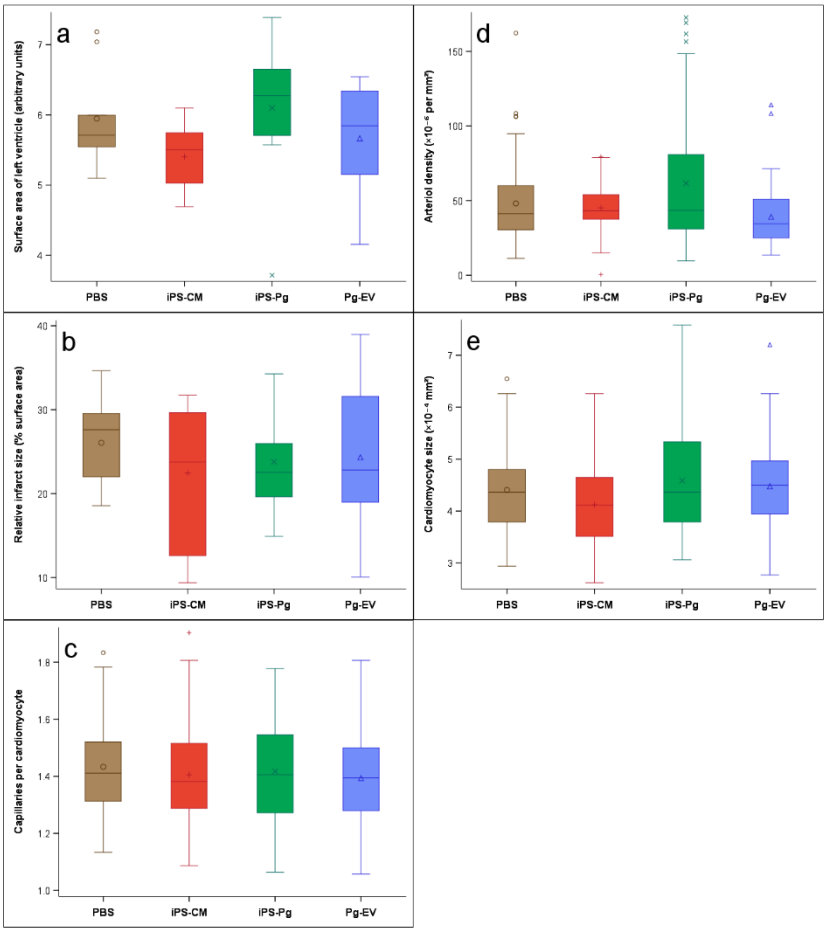

Supplemental Figure 11

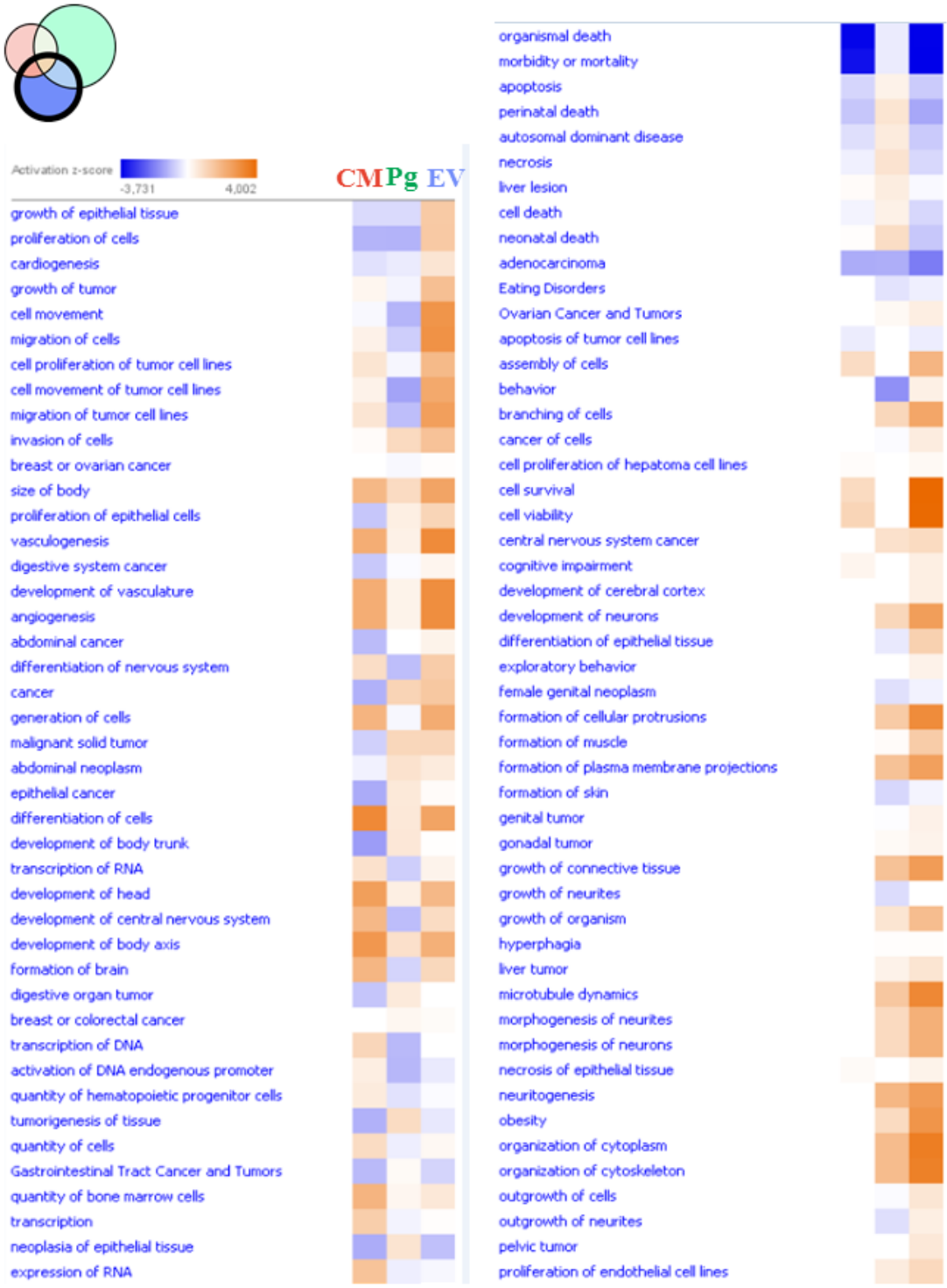

EV internalization video



Merged dmem +ev vf film (1).avi

HAL
archives-ouvertes.fr

Extracellular vesicles from human cardiovascular progenitors trigger a reparative immune response in infarcted hearts

Bruna Lima Correa, Nadia El Harane, Ingrid Gomez, Hocine Rachid Hocine, José Vilar, Manon Desgres, Valérie Bellamy, Kamaleswaran Keirththana, Chloé Guillas, Maria Perotto, et al.

▶ **To cite this version:**

Bruna Lima Correa, Nadia El Harane, Ingrid Gomez, Hocine Rachid Hocine, José Vilar, et al.. Extracellular vesicles from human cardiovascular progenitors trigger a reparative immune response in infarcted hearts. Cardiovascular Research, Oxford University Press (OUP), 2020, pp.cvaa028. 10.1093/cvr/cvaa028 . inserm-02563336

HAL Id: inserm-02563336
https://www.hal.inserm.fr/inserm-02563336

Submitted on 5 May 2020

HAL is a multi-disciplinary open access archive for the deposit and dissemination of scientific research documents, whether they are published or not. The documents may come from teaching and research institutions in France or abroad, or from public or private research centers.

L'archive ouverte pluridisciplinaire **HAL**, est destinée au dépôt et à la diffusion de documents scientifiques de niveau recherche, publiés ou non, émanant des établissements d'enseignement et de recherche français ou étrangers, des laboratoires publics ou privés.

Extracellular vesicles from human cardiovascular progenitors trigger a reparative immune response in infarcted hearts

Bruna Lima Correa [1†], Nadia El Harane[1†], Ingrid Gomez[1], Hocine Rachid Hocine[2], José Vilar[1],Manon Desgres[1], Valérie Bellamy[1], Keirththana Kamaleswaran [1], Chloé Guillas[1], Maria Perotto[1], Laetitia Pidial[1], Paul Alayrac[1], Thi Tran[1], Sisareuth Tan[3], Thomas Hamada[1], Dominique Charron[5], Alain Brisson[3], Nisa K. Renault[4], Reem Al-Daccak[5], Philippe Menasché[1,6*], and Jean-Sébastien Silvestre[1*]

1. INSERM UMRS 970, Paris Centre de Recherche Cardiovasculaire (PARCC), Université de Paris, 56, rue Leblanc, F-75015 Paris,
France;
2. Institut Curie, F-75005 Paris, France;
3. UMR-CBMN, CNRS—Université de Bordeaux—IPB, F-33600 Pessac, France;
4. Fujifilm Cellular Dynamics Inc, Madison, WI 53711, USA;
5. INSERM, UMRS-976, Hôpital Saint-Louis, F-75015 Paris, France; and
6. Department of Cardiovascular Surgery, Hôpital Européen Georges Pompidou, 20, rue Leblanc, F-75015 Paris, France

**.Corresponding authors.*
Tel: +33(0)1 56 09 36 22; fax: +33(0)1 56 09 32 61, E-mail:philippe.menasche@aphp.fr (P.M.);
Tel: +33 (0)1 53 98 80 60; fax: +33(0) 1 53 98 79 51, E-mail: jeansebastien.silvestre@inserm.fr (J.-S.S.)
†. The first two authors contributed equally to the study and are co-first authors

Abstract

The cardioprotective effects of human induced pluripotent stem cell-derived cardiovascular progenitor cells (CPC) are largely mediated by the paracrine release of extracellular vesicles (EV). We aimed to assess the immunological behaviour of EV-CPC, which is a prerequisite for their clinical translation. Flow cytometry demonstrated that EV-CPC expressed very low levels of immune relevant molecules including HLA Class I, CD80, CD274 (PD-L1), and CD275 (ICOS-L); and moderate levels of ligands of the natural killer (NK) cell activating receptor, NKG2D. In mixed lymphocyte reactions, EV-CPC neither induced nor modulated adaptive allogeneic T cell immune responses. They also failed to induce NK cell degranulation, even at high concentrations. These *in vitro* effects were confirmed *in vivo* as repeated injections of EV-CPC did not stimulate production of immunoglobulins or affect the interferon (IFN)-γ responses from primed splenocytes. In a mouse model of chronic heart failure, intra-myocardial injections of EV-CPC, 3 weeks after myocardial infarction, decreased both the number of cardiac pro-inflammatory Ly6Chigh monocytes and circulating levels of pro-inflammatory cytokines (IL-1α, TNF-α, and IFN-γ). In

a model of acute infarction, direct cardiac injection of EV-CPC 2 days after infarction reduced pro-inflammatory macrophages, Ly6Chigh monocytes, and neutrophils in heart tissue as compared to controls. EV-CPC also reduced levels of pro-inflammatory cytokines IL-1α, IL-2, and IL-6, and increased levels of the anti-inflammatory cytokine IL-10. These effects on human macrophages and monocytes were reproduced *in vitro*; EV-CPC reduced the number of pro-inflammatory monocytes and M1 macrophages, while increasing the number of anti-inflammatory M2 macrophages.

EV-CPC do not trigger an immune response either in *in vitro* human allogeneic models or in immunocompetent animal models. The capacity for orienting the response of monocyte/macrophages towards resolution of inflammation strengthens the clinical attractiveness of EV-CPC as an acellular therapy for cardiac repair.

Keywords: Acellular therapies, Heart Failure, Extracellular vesicles, Immunomodulatory effects

Introduction

Despite therapeutic improvements, chronic heart failure still carries a poor prognosis with a 5-year mortality averaging 50% [1]. When drug-based regimens are no longer effective, heart transplantation or mechanical assist devices may be indicated, but their invasiveness and limitations call for alternate options, include cell therapy. Even though, so far, cell therapy trials have largely failed to significantly improve patient outcomes, they have provided some insights into the mechanism of action of transplanted cells which appears to be predominantly mediated by paracrine signaling [2]. This concept is largely based on the observations that the secretome, including extracellular vesicles (EV), is as effective as the parent therapeutic cells in the treatment of experimental cardiomyopathies [3,4]. We have previously shown, in a mouse model of chronic heart failure, that EV released by embryonic stem cell derived cardiovascular progenitor cells (CPC) [5] and EV released by induced pluripotent stem cells (iPSC) derived CPC [6] were therapeutically effective. Others have shown this to be the case for the secretome of other cell types, primarily mesenchymal stem cells [7,8] and cardiac stem cells [9,10].

Extracellular vesicles are membrane-bound particles ranging in size from less than 100 nm to 1 µm and found in all biological fluids and conditioned media [11]. They are composed of a bi-lipid membrane, similar to the cell membrane, which encloses an aqueous, nucleus-free compartment, harboring mRNAs, microRNAs, proteins, lipids, and other bioactive molecules [12–16]. Although a consensus has not yet been reached on specific markers of EV subtypes, EV can be characterized by the expression of proteins like the tetraspanins (CD9, CD63 and CD81) and integrins while additional features of their profile depend on the phenotype of the parent cell [17–20]. Furthermore, while the molecular mechanisms underpinning the cardio-protective effects of EV are still under investigation, the therapeutic potential of EV likely relies on pleiotropic effects including angiogenesis, modulation of the inflammatory environment and, possibly, activation of cardiac intrinsic regenerative pathways[5,6,21–24].

Yet, to the best of our knowledge, most of the studies investigating the cardio-reparative effects of human EV have been conducted in immune-deficient experimental animal models. Although these studies provide valuable mechanistic insights, a more clinically relevant assessment of the immune

effects of EV, which is a prerequisite for their potential clinical use, requires their exposure to human cells and the use of immune-competent animal models. In the present study, we used tailored allogeneic *in vitro* human cell assays and immunocompetent mouse models of myocardial infarction (MI) to investigate the immune effects of EV derived from human CPC.

Material and Methods

Detailed Material and Methods are given in the Supplemental Material.

Ethics section

All procedures were approved by the Institutional Ethics Committee from the *Université de Paris-Descartes* (project #04073.01) and comply with European legislation (European Commission Directive 2010/63/EU) on animal care. All animals received humane care in compliance with the "Principles of Laboratory Animal Care" formulated by the National Society for Medical Research and the "Guide for the Care and Use of Laboratory Animals" prepared by the Institute of Laboratory Animal Resources and published by the National Institutes of Health (NIH guidelines). All animals received anesthesia by isoflurane (2.5L/min isoflurane at 1.5L/min of O_2) and were euthanized by dolethal injection at 140mg/kg. For *in vitro* tests with human cells, blood donors signed an informed consent and all methods and experimental protocols were approved by the institutional Ethics Committee (*Hôpital St. Louis*, Paris, France) and conducted in accordance with guidelines and regulation outlined in the Declaration of Helsinki.

Cell culture, EV preparation, quantification and characterization

a) Cell Culture and cell characterization

Cardiovascular progenitor cells differentiated from human iPSC (iCell® Cardiac Progenitor Cells, Cellular Dynamics International, Madison, WI) were cultured according to the manufacturer's directions (for a detailed protocol, see Supplementary Material). After 4 days of culture, cells were harvested and immune-phenotyped with antibodies against relevant immune molecules using fluorescence-activated cell sorting (FACS) (CANTO-II Flow Cytometer, BD Bioscience, DIVA and FlowJo software).

For human cell *in vitro* experiments, human peripheral blood mononuclear cells (PBMC) were prepared from blood samples from healthy donors using Ficoll gradient (Eurobio) centrifugation and cryopreserved for later use.

b) EV isolation

Conditioned media were collected, pre-cleared by centrifugation for 6 minutes at 1,200*g* and EV were pelleted by ultracentrifugation (rotor 70Ti-Beckman) for 16 hours at 100,000*g*.

c) EV quantification and characterization

Extracellular vesicles were quantified by Nanoparticle Tracking Analysis (NanoSight LM-14, Malvern) and characterized by FACS [25] after coupling with latex beads (Life Technologies, A37304) using a MACSplex kit (MACSPlex Exosome Kit human, Miltenyi Biotech) as follows to phenotype their membrane ligands.

In a second time, EV (25 µg of protein) were mixed with 4-µm Aldehyde/Sulfate Latex Beads at room temperature (RT); then suspended in Phosphate-Buffered Saline (PBS) and left at RT for another 2h. The coupling reaction was terminated by 100 mM glycine, and the mixture was centrifuged at 1,500 x g. The beads were then stained with conjugated antibodies for the relevant markers and analyzed by FACS.

Ultimately immuno-gold labeling and cryo-transmission electron microscopy (cryo-TEM) were also performed on EV. Gold nanoparticles (NP) were conjugated with an anti-CD81 monoclonal antibody (mAb) following procedures previously described [26]. Samples of EV were used either pure or diluted 10-fold with a HEPES ((4-(2-hydroxyethyl)-1-piperazineethanesulfonic acid)-buffered saline containing 150 mM NaCl and 10 mM HEPES, pH 7.4. Samples were then labeled for 1 h with 10-nm anti-CD81-gold-NP at 1-3 × 10^{15} gold-NP/L, at RT. Immuno-gold labeled samples were processed for cryo-TEM as follows. A 4-µL aliquot was deposited on an electron microscopy (EM) grid coated with a perforated carbon film. After draining the excess liquid with a filter paper, grids were quickly plunged into liquid ethane using a Leica EMCPC cryo-chamber, transferred to cryo-boxes and stored under liquid nitrogen until TEM observation. For cryo-TEM observation, grids were mounted onto a Gatan 626 cryoholder and transferred to a Tecnai F20 microscope (FEI) operated at 200 kV. Images were recorded with a USC1000-SSCCD camera (Gatan). These experiments were performed to best match the minimal Information for Studies of Extracellular Vesicles ("MISEV") guidelines[27].

On the basis of a previous study[6] in which the cardioprotective effects of 1.4x10^6 CPC could be recapitulated by delivering the amount of EV they had secreted in 48 hours, we selected in the present study the same EV dose which equates here to 1x10^{10} particles (100 µg of protein) concentrated in a 50-60µL-volume.

Allogeneic immune responses and immunomodulation assays

Tailored mixed lymphocyte reactions (MLR) were performed using PBMC from different donors. Briefly, responding PBMC ($1x10^5$ cells) were labeled with 2.5 µM carboxyfluorescein succinimidyl ester (CFSE, Thermofisher Scientific) and then co-cultured in Roswell Park Memorial Institute (RPMI) medium supplemented with 10% Fetal Bovine Serum (FBS, Gibco Life Technologies) in U-bottom 96-well plates (VWR) with human leukocyte antigen mismatched (HLA) mitomycin-C-treated (Sigma) stimulatory PBMC ($1x10^5$ cells), mitomycin-C-treated CPC (at CPC:PBMC ratios of 1:5 and 1:10), or increasing doses of EV (EV1: $5.5x10^8$, EV2: $5.5x10^9$ or EV3: $1.7x10^{10}$ particles) or PBS as a control. After 6 days of co-culture, cells were harvested and stained with anti-CD3-PE/Cy7, anti-CD4-APC, anti-CD8-APC-H7 antibodies and 7AAD (BD Biosciences). Proliferation and cell death of T-cell subsets were monitored by FACS.

In assays determining the immunomodulatory effects of CPC and EV-CPC, HLA-mismatched CFSE-labeled PBMC ($1x10^5$ cells) were stimulated with 1 µg/mL phytohemagglutinin (Sigma-Aldrich) in the presence or absence of mitomycin-C-treated CPC (at CPC: PBMC ratios of 1:5 and 1:10) or with increasing concentrations of EV (EV1: $5.5x10^8$, EV2:$5.5x10^9$ or EV3: $1.7x10^{10}$ particles) for 5 days. At the end of the co-culture, the proliferation and death rate of the T cells were monitored by FACS.

Natural killer cell degranulation

Natural Killer (NK) cells were isolated from PBMC by negative selection using immune-magnetic cell sorting (Miltenyi Biotech, Germany) according to the manufacturer's instructions. Experiments were conducted with NK cells primed overnight with recombinant human interleukine (Il), IL-15 (50 ng/mL) (Sigma) in RPMI medium supplemented with 10% FBS to ensure their proper expression of NK cell activating receptors and functionality. Cytokine-activated NK cells were cultured alone or in the presence of K562 cells used as positive controls (ATCC, USA), CPC (ratio 1:1) or increasing doses of EV ($5.5x10^8$; $5.5x10^9$ or $1.7x10^{10}$ particles) and labelled with an anti-CD107a-PE antibody (BD Bioscience). After 18 hours, cells were harvested, washed and stained with CD3-APC-H75R (BD Bioscience) and CD56-APC specific antibodies (BD Bioscience), and the expression of CD107a was analyzed on $CD3^-CD56^+$ NK cells by FACS.

Macrophage polarization assay

PBMC from healthy donors were suspended at a concentration of 100 million cells per mL in Monocyte Attachment Medium (Promocell) and seeded at a density of 1 million viable cells/cm^2 with a monocyte content ≥25% and 1.5 million viable cells/cm^2 for a monocyte content of <25% (4 million cells per P24-well). At day 0, monocytes were incubated for 90 min at 5% CO_2 and 37°C to allow adherence. Non-adherent cells were discarded by vigorously swirling the culture and aspirating the supernatant. Adherent cells were then washed and the appropriate amount of complete M0, M1, M2 Macrophage Generation Medium (Promocell) was added to the cells for 6 days. Under these conditions, monocytes differentiate into M1-like or M2-like polarized macrophages. After 6 days, the culture medium was replaced with fresh complete M0, M1, M2 Macrophage Generation Medium DXF with or without EV ($5.5x10^9$ particles per well). Macrophages were then incubated for another 2 days at 37°C and 5% CO_2. At day 8, the culture medium was supplemented with IFN-γ (50 ng/mL) and LPS (10 ng/mL) for M1 macrophage polarization, with 20 ng/mL IL-4 and 20ng/mL IL-13 for M2 macrophage polarization (all from Merck) or with macrophage colony-stimulating factor (MCSF) medium for M0 macrophages. Each of these conditions was exposed or not to EV ($5.5x10^9$ particles per well). The next day (D9), cells were detached with the Macrophage Detachment Solution DXF (Promocell) for 45 min at RT. Monocytes and macrophages were analyzed at day 9 of culture, after polarization and exposure to EV, as described above. They were suspended in MACSBuffer (Milteny), centrifuged for 10 min at 500 x g, counted and labelled at 200,000 cells per condition with anti-CD64 PE, anti-CD68 PE-Cy7, anti-CD80 PE-Cy5, anti-CD86 APC or BV605, anti-CD163 BV421, anti-CD206 BV711 and anti-CD14 FITC ((Fluorescein isothiocyanate) antibodies (all from BD Biosciences). Monocytes and macrophages were categorized by the following markers: Monocytes:CD14+; Pro-inflammatory monocytes: CD14+, CD86++; Macrophages: CD64+, CD68+; M1: CD64+, CD68+, CD80+, CD86+; M2a: CD64+, CD68+, CD206+; M2b: CD64+, CD 68+, CD163+. All antibodies were used at a dilution of 1:100. After incubation, cells were washed and suspended in 100 µL of MACS Buffer for FACS analysis. Events were acquired on a Fortessa X20 flow cytometer (BD Biosciences); results were analyzed with FlowJo software (FlowJo V10.4.2, FlowJo LLC) and are given as a percentage of the whole population. Experiments were performed in technical triplicates for each donor.

Bead-based multiplex immunoassay

A bead-based multiplex immunoassay (Bio-Rad) was used to measure the levels of multiple cytokines [basic Fibroblast Growth Factor, Eotaxin, G-CSF, GM-CSF, IFN-γ, IL-1β, IL-1ra, IL-2, IL-4, IL-5, IL-6, IL-7, IL-8, IL-9, IL-10, IL-12 (p70), IL-13, IL-15, IL-17A, IP-10, MCP-1 (MCAF), MIP-1α, MIP-1β, PDGF-BB, RANTES, Tumor Necrosis factor-alpha (TNF-α), and VEGF] from supernatants of macrophage cultures at day 9. Concentration were calculated using a standard curve (5 PL regression, with Bio-Plex Manager™ software).

Immunoglobulin assay following EV treatment

To assess whether EV-CPC could induce antibody production, mice were subcutaneously injected at day 1, 13 and 20 with either EV (n=5, at the dose of $1x10^{10}$ particles per injection) or PBS (n=5) according to a classical immunization protocol[28]. Blood samples were collected at days 10, 20 and 30 post injection. Ig isotypes in plasma were qualitatively detected using the mouse immunoglobulin isotyping ELISA kit (ThermoFisher Scientific).

Enzyme-linked immunospot

The enzyme-linked immunospot (ELISPOT) is a sensitive technique for the detection of cytokine-producing cells at the single cell level. The IFN-γ ELISPOT (Diacole) method was used for measuring the antigen-specific response to EV-CPC elicited by NK cells, T cells, antigen-specific Th1 $CD4^+$ and $CD8^+$ effector T cells. Primed splenocytes of each vaccinated mouse were isolated, plated (at a seeding density of 1.5 million cells/cm^2 in 96-well plates), and re-exposed to either EV ($2x10^9$ particles) or PBS *in vitro* for 21h; the positive control was a mixed solution of phorbol 12-myristate 13-acetate (PMA, 100ng/mL) and ionomycine (2ug/mL; both from Sigma) that triggers unspecific IFN-γ production. When spots indicating IFN-γ production appeared, they were counted using a Cellular Technology Ltd system (USA) and analyzed using ImmunoSpot 5.0.3 software. Results are reported as the mean of triplicate measurements of the number of IFN-γ spot-forming cells (SFCs) per $5x10^5$ plated cells.

Mouse model of myocardial infarction (MI) and administration of EV-CPC

Myocardial infarction was induced in C57BL/6JRj male mice (Janvier Laboratories) by permanent ligation of the left anterior descending coronary artery (LAD). In a first series of chronic heart

failure, mice received 3 echo-guided, trans-cutaneous injections of 10-20 µL each, in peri–infarcted myocardium, 3 weeks after MI. The experimental groups were as follows: PBS, CPC (1.4 million cells), EV-CPC (secreted by 1.4 million CPC in 48 hours, which was $1x10^{10}$ particles or 100 ug of protein) or lipopolysaccharide (LPS dose of 22.5 µg, used as a positive control of inflammation). Six additional mice were also infarcted but did not receive any injection (controls). Except for the LPS injection group, which had a 33% post-treatment mortality rate, all treated animals survived and were sacrificed 3 days after injection.

In an additional series of acute myocardial infarction, mice received similar transcutaneous echo-guided injections in 3 peri-infarcted areas of either PBS (vehicle control) or EV-CPC (secreted by $1.4x10^{6}$ CPC which was $1x10^{10}$ particles or 100 µg of proteins) 2 days after the infarct. Efforts were made to reproducibly control the degree of cardiac injury in each series of experiments by carefully standardizing the coronary artery ligation site 2–3 mm below the atria all the samples respected this histomorphometric inclusion criteria.

Tissue digestion and flow cytometry

Tissues (heart, spleen, femur and blood) were collected 3 days after EV-CPC injections in both acute and chronic models and kept on ice during all procedures (except for blood). Hearts were rinsed in PBS to remove blood clots. The left ventricle was isolated, minced with fine scissors and gently passed through the Bel-Art™ Scienceware™ 12-Well Tissue Disaggregator (Bel-Art Products). Cells from heart, spleen and bone marrow were then collected in PBS, filtered through a 40-µM nylon mesh (Falcon) and washed. Red blood cells were removed by using the Red Blood Cell Lysing Buffer (Sigma). Cells harvested from the heart were immuno-stained at 4°C for 30 min. Total cardiac immune cells were gated after staining with an Alexa Fluor 700-conjugated anti-CD45 antibody (BD Biosciences) and the following antibodies were used: PE/Cy7-conjugated anti-CD11b (BD Pharmingen), PA-conjugated anti-Ly6G (BD Pharmingen), BV421-conjugated anti-CD64 (Biolegend), APC-conjugated anti-F4/80 (Bio-Rad), FITC-conjugated anti-Ly6C (BD Pharmingen), Percp5.5-conjugated MHC class II (Biolegend), FITC-conjugated anti-CD45R/B220 (eBioscience) and BV421-conjugated anti-CD3 (BD Pharmingen). All antibodies were used at a dilution of 1:100. After incubation, cells were washed and suspended in 100 µL of PBS for FACS analysis. The total number of cells was normalized to heart weight. Events were acquired on an LSR II flow cytometer (BD Biosciences). Monocytes were categorized as $Ly6C^{high}$ monocytes

(CD45+CD11b^{+}F4/80^{-}Ly6G^{-}Ly6C^{high}), and Ly6C^{low} monocytes (CD45+CD11b^{+}F4/80^{-}Ly6G^{-} Ly6C^{low}). Neutrophils were categorized as CD45+CD11b^{+}Ly6G^{++}F4/80^{-}Ly6C^{med}, and macrophages, as CD45+CD11b^{+} Ly6G^{-}F4/80^{+} [29].

Bio-Plex ProTM

The bead-based multiplex immunoassay (Bio-Rad) was used to measure the levels of pro- and anti-inflammatory mediators from mouse plasma (chronic heart failure model) or cardiac tissue homogenates (chronic heart failure and acute myocardial infarction models), 3 days after EV-CPC injection. A 21-plex immunoassay panel (IL-1 α and β, IL-2, IL-3, IL-4, IL-5, IL-6, IL-9, IL-10, IL-12, IL-13, IL-17A, eotaxin, Granulocyte-colony stimulating factor (G-CSF), Granulocyte macrophage colony-stimulating factor (GM-CSF), IFN-γ, KC, Monocyte chemoattractant protein (MCP-1 or CCL-2), MIP-1α, RANTES and TNF-α) was used according to the manufacturer's directions and analysed on a Bio-Plex® 200 (Bio-Rad). Analyte concentration was calculated using a standard curve (5 PL regression, with Bio-Plex Manager™ software).

Statistical Analyses

For all analyses, the Wilcoxon signed rank test was used and a *p*-value <0.05 was considered statistically significant, Mann-Whitney test was also used to compare two groups. Analyses were conducted using GraphPad InStat3 (8.0.1).

Results

EV-CPC and their parental cells display an immune phenotype compatible with allogeneic applications

The iPSC-derived CPC express SSEA-1/CD15, a marker of loss of pluripotency, in line with their cardiac progenitor identity. Immunologically, they express low levels of HLA-I and costimulatory/regulatory CD274 [PDL1], CD275[ICOS-l] and CD86 molecules, low levels of CD80 and of the ligands of the NK cell activating receptor NKG2D, ULBP-1, ULBP 2/5/6 and MIC-A/B and they did not express HLA-II (Figure 1a). The EV-CPC also express CD15 of their parent cells. Immunologically, they do not express HLA-I, HLA-II or costimulatory CD86

molecules. They display low levels of CD80, PD-L1 and ICOS-1, and only modest levels of the ligands of NKG2D (Figure 1b).

To further characterize EV, we used the MACSplex kit to more extensively determine their surface marker profile. We detected CD9, CD29, CD49e, CD63, CD81 and CD326 (Epithelial Cell Adhesion Molecule-EPCAM), which are known to be abundantly expressed by EV, (Figure 1c and Supplemental Figure 1). The EV-CPC also expressed markers of an early differentiation stage including SSEA-4, CD133, CD105 and ROR1 and lacked the expression of markers not expected to be present on EV derived from CPC such as CD3, CD4 and CD14 (Supplemental Figure 1). The EV identity was further confirmed by the expression of CD81, as assessed by cryo-immuno gold electron microscopy (Figure 1d). EV consisted mostly of spherical vesicles ranging in size from 50 to 500 nm (Figure 1d-lower panel) and 40% of them were found to express the tetraspanin CD81.

EV-CPC neither induce T cell activation nor modulate their on-going proliferation

The capacity of both CPC and their secreted EV to activate T cells in allogeneic settings was then evaluated. Co-culture of PBMC with allogeneic mitomycin-C-treated PBMC significantly activated both $CD4^+$ and $CD8^+$ cells, increasing the percentage of proliferating cells from 4% to 40%. In contrast, neither $CD4^+$ nor $CD8^+$ cells responded to allogeneic mitomycin-c-treated CPC (Figure 2a). On the same note, PBMC cultured with EV-CPC maintained their basal proliferation rate and were not affected by EV (Figure 2a). The possibility of PBMC death by apoptosis as a potential cause of their non-proliferation was excluded by aminoactinomycine D7-AAD labeling (data not shown). Thus, neither CPC nor their secreted EV trigger any direct or indirect *in vitro* allogeneic T cell proliferation.

We then investigated the immunomodulatory capacity of EV-CPC in comparison to their parent cells. We evaluated PHA-induced T cell proliferation as an on-going T cell immune response model in the presence or absence of CPC or their secreted EV. The presence of CPC decreased both PHA-induced $CD4^+$ and $CD8^+$ T cell proliferation by approximately 33%, in a ratio-dependent manner (Figure 2b). In contrast, the presence of EV did not modulate PHA-induced $CD4^+$ or $CD8^+$ T cell proliferation (Figure 2b), suggesting that they neither inhibit nor promote a T cell-mediated on-going immune response.

EV-CPC do not induce NK degranulation

Similar to their parent cells, EV-CPC express ligands of the NKG2D receptor, albeit at a lower level. Therefore, we evaluated their capacity to trigger NK cell cytotoxicity in allogeneic settings by assessing their ability to induce degranulation of IL-15-primed NK cells. Compared to the classical NK cell target, (HLA-I-negative K562 cells), CPC modestly activated allogeneic NK cells. The percentage of NK cells specifically expressing the degranulation marker CD107a was approximately 26% in the presence of CPC compared to 45% in the presence of K562 cells. In contrast, the expression of CD107a on IL-15-primed NK cells was not affected by the presence of EV-CPC, even when a high dose of $1.7x10^{10}$ particles was used (Figure 3). Thus, in line with their expression of ligands of NK cell activating receptors, only CPC, but not their secreted EV, are able to modestly activate NK cells.

EV-CPC do not induce humoral nor cellular response *in vivo*

To validate our *in vitro* findings, we then investigated the immune behavior of EV-CPC in an immunocompetent mouse model subjected to an immunization protocol. Mice were subcutaneously injected 3 times (at day 1, 10, 20) with either EV-CPC (n=5) or PBS (n=5) and the humoral or cellular responses of injected mice against EV-CPC were determined. No statistically significant differences in immunoglobulin production were observed between controls and EV-CPC-treated mice at any time point (Figure 4a). To evaluate the cellular immune response, splenocytes from treated and untreated mice were re-challenged *in vitro* with EV-CPC or PBS and the production of IFN-γ was evaluated as a marker of effector T ($CD4^+$ and $CD8^+$) and NK cell activation. Neither the splenocytes from EV-CPC-treated mice nor those from untreated mice produced detectable levels of IFN-γ upon their re-exposure to EV-CPC (Figure 4b). Together, these data suggest that injecting immunocompetent recipients with EV-CPC is unlikely to trigger a pronounced humoral or cellular immune response.

Immuno-inflammatory effects of EV-CPC in an immunocompetent mouse model of chronic heart failure

We then investigated the immune response to EV-CPC in immunocompetent mice in which a MI had been created 3 weeks earlier. Inflammatory cells were harvested 3 days after treatment with PBS, CPC or EV-CPC. Lipopolysaccharide administration was used as a positive control to stimulate inflammation in the targeted cardiac tissue. As expected, the injection of LPS in the

myocardium altered the profile of myeloid cell lines (Figure 5a), thereby confirming the capacity for these mice to mount an appropriate response to this endotoxin [30]. In infarcted hearts which were left untreated (controls), the overall number of inflammatory cells was low, consistent with a lower level of inflammation in chronic heart failure compared to acute MI [31]. Furthermore, PBS injection did not lead to significant changes in the immune profile of heart tissue when compared to untreated animals, thereby ruling out a significant immune response to the needle poke or introduction of fluid. Likewise, injection of EV-CPC or their parental cells did not induce any significant alteration in the numbers of adaptive cells (B and T), innate macrophages or neutrophils, as compared to controls. In contrast, they significantly decreased the number of inflammatory $Ly6C^{high}$ monocytes without any pronounced effect on $Ly6C^{low}$ monocytes.

EV-CPC and CPC injection did not affect the number of circulating (blood) adaptive immune cells, neutrophils or $Ly6C^{low}$ monocytes (Supplementary Figure 2a). However, as compared to controls, and in contrast to EV, CPC injection reduced the number $Ly6C^{high}$ circulating monocytes. No significant difference between groups were observed in the immune profile of bone marrow (Supplemental Figure 3 a) or spleen cells (Supplemental Figure 3b), with the exception of a drastic drop of myeloid and lymphoid bone marrow cells in the LPS group [32].

The expression profile of blood cytokine levels was in accordance. Infarcted mice treated with EV-CPC or parental cells displayed decreased levels of the pro-inflammatory cytokines IL-1α, IL-1β, TNFα, and IFN-γ compared to the PBS control group (Figure 5b), while other cytokines were not affected (Supplemental Figure 2b).
Collectively, these data suggest that EV-CPC, similar to their parental cells, do not trigger any pronounced deleterious immune response in a chronic MI-induced left ventricle (LV) dysfunction model. They might rather downregulate pro-inflammatory compounds in cardiac tissue.

Immuno-inflammatory effects of EV-CPC in an immunocompetent mouse model of acute myocardial infarction

As the number of inflammatory cells in the infarcted heart was low 3 weeks post-infarct, the possibility was raised that the putative immunomodulatory potential of EV-CPC could have been missed due to the dampened inflammatory reaction at that stage of disease. Therefore, we assessed the immune-inflammatory effects of EV-CPC in an experimental model of acute MI which is

associated with a large increase of immune/inflammatory cells in the cardiac tissue. In this model, mice were injected with EV-CPC or PBS 2 days after the infarct, and, as in the chronic model, cardiac inflammatory cells were harvested 3 days after treatment. Compared to control PBS-injected mice, EV-CPC treatment resulted in a significant decrease in neutrophils (from 140 to 50 cells per mg of tissue, p=0.02) and pro-inflammatory Ly6C^{high} monocytes (from 160 to 70 cells per mg of tissue, p=0.01), but did not induce any significant differences in macrophages or adaptive T or B cell populations (Figure 6a). Cytokine profiling in cardiac tissue was in-line with these results, as EV-CPC induced a significant decrease in pro-inflammatory interleukins, IL-1α, IL-2, and IL-6, and a significant increase in the anti-inflammatory cytokine, IL-10. No noticeable differences were observed for other cytokines between the two groups (data not shown). EV-CPC treatment did not induce any significant alteration of tissue-resident cells in the bone marrow or the spleen (Supplemental Figure 4).

Collectively, our findings in the acute MI model support those observed in the chronic heart failure model and emphasize the capacity of EV-CPC to modulate immune/inflammatory responses towards a reparative profile.

EV-CPC shape macrophage polarization state

As our *in vivo* data had suggested that EV-CPC could act as modulators of monocyte/macrophage populations towards an anti-inflammatory phenotype, we assessed whether these effects were relevant to human cells. CD14+ monocytes were isolated from human PBMC and differentiated to M0-(M-CSF), M1-(LPS and IFNγ), or M2-macrophages (IL-4 and IL-13). Pro-inflammatory M1 macrophages were characterized as CD64+, CD68+, CD80+, CD86+ cells; and reparative macrophages as M2a (CD64+, CD68+, CD206+) or M2b (CD64+, CD68+, CD163+) (Supplementary Figure 5). Exposure of M0 to EV-CPC decreased the percentage of pro-inflammatory monocytes (CD14$^+$ CD86$^+$) by 2.20-fold (data not shown), and that of pro-inflammatory macrophages (CD64+ CD68+ CD86+ CD80+) by 2.26-fold. In this experimental setting, the percentage of anti-inflammatory macrophages M2a (CD64+ CD68+ CD206+) was increased by 1.66-fold, (Figure 7a). Exposure of M1 macrophages to EV-CPC did not impact the percentage of CD64+ CD68+ CD86+ CD80+ cells but raised by 1.64-fold the percentage of M2a cells, suggesting that even under pro-inflammatory conditions, EV-CPC favors the occurrence of anti-inflammatory M2 macrophages. Exposure of M2 macrophages to EV-CPC did not

significantly affect the percentage of M1, M2a or M2b cells (Figure 7a). Analysis of the culture supernatants confirmed the capacity of EV to modulate cytokine levels and, more specifically, to upregulate angiogenic and anti-inflammatory markers in the treated macrophages (Figure 7b).

16

Discussion

The principal findings of the present study are that EV derived from cardiovascular progenitor cells do not appear to be immunogenic and seem rather endowed with anti-inflammatory properties (Schematic representation).

The consistent observation of a discrepancy between the low engraftment rate of therapeutic cells and the maintenance of functional benefits beyond the disappearance of the grafted tissue has led the field to favor a paracrine mechanism of action whereby the transplanted cells release factors which stimulate endogenous repair pathways [20,24,33–36]. This mechanistic hypothesis is strengthened by the finding that the effects of transplanted cells can be recapitulated by the administration of their secretome[5,8]. This equivalence has been demonstrated in various and multiple preclinical models targeting different diseases[37] which lends further support for the therapeutic benefits of the cellular secretome. While this secretome is comprised of multiple biologically active components, one important class which has gained increasing interest is represented by EV [9,37–41]. All cell types secrete EV, but not all EVs are equivalent. For example, Barile et al [42] have shown that, in comparison with EV from mesenchymal stem cells, those released by cardiac stem cells have a greater therapeutic efficacy in a ischemic rat occlusion-reperfusion model. The proteomic profile from the two cell types is actually different, possibly leading to a release of factors by cardiac-committed cells which are better tailored to heart tissue repair. Therefore, and in-line with our previous studies, we have been committed to use EV secreted from cells phenotypically close to those of the target tissue. In this case, we use iPSC derived cardiovascular progenitors. These EV were primarily characterized by their size profile, surface markers and TEM characteristics which thus provided sound evidence for their identity.

While the composition of the EV cargo reflects that of their parental cells, it can be selectively enriched in, or deprived of, some molecules present in these cells[18]. This is confirmed in the present study by the finding that, in contrast to CPC, the secreted EV express extremely low levels of most immune relevant molecules. Yet, they did express the ligands for NK cell activating receptors, albeit at a lower level compared to their parent cells. This expression pattern strongly suggests that EV-CPC may be more immunologically neutral towards lymphoid populations and innate lymphoid NK cells than their parent cells. This idea is supported by the fact that EV-CPC did not

trigger allogeneic T cell activation either *in vitro*, as shown by the mixed lymphocyte reactions data. The EV-CPC are probably also unable to trigger neither T nor B cells response *in vivo*, since they were not able to affect the number of these adaptive cells upon their injection in immunocompetent infarcted mice. Further, EV-CPC did not trigger a humoral immune response, since their repeated delivery did not result in an increase in immunoglobulin production as compared to controls, thereby strengthening the idea that they may deviate the immune surveillance of the host. This makes them therapeutically attractive since, and in contrast to their parental allogeneic cells, their use in patients might not require immunosuppression. Of note, EV from other cell sources like antigen-presenting cells carry HLA-I and II antigens and can thus trigger T cell proliferation [43]. Conversely, EV from mesenchymal stem cells have been credited with immunosuppressive effects [44] which we did not find to be the case for EV-CPC in our *in vitro* studies. Taken together, these data highlight the critical influence of the parental cell phenotype on the ultimate immune properties of their secreted EV.

The fact that EV-CPC seem endowed with anti-inflammatory properties further supports the above notion. *In vivo*, we consistently observed that pro-inflammatory Ly6C^{high} monocytes were decreased in heart tissue in both acute MI and chronic heart failure models. This anti-inflammatory effect was more pronounced at the acute stage under the form of a concomitant decrease in neutrophils. Further evidence includes a decrease in heart and plasma cytokine levels in both acute and chronic settings and the trend for human innate myeloid monocytes/macrophages exposed to EV-CPC to shift their polarity towards an anti-inflammatory phenotype. Yet, EV-CPC were unable to reverse the pro-inflammatory M1 pattern once established concerning *in vitro* experiments with human cells, in contrast to exosomes from adipose-derived mesenchymal stromal cells which can reverse the M1 conversion of microglial cells subjected to oxygen and glucose deprivation [45].These divergent results might be due to differences in the content of the EV payload and/or the phenotype of the target cells.

Although the present experiments focused on the immune-inflammatory responses to EV and, as such, did not include functional assessments, it is noteworthy that in a previous study from our laboratory [6], EV from the same CPC source as in the present study were shown to improve post infarction contractile performance in a mouse model of chronic left ventricular dysfunction. The

transcriptomic study of these EV had highlighted the strong expression of 16 microRNAs broadly conserved across species, among which at least half, i.e., miR-92a [46], miR-24 [47], miR-93-5p [48], miR 20b-5p [49], miR-107 [50], miR 26a-5p [51], miR-16-5p[52] and miR-130b-3p [53] are to some extent involved in the regulation of inflammation. It is thus plausible that the effects of the EV cargo on the mitigation of immune-inflammatory responses demonstrated in the present study participate in the previously documented EV-associated preservation of post infarction heart function. Of note, these functional benefits were observed in an immune-deficient mouse model. However, recent work in our laboratory has reproduced this therapeutic effect in an immune-competent strain (unpublished data), suggesting that the possible link between the EV-related regulation of immune-inflammatory responses and the mitigation of post infarct heart injury is independent of the immune status of the recipient animals.

The finding of decreased circulating levels of IL-1α and IFN-γ in mice, following intramyocardial injection of EV three weeks earlier, suggests that these particles might induce a sustained systemic anti-inflammatory effect not strictly localized in the treated organ. It is thus conceivable that the opposite event may happen, i.e., that intravenously delivered EV, even though they are predominantly trapped in the lungs and spleen, may exert endocrine anti-inflammatory effects on remote organs, including the heart, as reported for mesenchymal stem cells[54]. This could explain the therapeutic efficacy of intravenously injected EV in Duchenne [55] and doxorubicin-induced cardiomyopathy [56] which share in common a chronic inflammation of the myocardial tissue [57,58]. Should this hypothesis be validated, it would reinforce the clinical attractiveness of EV by opening the way to systemic delivery, making such a treatment simple, non-invasive, readily available and economically affordable.

Funding: This work was supported by the *Institut National de la Santé et de la Recherche Médicale*; the *Assistance Publique Hôpitaux de Paris*; the *Université Paris Descartes*; the *Agence Nationale de la Recherche* (LabexRevive, ANR -10-LABX-73 to P.M.); the *Fondation de France* (FDF 00066471 to P.M. and FDF 00066471 J-S. S.), and the *Fondation pour la Recherche Médicale* (DEQ20160334910 to J-S. S. and P.M.).

Conflict of interests: The authors declare no competing financial interests.

References

1. Bui AL, Horwich TB, Fonarow GC. Epidemiology and risk profile of heart failure. *Nat Rev Cardiol*. 2011;8:30–41.
2. Gnecchi M, Zhang Z, Ni A, Dzau VJ. Paracrine mechanisms in adult stem cell signaling and therapy. *Circ Res*. 2008;103:1204–1219.
3. Gallet R, Dawkins J, Valle J, Simsolo E, de Couto G, Middleton R, Tseliou E, Luthringer D, Kreke M, Smith RR, Marbán L, Ghaleb B, Marbán E. Exosomes secreted by cardiosphere-derived cells reduce scarring, attenuate adverse remodelling, and improve function in acute and chronic porcine myocardial infarction. *Eur Heart J*. 2016;Sep 27. pii: ehw240. [Epub ahead of print].
4. Lai RC, Arslan F, Lee MM, Sze NSK, Choo A, Chen TS, Salto-Tellez M, Timmers L, Lee CN, El Oakley RM, Pasterkamp G, de Kleijn DPV, Lim SK. Exosome secreted by MSC reduces myocardial ischemia/reperfusion injury. *Stem Cell Res*. 2010;4:214–222.
5. Kervadec A, Bellamy V, El Harane N, Arakélian L, Vanneaux V, Cacciapuoti I, Nemetalla H, Périer M-C, Toeg HD, Richart A, Lemitre M, Yin M, Loyer X, Larghero J, Hagège A, Ruel M, Boulanger CM, Silvestre J-S, Menasché P, Renault NKE. Cardiovascular progenitor-derived extracellular vesicles recapitulate the beneficial effects of their parent cells in the treatment of chronic heart failure. *J Heart Lung Transplant*. 2016;35:795–807.
6. El Harane N, Kervadec A, Bellamy V, Pidial L, Neametalla HJ, Perier M-C, Lima Correa B, Thiébault L, Cagnard N, Duché A, Brunaud C, Lemitre M, Gauthier J, Bourdillon AT, Renault MP, Hovhannisyan Y, Paiva S, Colas AR, Agbulut O, Hagège A, Silvestre J-S, Menasché P, Renault NKE. Acellular therapeutic approach for heart failure: in vitro production of extracellular vesicles from human cardiovascular progenitors. *Eur Heart J*. 2018;39:1835–1847.
7. Timmers L, Lim SK, Hoefer IE, Arslan F, Lai RC, van Oorschot AAM, Goumans MJ, Strijder C, Sze SK, Choo A, Piek JJ, Doevendans PA, Pasterkamp G, de Kleijn DPV. Human mesenchymal stem cell-conditioned medium improves cardiac function following myocardial infarction. *Stem Cell Res*. 2011;6:206–214.
8. Gnecchi M, He H, Noiseux N, Liang OD, Zhang L, Morello F, Mu H, Melo LG, Pratt RE, Ingwall JS, Dzau VJ. Evidence supporting paracrine hypothesis for Akt-modified

mesenchymal stem cell-mediated cardiac protection and functional improvement. *FASEB J Off Publ Fed Am Soc Exp Biol*. 2006;20:661–669.

9. Ibrahim AG-E, Cheng K, Marbán E. Exosomes as critical agents of cardiac regeneration triggered by cell therapy. *Stem Cell Rep*. 2014;2:606–619.
10. Barile L, Lionetti V, Cervio E, Matteucci M, Gherghiceanu M, Popescu LM, Torre T, Siclari F, Moccetti T, Vassalli G. Extracellular vesicles from human cardiac progenitor cells inhibit cardiomyocyte apoptosis and improve cardiac function after myocardial infarction. *Cardiovasc Res*. 2014;103:530–541.
11. Zhang Y, Liu Y, Liu H, Tang WH. Exosomes: biogenesis, biologic function and clinical potential. *Cell Biosci* [Internet]. 2019 [cited 2019 Aug 19];9. Available from: https://www.ncbi.nlm.nih.gov/pmc/articles/PMC6377728/
12. Yuan A, Farber EL, Rapoport AL, Tejada D, Deniskin R, Akhmedov NB, Farber DB. Transfer of microRNAs by embryonic stem cell microvesicles. *PloS One*. 2009;4:e4722.
13. Vrijsen KR, Sluijter JPG, Schuchardt MWL, van Balkom BWM, Noort WA, Chamuleau S a. J, Doevendans P a. FM. Cardiomyocyte progenitor cell-derived exosomes stimulate migration of endothelial cells. *J Cell Mol Med*. 2010;14:1064–1070.
14. Sahoo S, Klychko E, Thorne T, Misener S, Schultz KM, Millay M, Ito A, Liu T, Kamide C, Agrawal H, Perlman H, Qin G, Kishore R, Losordo DW. Exosomes from human CD34(+) stem cells mediate their proangiogenic paracrine activity. *Circ Res*. 2011;109:724–728.
15. Chen D, Liu S, Ma H, Liang X, Ma H, Yan X, Yang B, Wei J, Liu X. Paracrine factors from adipose-mesenchymal stem cells enhance metastatic capacity through Wnt signaling pathway in a colon cancer cell co-culture model. *Cancer Cell Int*. 2015;15:42.
16. Cosme J, Liu PP, Gramolini AO. The cardiovascular exosome: current perspectives and potential. *Proteomics*. 2013;13:1654–1659.
17. Pols MS, Klumperman J. Trafficking and function of the tetraspanin CD63. *Exp Cell Res*. 2009;315:1584–1592.
18. Colombo M, Raposo G, Théry C. Biogenesis, secretion, and intercellular interactions of exosomes and other extracellular vesicles. *Annu Rev Cell Dev Biol*. 2014;30:255–289.
19. Henne WM, Buchkovich NJ, Emr SD. The ESCRT pathway. *Dev Cell*. 2011;21:77–91.
20. Théry C, Ostrowski M, Segura E. Membrane vesicles as conveyors of immune responses. *Nat Rev Immunol*. 2009;9:581–593.

21. Lauden L, Boukouaci W, Borlado LR, López IP, Sepúlveda P, Tamouza R, Charron D, Al-Daccak R. Allogenicity of human cardiac stem/progenitor cells orchestrated by programmed death ligand 1. *Circ Res*. 2013;112:451–464.
22. Fernandes S, Chong JJH, Paige SL, Iwata M, Torok-Storb B, Keller G, Reinecke H, Murry CE. Comparison of Human Embryonic Stem Cell-Derived Cardiomyocytes, Cardiovascular Progenitors, and Bone Marrow Mononuclear Cells for Cardiac Repair. *Stem Cell Rep*. 2015;5:753–762.
23. Hocine HR, Brunel S, Chen Q, Giustiniani J, Roman MJS, Ferrat YJ, Palacios I, Rosa O de la, Lombardo E, Bensussan A, Charron D, Jabrane-Ferrat N, Al-Daccak R. Extracellular Vesicles Released by Allogeneic Human Cardiac Stem/Progenitor Cells as Part of their Therapeutic Benefit. *STEM CELLS Transl Med* [Internet]. [cited 2019 Aug 19];0. Available from: https://stemcellsjournals.onlinelibrary.wiley.com/doi/abs/10.1002/sctm.18-0256
24. de Couto G, Gallet R, Cambier L, Jaghatspanyan E, Makkar N, Dawkins JF, Berman BP, Marbán E. Exosomal MicroRNA Transfer Into Macrophages Mediates Cellular Postconditioning. *Circulation*. 2017;136:200–214.
25. Davidson SM, Yellon DM. Exosomes and cardioprotection - A critical analysis. *Mol Aspects Med*. 2018;60:104–114.
26. Arraud N, Linares R, Tan S, Gounou C, Pasquet J-M, Mornet S, Brisson AR. Extracellular vesicles from blood plasma: determination of their morphology, size, phenotype and concentration. *J Thromb Haemost JTH*. 2014;12:614–627.
27. Théry C, Witwer KW, Aikawa E, Alcaraz MJ, Anderson JD, Andriantsitohaina R, Antoniou A, Arab T, Archer F, Atkin-Smith GK, Ayre DC, Bach J-M, Bachurski D, Baharvand H, Balaj L, Baldacchino S, Bauer NN, Baxter AA, Bebawy M, Beckham C, Zavec AB, Benmoussa A, Berardi AC, Bergese P, Bielska E, Blenkiron C, Bobis-Wozowicz S, Boilard E, Boireau W, Bongiovanni A, Borràs FE, Bosch S, Boulanger CM, Breakefield X, Breglio AM, Brennan MÁ, Brigstock DR, Brisson A, Broekman ML, Bromberg JF, Bryl-Górecka P, Buch S, Buck AH, Burger D, Busatto S, Buschmann D, Bussolati B, Buzás EI, Byrd JB, Camussi G, Carter DR, Caruso S, Chamley LW, Chang Y-T, Chen C, Chen S, Cheng L, Chin AR, Clayton A, Clerici SP, Cocks A, Cocucci E, Coffey RJ, Cordeiro-da-Silva A, Couch Y, Coumans FA, Coyle B, Crescitelli R, Criado MF, D'Souza-Schorey C, Das S, Chaudhuri AD, Candia P de, Junior EFDS, Wever OD, Portillo HA del, Demaret T, Deville S, Devitt A, Dhondt B, Vizio

DD, Dieterich LC, Dolo V, Rubio APD, Dominici M, Dourado MR, Driedonks TA, Duarte FV, Duncan HM, Eichenberger RM, Ekström K, Andaloussi SE, Elie-Caille C, Erdbrügger U, Falcón-Pérez JM, Fatima F, Fish JE, Flores-Bellver M, et al. Minimal information for studies of extracellular vesicles 2018 (MISEV2018): a position statement of the International Society for Extracellular Vesicles and update of the MISEV2014 guidelines. *J Extracell Vesicles*. 2018;7:1535750.

28. Gunasekaran M, Sharma M, Hachem R, Bremner R, Smith MA, Mohanakumar T. Circulating Exosomes with Distinct Properties during Chronic Lung Allograft Rejection. *J Immunol Baltim Md 1950*. 2018;200:2535–2541.
29. Zlatanova I, Pinto C, Bonnin P, Mathieu JRR, Bakker W, Vilar J, Lemitre M, Voehringer D, Vaulont S, Peyssonnaux C, Silvestre J-S. Iron Regulator Hepcidin Impairs Macrophage-Dependent Cardiac Repair After Injury. *Circulation*. 2019;139:1530–1547.
30. Prabhu SD, Frangogiannis NG. The Biological Basis for Cardiac Repair After Myocardial Infarction: From Inflammation to Fibrosis. *Circ Res*. 2016;119:91–112.
31. Cochain C, Auvynet C, Poupel L, Vilar J, Dumeau E, Richart A, Récalde A, Zouggari Y, Yin KYHW, Bruneval P, Renault G, Marchiol C, Bonnin P, Lévy B, Bonecchi R, Locati M, Combadière C, Silvestre J-S. The chemokine decoy receptor D6 prevents excessive inflammation and adverse ventricular remodeling after myocardial infarction. *Arterioscler Thromb Vasc Biol*. 2012;32:2206–2213.
32. Chandra R, Villanueva E, Feketova E, Machiedo GW, Haskó G, Deitch EA, Spolarics Z. Endotoxemia down-regulates bone marrow lymphopoiesis but stimulates myelopoiesis: the effect of G6PD deficiency. *J Leukoc Biol*. 2008;83:1541–1550.
33. Théry C, Zitvogel L, Amigorena S. Exosomes: composition, biogenesis and function. *Nat Rev Immunol*. 2002;2:569–579.
34. EL Andaloussi S, Mäger I, Breakefield XO, Wood MJA. Extracellular vesicles: biology and emerging therapeutic opportunities. *Nat Rev Drug Discov*. 2013;12:347–357.
35. Camussi G, Deregibus MC, Bruno S, Cantaluppi V, Biancone L. Exosomes/microvesicles as a mechanism of cell-to-cell communication. *Kidney Int*. 2010;78:838–848.
36. Camussi G, Deregibus M-C, Bruno S, Grange C, Fonsato V, Tetta C. Exosome/microvesicle-mediated epigenetic reprogramming of cells. *Am J Cancer Res*. 2011;1:98–110.

37. Lener T, Gioma M, Aigner L, Börger V, Buzas E, Camussi G, Chaput N, Chatterjee D, Court FA, Portillo HA del, O'Driscoll L, Fais S, Falcon-Perez JM, Felderhoff-Mueser U, Fraile L, Gho YS, Görgens A, Gupta RC, Hendrix A, Hermann DM, Hill AF, Hochberg F, Horn PA, Kleijn D de, Kordelas L, Kramer BW, Krämer-Albers E-M, Laner-Plamberger S, Laitinen S, Leonardi T, Lorenowicz MJ, Lim SK, Lötvall J, Maguire CA, Marcilla A, Nazarenko I, Ochiya T, Patel T, Pedersen S, Pocsfalvi G, Pluchino S, Quesenberry P, Reischl IG, Rivera FJ, Sanzenbacher R, Schallmoser K, Slaper-Cortenbach I, Strunk D, Tonn T, Vader P, Balkom BWM van, Wauben M, Andaloussi SE, Théry C, Rohde E, Giebel B. Applying extracellular vesicles based therapeutics in clinical trials - an ISEV position paper. *J Extracell Vesicles* [Internet]. 2015 [cited 2016 Oct 6];4. Available from: http://www.journalofextracellularvesicles.net/index.php/jev/article/view/30087

38. Xin H, Li Y, Cui Y, Yang JJ, Zhang ZG, Chopp M. Systemic administration of exosomes released from mesenchymal stromal cells promote functional recovery and neurovascular plasticity after stroke in rats. *J Cereb Blood Flow Metab*. 2013;33:1711–1715.

39. Kamata S, Miyagawa S, Fukushima S, Nakatani S, Kawamoto A, Saito A, Harada A, Shimizu T, Daimon T, Okano T, Asahara T, Sawa Y. Improvement of cardiac stem cell sheet therapy for chronic ischemic injury by adding endothelial progenitor cell transplantation: analysis of layer-specific regional cardiac function. *Cell Transplant*. 2014;23:1305–1319.

40. Vlassov AV, Magdaleno S, Setterquist R, Conrad R. Exosomes: current knowledge of their composition, biological functions, and diagnostic and therapeutic potentials. *Biochim Biophys Acta*. 2012;1820:940–948.

41. Menasché P. Stem cell–derived exosomes and the failing heart: Small cause, big effect. *J Thorac Cardiovasc Surg*. 2018;156:1089–1092.

42. Barile L, Cervio E, Lionetti V, Milano G, Ciullo A, Biemmi V, Bolis S, Altomare C, Matteucci M, Di Silvestre D, Brambilla F, Fertig TE, Torre T, Demertzis S, Mauri P, Moccetti T, Vassalli G. Cardioprotection by cardiac progenitor cell-secreted exosomes: role of pregnancy-associated plasma protein-A. *Cardiovasc Res*. 2018;114:992–1005.

43. Robbins PD, Morelli AE. Regulation of immune responses by extracellular vesicles. *Nat Rev Immunol*. 2014;14:195–208.

44. Börger V, Bremer M, Ferrer-Tur R, Gockeln L, Stambouli O, Becic A, Giebel B. Mesenchymal Stem/Stromal Cell-Derived Extracellular Vesicles and Their Potential as Novel Immunomodulatory Therapeutic Agents. *Int J Mol Sci*. 2017;18.
45. Jiang M, Wang H, Jin M, Yang X, Ji H, Jiang Y, Zhang H, Wu F, Wu G, Lai X, Cai L, Hu R, Xu L, Li L. Exosomes from MiR-30d-5p-ADSCs Reverse Acute Ischemic Stroke-Induced, Autophagy-Mediated Brain Injury by Promoting M2 Microglial/Macrophage Polarization. *Cell Physiol Biochem Int J Exp Cell Physiol Biochem Pharmacol*. 2018;47:864–878.
46. Lai L, Song Y, Liu Y, Chen Q, Han Q, Chen W, Pan T, Zhang Y, Cao X, Wang Q. MicroRNA-92a negatively regulates Toll-like receptor (TLR)-triggered inflammatory response in macrophages by targeting MKK4 kinase. *J Biol Chem*. 2013;288:7956–7967.
47. Tahamtan A, Teymoori-Rad M, Nakstad B, Salimi V. Anti-Inflammatory MicroRNAs and Their Potential for Inflammatory Diseases Treatment. *Front Immunol*. 2018;9:1377.
48. Liu J, Jiang M, Deng S, Lu J, Huang H, Zhang Y, Gong P, Shen X, Ruan H, Jin M, Wang H. miR-93-5p-Containing Exosomes Treatment Attenuates Acute Myocardial Infarction-Induced Myocardial Damage. *Mol Ther Nucleic Acids*. 2018;11:103–115.
49. You H, Zhang L, Chen Z, Liu W, Wang H, He H. MiR-20b-5p relieves neuropathic pain by targeting Akt3 in a chronic constriction injury rat model. *Synap N Y N*. 2019;73:e22125.
50. Gao Z-F, Ji X-L, Gu J, Wang X-Y, Ding L, Zhang H. microRNA-107 protects against inflammation and endoplasmic reticulum stress of vascular endothelial cells via KRT1-dependent Notch signaling pathway in a mouse model of coronary atherosclerosis. *J Cell Physiol*. 2019;234:12029–12041.
51. Kong B, Qin Z, Ye Z, Yang X, Li L, Su Q. microRNA-26a-5p affects myocardial injury induced by coronary microembolization by modulating HMGA1. *J Cell Biochem*. 2019;120:10756–10766.
52. Lei J, Fu Y, Zhuang Y, Zhang K, Lu D. LncRNA SNHG1 alleviates IL-1β-induced osteoarthritis by inhibiting miR-16-5p-mediated p38 MAPK and NF-κB signaling pathways. *Biosci Rep*. 2019;39.
53. Wang P, Zhang X, Li F, Yuan K, Li M, Zhang J, Li B, Liang W. MiR-130b attenuates vascular inflammation via negatively regulating tumor progression locus 2 (Tpl2) expression. *Int Immunopharmacol*. 2017;51:9–16.

54. Luger D, Lipinski MJ, Westman PC, Glover DK, Dimastromatteo J, Frias JC, Albelda MT, Sikora S, Kharazi A, Vertelov G, Waksman R, Epstein SE. Intravenously Delivered Mesenchymal Stem Cells: Systemic Anti-Inflammatory Effects Improve Left Ventricular Dysfunction in Acute Myocardial Infarction and Ischemic Cardiomyopathy. *Circ Res.* 2017;120:1598–1613.
55. Rogers RG, Fournier M, Sanchez L, Ibrahim AG, Aminzadeh MA, Lewis MI, Marbán E. Disease-modifying bioactivity of intravenous cardiosphere-derived cells and exosomes in mdx mice. *JCI Insight.* 2019;4.
56. Milano G, Biemmi V, Lazzarini E, Balbi C, Ciullo A, Bolis S, Ameri P, Di Silvestre D, Mauri P, Barile L, Vassalli G. Intravenous administration of cardiac progenitor cell-derived exosomes protects against doxorubicin/trastuzumab-induced cardiac toxicity. *Cardiovasc Res.* 2019;
57. Mavrogeni S, Papavasiliou A, Spargias K, Constandoulakis P, Papadopoulos G, Karanasios E, Georgakopoulos D, Kolovou G, Demerouti E, Polymeros S, Kaklamanis L, Magoutas A, Papadopoulou E, Markussis V, Cokkinos DV. Myocardial inflammation in Duchenne Muscular Dystrophy as a precipitating factor for heart failure: a prospective study. *BMC Neurol.* 2010;10:33.
58. Sun X, Shan A, Wei Z, Xu B. Intravenous mesenchymal stem cell-derived exosomes ameliorate myocardial inflammation in the dilated cardiomyopathy. *Biochem Biophys Res Commun.* 2018;503:2611–2618.

Figure legends

Figure 1: Surface marker profile of CPC and EV-CPC:

a & b) Representative flow cytometry histograms for the fluorescence intensity of surface markers on CPC (a) and EV-CPC (b). The percentage of positive cells (%) and geometric mean fluorescence intensity (MFI) are indicated. mAb (monoclonal antibody). c) Main surface marker profile of EV-CPC, as identified by a cocktail of 39 fluorescently-labeled bead populations, each coated with a specific antibody binding the respective EV surface epitope. These data were derived from 4 independent preparations of EV. Data are presented as box-and-whisker plots, with the midline representing the median and the whiskers representing maximum and minimum values. d) The upper and middle panels present representative cryo-TEM images of CD81+ and CD81- EV embedded in a thin film of frozen buffer. The lipid bilayer is clearly resolved (arrow in the upper panel). The lower panel presents the size distribution of CD81+ and CD81- EVs, determined over a total of 350 EV. The median sizes are 175 nM and 265 nM for CD81+ and CD81- EV, respectively. CPC: iPS-derived cardiovascular progenitor cells; EV: Extracellular vesicles from iPS-derived cardiovascular progenitor cells.

Figure 2: Effects of CPC and EV-CPC on allogeneic T-cell immune response.

a) CFSE-labeled peripheral blood mononuclear cells (PBMC) were cultured alone (negative control), with human leukocyte antigen-mismatched mitomycin C–treated PBMC (Allo PBMC from 2 different donors, positive control), with mitomycin C–treated CPC at different CPC:PBMC ratios (CPC1: 1:10; CPC2: 1:5), or with EV-CPC at different doses (EV1: $5.5x10^8$; EV2: $5.5x10^9$ and EV3: $1.7x10^{10}$ particles). Proliferation levels of $CD4^+$ and $CD8^+$ T cells were determined by loss of CFSE labelling.

b) CFSE-labeled human leukocyte antigen-mismatched PBMC were activated with phytohemagglutinin ((PHA)-positive control), alone (negative control), in the presence of mitomycin C–treated CPC at different CPC:PBMC ratios (CPC1: 1:10; CPC2: 1:5), or with EV-CPC at different doses (EV1: $5.5x10^8$; EV2: $5.5x10^9$ and EV3: $1.7x10^{10}$ particles). Proliferation levels of $CD4^+$ and $CD8^+$ T cells were determined by loss of CFSE labelling. The results are given as mean ± SD from 3 independent experiments performed in duplicate or triplicate. Wilcoxon signed rank test was used and a *p*-value <0.05 was considered statistically significant** $p \leq 0.01$; *** $p \leq 0.001$. Abbreviations as in Figure 1.

Figure 3: Effects of CPC and EV-CPC on NK cell degranulation.

a) Scatter plot of flow cytometry analysis showing the percentages of CD107a-positive cells in CD56+ IL-15-activated NK cells after overnight incubation with target cells: K562 (positive control), CPC or EV-CPC (EV1: $5.5x10^8$; EV2: $5.5x10^9$ and EV3: $1.7x10^{10}$ particles) at a 1:1 effector:target cell ratio.

b) Histogram presenting percentages of CD107a positive cells (mean ± SD) from 3 independent experiments performed in triplicate. The results are given as mean ± SD. Wilcoxon signed rank test was used, a p-value <0.05 was considered statistically significant. *** $p \leq 0.001$. Abbreviations as in Figure 1.

Figure 4: Humoral and cellular responses of vaccinated mice with PBS or EV-CPC.

a) Immunoglobulin isotype detection in plasma of vaccinated mice at days 10, 20, 30 and 37.

b) Spot counts of interferon-gamma (IFN-γ) detection secreted by splenocytes of each vaccinated mouse (technical triplicates), n = 6 per group. PBS: Phosphate-Buffered saline; other abbreviations as in Figure 1.

Figure 5: Inflammatory cell numbers in heart tissue and cytokine blood levels in the chronic heart failure model.

a) Heart tissue levels of immune cells: Three weeks after MI, mice were untreated (n=8-13) or injected with PBS (n=6-8), EV (n=7), CPC (n=6) or LPS (n=4). Three days after injection, the left ventricle was removed and analysed by FACS for the assessment of immune cells.

b) Circulating blood cytokine measurements, assessed by FACS using a Luminex® based–bead immuno assay. Untreated (n=3-5), PBS (n=4-6), EV (n=5-6), CPC (n=3-5) or LPS (n=3). The results are given as mean ± SD. Wilcoxon signed rank test was used, a p-value <0.05 was considered statistically significant. *$p \leq 0.05$; ** $p \leq 0.01$. Abbreviations as in Figure 4.

Figure 6: Inflammatory cell numbers and cytokine levels in heart tissue in the acute myocardial infarction model.

a) Heart tissue levels of immune cells: Two days after MI, mice were injected with PBS (n=6) or EV (n=6). Three days after injection, the left ventricle was removed and analysed by FACS for the assessment of immune cells.

b) Cardiac cytokine levels, as assessed by FACS using a Luminex® based–bead immuno-assay; PBS (n=5-6) or EV (n=6-7). The results are given as mean ± SD. Wilcoxon signed rank test was used, a p-value <0.05 was considered statistically significant. *$p \leq 0.05$. Abbreviations as in Figure 4.

Figure 7: Effects of EV-CPC on the expression of macrophage surface markers and cytokine expression profile.

a) Percentage of cell expressing specific surface markers in human macrophages (CD64+ and CD68+, n=3 or 4 different patients)**.** The results are given as mean ± SEM. Mann-Whitney Test was used to compare two groups and a p-value <0.05 was considered statistically significant.

b) Supernatants of macrophage cell culture at day 9 were analyzed by FACS using a Luminex bead-based immunoassay. Values have been normalized in reference to the untreated population in each case. Data were obtained from 4 different patients. The results are given as mean ± SD. Mann-Whitney Test was used to compare two groups and a p-value <0.05 was considered statistically significant; *$p \leq 0.05$.

M0: Undifferentiated macrophages; M1: Pro-inflammatory macrophages; M2: Anti-inflammatory macrophages; EV: Extracellular vesicles from iPS cell-derived cardiovascular progenitor cells.

Schematic representation: EV and cardiac inflammatory reaction. Extracellular vesicles (EV) obtained from iPS cell-derived cardiovascular progenitor cells (CPC) do not trigger an immune response either in *in vitro* human allogeneic settings or in immunocompetent experimental models. Of note, EV harbor an unchallenged capacity to fine-tune the response of monocyte/macrophages towards resolution of inflammation bolstering their therapeutic potential.

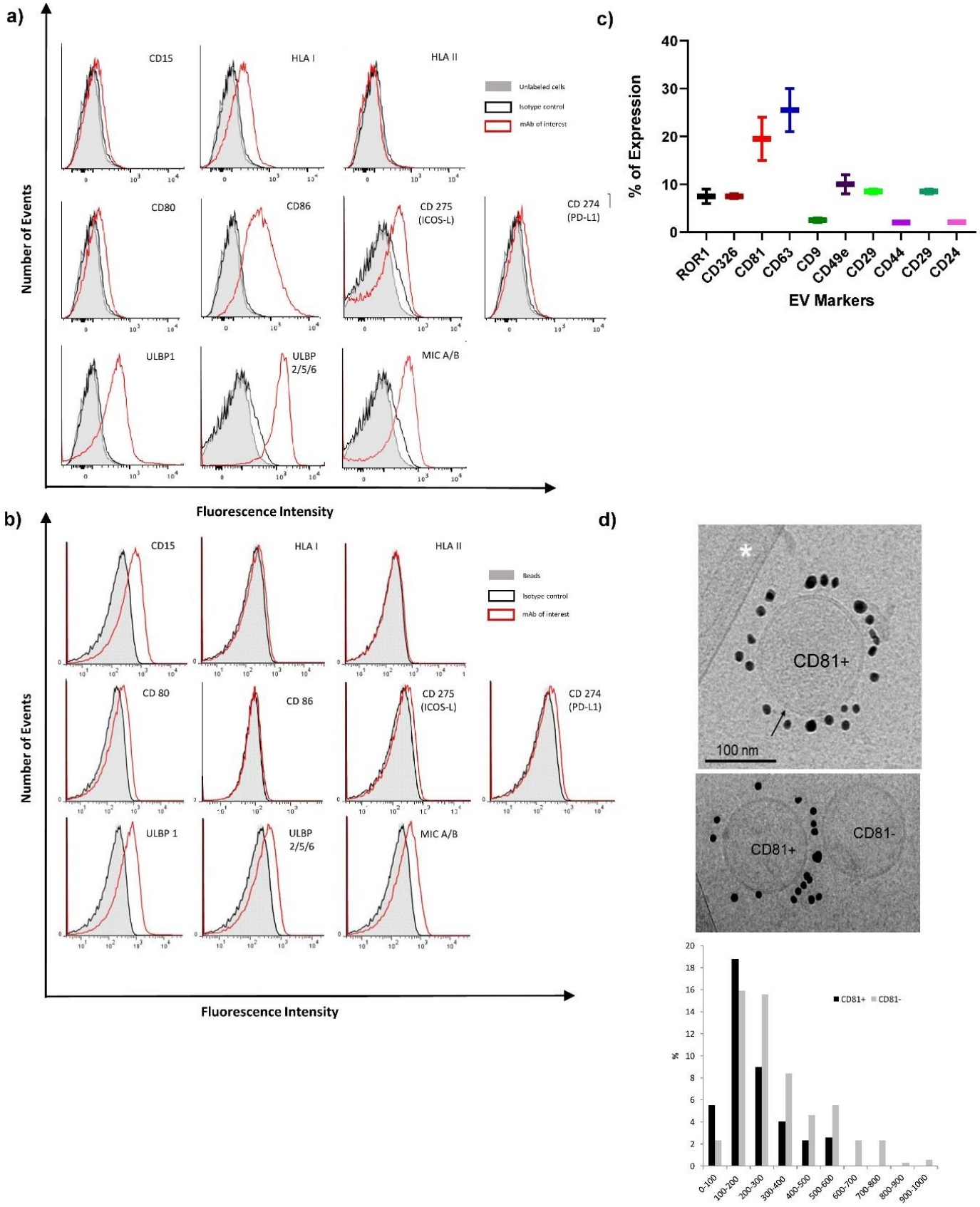
a)
CD15
HLA I
HLA II
Unlabeled cells
Isotype control
mAb of interest
CD80
CD86
CD 275 (ICOS-L)
CD 274 (PD-L1)
ULBP1
ULBP 2/5/6
MIC A/B
Number of Events
Fluorescence Intensity
b)
CD15
HLA I
HLA II
Beads
Isotype control
mAb of interest
CD 80
CD 86
CD 275 (ICOS-L)
CD 274 (PD-L1)
ULBP 1
ULBP 2/5/6
MIC A/B
Number of Events
Fluorescence Intensity
c)
% of Expression
ROR1
CD326
CD81
CD63
CD9
CD49e
CD29
CD44
CD29
CD24
EV Markers
d)
CD81+
100 nm
CD81+
CD81-
CD81+
CD81-
%
0-100
100-200
200-300
300-400
400-500
500-600
600-700
700-800
800-900
900-1000

Figure 1

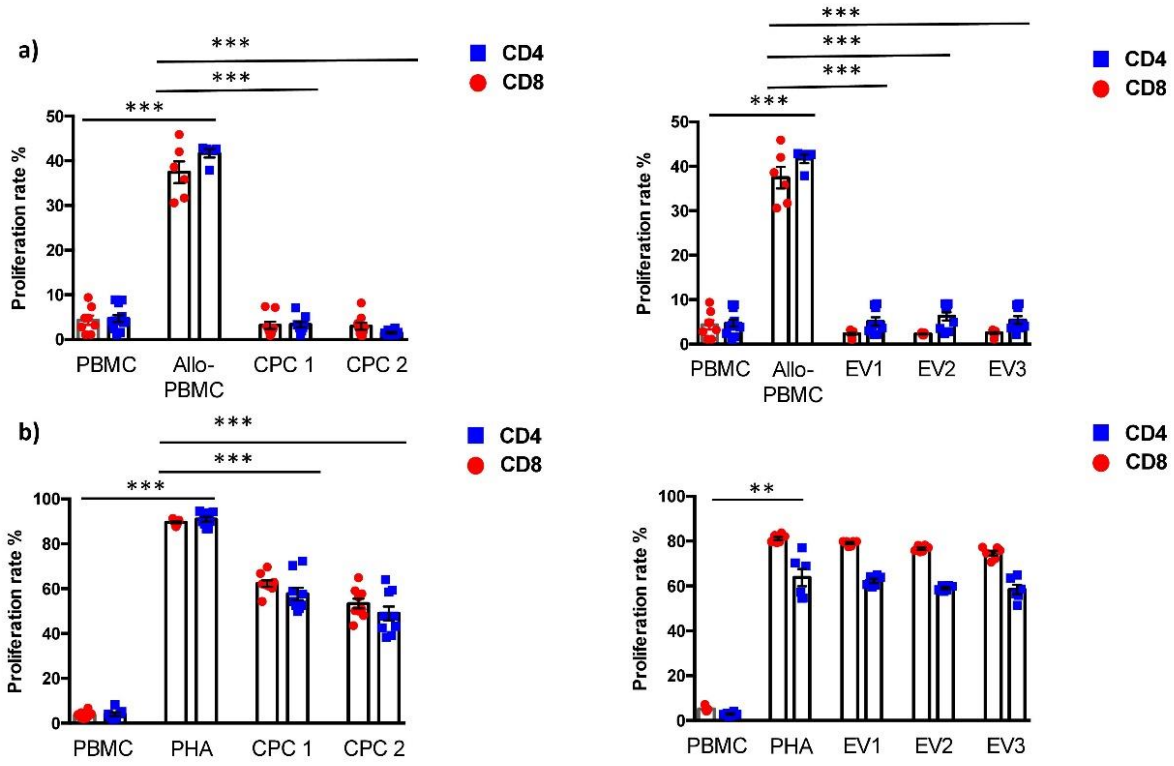
a)
***
***
***
CD4
CD8
Proliferation rate %
50
40
30
20
10
0
PBMC
Allo-PBMC
CPC 1
CPC 2
***
***
***
***
CD4
CD8
Proliferation rate %
PBMC
Allo-PBMC
EV1
EV2
EV3
b)
***
***
***
CD4
CD8
Proliferation rate %
100
80
60
40
20
0
PBMC
PHA
CPC 1
CPC 2
**
CD4
CD8
Proliferation rate %
PBMC
PHA
EV1
EV2
EV3

Figure 2

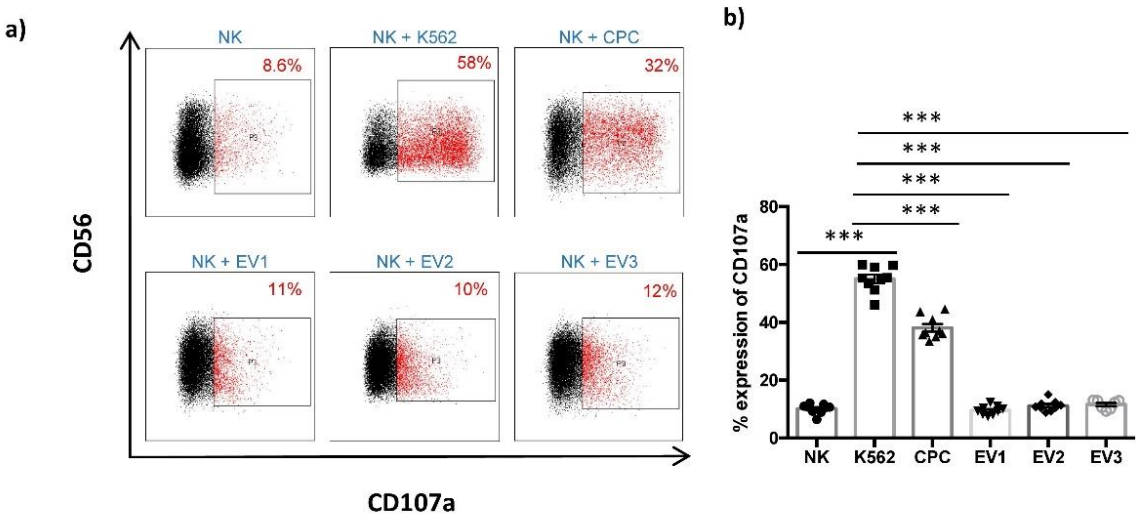
a)
NK
8.6%
NK + K562
58%
NK + CPC
32%
NK + EV1
11%
NK + EV2
10%
NK + EV3
12%
CD56
CD107a
b)
% expression of CD107a
***
***
***
***
***
80
60
40
20
0
NK
K562
CPC
EV1
EV2
EV3

Figure 3

a)

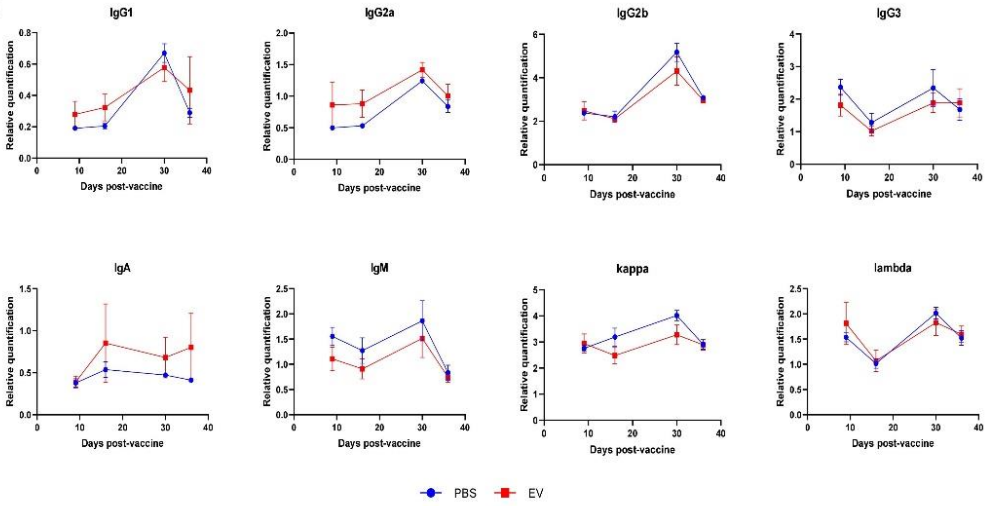

b)

Treatment	Immunized Mouse ID	Spot count Well 1	Spot count Well 2	Spot count Well 3	Ctl -	Ctl +
PBS	Mouse 1	4	0	0	0	152
	Mouse 2	0	0	0	0	39
	Mouse 3	0	0	0	0	111
	Mouse 7	0	1	0	0	120
	Mouse 8	0	0	0	0	113
	Mouse 12	0	0	0	0	80
EV	Mouse 4	0	0	0	0	44
	Mouse 5	0	1	1	0	191
	Mouse 6	2	0	0	0	98
	Mouse 9	1	1	0	1	112
	Mouse 10	0	0	4	0	33
	Mouse 11	0	0	0	0	28

Figure 4

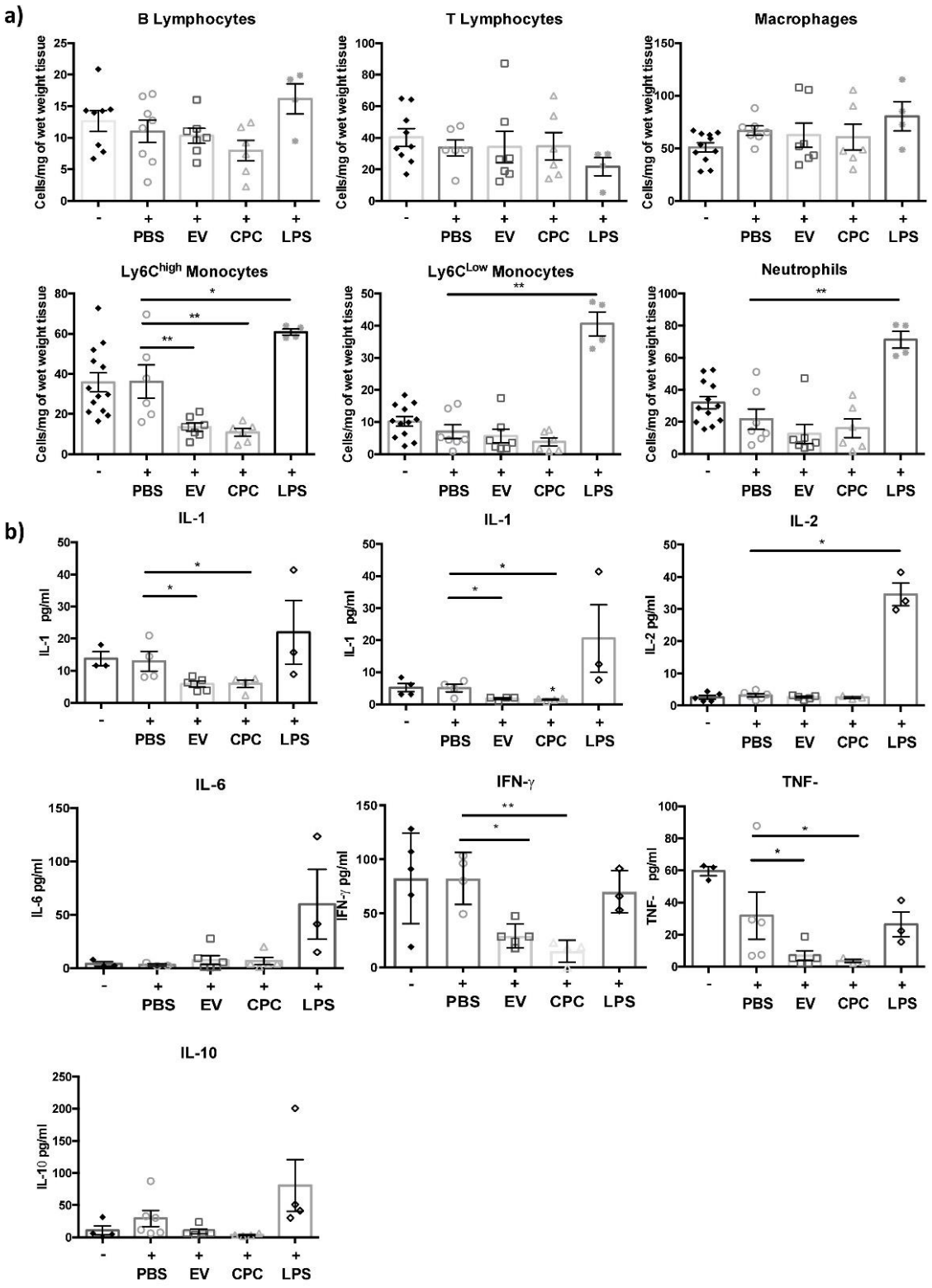
a)
B Lymphocytes
T Lymphocytes
Macrophages
Ly6C^high Monocytes
Ly6C^Low Monocytes
Neutrophils
Cells/mg of wet weight tissue
PBS
EV
CPC
LPS
b)
IL-1
IL-1
IL-2
IL-6
IFN-γ
TNF-
IL-10
IL-1 pg/ml
IL-2 pg/ml
IL-6 pg/ml
IFN-γ pg/ml
TNF- pg/ml
IL-10 pg/ml

Figure 5

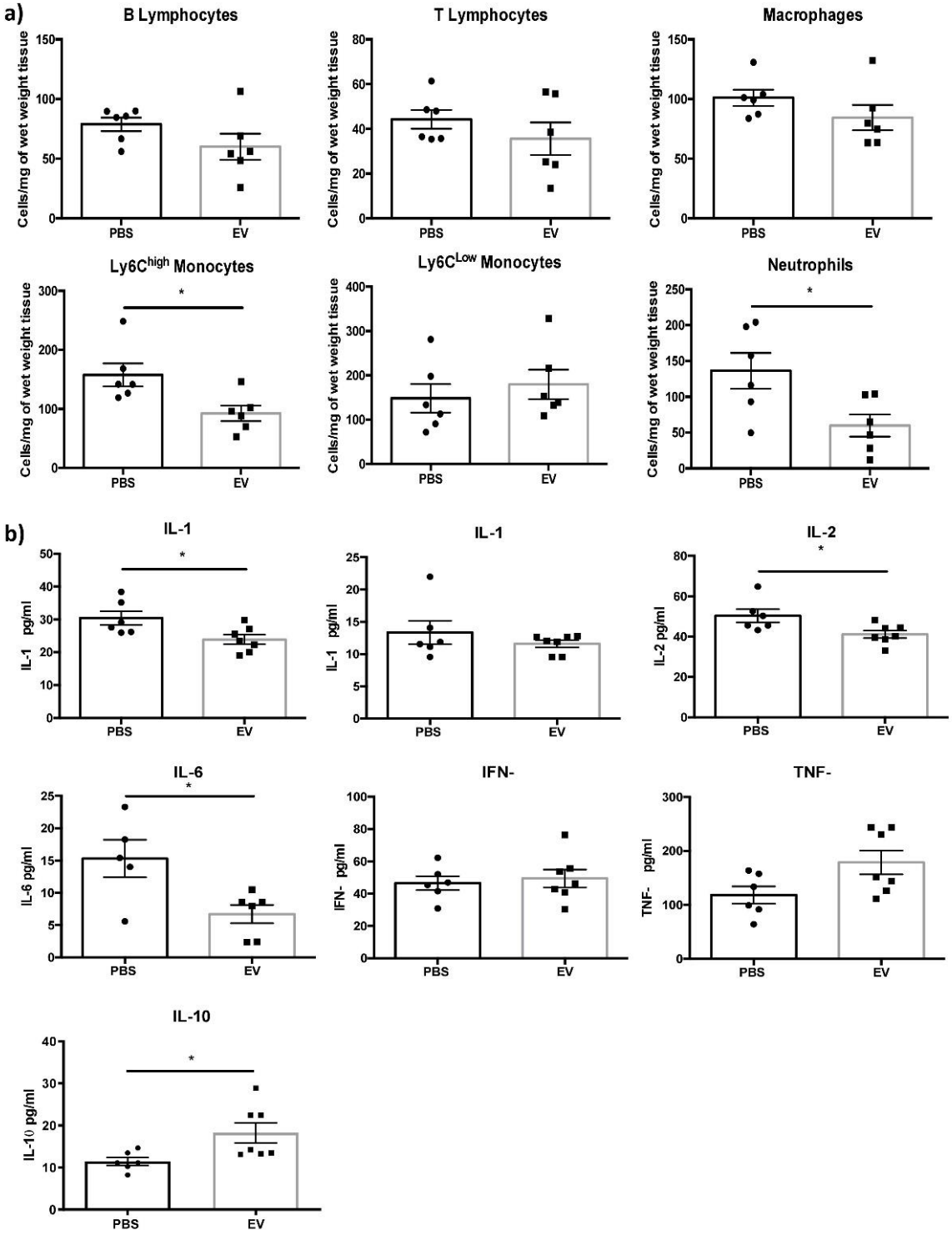
a)
B Lymphocytes
T Lymphocytes
Macrophages
Cells/mg of wet weight tissue
PBS
EV
Ly6C^high Monocytes
Ly6C^Low Monocytes
Neutrophils
*
b)
IL-1
IL-1
IL-2
IL-1 pg/ml
IL-2 pg/ml
IL-6
IFN-
TNF-
IL-6 pg/ml
IFN- pg/ml
TNF- pg/ml
IL-10
IL-10 pg/ml

Figure 6

a)

Cell marker (CD)	M0	M0 + EV	p-value	M1	M1 + EV	p-value	M2	M2 + EV	p-value
CD80+/ CD86+	58.1 % (+/-6.4)	25.6 % (+/- 7.6)	p≤ 0.05	88.1 % (+/- 3.6)	89.9% (+/- 4.9)	p≥0.05	33.1% (+/- 14.0)	34.2% (+/-16.6)	p≥0.05
CD206+	40.1 % (+/- 12.8)	66.6 % (+/- 15.08)	p≤0.05	13.9 % (+/-3.5)	22.9 % (+/- 2.3)	P≤0.05	63.7 % (+/- 18.7)	66.2 % (+/- 16.0)	p≥0.05
CD163+	22.9 % (+/-13.2)	34.5 % (+/- 17.8)	p≥0.05	1.7 % (+/- 0.8)	3.1 % (+/- 1.7)	p≥0.05	34.2 % (+/-23.4)	40.8 % (+/-36.6)	p≥0.05

b)

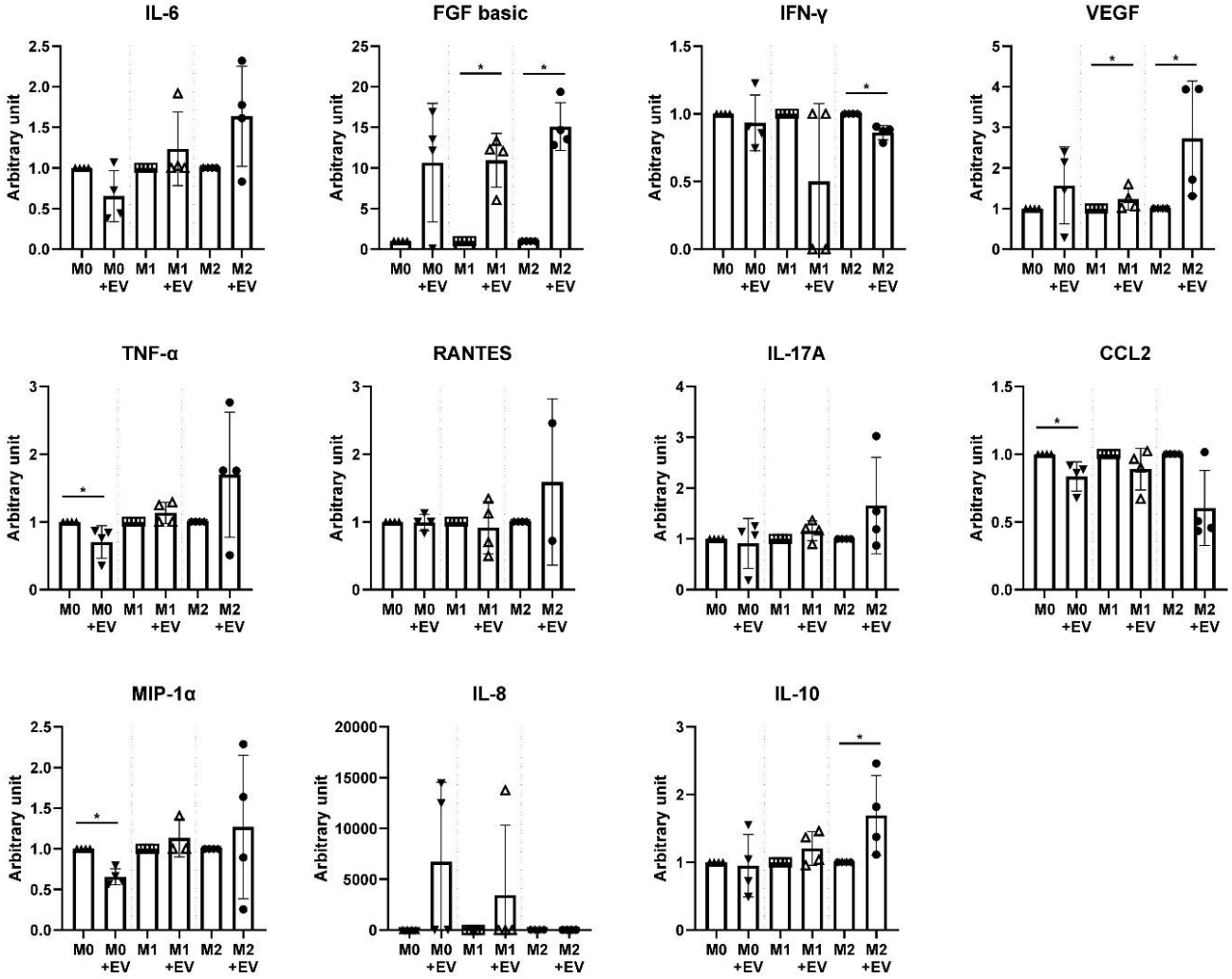

Figure 7

Visual Abstract

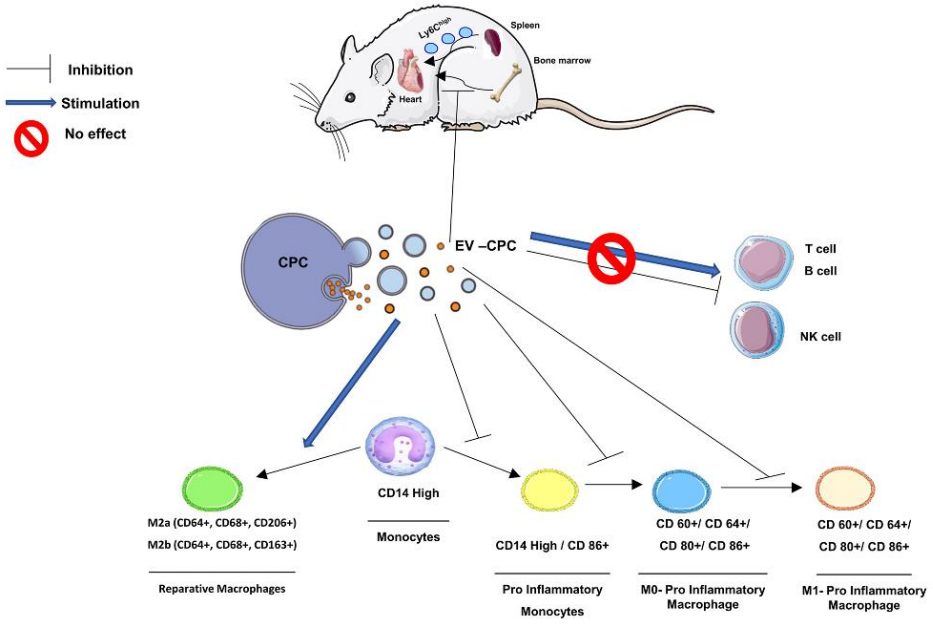

Cardiovasc Res, Volume 117, Issue 1, 1 January 2021, Pages 292–307, https://doi.org/10.1093/cvr/cvaa028
The content of this slide may be subject to copyright: please see the slide notes for details.

OXFORD UNIVERSITY PRESS

Supplemental Material

Cell culture

Cryopreserved iPSC-CPC were thawed and plated at a density of 78,000 cells/cm^2 on fibronectin-coated flasks (ref.: 11051407001, Roche Applied Sciences, Indianapolis, IN, USA) and cultured 4 days at 7% CO_2 and 37°C in serum-free media according to the proliferation protocol recommended by the manufacturer: William's E medium (ref.: A12176-01, Life Technologies, Saint Aubin, France) with Cocktail B from hepatocyte maintenance supplement pack (ref.: CM4000, Life Technologies), 25µg/mL Gentamicin (ref.: 15750, Life Technologies) and bFGF, 1µg/mL (Miltenyi, ref.: 130-093-842). The particle concentration in the media prior to exposure to cells (virgin media) was $4x10^8$ particles/mL. During CPC culture, the media was refreshed on day 2, and at day 4, the conditioned media (containing the EV secreted over the previous 48 hours) was collected for EV isolation. The particle concentration in the conditioned media was 1000-fold higher than in the virgin media alone.

Quantification and size distribution of EV

Nanoparticle tracking analysis (NTA) (NanoSight LM-14, Malvern) of EV-CPC preparation detected a poly-disperse population of particles ranging primarily from approximately 50 to 550 nm, with a small population at around 1000 nm. The majority of particles (~70%) in our preparations were in the size range of small particles (approximately 50–200 nm) as shown in Supplemental Figure 1b.

Dose of EV-CPC

The doses used are expressed in different metrics according to MISEV guidelines. The EV-CPC secreted by an equivalent amount of $1.4x10^6$ of CPC correspond to $1x10^{10}$ (+/-3000) particles, as quantified by NTA and 100 µg of proteins, as measured by BCA (Thermo Scientific).

Bioactivity assays for EV-CPC

Each batch of EV-CPC was tested *in vitro* using angiogenesis and viability assays described in our previous work [6] and which basically entail the measurements of scratch-induced endothelial cell wound healing and viability of H9c2 cardiomyoblasts stressed by serum deprivation, respectively.

EV-CPC characterization

To test if the effect on the secretome of EV-CPC is not due to components of the cell culture media alone (composed by William's E medium; Cocktail B and human bFGF), we used the H9c2 cell viability assay described in our previous work [6]. As expected, the viability of stressed cells following their exposure to EV-CPC robustly outweighed those incubated in the presence of the media alone (362 % *vs.* 234%.

To separate the protein load co-purified with EV from EV, we used size exclusion chromatography (qEV isolation system, Izon Science, Oxford, UK) and assessed the bioactivity of the isolated fractions with the above-mentioned cell viability assay [6]. The EV –CPC + protein bulk yielded a viability of 398% compared to the negative control. This effect was decreased by 2.6-fold with the only EV-enriched fraction and 1.3-fold with the protein-enriched fraction, thereby supporting the use of the whole secretome to leverage the synergystic protection afforded by each fraction separately.

Concerning EV-CPC stability, we incubated EVs during 9 days at 37°C and tested their bioactivity at different time points: Day 0, Day 2, Day 6 and Day 9, using a cell viability assay previously described [6] and in which H9c2 cells are stressed by serum deprivation. Compared with the control, viability increased by 3.6-fold at Day 0; 2.8-fold at Day 2; 2.5-fold at Day 6 and 2.0-fold at Day 9.

EV-CPC did not express Calnexin, as expected for EV (data no shown).

Supplemental Figures

Supplemental Figure 1: a) Fluorescence intensity of EV-CPC surface marker. EVs from 4 independent productions were captured by a set of 39 bead-linked antibodies, followed by staining with a cocktail of anti-CD9, anti-CD63 and anti CD81-APC antibodies. REA and mIgG1 indicate isotype control-beads, i.e. beads linked to an antibody which does not bind EV. CPC: iPS cell-derived cardiovascular progenitor cells; EV: Extracellular vesicles from iPS cell-derived cardiovascular progenitor cells. Data are presented as box-and-whisker plots, with the midline representing the median and the whiskers representing maximum and minimum values. b) Nanoparticle tracking analysis of EV-CPC preparation detected a poly-disperse population of particles ranging primarily from approximately 50 to 550 nm, with predominantly small particles.

Supplemental Figure 2: Circulating blood levels of inflammatory cells and cytokines in the chronic myocardial infarction model. Three weeks after MI, mice were untreated (n=5) or injected with PBS (n=6-8), EV (n=7), CPC (n=6) or LPS (n=4). Three days after injections, the plasma was processed by flow cytometry for the assessment of immune cells (a) and inflammatory mediators (b), using a luminex bead-based multiplex assay; untreated (n=5), PBS (n=4), EV (n=5), CPC (n=4) or LPS (n=3). Results are given as mean ± SD. PBS: Phosphate-Buffered Saline; LPS: Lipopolysaccharide; other abbreviations as in Supplemental Figure 1. The histogram at the far left corresponds to the group of mice which underwent myocardial infarction but did not receive any treatment.
Wilcoxon signed rank test was used, a p-value <0.05 was considered statistically significant. * $p \leq 0.01$.

Supplemental Figure 3: Spleen and Bone marrow inflammatory cells in the chronic myocardial infarction model. a) Three weeks after MI, mice were untreated (n=5) or injected with PBS (n=6-7), EV (n=7), CPC (n=6) or LPS (n=4). Three days after injections, the spleen was processed by flow cytometry for the assessment of immune cells. The results represent the mean ± SD of the number of cells/g of tissue. b) Tree days after treatment, the bone marrow was collected flushing one femur of each mice and immune cells were analyzed by flow cytometry. Untreated (n=5), PBS (n=6-8), EV (n=7), CPC (n=6) or LPS (n=4) * $p \leq 0.05$; Same abbreviations as in Supplemental Figure 2. Wilcoxon signed rank test was used, a p-value <0.05 was considered statistically significant. *$p < 0.05$; ** $p \leq 0.01$.

Supplemental Figure 4: Spleen and Bone marrow inflammatory cell number in the acute myocardial infarction model. a) Two days after MI, mice were injected with PBS (n=6) or EV (n=6). Three days after injections, the bone marrow was collected by flushing one femur and processed by flow cytometry for the assessment of immune cells. b) Three days after injections, the spleen was processed by flow cytometry for the assessment of immune cells.

Supplemental Figure 5: Schematic representation of polarization of human macrophages into M0, M1 or M2 macrophages with or without exposure to EV-CPC. EV= Extracellular vesicles from iPS cell-derived cardiovascular progenitor cells.

Supplemental Figure 1

a)

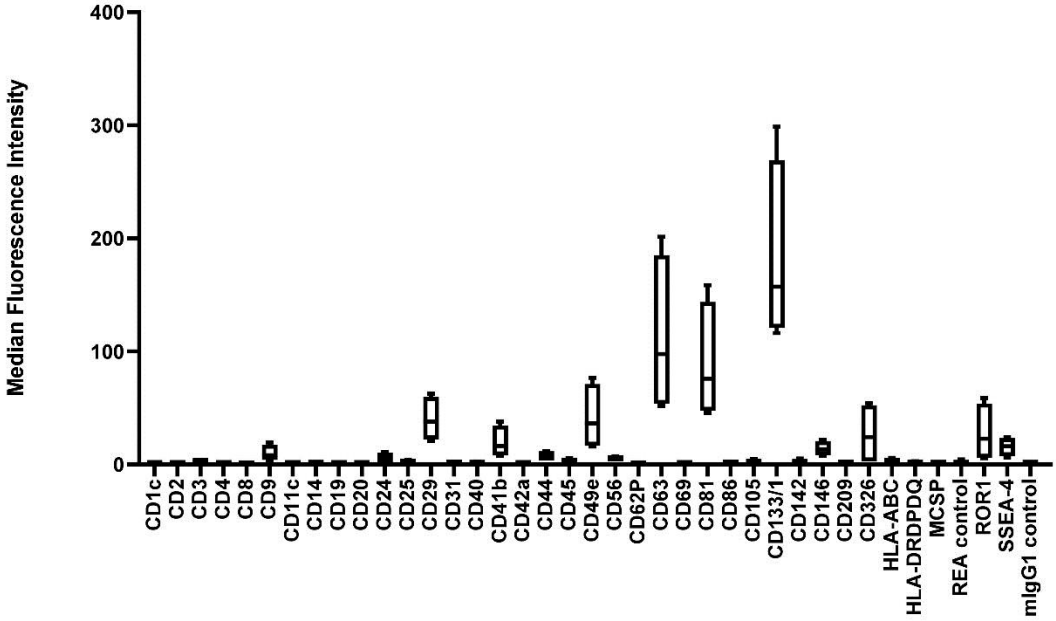

b)

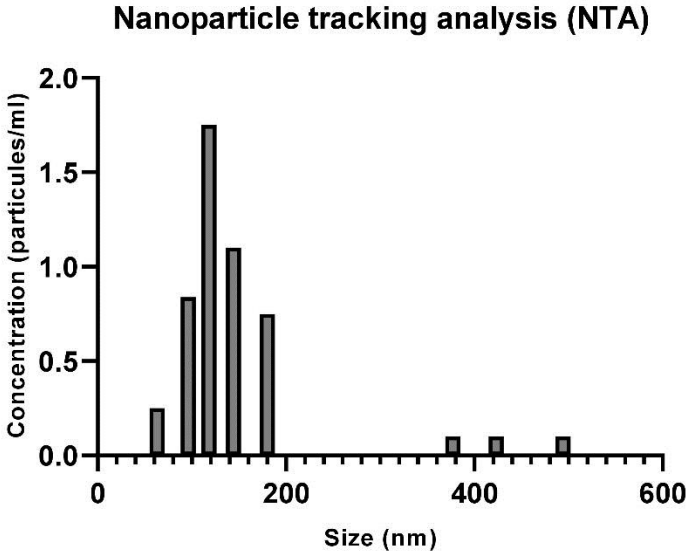

Supplemental Figure 2

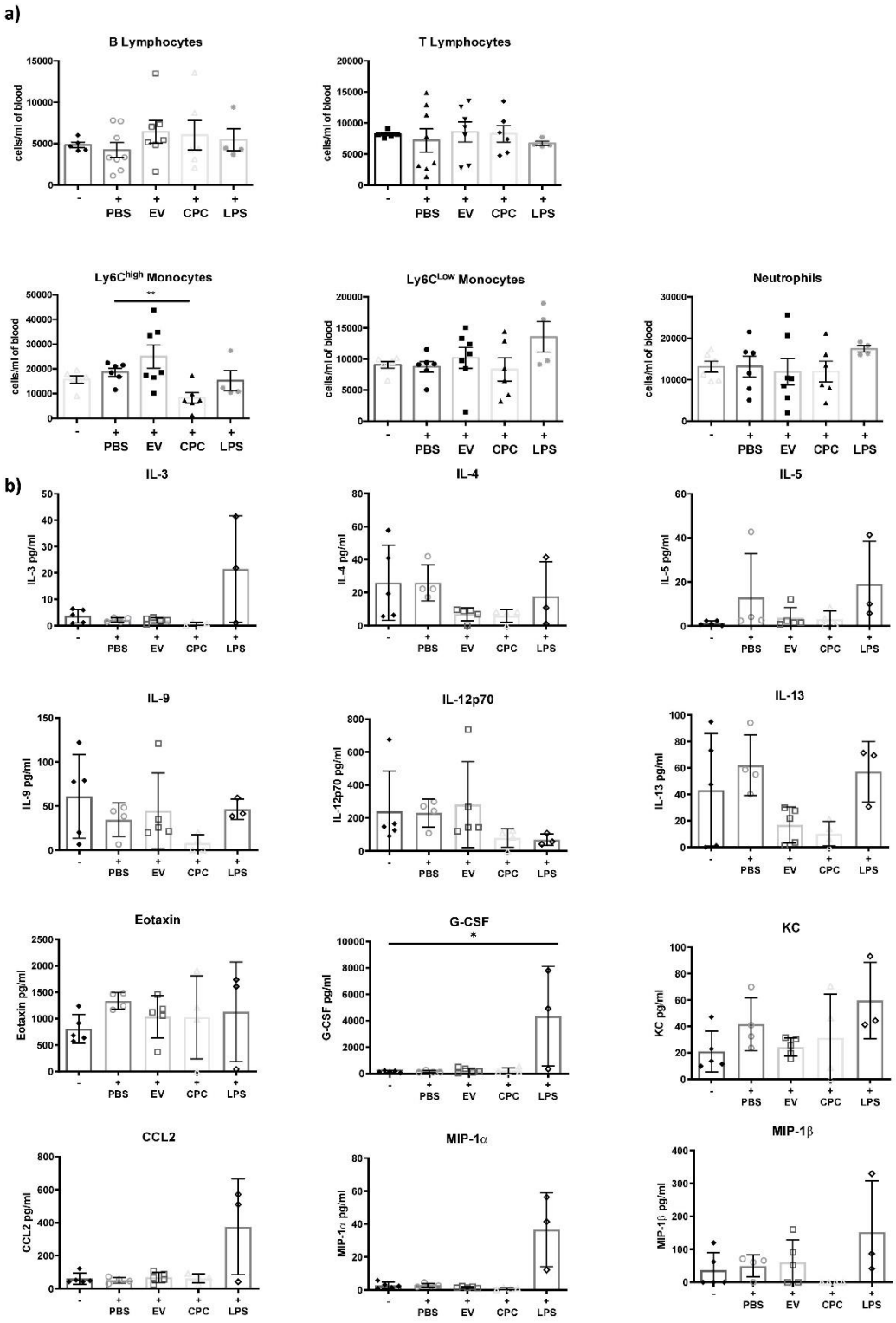

Supplemental Figure 3

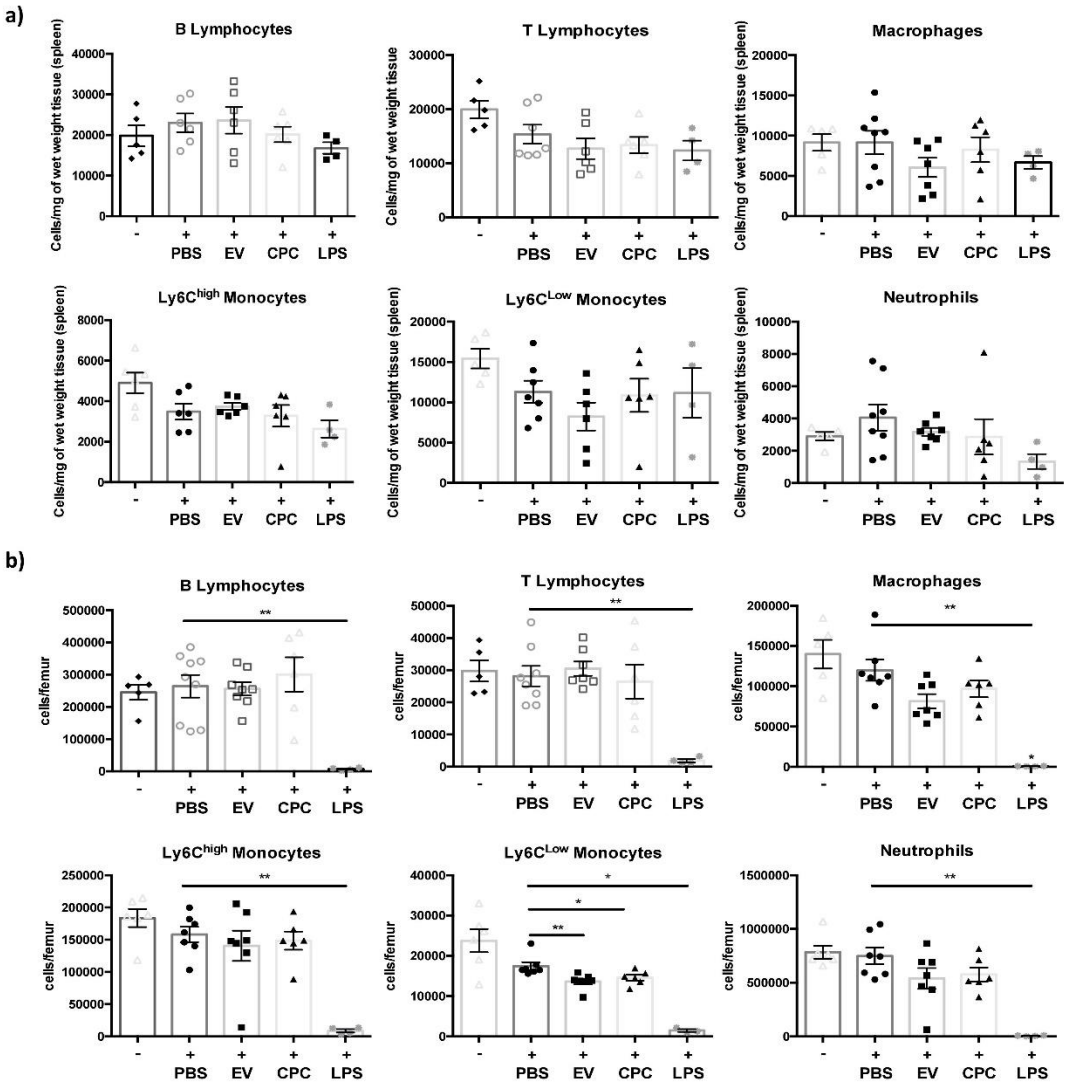

Supplemental Figure 4

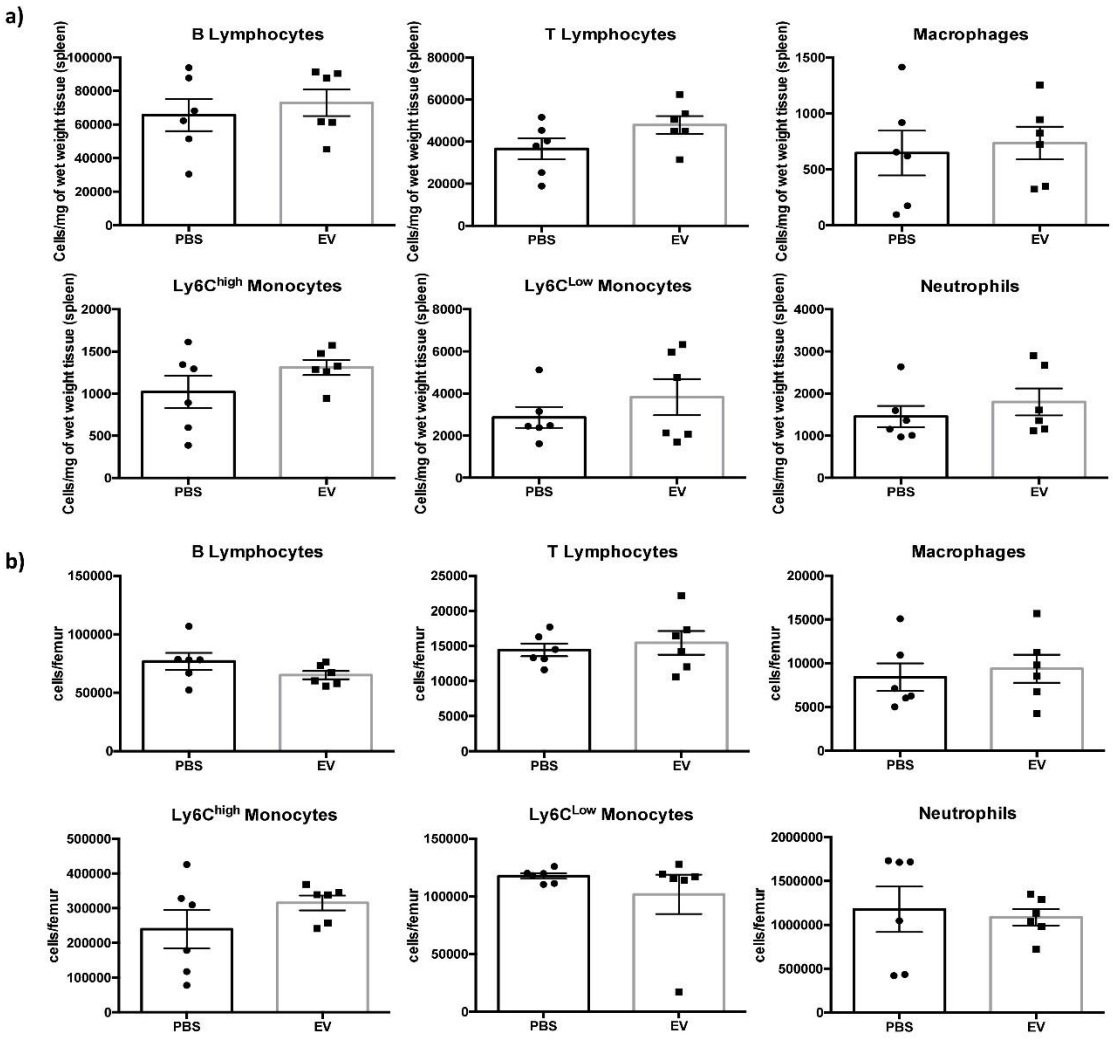

Supplemental Figure 5

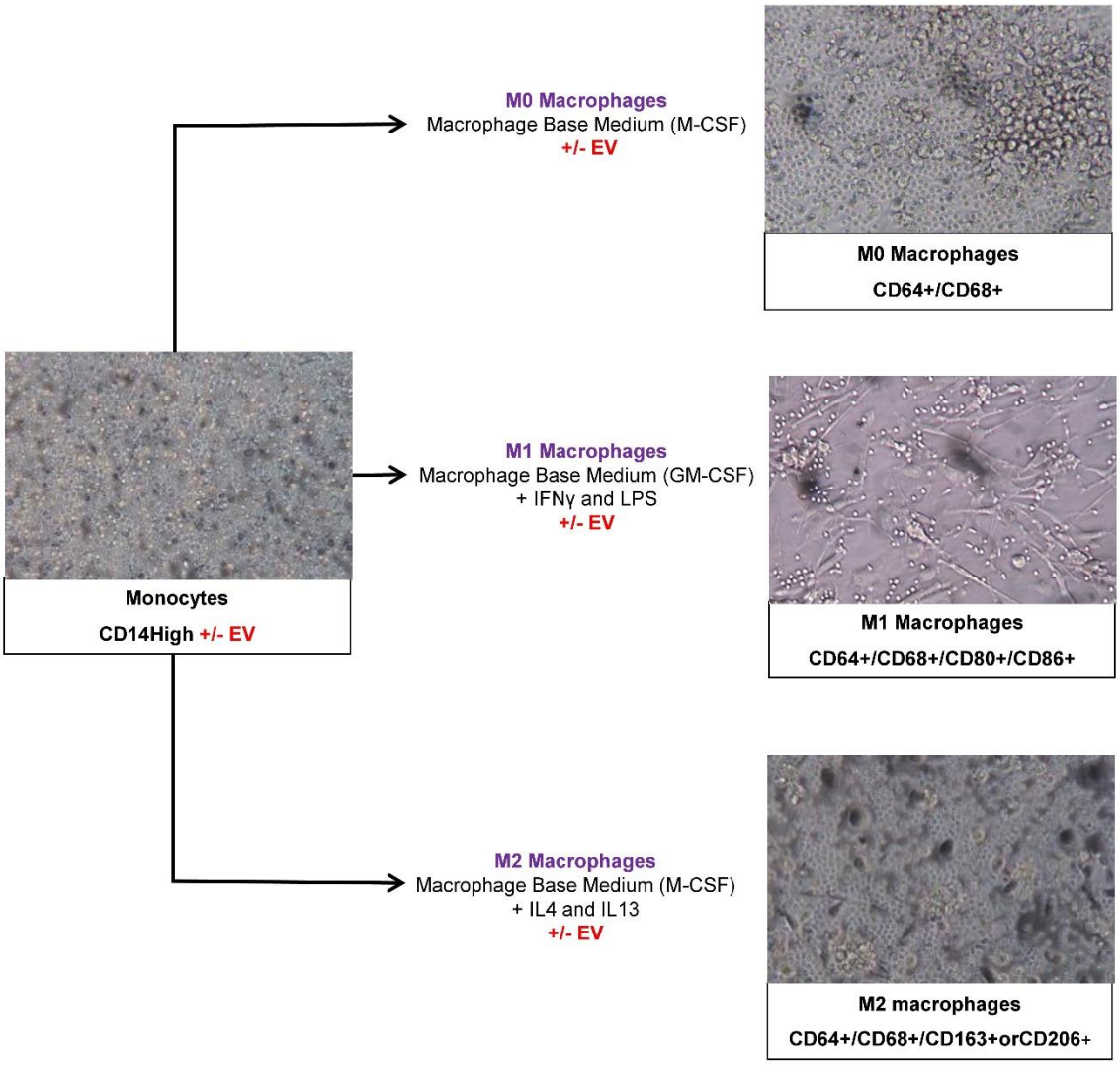

Do Extracellular Vesicles Improve Cardiac Function by Generating New Cardiomyocytes?

Bruna Lima Correa*, MSc[1], Nadia El Harane*, PhD[2], Manon Desgres, MSc[1], Maria Perotto, MD[3], Paul Alayrac, MSc[1], Chloé Guillas, MSc[1], Laetitia Pidial, MSc[1], Valérie Bellamy, BS[1], Emilie Baron, MD[4], Gwennhael Autret, MSc[1], Keirththana Kamaleswaran, MSc[1], Chloé Pezzana, MSc[1], Marie-Cécile Perier, MsC[1], José Vilar, PhD[1], Antonio Alberdi, PhD[5], Nisa Renault, PhD[6], Massimiliano Gnecchi, MD, PhD[3], Jean-Sébastien Silvestre, PhD[1], Philippe Menasché, MD, PhD,[1,7].

Short Title: Extracellular Vesicles for Heart Failure

Affiliations

1. Université de Paris, PARCC, Inserm, F-75015 Paris, France
2. University of Geneva, Translational Research Centre in Onco-hematology, Department of Medicine, Geneva, Switzerland
3. Department of Molecular Medicine, Unit of Cardiology, University of Pavia, Pavia, Italy. and Laboratory of Experimental Cardiology for Cell and Molecular Therapy, Fondazione IRCCS Policlinico San Matteo, Pavia, Italy.
4. Department of Cardiology, Hôpital Européen Georges Pompidou, F-75015 Paris, France
5. Inserm, UMRS-976, Hôpital Saint-Louis, Paris, France
6. Fujifilm Cellular Dynamics, Inc, Madison, Wisconsin, USA.
7. Department of Cardiovascular Surgery, Hôpital Européen Georges Pompidou, F-75015 Paris, France

Address for correspondence

Philippe Menasché
Department of Cardiovascular Surgery
Hôpital Européen Georges Pompidou
20, rue Leblanc
75015 Paris, France
Email : philippe.menasche@aphp.fr
Phone : +33(0)1 56 09 36 22
Fax : +33(0)1 56 09 32 61

or Jean-Sébastien Silvestre
INSERM 970, team 6
Paris Centre de Recherche Cardiovasculaire
56, rue Leblanc
75015, Paris, France
Email : jean-sebastien.silvestre@inserm.fr
Phone: +33 (0)1 53 98 80 60
Fax: +33(0) 1 53 98 79 51

Word count: 7472

Key words:
Heart failure, extracellular vesicles, acellular therapy, cardiac cell proliferation, myocardial fibrosis

Abstract

Background: Extracellular vesicles (EV) mediate the therapeutic effects of stem cells but it is unclear whether this involves cardiac regeneration mediated by endogenous cardiomyocyte proliferation.

Methods: Bi-transgenic MerCreMer/ZEG (n=15/group) and Mosaic Analysis With Double Markers (MADM; n=6/group) mice models underwent permanent coronary artery ligation and received, 3 weeks later, 10 billion EV (from human iPS-derived cardiovascular progenitor cells [CPC]), or saline, injected percutaneously under echo guidance in the peri-infarcted myocardium. Endogenous cardiomyocyte proliferation was tracked by EdU labeling and biphoton microscopy. End points, including cardiac function (echocardiography and MRI), histology and transcriptomics were blindly assessed 4-6 weeks after injections.

Results: Ejection fraction of control hearts decreased over the study period while it increased in both EV-treated groups. Echocardiographic changes from baseline were thus significantly different between EV groups and controls: 20.7% ± 10.5 % (p=0.048) and 28.0% ± 11.0 %, (p=0.045) for MerCreMer/ZEG versus controls and MADM versus controls, respectively (mean ± SEM). This improvement was confirmed by MRI. However, there was no proliferation of cardiomyocytes in either transgenic mouse model and this was confirmed by the absence of activation of the Hippo pathway. EV administration reduced infarct size by 11.9 ± 5.75% (p=0.04), decreased expression of several pro-fibrotic genes compared with controls and triggered an overexpression of the anti-fibrotic miRNA 133-a1 compared to controls (n=3/group; p=0.001). Experiments with an anti-miR133-a demonstrated that the cardio-reparative effects of EV were partly abrogated.

Conclusions: EV-CPC improve cardiac function by mechanisms independent of cardiomyocyte proliferation and which may include the regulation of fibrosis.

This paper was presented at The Society of Thoracic Surgeons annual meeting, January 29-31, 2021.

Abbreviations

Extracellular vesicles (EV)

Mosaic Analysis With Double Markers (MADM)

iPS (induced pluripotent stem cells)

iPS-derived cardiovascular progenitor cells (CPC)

EdU (5-ethynyl-2´-deoxyuridine)

Magnetic resonance imaging ([MRI)

Left ventricular ejection fraction (LVEF)

Extracellular vesicles from iPS-derived cardiovascular progenitor cells (EV-CPC)

Nanoparticle Tracking Analysis (NTA)

Minimal Information for Studies of Extracellular Vesicles (MISEV)

Green fluorescent protein (GFP)

Transgene (Tg)

Myosin heavy chain (MHC)

Myocyte enhancer factor-2 (MEF-2)

Optimal Cutting Temperature compound (OCT)

Real-Time Quantitative Reverse Transcription Polymerase Chain Reaction (qRT-PCR)

Fibroblast Activated Protein (FAP)

Room temperature (RT)

Troponin T (TnT)

Fluorescein (FITC)

Lectin Wheat Germ Agglutinin (WGA)

Ribonucleic acid (RNA)

Glyceraldehyde 3-phosphate dehydrogenase (GAPDH)

Hydroxymethylbilane synthase (Hmbs)

LVEDV (left ventricular end-diastolic volume)

LVESV (left ventricular end-systolic volume)

Col (Collagen)

Lysyl oxidase (LOX)

Matrix Metalloproteinase 3 (MMP3)

Micro-ARN (miR)

Bromodeoxyuridine (BrdU)

Yes-associated protein 1 (YAP)

Introduction

Except for cardiac transplantation, the current treatments of ischemic heart failure do not address the root cause of the disease, i.e., the loss of a large number of cardiomyocytes and this observation has been a strong incentive for transplanting therapeutic stem cells with the hope of replacing tissue loss by new functional cardiac cells. Experimentally, several cell types of distinct origins (skeletal myoblasts, bone marrow cells, mesenchymal stromal cells, putative c-kit$^+$ cardiac stem cells, cardiosphere-derived cells and pluripotent stem cell-derived cardiomyocytes [1–9]) have been shown to improve cardiac function and attenuate adverse left ventricular remodelling. However, the parallel and consistent observation that few, if any, of these cells engrafted permanently has led to challenge the exogenous cell-based "remuscularization" hypothesis and led to consider an alternate mechanism of action based on the paracrine harnessing of endogenous pathways contributing to cardiac repair.[10] Further mechanistic insights have then led to recognize that these paracrine effects were largely mediated by biomolecules packaged in extracellular vesicles (EV). These nanoparticles harbour a biologically rich cargo made of proteins, lipids and nucleic acids that they shuttle into recipient cells, thereby modulating their function. The most compelling evidence for the role of EV as mediators of the stem cells effects has come from the findings that they could recapitulate the cardio-protective potential of their parent cells in pre-clinical models of multiple diseases including ischemic heart injury.[11–13] In a clinical perspective, EV-based therapies are currently raising a growing interest because of their attractive features including a large-scale production more akin to that of a pharma-type product,[14] their lack of immunogenicity (depending of the parental cells). [15]

However, the precise mechanism(s) whereby EV improve cardiac function remain elusive. Since one of them could be the induction of cardiomyocyte proliferation, the present study was designed to assess, with the use of two transgenic models, whether EV could trigger endogenous cardiomyocyte proliferation in the setting of chronic heart failure.

Ethics section

All procedures were approved by the Institutional Ethics Committee from Paris University (project #04073.01) and complied with European legislation (European Commission Directive 2010/63/EU) on animal care. All animals received anesthesia by isoflurane (1.5 L/min isoflurane at 0.8-1.0L/min of O_2) and were euthanized by an overdose of isoflurane (3.5 L/min isoflurane at 2.0 L/min of O_2).

Cell Culture, Extracellular Vesicle Preparation and Characterization

Cell Culture and EV isolation

Cryopreserved cardiovascular progenitor cells differentiated from human induced pluripotent stem cells (iPSC-CPC) (CPC-301-020-001-PT, iCell®, Cellular Dynamics International, Madison, WI) were thawed and plated at a density of 78,000 cells/cm^2 on fibronectin-coated flasks (Roche Applied Sciences, St. Quentin Fallavier, France) and cultured for 4 days with 7% CO_2 at 37°C in serum-free media (William's E medium) with Cocktail B from hepatocyte maintenance supplement pack, 25µg/mL Gentamicin (Life Technologies, Illkirch, France) and bFGF, 1µg/mL (Miltenyi, Bergisch Gladbach, Germany). During iPSC-CPC culture, the media was refreshed on day 2 and on day 4, the conditioned media containing the EVs secreted over the previous 48 hours was collected for EV isolation. Conditioned media was then pre-cleared by centrifugation for 6 minutes at 1200 *g* and EVs were pelleted by ultracentrifugation for 16 hours at 100,000 *g*.

EV quantification

Extracellular vesicles were quantified by Nanoparticle Tracking Analysis (NanoSight LM-14, Malvern, Palaiseau, France), and protein content was measured by BCA (Thermo Scientific, Illkirch, France) as previously described.[15,16] The EV-CPC were characterized following the MISEV guidelines,[17] using evaluation of CD9, CD81, CD63 expression by Western Blot, immuno-gold labeling cryo-transmission electron microscopy and flow cytometry. Each batch of EV-CPC was tested *in vitro* using scratch-induced endothelial cell wound healing and H9c2 cardiomyoblasts viability assays, as previously described.[15]

Generation of the MerCreMer/ZEG mouse model

MerCreMer/ZEG mice harbor a tamoxifen inducible Cre-recombinase under the genetic control of the cardiomyocyte-specific alpha myosin-heavy chain promoter (MerCreMer transgene) and a ubiquitously expressed floxed LacZ gene plus stop codon upstream of a GFP locus[18] (ZEG transgene). These mice were obtained by breeding a MerCreMer female mouse (B6.Cg-Tg (ACTB-Bgeo/GFP) 21Lbe/J) with a ZEG male mouse (Tg(CAG-Bgeo/GFP)21Lbe/J) which were kindly provided by Professor Richard Lee, Harvard University. For genotyping, tail tips were sampled, DNA extracted, and polymerase chain reaction (PCR) was performed to identify double transgenic animals with primers listed in the Supplemental Material section. Double heterozygous MerCreMer-ZEG mice were used for the subsequent experiments.

Generation of the mosaic analysis with double markers (MADM) mouse model

Mosaic analysis with double markers mice with a high lox-induced efficiency upon recombination (MADM-ML) were obtained from the Jackson laboratory (JAX, Bar Harbor, Maine): Igs2tm1(ACTB-EGFP,-tdTomato)Zng/Igs2tm2(ACTB-tdTomato,-EGFP)Zng/J. To allow a cardiac-specific labelling, we crossed MADM-ML mice with animals expressing a constitutive cardiac-specific alpha myosin-heavy chain–Cre obtained from JAX laboratory: B6.FVB-Tg(Myh6-cre)2182Mds/J. In this model, cardiomyocytes that successfully divide in the presence of a cell-type-specific Cre-recombinase produce daughter cells that are either red, green, red and green (yellow) or colorless, based on allelic recombination of fluorescent reporters; however, if the cardiomyocytes fail to divide, they remain double-colored (yellow) if recombination occurs or colorless if there is no recombination. The identification of these animals was performed by PCR on DNA extracted from tail tips with primers listed in the Supplemental Materials section.

Experimental model of chronic heart failure

Myocardial infarction (MI) was induced in MerCreMer/ZEG, MADM and C57BL/6J mice by permanent ligation of the left coronary artery. Two different protocols of infarction were implemented which differed by the timing of the treatment: in MerCreMer/ZEG and MADM mice, a chronic protocol was used with treatment given 3 weeks after the infarction and sacrifice 4-6 weeks thereafter. In the MerCreMerZEG series of mice, Cre recombinase expression was induced by a tamoxifen-containing diet (1-2 mg/pellet; 14 mg total; Envigo, Gannat, France) given for 14 days, followed by a 5-day wash-out before induction of infarction. In the C57BL/6J model, one part of the animals underwent an acute protocol with treatment implemented 3 days after infarction and sacrifice 2 days later for tissue collection and transcriptomic analysis; the remainder of mice went through the chronic protocol with sacrifice 4-6 weeks after treatment.

Regardless of the timing, EV or a control PBS solution were injected trans-cutaneously to avoid a second surgical procedure and its attendant mortality. To this end, mice were anesthetized with 2.5% isoflurane and immobilized on the VisualSonics (Amsterdam, The Netherlands) platform, as previously described .[19] Three injections of 15 µL each were performed under echocardiographic guidance in the anterior wall of the left ventricle (LV) in the peri-infarction zone, two in long axis view and one in lateral view. Extracellular vesicles were delivered at a dose of $1x10^{10}$ (±3000) particles quantified by NTA, secreted by 1.4 million iPSC-CPC corresponding to 100 µg of proteins (BCA). In a separate set of experiments, 20µM of the anti-miR 133-a (Ambion by Life Technologies) were also co-delivered with EV. An equivalent volume of 45 µL was delivered in all PBS-injected control hearts. The different protocols are summarized in Figure 1.

Echocardiography

Three weeks after MI, all mice underwent a two-dimensional echocardiography (2 VEVO 2100 , Visualsonics [Amsterdam, The Netherlands]). Images were acquired in long axis view in B-mode (VEVO Lab) and all parameters were calculated according to a previously described protocol.[20] All animals with a left ventricular ejection fraction (LVEF) > 45% were excluded. They were then

assigned to the control and experimental groups to ensure that baseline values LVEF and left ventricular endsystolic (LVESV) and endiastolic (LVEDV) were well balanced between groups, thereby minimizing biases in the subsequent assessment of treatment effects. Four to six weeks after treatment, cardiac echography was performed again under the same conditions by the same operator blinded to the treatment groups.

Magnetic Resonance Imaging (MRI)

To validate echocardiographic results with a more operator-independent technique, 11 mice in the MerCreMer/ZEG series (EV n=5, PBS n=6) underwent MRI imaging in a Bruker BioSpec (Bruker, Wissembourg, France) adapted for small animal studies with a 4.7 Tesla magnetic field. Images were acquired for 85s each using a FLASH-cine IntraGate technology and 1.03 mm-thick slices were oriented along the heart's short axis. Image analysis was carried out using the Cvi42 software (Circle Cardiovascular Imaging Inc. Calgary, Canada) for Windows 7 by two blinded operators.

5-ethynyl-2´-deoxyuridine (EdU) protocol

Osmotic minipumps (Alzet, Cupertino, CA) delivering EdU (EdU-Click 647 cell proliferation assay, Baseclick, Neuried, Germany) at 1µg per hour per gram body weight were subcutaneously implanted for 7-10 days. Mice were sacrificed at 4-6weeks following pump implantation and hearts and liver were collected.

HL-1 cells and 3T3 cells culture

Murine cardiomyocyte cells (HL-1 cells generously provided by Pr. Claycomb, LSU Health, School of Medicine, New Orleans, LA) or NIH/3T3 fibroblasts (ATCC® CRL-1658™, ATCC, Molsheim, France) were seeded at 250,000 cells per well and cultured until confluence in a 6-well plate. When confluence was reached, culture media was replaced with serum-deprived media and cells were treated with either EV-CPC (10.10^9 particles per well) or 0.1 µm filtered PBS for 24 hours. Cells were then washed with filtered PBS and subsequently lysed with 800 µl QIAzol reagent (Qiagen, Courtaboeuf, France). Sample lysates were transferred into new tubes for miRNA extraction and quantification of miR 133-a by qRT-PCR.

MEF2 detection

Nuclear extraction of EV-CPC was performed using the Nuclear Extraction Kit (Abcam) and the extracts were quantified using BCA (ThermoScientific) for protein content. High throughput ELISA assay was used to quantify the MEF2 transcription factor (Abcam, Cambridge, UK) in EV-CPC.

Immunohistochemistry and immunofluorescence microscopy

After sacrifice, explanted hearts were washed in PBS, submerged in Optimal Cutting Temperature compound (OCT, Tissue-Tek; Sakura Finetek, Villeneuve-d'Ascq, France), frozen in liquid nitrogen and stored at -80°C until sectioning. Hearts were cryo-sectioned into 5-10µm thin-sections and an average of 12 tissue sections of different ventricular locations per heart were used for

staining. To stain slides for Green Fluorescent Protein, cardiac Troponin T (TnT) and Fibroblast Activated Protein (FAP), fixation was performed with 4% paraformaldehyde for 15 minutes at room temperature (RT). Membrane permeabilization was achieved with 1% triton X-100 in PBS for 20 minutes at RT and non-specific epitopes were blocked with 5% bovine serum albumin (BSA) for 30 minutes at RT.

Triple GFP/TnT/ EDU staining

In the MerCreMer/ZEG mouse model, it was first necessary to check that after administration of Tamoxifen, mice expressed GFP exclusively in cardiomyocytes. A double staining for GFP and cardiac Troponin T was then performed with the relevant antibodies (FITC-conjugated anti-GFP, unconjugated anti-Troponin T and Texas red-conjugated secondary anti-rabbit antibody, all from Abcam). EdU was revealed according to the manufacturer's instruction by a click chemical reaction which yields a fluorescent dye (Cy5 Azide alternative). Nuclei were stained with 4', 6-diamidino-2-phenylindole (DAPI, Calbiochem, Lyon, France).

Double FAP/ TnT staining

Slides stained for FAP and TnT underwent a similar protocol using unconjugated anti-FAP (Fisher Scientific, Illkirch, France) and anti-TnT (Abcam) antibodies and Alexa 488-conjugated anti-rabbit (Life Technologies) and Alexa 594-conjugated anti-mouse secondary antibodies, respectively (Life Technologies). Nuclei were stained with DAPI.

Lectin Wheat Germ Agglutinin (WGA) and Isolectin staining

Slides stained for WGA and Isolectin underwent a similar protocol except that they were fixed for 10 minutes in acetone. Isolectin B4 and WGA were coupled to FITC and tetramethylrhodamine, respectively.

Hematoxylin/eosin staining

Thawed tissue sections were fixed in acetone for 10 minutes, washed 5 minutes in PBS and immersed for 2 seconds in hematoxylin and eosin (Sigma, Lyon, France). All slides stained were scanned with a slide scanner (NanoZoomer, Hamamatsu, Massy, France) and analyzed through the NDP view 2.5 software or the Metamorph® software (Molecular Devices, San Jose, CA) for fibrotic area calculation. Infarct size was calculated as the perimeter of the stained infarct area divided by the total perimeter of the section and expressed as a percentage.

Image analysis

Images were analyzed by Qcapture (QImaging, Surrey, Canada), observed using a Leica DM 2000 optical microscope and quantified manually using the Metamorph® or Image J softwares.

RNA expression on mice hearts or murine cultivated cells

RNA extraction

RNAs were extracted from heart tissue cryo-sections (200-400 µm) or cultured cardiomyocytes and fibroblasts following the manufacturer's instructions and the concentration and purity of samples were evaluated with the NanoDrop® Spectrophotometer (ThermoFisher Scientific, Illkirch, France).

Affymetrix microarray analysis

RNA quantification and quality control were performed using the HT Standard RNA LabChip Kit and the Caliper LabChip Microfluidics System (Perkin Elmer, Villebon sur Yvette, France). One-hundred nanograms of total RNA were amplified, labeled, and fragmented using GeneChip WT. Each sample was hybridized onto Mouse Clariom D, washed, and stained with the Affymetrix® Fluidics Station 450. Array scanning was performed with the Affymetrix® GeneChip Scanner 3000 7G using the Command Console software (ThermoFisher Scientific, Illkirch, France) and then analyzed using the Affymetrix® rma-sketch routine. Subsequently, differentially expressed genes (DEGs) were selected using one-way analysis of variance (ANOVA) using the Affymetrix Transcriptome Analysis Console (TAC) software v.1.0. The fold change (FC) ($2 \geq -2$) of every gene, together with their corresponding p value (0.05) were used for selection of DEGs.

Real-time quantitative PCR

q RT-PCR was used to assess the expression of genes involved in fibrosis, apoptosis, autophagy, proliferation and miR-133-a1 expression. The list of primers is indicated in the Supplemental Materials. The primers were designed using Primer Blasy with an annealing temperature of 50-60°C. First-strand cDNA was synthetized from 250 ng of total mRNA with random hexamer primers using the RevertAid first-strand cDNA synthesis kit (Thermo Scientific). Quantitative PCR was carried out in 384-well plates on cDNA products diluted to 1/25 in duplicate using SYBR Green on a LightCycler® 480 (Roche) with the following parameters: initial denaturation step (95°C, 5 min), then 40 cycles composed of denaturation (95°C, 30 s) and annealing/extension steps (60°-50°C for 15 s, 72°C for 15s). Hmbs or GADPH were used as the housekeeping genes. The ratio between the amount of a target gene and that of the endogenous reference was then determined.

Statistical Analysis

Apart from genome-wide analyses, Mann-Whitney or Student t-Test were used. Analyses were conducted using GraphPad InStat3 (8.0.1) and performed by an independent statistician blinded to the treatment groups. Values are given as means ± standard error of the mean (SEM) and a p value <0.05 was considered statistically significant. Mice that died within 24 hours of coronary artery ligation surgery (<10% in all genotypes studied) were excluded from subsequent analyses.

RESULTS

EV-CPC quantification

The majority of EVs (~70%) were in the size range of approximately 50 to 200 nm. The concentration of particles of the size of small EV in the media prior to cell exposure was $4x10^8$ particles/mL, as measured by NTA. This value represented the background noise which was taken into account when the actual number of EV released by the CPC (higher by two logs) was measured.

EV-CPC improved cardiac function without affecting endogenous cardiomyocyte proliferation

In MerCreMer/ZEG mice, LVEF increased by 18.9% ± 0.2% from baseline in the EV-treated hearts whereas it decreased by 2.3% ± 0.2% in the PBS group (Figure 2 a and b). This was associated with a decrease of LVEDV and LVESV by 3% ± 0.2% and 4% ± 0.3%, respectively, in the EV-treated group which contrasted with an increase by 20% ± 0.2% and 24% ± 0.2%, respectively, in the control group. This improvement of LVEF following EV injections was confirmed by MRI (Figure 2c). In this model a 4-OH-tamoxifen pulse induced green fluorescent protein (GFP) expression only in cardiomyocytes, with 80% of them expressing the fluorescent protein. The number of proliferating (EdU^+) cardiomyocytes (TnT^+) did not differ between groups and averaged 10.6 ± 2.7 cells in the infarct area, 18.9 ± 5.7 cells in the peri-infarcted area and 23.7 ± 8.5 cells in remote area in control mice whereas in EV-treated hearts, the corresponding values were 9.2 ± 1.9, 14.2 ± 3.5 and 11.4 ± 2.7, respectively (Figure 3 a and b). These values represented approximately 0.6% and 1.7% of the total cardiomyocyte content per tissue section. Importantly, all proliferating double-positive EdU^+ TnT^+ cardiomyocytes stained positive for GFP (Figure 3 c), thereby demonstrating that cardiac proliferation derived from pre-existing cardiomyocytes. In line with these findings, there was no upregulation of YAP which transcriptionally activates genes that promote cardiomyocyte proliferation (Figure 3 d).

MADM mice featured a similar pattern as intra-cardiac administration of EVs improved LVEF by 13.3% ± 0.16 % from baseline whereas it decreased by 14.4% ± 0.16 % in the control PBS-injected group (Figure 2 d and e). Likewise, there was a decrease of LVESV by 21% ± 0.2% in EV-treated hearts contrasting with an increase of 42% ± 0.2% in the control group. However, in keeping with the data obtained with the MerCreMer/ZEG model, we failed to show any difference in the number of single-colored cells between the two groups, thereby indicating a similar rate of cardiomyocyte proliferation independent of the EV treatment (Figure 3 e and f). Taken together, these results suggest that EV administration did not promote proliferation of pre-existing cardiomyocytes in the failing heart.

EV-CPC decreased infarct size and fibrosis

Conversely, EV administration reduced myocardial fibrosis. Indeed, MerCreMer/ZEG mice injected with PBS had a mean infarct size of 49% ± 10.7 % versus 36.6% ± 12.7 % in those that had received EV, yielding a significant difference of 12.4% ± 5.7 % (Figure 4 a and b). This was

paralleled by a decreased (albeit not significantly) expression of several pro-fibrotic mRNAs (Col 1a1, Col 3a1, Lox, MMP3) and a significant decrease in the number of FAP-positive cells[21] in EV-treated hearts compared to controls (Figure 4c). Likewise, in the C57BL/6J mice in which transcriptomics studies were performed acutely (i.e., 5 days post MI, 2 days post intervention) pro-fibrotic genes were also down-regulated, the difference between EV-treated and PBS controls being significant for MMP3 (p=0.0352) and Elastin (p=0.0058). Capillary density and cardiomyocyte hypertrophy did not differ between groups(data not shown).

To provide additional insight into the mechanism(s) of EV-induced cardiac repair, genome-wide microarrays were used to assess the differential expression of RNAs in the myocardial tissue of EV-CPC-treated MerCreMer/ZEG mice compared with PBS-injected animals (Figure 5a). Out of the 64,000 gene arrays, 14 genes were differentially expressed, of which 9 have been studied in mammalians (Table 1) In line with the histological findings, the anti-fibrotic miR-133-a1[22,23] and its pseudo-gene Gm21747 were found significantly upregulated compared with controls (by 2.13 and 2.94 fold, respectively, Table 1). However, only small amounts of miR-133-a1 were found in EV-CPC (data not shown), making unlikely that its increased expression in the EV-treated hearts was due to an EV-mediated direct transfer. As an alternate possibility was that EV foster an endogenous overexpression of miR-133-a1 in targeted cardiac resident cells, we looked for the expression, in the EV cargo, of the transcription factor MEF2, which is a miR-133-a1 activator [22,24] and actually found it increased (Figure 5b). Additional *in vitro* experiments confirmed the upregulation of miR133-a1 in cardiomyocytes (Figure 5c), but not in fibroblasts (data not shown), when these cell types were incubated in the presence of EV. In an attempt to further assess the potential relationship between the increased expression of miR133-a1 and the EV-induced improvement in heart function, we conducted an additional series of *in vivo* experiments where C57BL/6J mice were injected with EV-CPC, PBS or a mix of EV-CPC and anti-miR-133-a. In keeping with the previous functional data, EV-CPC improved significantly LVEF by 14.76 % ± 6.20% compared to PBS controls 4-6 weeks after treatment whereas this protective effect was partly abrogated by the anti-miR133-a antagomir (Figure 5d).

DISCUSSION

Over the past years, cell transplantation has emerged as a possible new treatment of heart failure. As it often occurs, the enthusiastic claims of experimental studies have not been matched by the suboptimal outcomes of most clinical trials. Nevertheless, some hints of efficacy have been reported that justify to further explore this therapeutic option and have fueled the numerous experimental studies aimed at understanding the mechanism(s) of action of the transplanted cells [25]. One of the most important results of these studies has been the recognition that, once engrafted, the transplanted cells did not physically replace the dead cardiomyocytes but rather acted via paracrine mechanisms by fostering endogenous repair pathways through the release of a wide blend of biological factors, many of them being enclosed in EV. These nanoparticles are now recognized as key players in intercellular communication but the mechanisms by which EV protect the heart

are yet unsettled. They likely depend on the composition of their cargo, which is itself influenced by the phenotype of the parental cells. However, while it has been reported that once internalized into the recipient cells, the constituents of the vesicular cargo could modulate signaling pathways involved in the stimulation of angiogenesis and the mitigation of inflammation, apoptosis and fibrosis, [15,16,21,26] little is still known about the potential capacity of EV to trigger cardiomyocyte proliferation. The present study was designed to address this issue.

The main results of our present work can be summarized as follows: (1) EV preserve cardiac function of chronically infarcted hearts, (2) this preservation occurs in the absence of generation of new cardiomyocytes, but (3) it rather seems to be mediated by a regulation of myocardial fibrosis.

Several reports have already shown that EV released by CPC, either native[12,27] or differentiated from pluripotent stem cells [16,20] improve function of chronically infarcted hearts. The present study confirms these data across three different mouse strains and with the use of two imaging modalities (echocardiography and MRI). Although the differences failed to be statistically significant, there was a clear trend towards a 6-fold decrease in both LVEDV and LVESV in the MerCreMer/ZEG mice treated with EV compared with PBS-injected control hearts whereas the MADM and C57BL/6J mice exhibited a preferential reduction in LVESV. These data suggest that EV predominantly preserve systolic function.

To track endogenous cardiogenesis, we used two well-characterized transgenic models which allow to assess whether new cardiomyocytes have been generated and, if so, whether they derive from mobilization of putative endogenous cardiac progenitor cells or re-induction of a mitotic cycle in host mature cardiomyocytes. Our data failed to demonstrate an EV-induced cardiomyocyte proliferation with either model. In the MerCreMer/ZEG experiments, a triple immunostaining allowed to label host cardiomyocytes expressing both cTnT (constitutively) and GFP (following the tamoxifen pulse chase) as well as EdU for those which had proliferated. The advantage of using EdU is that, in contrast to the commonly used proliferation marker BrdU, its detection does not require harsh denaturants and can thus be multiplexed with fluorescent proteins like GFP. In these experiments, there was no difference in the number of these triple-positive cardiomyocytes between the control and EV groups. To double-check these findings, we also used the MADM model which provides unambiguous evidence for cell division directly related to cytokinesis [28,29] as the latter is needed to generate individual green (GFP^+) and red ($tdTomato^+$) cells (a binucleated cell would be double-labeled and appear yellow). In our experiments, the ratio of single-colored cells to double-colored cells was identical in the two groups, thereby ruling out again an effect of EV on cell proliferation. Although one could argue that newly generated cardiomyocytes might have originated not from the already mature ones but from endogenous progenitors, this is unlikely since such cells would have been positive for both cTnT and EdU but negative for GFP, which did not actually happen. In line with this finding, YAP which is a downstream transcriptional regulator of the Hippo pathway was not expressed in EV-treated hearts in contrast to its strong expression in the still proliferating neonatal myocardial tissue used as a control. The downregulation of YAP indicates that the Hippo pathway was not activated, which is known to occur shortly after birth and induces the arrest of cardiomyocyte proliferation [30] and our

data are thus consistent with the finding that cardiac deletion of YAP suppresses cardiomyocyte proliferation[31]. Another contributor to this arrest is the switch from anaerobic glycolysis to oxidative phosphorylation.[32] However, there is no reason to postulate that EV could reverse this switch and restore an energetic milieu fostering cardiomyocyte proliferation. At the opposite, they have been reported to shuttle mitochondria as part of the package they transfer into recipient cells [33,34] and, as such, could rather favor mitochondria-based oxidative metabolism. Altogether, our results are in line with the concept that division of cardiomyocytes stops shortly after birth. Even if isotopic studies have a documented a subsequent slow turn-over during the lifetime,[35] the number of newly generated cardiomyocytes is by far too low to cope with the massive loss of these cells which is a hallmark of severe ischemic heart failure and it does not seem that EV induce heart repair by increasing this number. In support of this conclusion, four publications listed in a meta-analysis [36] that used EV from CPC did not detect either an EV-induced cardiomyocyte proliferation while they reported a cardio-protective effect.

However, the lack of *de novo* cardiomyocyte proliferation did not preclude an improvement in heart function which was related, at least in part, to a mitigation of fibrosis demonstrated histologically and by the trend for a downregulation of fibrosis-inducing genes in the myocardial tissue. The effects of EV on the mitigation of fibrosis have been documented in previous studies [26] and are consistent with their ability to modulate ischemia-induced myocardial inflammation.[15] Of note, in the present study, there was a significantly decreased immune-histochemical expression of Fibroblast Activated Protein (FAP) whose inactivation by chimeric antigen receptor T-lymphocytes has recently been shown to contribute to improve heart function.[21] In line with this hypothesis, there was an increased expression of the anti-fibrotic miR-133-a1 in the EV-treated hearts.[22] However, since only small amounts of this miR were present in the EV, induction of its endogenous expression by some other EV components rather than an EV-mediated transfer appears a more plausible mechanism.[37] This hypothesis is consistent with our finding of increased levels of MEF2,[24] which is an inducer of miR-133-a1, in the EV cargo and with the increased miR-133-a1 expression in cultured cardiomyocytes following their exposure to EV-CPC. It is thus mechanistically plausible that the EV-mediated transfer of MEF2 triggered the upregulation of endogenous miR-133-a1. To further assess the role of miR-133-a1, a separate series of experiments were performed with an anti-miR-133-a1 antagomir. The functional outcomes were intermediary between those of control PBS-injected and EV-treated hearts. This result confirms the likely contribution of miR-133-a1 to the EV-associated cardiac repair; at the same time, it highlights that the protective effects of EV cannot be reduced to a single compound and rather result from the cooperative action of the multiple constituents of their cargo. The practical implication is that deconstructing the EV cargo may not be the most effective approach for leveraging its reparative capacities, supporting our choice to rather target the EV-enriched secretome for our clinical trial under preparation.

In conclusion, the results of this study confirm that EV from CPC have cardio-protective effects which do not seem to involve the generation of new cardiomyocytes but are more likely mediated by a regulation of myocardial fibrosis. Other strategies currently aim at inducing such a cardiac "regeneration" by lifting checkpoint inhibitors (like the Hippo pathway),[38] overexpressing

cell-cycle regulators [29] or converting host fibroblasts into cardiomyocytes.[39,40] Their clinical feasibility, efficiency and safety still remain to be established and in the meantime the use of EV could yet be a more user-friendly and effective addition to the current armamentarium of therapies against heart failure.

Acknowledgements
Pierre Johanne, Xavier Loyer, Stephan Malzan, Michael Robillard

Funding: This work was supported by INSERM, the LabexRevive (10-LABX-0073), Assistance Publique-Hôpitaux de Paris, the University of Paris, the Fondation de France (PME20180639496), the Fondation pour la Recherche Médicale (DEQ20160334910), Agence Nationale de la Recherche (ANR-17-CE18-0003).

REFERENCES

1. Bu L, Jiang X, Martin-Puig S, Caron L, Zhu S, Shao Y, Roberts DJ, Huang PL, Domian IJ, Chien KR. Human ISL1 heart progenitors generate diverse multipotent cardiovascular cell lineages. *Nature*. 2009;460:113–117.

2. Laugwitz K-L, Moretti A, Lam J, Gruber P, Chen Y, Woodard S, Lin L-Z, Cai C-L, Lu MM, Reth M, Platoshyn O, Yuan JX-J, Evans S, Chien KR. Postnatal isl1+ cardioblasts enter fully differentiated cardiomyocyte lineages. *Nature*. 2005;433:647–653.

3. Beltrami AP, Barlucchi L, Torella D, Baker M, Limana F, Chimenti S, Kasahara H, Rota M, Musso E, Urbanek K, Leri A, Kajstura J, Nadal-Ginard B, Anversa P. Adult cardiac stem cells are multipotent and support myocardial regeneration. *Cell*. 2003;114:763–776.

4. Sultana N, Zhang L, Yan J, Chen J, Cai W, Razzaque S, Jeong D, Sheng W, Bu L, Xu M, Huang G-Y, Hajjar RJ, Zhou B, Moon A, Cai C-L. Resident c-kit(+) cells in the heart are not cardiac stem cells. *Nat Commun*. 2015;6:8701.

5. Thomson JA, Itskovitz-Eldor J, Shapiro SS, Waknitz MA, Swiergiel JJ, Marshall VS, Jones JM. Embryonic stem cell lines derived from human blastocysts. *Science*. 1998;282:1145–1147.

6. Ebelt H, Jungblut M, Zhang Y, Kubin T, Kostin S, Technau A, Oustanina S, Niebrügge S, Lehmann J, Werdan K, Braun T. Cellular cardiomyoplasty: improvement of left ventricular function correlates with the release of cardioactive cytokines. *Stem Cells Dayt Ohio*. 2007;25:236–244.

7. Ménard C, Hagège AA, Agbulut O, Barro M, Morichetti MC, Brasselet C, Bel A, Messas E, Bissery A, Bruneval P, Desnos M, Pucéat M, Menasché P. Transplantation of cardiac-committed mouse embryonic stem cells to infarcted sheep myocardium: a preclinical study. *Lancet Lond Engl*. 2005;366:1005–1012.

8. Qiao H, Zhang H, Yamanaka S, Patel VV, Petrenko NB, Huang B, Muenz LR, Ferrari VA, Boheler KR, Zhou R. Long-term improvement in postinfarct left ventricular global and regional contractile function is mediated by embryonic stem cell-derived cardiomyocytes. *Circ Cardiovasc Imaging*. 2011;4:33–41.

9. Synthetic extracellular matrix mimic hydrogel improves efficacy of mesenchymal stromal cell therapy for ischemic cardiomyopathy. - PubMed - NCBI [Internet]. 2020 [cited 2020 Apr 21];Available from: https://www.ncbi.nlm.nih.gov/pubmed/29341932

10. Gnecchi M, Zhang Z, Ni A, Dzau VJ. Paracrine mechanisms in adult stem cell signaling and therapy. *Circ Res*. 2008;103:1204–1219.

11. Adamiak M, Cheng G, Bobis-Wozowicz S, Zhao L, Kedracka-Krok S, Samanta A, Karnas E, Xuan Y-T, Skupien-Rabian B, Chen X, Jankowska U, Girgis M, Sekula M, Davani A, Lasota S, Vincent RJ, Sarna M, Newell KL, Wang O-L, Dudley N, Madeja Z, Dawn B,

Zuba-Surma EK. Induced Pluripotent Stem Cell (iPSC)-Derived Extracellular Vesicles Are Safer and More Effective for Cardiac Repair Than iPSCs. *Circ Res*. 2018;122:296–309.

12. Barile L, Milano G, Vassalli G. Beneficial effects of exosomes secreted by cardiac-derived progenitor cells and other cell types in myocardial ischemia. *Stem Cell Investig* [Internet]. 2017 [cited 2019 Aug 19];4. Available from: https://www.ncbi.nlm.nih.gov/pmc/articles/PMC5723752/

13. Chen L, Wang Y, Pan Y, Zhang L, Shen C, Qin G, Ashraf M, Weintraub N, Ma G, Tang Y. Cardiac progenitor-derived exosomes protect ischemic myocardium from acute ischemia/reperfusion injury. *Biochem Biophys Res Commun*. 2013;431:566–571.

14. Jeyaram A, Jay SM. Preservation and Storage Stability of Extracellular Vesicles for Therapeutic Applications. *AAPS J*. 2017;20:1.

15. Lima Correa B, El Harane N, Gomez I, Rachid Hocine H, Vilar J, Desgres M, Bellamy V, Keirththana K, Guillas C, Perotto M, Pidial L, Alayrac P, Tran T, Tan S, Hamada T, Charron D, Brisson A, Renault NK, Al-Daccak R, Menasché P, Silvestre J-S. Extracellular vesicles from human cardiovascular progenitors trigger a reparative immune response in infarcted hearts. *Cardiovasc Res* [Internet]. [cited 2020 Apr 21];Available from: https://academic.oup.com/cardiovascres/advance-article/doi/10.1093/cvr/cvaa028/5734650

16. El Harane N, Kervadec A, Bellamy V, Pidial L, Neametalla HJ, Perier M-C, Lima Correa B, Thiébault L, Cagnard N, Duché A, Brunaud C, Lemitre M, Gauthier J, Bourdillon AT, Renault MP, Hovhannisyan Y, Paiva S, Colas AR, Agbulut O, Hagège A, Silvestre J-S, Menasché P, Renault NKE. Acellular therapeutic approach for heart failure: in vitro production of extracellular vesicles from human cardiovascular progenitors. *Eur Heart J*. 2018;39:1835–1847.

17. Théry C, Witwer KW, Aikawa E, Alcaraz MJ, Anderson JD, Andriantsitohaina R, Antoniou A, Arab T, Archer F, Atkin-Smith GK, Ayre DC, Bach J-M, Bachurski D, Baharvand H, Balaj L, Baldacchino S, Bauer NN, Baxter AA, Bebawy M, Beckham C, Zavec AB, Benmoussa A, Berardi AC, Bergese P, Bielska E, Blenkiron C, Bobis-Wozowicz S, Boilard E, Boireau W, Bongiovanni A, Borràs FE, Bosch S, Boulanger CM, Breakefield X, Breglio AM, Brennan MÁ, Brigstock DR, Brisson A, Broekman ML, Bromberg JF, Bryl-Górecka P, Buch S, Buck AH, Burger D, Busatto S, Buschmann D, Bussolati B, Buzás EI, Byrd JB, Camussi G, Carter DR, Caruso S, Chamley LW, Chang Y-T, Chen C, Chen S, Cheng L, Chin AR, Clayton A, Clerici SP, Cocks A, Cocucci E, Coffey RJ, Cordeiro-da-Silva A, Couch Y, Coumans FA, Coyle B, Crescitelli R, Criado MF, D'Souza-Schorey C, Das S, Chaudhuri AD, Candia P de, Junior EFDS, Wever OD, Portillo HA del, Demaret T, Deville S, Devitt A, Dhondt B, Vizio DD, Dieterich LC, Dolo V, Rubio APD, Dominici M, Dourado MR, Driedonks TA, Duarte FV, Duncan HM, Eichenberger RM, Ekström K, Andaloussi SE, Elie-Caille C, Erdbrügger U, Falcón-Pérez JM, Fatima F, Fish JE, Flores-Bellver M, et al. Minimal information for studies of extracellular vesicles 2018 (MISEV2018): a position statement of the International Society for Extracellular Vesicles and update of the MISEV2014 guidelines. *J Extracell Vesicles*. 2018;7:1535750.

18. Chan SS-K, Shueh Y-Z, Bustamante N, Tsai S-J, Wu H-L, Chen J-H, Hsieh PCH. Genetic Fate-Mapping for Studying Adult Cardiomyocyte Replenishment After Myocardial Injury [Internet]. In: Lee RJ, editor. Stem Cells for Myocardial Regeneration: Methods and Protocols. Totowa, NJ: Humana Press; 2010 [cited 2021 Jan 6]. p. 201–211.Available from: https://doi.org/10.1007/978-1-60761-705-1_13

19. Toeg HD, Tiwari-Pandey R, Seymour R, Ahmadi A, Crowe S, Vulesevic B, Suuronen EJ, Ruel M. Injectable small intestine submucosal extracellular matrix in an acute myocardial infarction model. *Ann Thorac Surg*. 2013;96:1686–1694; discussion 1694.

20. Kervadec A, Bellamy V, El Harane N, Arakélian L, Vanneaux V, Cacciapuoti I, Nemetalla H, Périer M-C, Toeg HD, Richart A, Lemitre M, Yin M, Loyer X, Larghero J, Hagège A, Ruel M, Boulanger CM, Silvestre J-S, Menasché P, Renault NKE. Cardiovascular progenitor-derived extracellular vesicles recapitulate the beneficial effects of their parent cells in the treatment of chronic heart failure. *J Heart Lung Transplant*. 2016;35:795–807.

21. Aghajanian H, Kimura T, Rurik JG, Hancock AS, Leibowitz MS, Li L, Scholler J, Monslow J, Lo A, Han W, Wang T, Bedi K, Morley MP, Linares Saldana RA, Bolar NA, McDaid K, Assenmacher C-A, Smith CL, Wirth D, June CH, Margulies KB, Jain R, Puré E, Albelda SM, Epstein JA. Targeting cardiac fibrosis with engineered T cells. *Nature*. 2019;573:430–433.

22. Li N, Zhou H, Tang Q. miR-133: A Suppressor of Cardiac Remodeling? *Front Pharmacol* [Internet]. 2018 [cited 2020 Apr 21];9. Available from: https://www.frontiersin.org/articles/10.3389/fphar.2018.00903/full

23. Izarra A, Moscoso I, Levent E, Cañón S, Cerrada I, Díez-Juan A, Blanca V, Núñez-Gil I-J, Valiente I, Ruíz-Sauri A, Sepúlveda P, Tiburcy M, Zimmermann W-H, Bernad A. miR-133a Enhances the Protective Capacity of Cardiac Progenitors Cells after Myocardial Infarction. *Stem Cell Rep*. 2014;3:1029–1042.

24. Liu N, Williams AH, Kim Y, McAnally J, Bezprozvannaya S, Sutherland LB, Richardson JA, Bassel-Duby R, Olson EN. An intragenic MEF2-dependent enhancer directs muscle-specific expression of microRNAs 1 and 133. *Proc Natl Acad Sci*. 2007;104:20844–20849.

25. Gnecchi M. Cell Therapy for Heart Regeneration: Learning from the Past to Build a Brighter Future. *STEM CELLS Transl Med*. 2018;7:702–704.

26. Rogers RG, Ciullo A, Marbán E, Ibrahim AG. Extracellular Vesicles as Therapeutic Agents for Cardiac Fibrosis. *Front Physiol* [Internet]. 2020 [cited 2020 Dec 28];11. Available from: https://www.ncbi.nlm.nih.gov/pmc/articles/PMC7255103/

27. Barile L, Lionetti V, Cervio E, Matteucci M, Gherghiceanu M, Popescu LM, Torre T, Siclari F, Moccetti T, Vassalli G. Extracellular vesicles from human cardiac progenitor cells inhibit cardiomyocyte apoptosis and improve cardiac function after myocardial infarction. *Cardiovasc Res*. 2014;103:530–541.

28. Ali SR, Hippenmeyer S, Saadat LV, Luo L, Weissman IL, Ardehali R. Existing cardiomyocytes generate cardiomyocytes at a low rate after birth in mice. *Proc Natl Acad Sci U S A*. 2014;111:8850–8855.

29. Mohamed TMA, Ang Y-S, Radzinsky E, Zhou P, Huang Y, Elfenbein A, Foley A, Magnitsky S, Srivastava D. Regulation of Cell Cycle to Stimulate Adult Cardiomyocyte Proliferation and Cardiac Regeneration. *Cell*. 2018;173:104-116.e12.

30. Zheng M, Jacob J, Hung S-H, Wang J. The Hippo Pathway in Cardiac Regeneration and Homeostasis: New Perspectives for Cell-Free Therapy in the Injured Heart. *Biomolecules* [Internet]. 2020 [cited 2020 Nov 24];10. Available from: https://www.ncbi.nlm.nih.gov/pmc/articles/PMC7407108/

31. Xin M, Kim Y, Sutherland LB, Murakami M, Qi X, McAnally J, Porrello ER, Mahmoud AI, Tan W, Shelton JM, Richardson JA, Sadek HA, Bassel-Duby R, Olson EN. Hippo pathway effector Yap promotes cardiac regeneration. *Proc Natl Acad Sci*. 2013;110:13839–13844.

32. Nakada Y, Canseco DC, Thet S, Abdisalaam S, Asaithamby A, Santos CX, Shah AM, Zhang H, Faber JE, Kinter MT, Szweda LI, Xing C, Hu Z, Deberardinis RJ, Schiattarella G, Hill JA, Oz O, Lu Z, Zhang CC, Kimura W, Sadek HA. Hypoxia induces heart regeneration in adult mice. *Nature*. 2017;541:222–227.

33. Balbi C, Costa A, Barile L, Bollini S. Message in a Bottle: Upgrading Cardiac Repair into Rejuvenation. *Cells*. 2020;9.

34. Doulamis IP, Guariento A, Duignan T, Orfany A, Kido T, Zurakowski D, del Nido PJ, McCully JD. Mitochondrial transplantation for myocardial protection in diabetic hearts. *Eur J Cardiothorac Surg*. 2020;57:836–845.

35. Bergmann O, Bhardwaj RD, Bernard S, Zdunek S, Barnabé-Heider F, Walsh S, Zupicich J, Alkass K, Buchholz BA, Druid H, Jovinge S, Frisén J. Evidence for cardiomyocyte renewal in humans. *Science*. 2009;324:98–102.

36. Wendt S, Goetzenich A, Goettsch C, Stoppe C, Bleilevens C, Kraemer S, Benstoem C. Evaluation of the cardioprotective potential of extracellular vesicles – a systematic review and meta-analysis. *Sci Rep*. 2018;8:1–14.

37. Tkach M, Théry C. Communication by Extracellular Vesicles: Where We Are and Where We Need to Go. *Cell*. 2016;164:1226–1232.

38. Leach JP, Heallen T, Zhang M, Rahmani M, Morikawa Y, Hill MC, Segura A, Willerson JT, Martin JF. Hippo pathway deficiency reverses systolic heart failure after infarction. *Nature*. 2017;550:260–264.

39. Murry CE, Pu WT. Reprogramming Fibroblasts into Cardiomyocytes. *N Engl J Med*. 2011;364:177–178.

40. Murry CE, Kay MA, Bartosek T, Hauschka SD, Schwartz SM. Muscle differentiation during repair of myocardial necrosis in rats via gene transfer with MyoD. *J Clin Invest.* 1996;98:2209–2217.

Figure Legends

Figure 1: Experimental protocols

Figure 2: Functional effects of EV-CPC

MerCreMerZEG series: (a) Echocardiographic data of left ventricular ejection fraction expressed at baseline and at the end of study or (b) as percent changes from baseline. Each group comprised 15 mice.
MerCreMerZEG series: (c) Magnetic Resonance Imaging data of left ventricular ejection fraction expressed in absolute values. There were 5 and 6 mice in the EV and PBS groups, respectively.
MADM series: (d) Echocardiographic data of left ventricular ejection fraction expressed at baseline and at the end of study or (e) as percent changes from baseline. Each group comprised 6 mice.
*$p \leq 0.05$

Figure 3: Lack of EV-induced cardiomyocyte proliferation

(a) Mean number of proliferating cardiomyocytes (EdU+ and cTnT+) after 7 or (b) 10 days of EdU delivery (5 mice in each group for each timing).
(c) Representative fluorescence microscopic imaging of triple immune-staining for cTnT, GFP and EdU in MerCreMer/ZEG mice. Arrow points to a proliferating cardiomyocyte.
(d) Increased expression of YAP as assessed by RT-PCR in EV-CPC (n=6) and PBS (n=6) injected hearts; the controls were newborn resected hearts (n=4).
(e) Cardiomyocyte proliferation in MADM mice expressed as the percentage of single-colored cardiomyocytes and showing similar results in the PBS-injected and EV-CPC-treated groups
(f) Representative fluorescence of bi-photon imaging.
*$p \leq 0.05$

Figure 4: EV-CPC and fibrosis Modulation

(a) Infarct size expressed as a ratio between the perimeter of the infarct and the total perimeter of the section (H&E staining). There were 15 and 13 mice in the EV and PBS groups, respectively.
(b) Representative images of the infarct area in a control and an EV-treated heart (Sirius red staining). Arrows point to infarcted area
(c) Quantification of FAP in peri-infarcted area in EV-CPC (n=15) and PBS (n=13) injected hearts.
(d) Representative immunostaining for Fibroblast Activated Protein (FAP, green) and cardiac Troponin T (red) in the left ventricular free wall sections from a PBS- and an EV-CPC-injected heart. (20X).
*$p \leq 0.05$ ** $p \leq 0.005$

Figure 5: EV-CPC and mechanistic effects of miR-133a

(a) Hierarchical clustering of the Whole Transcript (WT) Expression Arrays was performed using mRNAs from control and treated hearts and differentially expressed genes (DEG) were selected using

one-way analysis of variance (ANOVA). The fold change (FC) of every gene, together with their corresponding p-value, were used for selection of DEGs with a cutoff of 2.0.
(b) Expression of MEF2 in EV-CPC. The control was nuclear extracts provided by the manufacturer (2 technical replicates).
(c) Expression levels of miR-133a1 in HL-1 cells treated with PBS or EV after a 24-hour incubation.
(d) Echocardiographic data of left ventricular ejection fraction in C57BL/6J mice expressed at baseline and at the end of study or (e) as percent changes from baseline and showing a partial abrogation of the protective effects of EV-CPC in the presence of an miR133-a antagomir. Each group comprised 6 mice.
$*p \leq 0.05$

Figure 6: List of the differentially expressed genes between the EV-CPC- and PBS- groups (n=3 for each group).

Visual Abstract

Figure 1

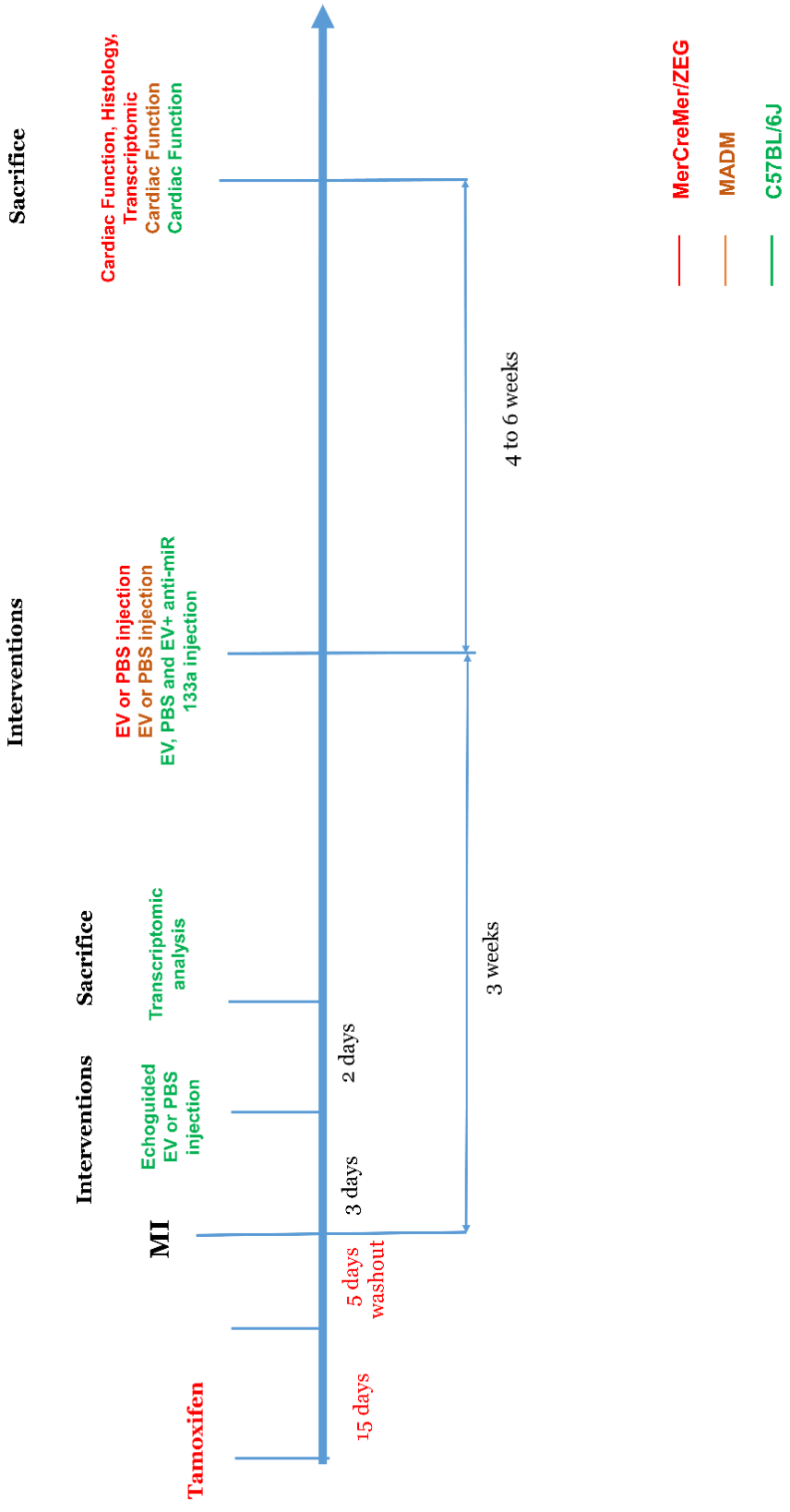
Sacrifice
Cardiac Function, Histology, Transcriptomic
Cardiac Function
Cardiac Function
Interventions
EV or PBS injection
EV or PBS injection
EV, PBS and EV+ anti-miR 133a injection
4 to 6 weeks
Sacrifice
Transcriptomic analysis
Interventions
Echoguided EV or PBS injection
2 days
3 weeks
MI
3 days
5 days washout
15 days
Tamoxifen
MerCreMer/ZEG
MADM
C57BL/6J

Figure 2

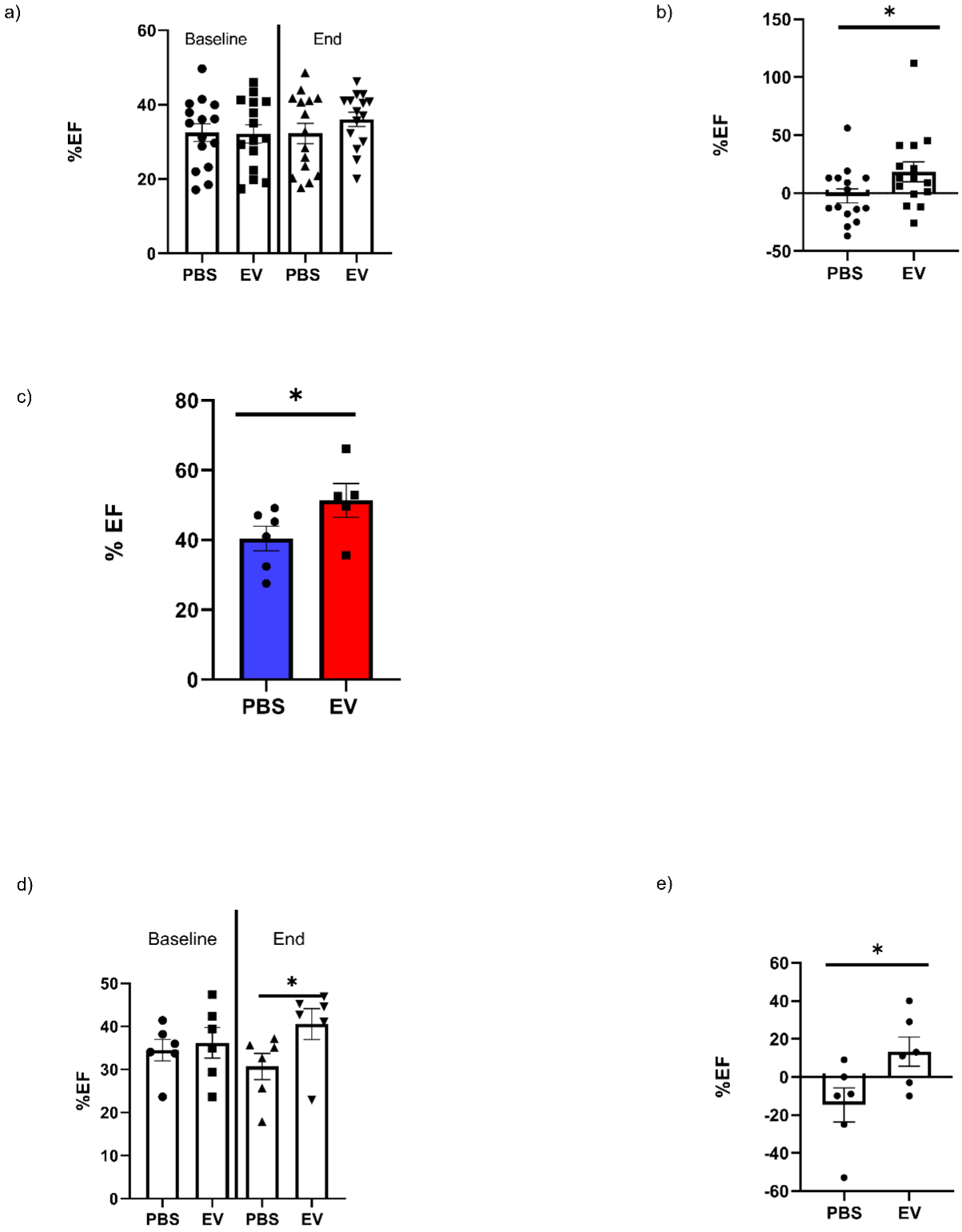
a)
Baseline
End
%EF
60
40
20
0
PBS
EV
PBS
EV
b)
*
150
100
50
0
-50
%EF
PBS
EV
c)
*
80
60
40
20
0
% EF
PBS
EV
d)
Baseline
End
*
50
40
30
20
10
0
%EF
PBS
EV
PBS
EV
e)
*
60
40
20
0
-20
-40
-60
%EF
PBS
EV

Figure 3

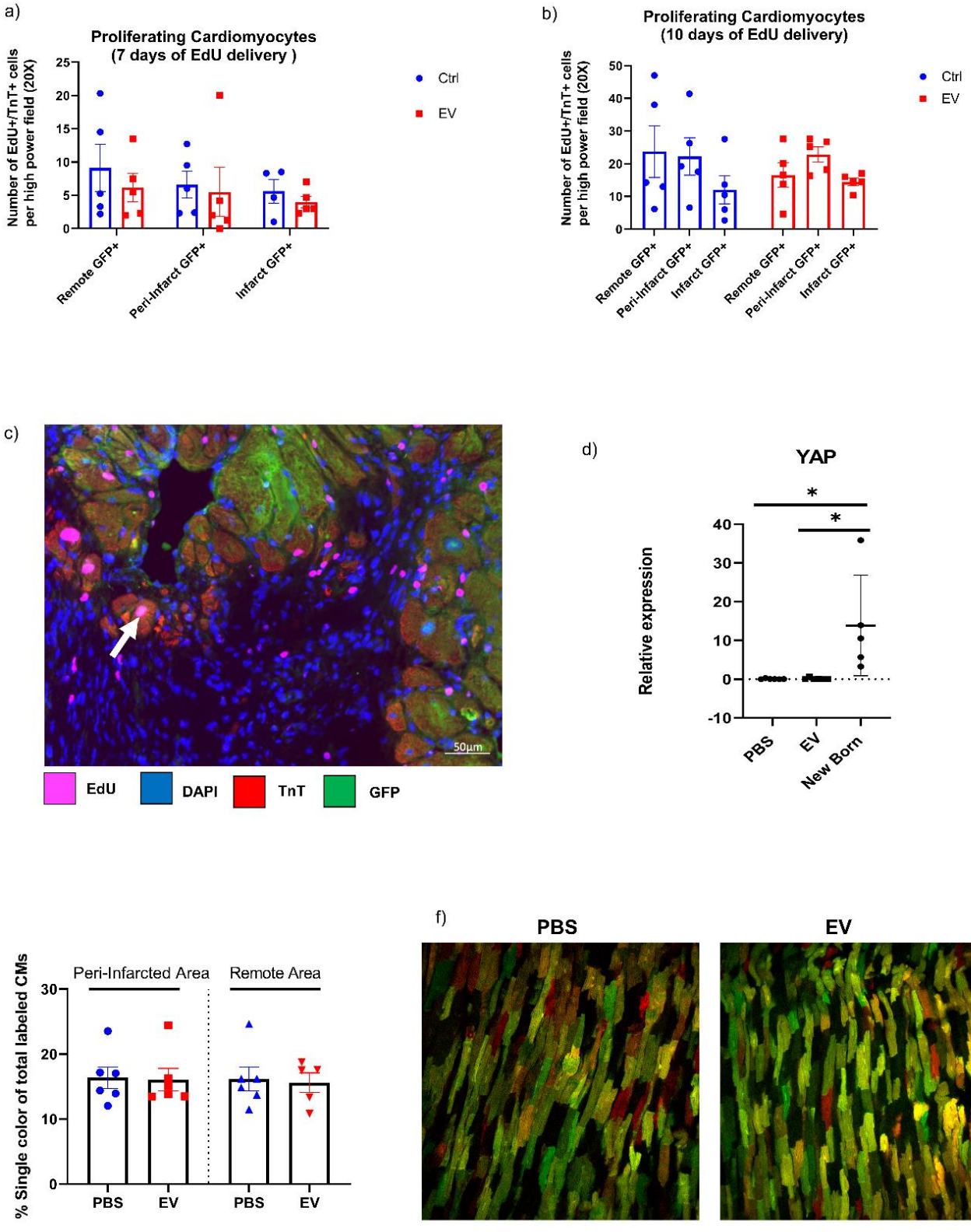
a)
Proliferating Cardiomyocytes
(7 days of EdU delivery)
Number of EdU+/TnT+ cells per high power field (20X)
Ctrl
EV
Remote GFP+
Peri-Infarct GFP+
Infarct GFP+
b)
Proliferating Cardiomyocytes
(10 days of EdU delivery)
Number of EdU+/TnT+ cells per high power field (20X)
Ctrl
EV
Remote GFP+
Peri-Infarct GFP+
Infarct GFP+
Remote GFP+
Peri-Infarct GFP+
Infarct GFP+
c)
50µm
EdU
DAPI
TnT
GFP
d)
YAP
Relative expression
PBS
EV
New Born
e)
Peri-Infarcted Area
Remote Area
% Single color of total labeled CMs
PBS
EV
PBS
EV
f)
PBS
EV

Figure 4

a)

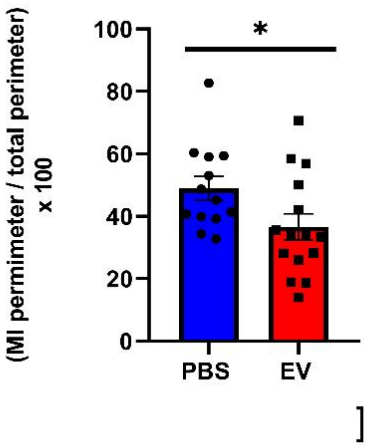

b)

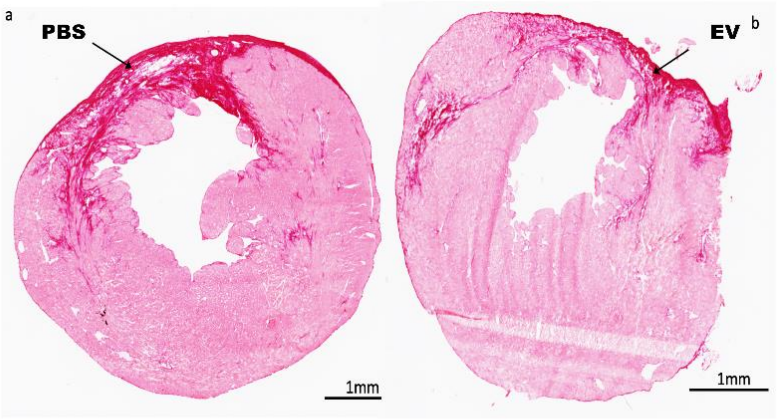

c)

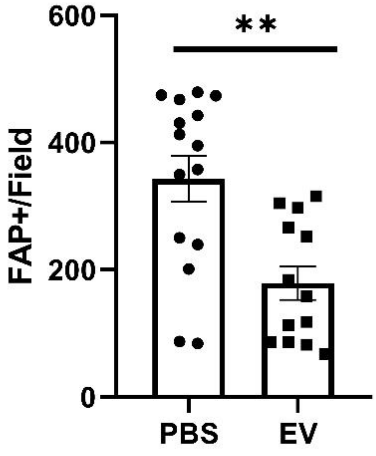

Field= 309577 µm^2

d)

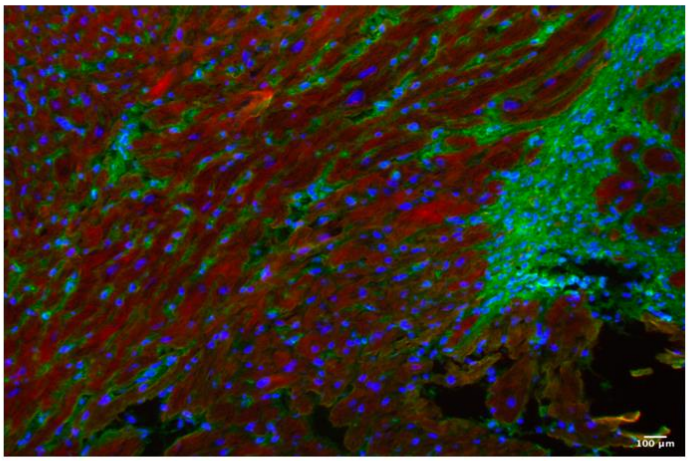

DAPI TnT FAP

Figure 5

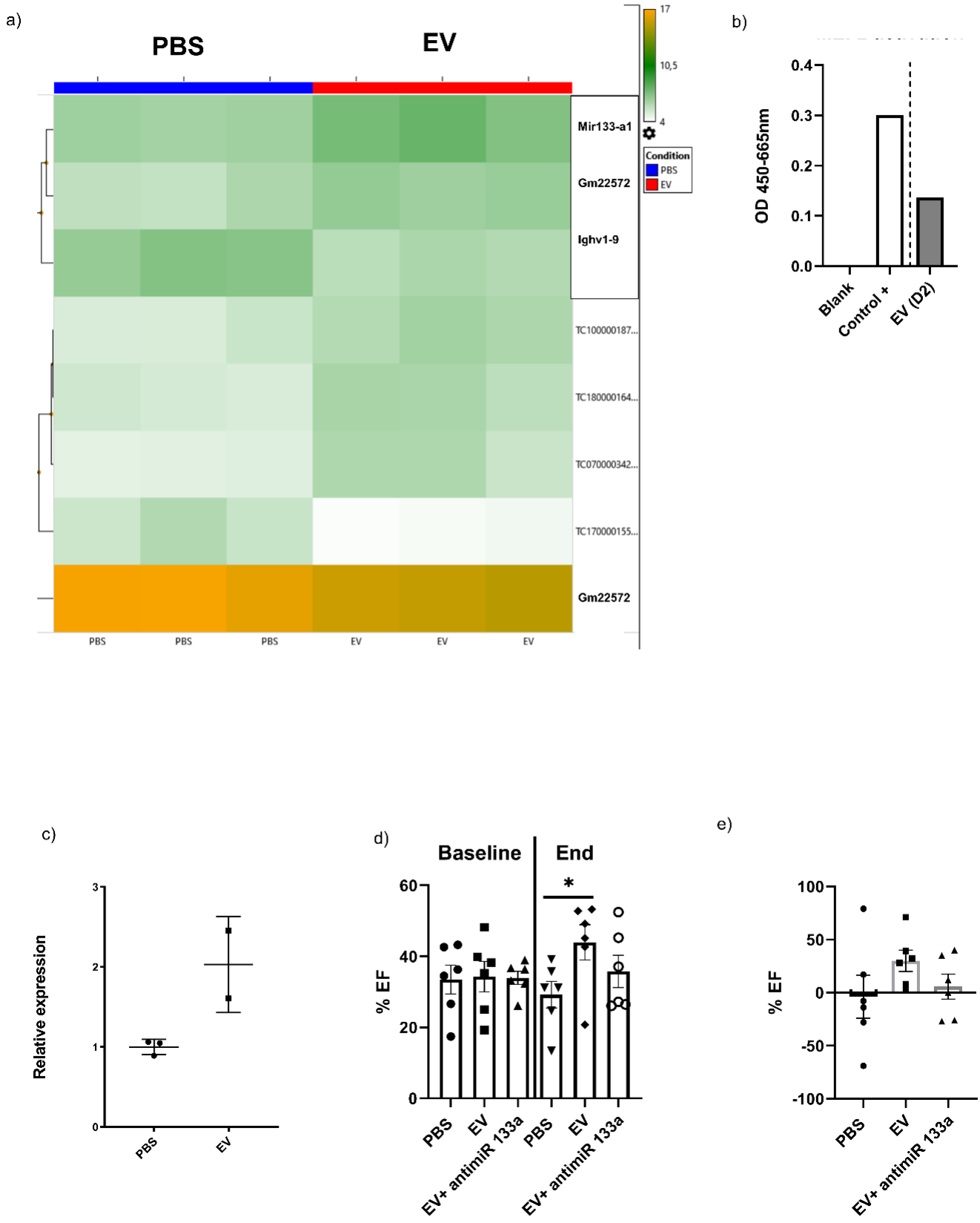
a)
PBS
EV
17
10,5
4
Condition
PBS
EV
Mir133-a1
Gm22572
Ighv1-9
TC100000187...
TC180000164...
TC070000342...
TC170000155...
Gm22572
PBS
PBS
PBS
EV
EV
EV
b)
OD 450-665nm
0.4
0.3
0.2
0.1
0.0
Blank
Control +
EV (D2)
c)
Relative expression
3
2
1
0
PBS
EV
d)
Baseline
End
*
% EF
60
40
20
0
PBS
EV
EV+ antimiR 133a
PBS
EV
EV+ antimiR 133a
e)
% EF
100
50
0
-50
-100
PBS
EV
EV+ antimiR 133a

Figure 6

Probe ID	FC	P-val	Gene Symbol	Description	Group
TC1800000982.mm.1	2,13	0,0015	Mir133a-1	microRNA 133a-1; **miRNA**, **non-coding RNA**; 68nt; expressed on heart; cell differentiation, cell population proliferation, response to stimulus, system development	Precursor_microRNA
TC0900003162.mm.1	5,7	0,0291	Mir5128	microRNA 5128; **miRNA**, **non-coding RNA**; 84nt; expressed on cardiac precursor; response to stimulus	Precursor_microRNA
TC1100002649.mm.1	-3,13	0,0441	Tgtp2	T cell specific GTPase 2; expressed on musculoskeletal system; hydrolase, IFNG-inducible GTPase, participate on vesicular transport; response to stimulus	Multiple_Complex
TC0500001693.mm.1	-2,42	0,0494	Mir7038	microRNA 7038; **miRNA**, **non-coding RNA**; 71nt; expressed on heart;	Precursor_microRNA
TC0700000324.mm.1	4,42	0,0497	Vmn1r113	vomeronasal 1 receptor 113; expressed on heart;	Coding
TC0200000400.mm.1	2,02	0,0044	Gm22572	**snRNA**; 105nt; Expressed on heart; cell nucleus; processing of pre messenger RNAs	Small_RNA
TC1400001667.mm.1	2,22	0,0129	Gm24916	**snoRNA**, **non-coding RNA**; 79nt; Expressed on heart	Small_RNA
TC0400000944.mm.1	-2,07	0,0328	Gm22804	**snoRNA**, **non-coding RNA**; 101nt; Expressed on heart	Small_RNA
TC1800000981.mm.1	2,94	0,0456	Gm21747; Mir133a-1hg	**lncRNA**; 4161nt; expressed on heart, expressed on cardiac precursor; antisense to Mib1 and host to Mir1a-2, Mir133a-1	NonCoding

Visual Abstract

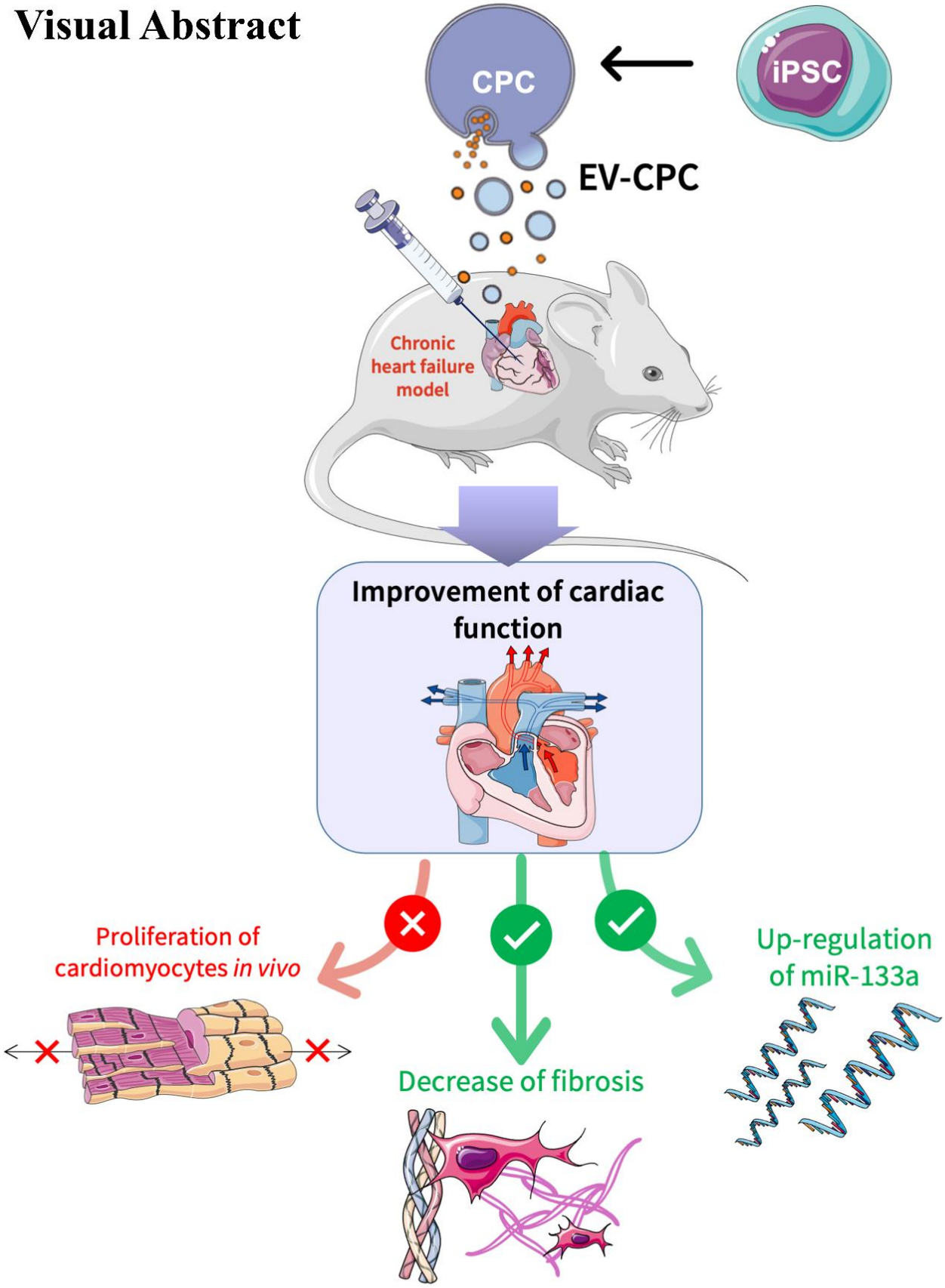

Supplemental Materials

Generation of the MerCreMer/ZEG mouse model

For genotyping, tail tips were sampled, DNA extracted, and PCR were performed to identify doubly transgenic animals with the following primers:
MerCreMer forward: 5′-GTCTGAC TAGGTGTCCTTCT-3′;
MerCreMer backward: 5′-CGTCCTCCTGCTGGTA TAG-3′;
ZEG forward: 5′-AAGTTCATCTGCACCACCG-3′;
ZEG backward: 5′-TCCTTGAAGAAGATGGTGCG-3′;
ZEG control forward: 5′-CTAGGCCA CAGAATTGAAAGATCT-3′;
and ZEG control backward: 5′-GTAGGTG GAAATTCTAGCATCATCC-3′.
Double heterozygous MerCreMer-ZEG mice were used for the subsequent experiments.

Generation of the MADM (mosaic analysis with double markers) mouse model

The identification of these animals was performed by PCR on extract DNA from tail tips with the following primers:
MADM-ML F1: 5'-AACTGGGCATGTGGAGACAGAGAA-3';
MADM-ML F2: 5'-GACCGCCGTCCTCGAAGTTCATCA-3';
MADM-ML F3: 5'GTTGCCGTCGTCCTTGAAGAAGAT-3';
MADM-ML Wild-type forward: 5'AATCCTTCAGCTGCCCACTCTACT-3';
MADM-ML Wild-type backward: CCCCAGGCATTTCTGCTTTTTCTGT-3'.
Myh6-Cre specific: 5' AGAAGCCTAGCCCACACCAGAAAT-3';
Myh6-Cre common: 5'AGAAGCCTAGCCCACACCAGAAAT-3';
Myh6-Cre endogenous: 5'CCCTGGTGCACCTGCTTGGGTTTC-3'.

Real-time quantitative PCR

q RT-PCR was used to assess the expression of genes involved in fibrosis, apoptosis, autophagy, proliferation and miR 133-a expression. The list of primers is indicated below:

Col 1a1:

(F 5'ATTCCCGTTCGAGTACGGAA 3'; R 3'CTCGATCTCGTTGGATCCCT 5'),

Col 3a1:

(F 5'AAAGAGGATCTGAGGGCTCG 3'; R 5'TCACCTCCAACTCCAGCAAT3'),

Col 1a2:

(F 5' CGATGGCTGCTCCAAAAAGA 3'; R 5' AATGTCAAGGAATGGCAGGC 3'),

Lox:

(F 5' TGAACAAATAGCGGAGGGGC 3'; R 5' GAAAGCGCACAGAGTCTGGA 3'),

Bcl-2:

(F 5'TCTGGTTGGGATTCCTACGG 3'; R 5' AGGAGGGTTTCCAGATTGGG 3')

Elastin:

(F 5' CAGCTAAATACGGTGCTGCTG 3'; R 5'AATCCGAAGCCAGGTCTTG 3')

MMP3:

(F5'CTTCTGCAACTCCGACATCGT 3'; R 5' GGGGCATCTTACTGAAGCCTC3')

P53:

(F5'CTCACTCCAGCTACCTGAAGA 3'; R 5'AGAGGCAGTCAGTCAGTCTGAGTCA3')

Bax:

(F 5' GTCCCGCCTCTTCAC CTT TCAG 3'; R 5'GATTCTGGTGTTTCCCCGTTGG 3')

Caspase 3:

(F 5'GGACAGCAGTTACAAAATGGATTA 3'; R 5' CGGCA GGCC TGAA TGAT GAAG 3')

Perostin:

(F 5' FACGGAGCTCAGGGCTGAAGATG 3'; R 5'GTTT GGGCCC TGA TCCCGAC 3')

Yap:

(F 5' AGGAGAGACTGCGGTTGAAA 3'; R 5' CCTGAGACATCCAG GAGAA)

Fibronectin1 (Fn):

(F 5' CGAAGAGCCCTTACAGTTCCA 3', R 5' ATCTGTA GGCTGGT TCAGGC 3')

Actin Alpha 2 (Acta2):

(F 5'AGATCAAG ATCATTGCCCCTCC 3', R 5' TTGTGTGCTAGAGGCAGAGC 3')

miR 133-a: (MIMAT0000427: 5' UUUGGUCCCC UUCAACCAGCUG).

V) Discussion

Chronic heart failure affects several million people around the world and is the main cause of repeated hospitalizations with an attendant high economic burden. Furthermore, due to the aging of the population, the incidence of this pathology should continue to increase in the coming years. [158] Despite the progress in the drug-based management of patients, a significant portion of them requires other treatment options, among which stem cells are rising a growing interest for treating those who have exhausted conventional treatments and are not eligible for more invasive procedures, such as the implantation of an assist device or a heart transplant. These limitations justify that research on stem cell therapies continues to grow although clinical trials have so far failed to demonstrate clear and clinically relevant benefits. This is well illustrated by the fact that in November 2020, the words "stem cells" and "heart failure" generated 105 hits on the ClinicalTrials.gov website.

During these past decades, however, there has been a major paradigm shift in the putative mechanism of action of stem cells. While the original hypothesis was that transplanted cells could physically replace damaged cardiomyocytes, the general opinion today rather supports a paracrine effect of these cells. This hypothesis is based on several consistent findings: (1) a functional benefit of transplanted cells is still present while almost all of them have disappeared; [159] (2) an upregulation of cardio-protective signaling pathways in target tissues is triggered by transplanted stem cells; [160] (3) several types of cells release bioactive factors into their surrounding environment, which is consistent with this activation of endogenous repair pathways. While confirmation of this paracrine hypothesis has been brought by the observations of functional benefits after administration of conditioned medium [83] into the tissue, the biological factors and mechanisms of action underlying these beneficial effects have long remained unknown.

More recently, many of these factors have been shown to be packaged in EV, heterogeneous nanoparticles shown to harbor a biologically active content made up of proteins, lipids and mainly non-coding nucleic acids [161] and to play a key role in intercellular communication.

Thanks to their ability to transfer their cargo to target cells and to consecutively trigger physiologically-relevant functional modifications (activation, proliferation, differentiation) in the latter, EV have largely justified their interest in regenerative medicine and more specifically

in preclinical models of stroke, [162,163] acute kidney injury, [164] ischemic cardiomyopathy [94,165–169] and ischemia of the lower limbs.[170]

The phase I of the ESCORT clinical trial, based on the transplant of a patch cellularized with ESC-derived CPC, showed encouraging results, [171] with the caveat that the logistics, quality controls and regulation inherent in the use of ESC-derived differentiated cells are difficult to manage in the perspective of a large-scale use. As the clinical study was proceeding, we tried to elucidate the mechanisms of action of these cells and in particular their paracrine effects. Thus, in a mouse model of chronic post-infarction heart failure, we compared the transplantation of the ESC-CPC similar to those which were transplanted in patients with the sole administration of the EV they secreted and found that the functional benefits of CPC could be recapitulated by a single injection of their vesicles. These results were published in the *Journal of Heart and Lung Transplantation*. [157] We then moved to a second study to determine whether this functional equivalence between cells and EV could be reproduced if the CPC were derived from iPS cells instead of ESC (for reasons of easier availability) and whether the outcomes would then be influenced by the state of differentiation of the cells (CPC versus more mature cardiomyocytes). *In vitro* bioactivity assays were conducted and concluded that EV-CPC from hiPS cells were internalized by target cells, increased cell survival and proliferation as well as endothelial cell migration in a dose-dependent manner, and stimulated vascular tube formation and cardiomyocyte proliferation. The EV are specifically enriched in miRNAs and most of the 16 phylogenetically conserved miRNAs that were identified in EV-CPC were found to be associated with tissue repair pathways, thereby suggesting a possible mechanistic link between this payload and the EV-associated cardio-protective effects. Injection of these iPS cell-derived EV-CPC into an immune-deficient mouse model of chronic post infarction heart failure confirmed these benefits by showing a significant improvement of cardiac function. Of note, cardiomyocytes only produced minimal amounts of EV, in line with the finding that early-differentiated cells have the higher secretory potential [172] which supports our choice of CPC as EV producers. I was involved in this study and am thus among the authors of the paper which was published in the *European Heart Journal* [173] (page number 61).

The previous studies were performed in immune-deficient mice, which does not correspond to a clinical scenario. Furthermore, as discussed above, myocardial infarction elicits a bi-phasic inflammatory response with an initial leukocyte infiltration into the infarcted area to phagocytize necrotic cardiomyocytes followed by efferocytosis (a physiological process characterized by the phagocytosis of apoptotic immune cells) mainly carried out by

macrophages to reduce inflammation. [174] Overall, the duration and extent of inflammation depend on neutrophil, monocyte and macrophage trafficking [175,176] and a prolonged and uncontrolled post-infarction inflammatory response results in adverse cardiac remodeling and progression to heart failure. [24] Reducing inflammation may therefore help to limit remodeling and thus attenuate progression to severe heart failure [174,177]. Understanding if EV-CPC are immunogenic and can modulate the resolution of inflammation after MI is therefore critical for clinical applications and prompted our next study.

Its primary objective was to investigate the immunological patterns of EV *in vivo* and *in vitro*. In summary, EV-CPC were found to express very low levels of immune relevant molecules. They neither induced nor modulated adaptive allogeneic T cell immune responses. They also failed to induce NK cell degranulation. These *in vitro* effects were confirmed *in vivo* as repeated injections of EV-CPC did not stimulate production of immunoglobulins or affect the interferon (IFN)-γ responses from primed splenocytes. In a mouse model of chronic heart failure, intra-myocardial injections of EV-CPC at a chronic stage decreased both the number of cardiac pro-inflammatory Ly6C- high monocytes and circulating levels of pro-inflammatory cytokines (IL-1α, TNF-α, and IFN-γ). At the acute stage of the infarction, direct cardiac injection of EV-CPC reduced pro-inflammatory macrophages, Ly6C-high monocytes and neutrophils in heart tissue compared to controls. EV-CPC also reduced levels of pro-inflammatory cytokines IL-1α, IL-2, and IL-6, and increased levels of the anti-inflammatory cytokine IL-10. These effects were reproduced *in vitro* on human macrophages and monocytes; EV-CPC reduced the number of pro-inflammatory monocytes and M1 macrophages, while increasing the number of anti-inflammatory M2 macrophages. In summary, EV-CPC did not trigger an immune response and were able to shift the response of monocyte/macrophages towards resolution of inflammation. These characteristics reinforce the clinical attractivity of EV in that their use in patients can be envisioned without the need for immunosuppressive drugs while their anti-inflammatory effects might not be fraught with some of the side-effects of conventional drugs (i.e., corticosteroids or monoclonal antibodies). Namely, there are several reassuring arguments about the safety of EV-based therapies: (1) EV are naturally produced in the human body, (2) their cargo, when it is let unmodified, only comprises physiological components, and (3) blood transfusions are unavoidably associated with the co-delivery of large amounts of EV without the report of specific adverse events. These results have been published in *Cardiovascular Research* [178] and I am a co-first author (page number 102) .

Although mitigation of inflammation has been shown to be an important mechanism of action of EV, this does not preclude other protective pathways to be involved. As one of them might be the generation of new cardiomyocytes to replenish the pool of those which have been lost, the last objective investigated in this thesis was to elucidate if EV-CPC could promote *de novo* cardiogenesis, and if it is the case, from which source of cells the proliferation came from (either pre-existing cardiomyocytes re-entering a mitotic cycle or progenitor cells mobilized from putative endogenous niches). To that end, we used two transgenic mice models. The first was the double transgenic fate-mapping MerCreMer/ZEG model which allows to distinguish whether putative new cardiomyocytes originate from the division of preexisting ones (GFP+, TnT+, EdU+) or differentiate from endogenous progenitors, in which case they would stain positive for TnT+/EdU+ but negative for GFP. Since a cardiomyocyte is only considered proliferative if it goes through complete cytokinesis, we then used the Mosaic Analysis With Double Markers Model (MADM) mouse model which allows to assess this end point. In this model, the proliferation of new cardiomyocytes derived from the pre-existing ones or from progenitors will stain either red or green whereas cardiomyocytes that fail to divide remain double-colored as yellow. Consequently, if proliferation occurs in the treatment group, the ratio of single-colored cells to the double-colored ones will be greater than in the control saline-injected group. In both immunocompetent transgenic mouse models, echocardiography showed an improvement of the cardiac function which was confirmed by Magnetic Resonance Imaging (MRI). However, in the MerCreMer/ZEG experiments, the number of new cardiomyocytes (TnT+/EdU+/GFP+) was modest and did not significantly differ between EV-treated hearts and controls, in line with the non-activation of the Hippo pathway. For MADM mice, a similar result was found as the number of single-colored cells did not differ between both groups. Thus, the improved functional outcomes of EV could not be ascribed to a *de novo* cardiogenesis (nor to an increased angiogenesis or a cardiomyocyte hypertrophy). However, it was associated with an infarct size reduction which correlated with the trend towards down regulation of pro-fibrotic genes (such Col 1a1, Col 3a1, Col 1a2, Elastin and MMP3). In keeping with these data, the anti-fibrotic miR 133-a-1 was found to be overexpressed in EV-treated MerCreMer/ZEG hearts (and additional *in vitro* experiments confirmed the ability of cardiomyocytes to increase their expression of this miR following incubation in the presence of EV). Since this miR is only present in small amounts in the EV cargo, its increased expression in the myocardium more likely reflects an endogenous upregulation, possibly triggered by MEF2 (present in the EV cargo) which is one of its activators. To further investigate the contribution of miR 133-a-1, a last series of experiments on C57BL/6J mice was conducted which showed that co-injection of

the anti-miR133a-1 with EV partly abrogated their protective effects. That this abrogation is only partial supports that attributing the effects of EV to a single component would be unrealistically reductionist given the multiplicity of the biomolecules packaged in the EV cargo and the additional effects of extravesicular soluble factors (particularly proteins). This justifies our choice, in a clinical perspective, to use the EV-enriched secretome rather than trying to deconstruct it to isolate a single compound. These results have been accepted for presentation at the 2021 Annual Meeting of the Society of Thoracic Surgeons and the corresponding manuscript has been submitted to *the Annals of Thoracic Surgery*. I am a co-first author (page number 148) of this paper.

A common feature of all these studies has been to use EV secreted by CPC. The choice of this parental cell phenotype was largely based on studies suggesting the superiority of using source cells as close as possible to those of the target tissue [179,180]. However, EV from MSC have also shown excellent cardio-protective effects [165,166,181] and additional head-to-head comparisons are likely required to further validate the optimal parental cells in relation with the target indication.

VI) Conclusions and perspectives

The main objective of our laboratory is to develop a new biological treatment based on the administration of EV from hiPS-CPC because this cell-free therapy offers significant advantages in clinical practice such as a better control over batch consistency, the potential for a large-scale production more akin to that of a pharma-type product, the possibility of cryo-preservation without loss of efficacy after thawing, thereby enabling an off-the-shelf availability and the avoidance of adverse events possibly associated with cells such arrhythmias, tumors (EV have no replicative abilities) and allo-immunization. The data acquired during my thesis regarding the efficacy of EV-CPC and some of their presumed mechanism(s) of action are part of the preclinical package required for moving to a phase I clinical trial. Clearly, this translation raises technical challenges that we are currently addressing with our industrial partner CDI (Cellular Dynamics International, Madison, WI, USA, the provider of the CPC) and our collaborators at the Advanced Therapy Medicinal Products (ATMP Méary platform) located at *hôpital Saint-Louis*. This translational process requires that all steps are performed under Good Manufacturing Practice conditions and in compliance with the regulatory guidelines edited by the French agency (*Agence nationale de sécurité du medicament et des produits de santé).*

In brief, the process is divided into two main phases. The upstream phase comprises the reprogramming of hematopoietic stem cells into iPS cells, their differentiation in CPC and their subsequent scale-up until they are cryopreserved. These steps are performed in CDI facilities according to proprietary procedures. The downstream phase is performed in the ATMP platform of hôpital Saint-Louis and entails an ultimate brief culture of the thawed progenitor cells (partly in a serum-free dedicated medium), collection of the cell-derived conditioned medium, its filtration/concentration and final fill and finish. Each of these steps has to be tightly characterized to ensure its robustness, efficacy and reproducibility since, in contrast to conventional drugs where changes in the sequence of production steps are expected to only minimally alter the final product, the structural complexity of biopharmaceuticals requires for optimizing their characterization and batch-to-batch consistency that the production process be tightly controlled from beginning to end (hence the formula: “the process is the product”). While some aspects to this process cannot be yet fully disclosed for intellectual property-associated reasons, others can be more openly discussed

and will be briefly addressed as they are also part of the research perspectives of our laboratory.

Drug formulation, storage and stability

Clinical grade EV-CPC are formulated as a liquid suspended in a neutral solvent (PBS). However, research is carried out on methods used to increase drug stabilization and extend their shelf life. Among them, lyophilization (freeze drying) is of the most effective. [182] Recent experiments in our laboratory have shown that EV could be safely freeze-dried without losing their bioactivity upon subsequent thawing. [183] Storing EV in a freeze-dried formulation could further enhance their user-friendliness.

a) Efficacy *in vitro and in vivo*

Efficacy is defined in the context of evidence-based medicine as the capacity of a therapy to positively influence the course or duration of a disease at the dose tested in the patient population or model for which it is designed [184]. This is why several *in vitro* and *in vivo* tests are required. Here below we will detail the tests that have been or are still in the process of being developed in our laboratory and to which I still participate.

In vitro

We have previously described the viability and angiogenesis [173] assays that were used for assessing the bioactivity of EV. However, to further explore their potency, other tests are still needed and to this end we are currently developing two assays: the first aims at assessing the effects of EV on the apoptosis of human cardiomyocytes (derived from iPS cells) induced by staurosporine; the second assay aims at assessing the effects of EV on the cytotoxicity incurred by the same cell type when subjected to a doxorubicin-induced injury. This drug is known to damage cardiac cells by different mechanisms including the blockade of aerobic respiration in the mitochondria increasing the oxidative stress, [185] changes in gene expression with decreased expression of the contractile proteins,[186] induction of apoptosis by inhibition of topoisomerase II and collapse of the whole troponin network leading to cytoskeletal disorganization and cardiomyocyte death. [187] The goal of the *in vitro* tests is to evaluate the viability, oxidative stress and cytoskeletal disorganization following exposure of human cardiomyocytes to doxorubicin and to assess whether, and to what extent, EV can provide some rescue. Although critically important to provide proof-of-concept data and mechanistic cues, these *in vitro* assays are of only limited relevance to the *in vivo* settings and

thus need to be complemented by animal studies to further investigate the disease-modifying properties of any biologics intended for human use.

In vivo

For a while, the evaluation of stem cells and then of their secretome has focused on ischemic cardiomyopathies and, as shown in the papers presented in this Thesis, we have used the conventional model for this type of diseases, i.e., the induction of a myocardial infarction by a permanent coronary artery occlusion. More recently, however, we have extended our portfolio of animal models in two directions to better stick to the current clinical scenarios:

One model entails an ischemia/reperfusion protocol (preferentially in rats) which is closer to contemporary practice patterns whereby patients with an acute myocardial infarction usually undergo an emergent revascularization.

The second model which is more challenging is that of a nonischemic cardiomyopathy which is relevant in view of the increased prevalence of this condition. [186,188] In the clinics, heart failure of a nonischemic origin can be due to a variety of etiologies (hypertension, valve disease, genetic mutations, congenital abnormalities, arrhythmias, toxic causes). In the laboratory, we have selected to focus on anthracycline-induced cardiomyopathies because of the high prevalence of this late complication in cancer survivors [189] and the lack of current efficacious treatments. [188,190] Experiments testing the effects of our EV-CPC in this setting are currently under way.

b) Route of administration, dosing and EV targeting

Most of stem cells studies, both experimental and clinical, have entailed an intramyocardial route for delivery since it is the only one which provides a direct access to the target tissue and this approach was further rationalized by the initial belief that transplanted cells would engraft persistently. Logically, most of the initial EV studies have also used direct intramyocardial injections and this has actually been the case in the papers presented in this Thesis. More recently, this approach has been challenged for two main reasons: first, the temporal discrepancy between the disappearance of the transplanted cells and the persistence of a functional benefit has questioned the idea that their physical presence in the

heart was a prerequisite to their therapeutic effect; second, several studies have reported that repeated dosing was likely to optimize functional outcomes, [191,192] thereby implying the use of a less invasive route than open-chest procedures. These considerations have fuelled an increased interest in an intravenous mode of delivery. Experimental studies reviewed in *Wysoczynski et al*. [193] have documented the efficacy of intravenous cell injections and these data are now supported by those of early clinical trials. [194] Likewise, in a meta-analysis of the effects of EV after myocardial infarction, the route for EV delivery (intramyocardial or intravenous) was not identified as a predictor of a successful outcome. [195] The efficacy of intravenous EV infusions also looks relevant to nonischemic cardiomyopathies [196–198] and we are currently testing this route for delivering our EV-CPC in the doxorubicin-induced cardiomyopathy model. The mechanism(s) by which systemic injections of cells or their secretome can elicit cardio-protective effects is still elusive given their predominant homing in lungs, spleen and liver. However, studies have shown that once sequestered systemically, EV could trigger changes in endogenous immune cell populations shifting their phenotype towards an anti-inflammatory pattern [199–201] and these cells might then convey the protective signals remotely to the heart. [202] Whether, despite this systemic mode of action, the functional benefits of intravenous delivered EV could still be improved by their more selective targeting to the heart through engineering of the parental cells [203] or the EV themselves [204] is an important area of research currently under intense investigation. In cases where an open-chest procedure is considered for patient-related reasons, the direct intramyocardial delivery is still sound but its benefits are likely to be optimized by incorporation of the secretome in a hydrogel enabling its controlled release, thereby extending its time of exposure to the target myocardium. [205]

Another clinically relevant but still unsettled issue pertains to EV dosing. Throughout our studies, we have used a number of EV corresponding to their production by the number of cells previously shown to be functionally effective (1.4 million). While this "cell equivalent" metrics is one option, others are also available such as the absolute number of particles, amount of vesicle protein or vesicle number to protein ratio. Regardless of the metrics, dose-relationship studies are thus mandatory to fine-tune the optimal number of EV in relation with a given route for delivery. The main additional translational issues that need to be addressed before moving to an EV clinical trial pertain to toxicology, tumorigenicity and biodistribution. The same EV-CPC as those used in my studies but upgraded for a human use, as discussed above, will undergo the relevant assays under Good Laboratory

Practice conditions and in compliance with the regulation on Biological Medications but their description is beyond the scope of this Thesis.

c) Scientific impact

In conclusion, the results presented in this Thesis reinforce the growing interest in EV as acellular biologics endowed with cardio-reparative properties and which, as such, could find a place in the armamentarium of therapies of cardiac diseases. Many issues still remain to be addressed but these data could hopefully contribute to move the field closer to clinical applications by providing additional safety and efficacy data. Despite organ specificities, tissue repair is a cross-disciplinary field and these data collected in the cardiac area might also be relevant to other medical applications with regard to both basic EV-related biology and clinically-oriented production processes.

Résumé

Les vésicules extracellulaires (EV) sont des nanoparticules sécrétées par toutes les cellules de l'organisme et qui jouent un rôle majeur dans la communication inter-cellulaire. Les EV sont constituées d'une bicouche lipidique délimitant un contenu varié constitué de protéines solubles ou membranaires, de lipides, de métabolites et d'acides nucléiques. Ces vésicules, hétérogènes en taille (50nm-1000nm) et d'origines cellulaires diverses sont classées en trois catégories : exosomes, microvésicules et microparticules. Il semble de plus en plus acquis qu'elles sont les médiateurs principaux des effets paracrines des cellules souches dont elles peuvent reproduire le bénéfice dans de multiples modèles pré-cliniques. Dans une perspective clinique, l'utilisation des VE se traduirait par une probable simplification des problèmes inhérents à la production, la reproductibilité, aux contrôles-qualité et donc à la réglementation par rapport à la greffe de cellules-mères dont elles sont issues.

Notre projet est donc désormais ciblé sur cette « thérapie cellulaire sans cellules » fondée sur la seule administration au patient des EV et n'exploitant plus les cellules que comme sources in vitro de leur production. L'un des pré-requis importants à une telle utilisation clinique des EV est néanmoins une meilleure identification des facteurs qu'elles véhiculent et la compréhension de leur contribution respective aux effets globalement cardio-protecteurs observés expérimentalement.

Pour des raisons épidémiologiques, il est également important de savoir si ces EV pourraient être efficaces dans le traitement de certaines cardiopathies ischémiques et non ischémiques. C'est à ces questions que tentera de répondre cette thèse qui est ainsi structurée en trois objectifs principaux.

-L'objectif 1 a exploré l'hypothèse que les EV issues de progéniteurs cardiovasculaires (CPC) dérivés d'iPSC étaient aussi efficaces que leurs cellules mères, ainsi que les cellules souches embryonnaires (ESC) et que les EV que sécrètent ces dernières. À cette fin, un modèle murin immunodéficient d'insuffisance cardiaque chronique a été généré et les résultats ont confirmé l'équivalence fonctionnelle entre les cellules et leur EV expliquée par une transcription accrue des gènes cardio-protecteurs dans les tissus cardiaques. Les mécanismes d'action des EV in vitro ont été en partie élucidés révélant ainsi des effets pro-angiogéniques sur des cellules endothéliales, des effets prolifératifs des cardiomyoblastes des rats et sur des cardiomyocytes humains. Les objectifs 2 et 3 ont donc été menés afin d'élucider les mécanismes d'action des EV.

- L’objectif 2 concerne le caractère immunologique des EV étudié in vivo chez la souris et in vitro sur des cellules mononuclées sanguines périphériques humaines. Nous avons d’abord montré par des test MLR (mixed lymphocyte reaction) utilisant des cellules effectrices provenant de plusieurs donneurs que les EV ne provoquent pas de prolifération de lymphocytes T et n’augmentent pas la dégranulation des cellules NK. L'exposition des macrophages aux EV diminue le pourcentage des monocytes et des macrophages M1 pro-inflammatoires (et leurs médiateurs) tout en augmentant le nombre de macrophages M2 anti-inflammatoires (et leurs médiateurs) lorsqu’ils sont indifférenciés dans un état M0. En revanche, les EV ne sont pas capables d’inverser le phénotype M1 une fois qu’il est acquis. Nous avons ensuite caractérisé la réponse immunitaire aux EV in vivo et avons constaté, dans un modèle de dysfonction ventriculaire gauche chronique, que les EV atténuent l’inflammation, notamment en diminuant le nombre des précurseurs des macrophages pro-inflammatoires (Lyh6 High) dans le tissu cardiaque ainsi que les médiateurs pro-inflammatoires circulants. Cette propriété anti-inflammatoire est davantage confirmée au stade aigu de l’infarctus du myocarde avec une diminution significative des cellules pro-inflammatoires (monocytes, macrophages et neutrophiles) et des médiateurs pro-inflammatoires, et une augmentation des médiateurs anti-inflammatoires circulants. De plus, les EV n’induisent pas de réponse humorale (pas de production d’immunoglobulines) ou cellulaire (pas de production d’IFN γ par les splénocytes) dans un modèle vaccinal. L’ensemble de ces résultats suggèrent que les EV ont un effet globalement immuno-modulateur et qu’en tous cas, l’absence de réponse allo-immune (même s’il s’agit plus précisément ici d’une réponse xéno-immune puisque dans ces modèles ce sont des EV d’origine humaine qui ont été administrées à des souris) renforce leur attractivité clinique.

- L’objectif 3 a cherché à établir si les effets cardio-protecteurs des EV impliquent une augmentation du pool myocardique de cellules contractiles. A cet effet, nous avons utilisé un modèle de souris doublement transgéniques MerCreMer/ZEG qui a permis d’établir si une partie du bénéfice attribué à l’administration de VE viendrait d’un accroissement de la masse de cellules contractiles par mobilisation de cellules souches/progénitrices endogènes et/ou réinduction d’un cycle mitotique chez les cardiomyocytes déjà différenciés. Après une administration de tamoxifène les souris MerCreMer/ZEG expriment de façon constitutive la molécule Green Fluorescent Protein (GFP) uniquement dans les cardiomyocytes. Notre protocole a comporté une injection des EV intra-myocardique per-cutanée, sous contrôle échocardiographique, trois semaines après la création d’un infarctus du myocarde (par

ligature permanente de l'artère coronaire gauche), ainsi que l'administration d'EdU via des pompes osmotiques implantables (pendant 1 semaine au moment de l'administration des EV). Les souris ont été sacrifiées 4-6 semaines après l'injection des EV avec évaluation par échographie et, pour certaines d'entre elles, imagerie par résonance magnétique (IRM) complétées par l'examen histologique des cœurs explantés. Ainsi conçu, ce protocole devait permettre de savoir si l'injection des EV entraîne un accroissement de la masse de cellules contractiles par mobilisation de cellules souches endogènes (augmentation du nombre de cellules GFP négatives et EdU positives) ou réinduction d'un cycle mitotique chez les cardiomyocytes déjà différenciés (augmentation des cellules à la fois GFP et EdU-positives). Sur 60 souris ayant subi un infarctus, 37 ont survécu et 30 ont été stratifiées, en fonction de leur fraction d'éjection de base (≤45%), en deux groupes équivalents, l'un recevant les injections de EV (secrétées par 1.4 millions de CPC ou 10 milliards de particules) et l'autre, un volume équivalent du solvant de resuspension (saline). Nos résultats ne montrent aucune prolifération cardiomyocitaire car il n'existe pas de différence significative dans le nombre de cardiomyocytes (doublement positifs pour la troponine T et EdU) entre le groupe traité par les EV et les contrôles. Néanmoins nous avons observé une amélioration significative de la fonction cardiaque (par échocardiographie [15 souris par groupe] et IRM [6 contrôles et 5 EV]) ainsi qu'une diminution de la taille de l'infarctus et de la fibrose chez les souris injectées avec les EV. Cette modulation de la fibrose s'accompagne d'une augmentation du miRNA anti-fibrotique 133-a dans le tissu cardiaque des animaux traités par les EV (analyse transcriptomique) ainsi que d'une diminution de l'expression des ARNs pro-fibrotiques (Col1a2, Col3a1, Lox, Col1a2, Elastin et Mmp3) et de la protéine FAP (Fibroblast activation protein). En concordance avec ces résultats, YAP qui est un régulateur transcriptionnel en aval de la voie Hippo n'a pas été exprimé dans les cœurs traités par les EV contrairement à sa forte expression dans le tissu myocardique néonatal utilisé comme témoin. Dans ce travail, la prolifération cardiomyocytaire s'est fondée sur la quantification de la synthèse d'ADN par la détection de l'EdU en phase S. Néanmoins un cardiomyocyte est seulement considéré prolifératif s'il y a cytokinèse. Aussi, avons-nous cherché à valider ces premiers résultats à l'aide d'un autre modèle de souris transgénique (MADM ; mosaic analysis with double markers) où les nouveaux cardiomyocytes provenant de ceux préexistants ou de progéniteurs sont GFP+ ou tdTomato+ (une cellule qui est binucléé et n'a pas subi de cytokinèse apparaitra jaune). Si donc il y a une prolifération dans le groupe traité, le nombre de cardiomyocytes GFP+ ou tdTomato+ sera augmenté. Ces souris ont également été réparties en 2 groupes de 6 (l'un injecté par les EV à la même concentration précédemment utilisé et l'autre injecté avec

le seul milieu de resuspension, 3 semaines après création de l'infarctus). Nous avons retrouvé des résultats identiques, à savoir une amélioration de la fonction cardiaque 4-6 semaines après les injections, sans augmentation concomitante du nombre de nouveaux cardiomyocytes. Enfin, la mise en évidence par analyse transcriptomique d'une forte expression du miRNA 133-a dans les cœurs injectés avec les EV suggère qu'il pourrait fortement contribuer aux effets anti-fibrotiques observés dans ce groupe et ainsi, indirectement, à l'amélioration de la fonction cardiaque. Pour vérifier cette hypothèse, une étude in vivo a été menée. Le protocole d'induction de la dysfonction ventriculaire gauche reste identique et comporte 3 groupes expérimentaux : contrôle (PBS), EV et EV+anti-miR 133-a. Les résultats fonctionnels du groupe traité par les EV+anti-miR 133-a étaient intermédiaires entre ceux des cœurs témoins injectés au PBS et traités par les EV. Cette hypothèse est cohérente avec l'observation de niveaux accrus de MEF2 (dans le cargo des EV) qui est un inducteur de miR-133-a1, ainsi qu'une augmentation de l'expression de miR-133-a1 dans les cardiomyocytes murins en culture à la suite de leur exposition aux EV. Il est donc mécanistiquement plausible que le transfert de MEF2 médié par les EV ait déclenché la régulation à la hausse du miR-133-a1 endogène. En même temps, il souligne que les effets protecteurs des EV ne peuvent être réduits à un seul composé et résultent plutôt de l'action coopérative des multiples constituants de leur cargaison.

Objectif 4 : Il consiste à évaluer le potentiel thérapeutique des EV dans un modèle de cardiopathie induite par les anthracyclines. La mise au point d'un protocole de cardiomyopathie chimio-toxique s'est révélée longue et complexe, conduisant, au fil des résultats, à de multiples ajustements de dose, de source et de chronologie d'administration de la drogue ainsi qu'à un changement de souche de souris. La cardiotoxicité de la doxorubicine est désormais induite par 3 injections intra-péritonéales hebdomadaires de la drogue (4mg/kg par injection, soit une dose cumulée de 12 mg/kg au terme des 3 semaines de traitement). La fonction ventriculaire gauche sera évaluée par échocardiographie et/ou IRM 6 semaines après la 1ère injection de la drogue et les EV ou un volume équivalent du milieu de suspension seront injectés par voie intraveineuse à la dose de 30 milliards répartis en 3 injections distantes de 5 jours. L'effet des EV sur la fonction ventriculaire gauche (volumes et fraction d'éjection) sera évalué 21 jours après le début du traitement avec une analyse histologique (apoptose, fibrose, prolifération cellulaire, réponse immune, angiogenèse) dans la foulée des explorations fonctionnelles. L'objectif 4 est toujours en cours de développement. Il est à

prévoir que de nouveaux changements pourraient encore intervenir dans la chronologie d'administration des traitements, leurs modalités et le moment de leur évaluation finale.

Enfin dans une perspective translationnelle (d'utilisation des EV en clinique) dans le traitement de l'insuffisance cardiaque, l'expansion à grande échelle de cellules progénitrices cardio-vasculaires (différenciées à partir de cellules somatiques induites à la pluripotence) dans un milieu de grade clinique ; la caractérisation phénotypique des cellules au terme de cette phase de culture ainsi que leur secretome; la mise au point d'une purification par filtration à flux tangentiel sont en cours de développement par notre collaborateur au laboratoire de thérapie cellulaire de l'hôpital Saint-Louis avec l'objectif de mener un essai clinique dans l'année à venir.

Mots Clés : Vésicules extracellulaires, Secretome, Biotechnologies, Thérapie Cellulaire, Réparation Cardiaque, Insuffisance Cardiaque.

Abstract

Extracellular vesicles (EV) are nanoparticles secreted by all cell types in the body, they play a major role in intercellular communication and seems to be the main mediators of paracrines effects exercised by stem cells. From a clinical point of view, the use of EV will result in a probable simplification of the problems inherent in production, reproducibility, quality control and regulation of relations with the graft of mother cells. Our project is therefore now focused on this "cell-free cell therapy" based on the sole administration of EV to the patient and no longer using the cells which are *in vitro* sources of their production. Important prerequisites for the clinical use of EV are also included in the best identification of relevant factors and understanding of the respective contribution to the overall cardioprotective effects observed experimentally.

The first article explored the hypothesis that EV from cardiovascular progenitor cells (CPC) derived from iPSC were as effective as their mother cells and as efficient as embryonic stem cells (ESC). To this purpose, an immunodeficient mouse model of chronic heart failure was generated and the results have actually confirmed the functional equivalence between the cells and their EV which were shown to share in common an increased transcription of cardio-protective genes in heart tissue.

The second article looked at the immunological effects of EV-CPC. At this stage, we turned to iPSC as the source of the CPC (otherwise very similar to those from ESC previously tested) and switched to an immune-competent mouse model in both acute and chronic myocardial ischemia settings. The data showed that these EV-CPC do not trigger an immune response (at least in this xenogenic context) either *in vitro* or in the animal models and at the same time unraveled the capacity of EV to fine-tune the response of monocyte/macrophages towards a resolution of inflammation that likely bolsters their therapeutic potential.

The third paper was designed to assess whether EV-CPC could trigger cardiomyocyte proliferation and, if so, which was the source of these newly generated cardiomyocytes. To this end, we used two lineage-tracing models and have shown that while EV actually failed to induce cardiogenesis, their cardio-protective effects could still be confirmed and likely accounted for, at least in part, to a modulation of cardiac fibrosis. Overall, these data are thus consistent with the currently prevailing hypothesis that the regulation of immune inflammatory responses by transplanted cells or, in our case, their EV-enriched secretome is a major mechanism whereby these biologics improve heart function.

Key words; Extracellular Vesicles, Secretome, Biotechnology, Cardiac Repair, Heart Failure, Cell Therapy.

References

1. McMurray, J. J. V. *et al.* ESC Guidelines for the diagnosis and treatment of acute and chronic heart failure 2012. *Eur. J. Heart Fail.* **14**, 803–869 (2012).
2. Ejection Fraction Heart Failure Measurement. *www.heart.org* https://www.heart.org/en/health-topics/heart-failure/diagnosing-heart-failure/ejection-fraction-heart-failure-measurement.
3. 2016 ESC Guidelines for the diagnosis and treatment of acute and chronic heart failure | European Heart Journal | Oxford Academic. https://academic.oup.com/eurheartj/article/37/27/2129/1748921.
4. Benjamin, E. J. *et al.* Heart Disease and Stroke Statistics-2019 Update: A Report From the American Heart Association. *Circulation* **139**, e56–e528 (2019).
5. L'insuffisance cardiaque en chiffres. *Fondation pour la Recherche Médicale* https://www.frm.org/recherches-maladies-cardiovasculaires/insuffisance-cardiaque/l-insuffisance-cardiaque-en-chiffres.
6. Cardiomyocyte death: mechanisms and translational implications. https://www.ncbi.nlm.nih.gov/pmc/articles/PMC3252742/.
7. Cardiac Disease - Creative Diagnostics. https://www.creative-diagnostics.com/Cardiac-Disease.htm.
8. Katz, A. M. & Konstam, M. A. *Heart Failure: Pathophysiology, Molecular Biology, and Clinical Management*. (Lippincott Williams & Wilkins, 2012).
9. Garg, R. & Yusuf, S. Overview of randomized trials of angiotensin-converting enzyme inhibitors on mortality and morbidity in patients with heart failure. Collaborative Group on ACE Inhibitor Trials. *JAMA* **273**, 1450–1456 (1995).
10. Branger et Samuel - 2017 - Photo's Jasper Zwartjes, Stefan Nimmersgern.pdf.

11. Kübler, W. & Haass, M. Cardioprotection: definition, classification, and fundamental principles. *Heart* **75**, 330–333 (1996).
12. Grigorian Shamagian Lilian *et al.* Perspectives on Directions and Priorities for Future Preclinical Studies in Regenerative Medicine. *Circ. Res.* **124**, 938–951 (2019).
13. Riehle, C. & Bauersachs, J. Key inflammatory mechanisms underlying heart failure. *Herz* **44**, 96–106 (2019).
14. Bollini, S., Smits, A. M., Balbi, C., Lazzarini, E. & Ameri, P. Triggering Endogenous Cardiac Repair and Regeneration via Extracellular Vesicle-Mediated Communication. *Front. Physiol.* **9**, (2018).
15. Cellular and Molecular Immunology - 6th Edition. https://www.elsevier.com/books/cellular-and-molecular-immunology/abbas/978-1-4160-3122-2.
16. Vincenzo, B., Asif, I. J., Nikolaos, P. & Francesco, M. Adaptive Immunity and Inflammation. *Int. J. Inflamm.* **2015**, (2015).
17. Maione, F. *et al.* Interleukin-17A Exacerbates Ferric Chloride-Induced Arterial Thrombosis in Rat Carotid Artery. *International Journal of Inflammation* vol. 2014 e247503 https://www.hindawi.com/journals/iji/2014/247503/ (2014).
18. Zambrano-Zaragoza, J. F., Romo-Martínez, E. J., Durán-Avelar, M. de J., García-Magallanes, N. & Vibanco-Pérez, N. Th17 cells in autoimmune and infectious diseases. *Int. J. Inflamm.* **2014**, 651503 (2014).
19. Choi, J.-M. & Bothwell, A. L. M. The Nuclear Receptor PPARs as Important Regulators of T-Cell Functions and Autoimmune Diseases. *Mol. Cells* **33**, 217–222 (2012).
20. Zlatanova, I., Pinto, C. & Silvestre, J.-S. Immune Modulation of Cardiac Repair and Regeneration: The Art of Mending Broken Hearts. *Front. Cardiovasc. Med.* **3**, (2016).

21. Live Combined Bacillus subtilis and Enterococcus faecium Ameliorate Murine Experimental Colitis by Immunosuppression. https://www.ncbi.nlm.nih.gov/pmc/articles/PMC4170745/.
22. Contradictory Immune Response in Post Liver Transplantation Hepatitis B and C. https://www.hindawi.com/journals/iji/2014/814760/.
23. Pereira da Silva, L., Miguel Neves, B., Moura, L., Cruz, M. T. & Carvalho, E. Neurotensin decreases the proinflammatory status of human skin fibroblasts and increases epidermal growth factor expression. *Int. J. Inflamm.* **2014**, 248240 (2014).
24. Moreau, R. *et al.* Acute-on-chronic liver failure is a distinct syndrome that develops in patients with acute decompensation of cirrhosis. *Gastroenterology* **144**, 1426–1437, 1437.e1–9 (2013).
25. Sutton Martin G. St. John & Sharpe Norman. Left Ventricular Remodeling After Myocardial Infarction. *Circulation* **101**, 2981–2988 (2000).
26. Prabhu, S. D. Post-infarction ventricular remodeling: an array of molecular events. *J. Mol. Cell. Cardiol.* **38**, 547–550 (2005).
27. Pinto, A. R. *et al.* Revisiting Cardiac Cellular Composition. *Circ. Res.* **118**, 400–409 (2016).
28. Frangogiannis, N. G. Regulation of the inflammatory response in cardiac repair. *Circ. Res.* **110**, 159–173 (2012).
29. Yan, X. *et al.* Temporal dynamics of cardiac immune cell accumulation following acute myocardial infarction. *J. Mol. Cell. Cardiol.* **62**, 24–35 (2013).
30. Improved Generation of Induced Cardiomyocytes Using a Polycistronic Construct Expressing Optimal Ratio of Gata4, Mef2c and Tbx5. - PubMed - NCBI. https://www.ncbi.nlm.nih.gov/pubmed/26649751.

31. Boufenzer, A. *et al.* TREM-1 Mediates Inflammatory Injury and Cardiac Remodeling Following Myocardial Infarction. *Circ. Res.* **116**, 1772–1782 (2015).
32. Chen, B., Brickshawana, A. & Frangogiannis, N. G. The functional heterogeneity of resident cardiac macrophages in myocardial injury: CCR2+ cells promote inflammation, whereas CCR2− cells protect. *Circ. Res.* **124**, 183–185 (2019).
33. Dewald, O. *et al.* CCL2/Monocyte Chemoattractant Protein-1 regulates inflammatory responses critical to healing myocardial infarcts. *Circ. Res.* **96**, 881–889 (2005).
34. Identification of splenic reservoir monocytes and their deployment to inflammatory sites. - Abstract - Europe PMC. https://europepmc.org/article/med/19644120.
35. Varda-Bloom, N. *et al.* Cytotoxic T lymphocytes are activated following myocardial infarction and can recognize and kill healthy myocytes in vitro. *J. Mol. Cell. Cardiol.* **32**, 2141–2149 (2000).
36. Souders, C. A., Bowers, S. L. K. & Baudino, T. A. Cardiac fibroblast: the renaissance cell. *Circ. Res.* **105**, 1164–1176 (2009).
37. Shinde, A. V. & Frangogiannis, N. G. Fibroblasts in myocardial infarction: a role in inflammation and repair. *J. Mol. Cell. Cardiol.* **70**, 74–82 (2014).
38. Saxena, A. *et al.* IL-1 induces proinflammatory leukocyte infiltration and regulates fibroblast phenotype in the infarcted myocardium. *J. Immunol. Baltim. Md 1950* **191**, 4838–4848 (2013).
39. Epelman, S., Liu, P. P. & Mann, D. L. Role of Innate and Adaptive Immunity in Cardiac Injury and Repair. *Nat. Rev. Immunol.* **15**, 117–129 (2015).
40. Dobaczewski, M., Gonzalez-Quesada, C. & Frangogiannis, N. G. The extracellular matrix as a modulator of the inflammatory and reparative response following myocardial infarction. *J. Mol. Cell. Cardiol.* **48**, 504–511 (2010).

41. Trial, J. *et al.* Fibronectin fragments modulate monocyte VLA-5 expression and monocyte migration. *J. Clin. Invest.* **104**, 419–430 (1999).
42. Korf-Klingebiel, M. *et al.* Myeloid-derived growth factor (C19orf10) mediates cardiac repair following myocardial infarction. *Nat. Med.* **21**, 140–149 (2015).
43. Schuleri, K. H. *et al.* Autologous mesenchymal stem cells produce reverse remodelling in chronic ischaemic cardiomyopathy. *Eur. Heart J.* **30**, 2722–2732 (2009).
44. Hofmann, U. *et al.* Activation of CD4+ T lymphocytes improves wound healing and survival after experimental myocardial infarction in mice. *Circulation* **125**, 1652–1663 (2012).
45. Stabile, E. *et al.* Impaired arteriogenic response to acute hindlimb ischemia in CD4-knockout mice. *Circulation* **108**, 205–210 (2003).
46. Li, J. *et al.* VEGF, flk-1, and flt-1 expression in a rat myocardial infarction model of angiogenesis. *Am. J. Physiol.* **270**, H1803-1811 (1996).
47. Zymek, P. *et al.* The role of platelet-derived growth factor signaling in healing myocardial infarcts. *J. Am. Coll. Cardiol.* **48**, 2315–2323 (2006).
48. Chen, C.-W. *et al.* Human Pericytes for Ischemic Heart Repair. *Stem Cells Dayt. Ohio* **31**, 305–316 (2013).
49. Prabhu, S. D. & Frangogiannis, N. G. The Biological Basis for Cardiac Repair After Myocardial Infarction: From Inflammation to Fibrosis. *Circ. Res.* **119**, 91–112 (2016).
50. Devaux, B., Scholz, D., Hirche, A., Klövekorn, W. P. & Schaper, J. Upregulation of cell adhesion molecules and the presence of low grade inflammation in human chronic heart failure. *Eur. Heart J.* **18**, 470–479 (1997).
51. Poss, K. D., Wilson, L. G. & Keating, M. T. Heart regeneration in zebrafish. *Science* **298**, 2188–2190 (2002).
52. Tanaka, E. M. Regeneration: if they can do it, why can't we? *Cell* **113**, 559–562 (2003).

53. Chien, K. R. *et al.* Regenerating the field of cardiovascular cell therapy. *Nat. Biotechnol.* **37**, 232–237 (2019).
54. Eschenhagen, T. *et al.* Cardiomyocyte Regeneration: A Consensus Statement. *Circulation* **136**, 680–686 (2017).
55. Rasmussen Tara L., Raveendran Ganesh, Zhang Jianyi, & Garry Daniel J. Getting to the Heart of Myocardial Stem Cells and Cell Therapy. *Circulation* **123**, 1771–1779 (2011).
56. Soonpaa Mark H. & Field Loren J. Survey of Studies Examining Mammalian Cardiomyocyte DNA Synthesis. *Circ. Res.* **83**, 15–26 (1998).
57. Bergmann, O. *et al.* Evidence for cardiomyocyte renewal in humans. *Science* **324**, 98–102 (2009).
58. Wu, S. M. *et al.* Developmental origin of a bipotential myocardial and smooth muscle cell precursor in the mammalian heart. *Cell* **127**, 1137–1150 (2006).
59. Priest, C. A., Manley, N. C., Denham, J., Wirth, E. D. & Lebkowski, J. S. Preclinical safety of human embryonic stem cell-derived oligodendrocyte progenitors supporting clinical trials in spinal cord injury. *Regen. Med.* **10**, 939–958 (2015).
60. Schwartz, S. D. *et al.* Human embryonic stem cell-derived retinal pigment epithelium in patients with age-related macular degeneration and Stargardt's macular dystrophy: follow-up of two open-label phase 1/2 studies. *Lancet Lond. Engl.* **385**, 509–516 (2015).
61. Kikuchi, T. *et al.* Human iPS cell-derived dopaminergic neurons function in a primate Parkinson's disease model. *Nature* **548**, 592–596 (2017).
62. Diekman, B. O. & Guilak, F. Stem cell-based therapies for osteoarthritis: Challenges and opportunities. *Curr. Opin. Rheumatol.* **25**, 119–126 (2013).
63. Rahim, F., Arjmand, B., Shirbandi, K., Payab, M. & Larijani, B. Stem cell therapy for patients with diabetes: a systematic review and meta-analysis of metabolomics-based risks and benefits. *Stem Cell Investig.* **5**, (2018).

64. Sanganalmath, S. K. & Bolli, R. Cell therapy for heart failure: a comprehensive overview of experimental and clinical studies, current challenges, and future directions. *Circ. Res.* **113**, 810–834 (2013).

65. Translational cardiac stem cell therapy: advancing from first-generation to next-generation cell types | npj Regenerative Medicine. https://www.nature.com/articles/s41536-017-0024-1.

66. Murry, C. E., Wiseman, R. W., Schwartz, S. M. & Hauschka, S. D. Skeletal myoblast transplantation for repair of myocardial necrosis. *J. Clin. Invest.* **98**, 2512–2523 (1996).

67. Dowell, J. D., Rubart, M., Pasumarthi, K. B. S., Soonpaa, M. H. & Field, L. J. Myocyte and myogenic stem cell transplantation in the heart. *Cardiovasc. Res.* **58**, 336–350 (2003).

68. Menasché, P. *et al.* The Myoblast Autologous Grafting in Ischemic Cardiomyopathy (MAGIC) trial: first randomized placebo-controlled study of myoblast transplantation. *Circulation* **117**, 1189–1200 (2008).

69. Orlic, D. *et al.* Bone marrow cells regenerate infarcted myocardium. *Nature* **410**, 701–705 (2001).

70. Jackson, K. A. *et al.* Regeneration of ischemic cardiac muscle and vascular endothelium by adult stem cells. *J. Clin. Invest.* **107**, 1395–1402 (2001).

71. Caplan, A. I. Mesenchymal stem cells. *J. Orthop. Res. Off. Publ. Orthop. Res. Soc.* **9**, 641–650 (1991).

72. Williams, A. R. & Hare, J. M. Mesenchymal stem cells: biology, pathophysiology, translational findings, and therapeutic implications for cardiac disease. *Circ. Res.* **109**, 923–940 (2011).

73. Toma, C., Pittenger, M. F., Cahill, K. S., Byrne, B. J. & Kessler, P. D. Human mesenchymal stem cells differentiate to a cardiomyocyte phenotype in the adult murine heart. *Circulation* **105**, 93–98 (2002).

74. Noiseux, N. *et al.* Mesenchymal stem cells overexpressing Akt dramatically repair infarcted myocardium and improve cardiac function despite infrequent cellular fusion or differentiation. *Mol. Ther.* **14**, 840–850 (2006).
75. Hare, J. M. *et al.* Comparison of allogeneic vs autologous bone marrow–derived mesenchymal stem cells delivered by transendocardial injection in patients with ischemic cardiomyopathy: the POSEIDON randomized trial. *JAMA* **308**, 2369–2379 (2012).
76. Desgres, M. & Menasché, P. Clinical Translation of Pluripotent Stem Cell Therapies: Challenges and Considerations. *Cell Stem Cell* **25**, 594–606 (2019).
77. Bu, L. *et al.* Human ISL1 heart progenitors generate diverse multipotent cardiovascular cell lineages. *Nature* **460**, 113–117 (2009).
78. Laugwitz, K.-L. *et al.* Postnatal isl1+ cardioblasts enter fully differentiated cardiomyocyte lineages. *Nature* **433**, 647–653 (2005).
79. Thomson, J. A. *et al.* Embryonic stem cell lines derived from human blastocysts. *Science* **282**, 1145–1147 (1998).
80. Differentiation of human embryonic stem cells and induced pluripotent stem cells to cardiomyocytes: a methods overview. - PubMed - NCBI. https://www.ncbi.nlm.nih.gov/pubmed/22821908.
81. Menasché, P. *et al.* Transplantation of Human Embryonic Stem Cell-Derived Cardiovascular Progenitors for Severe Ischemic Left Ventricular Dysfunction. *J. Am. Coll. Cardiol.* **71**, 429–438 (2018).
82. Takahashi, K. & Yamanaka, S. Induction of pluripotent stem cells from mouse embryonic and adult fibroblast cultures by defined factors. *Cell* **126**, 663–676 (2006).
83. Gnecchi, M., Zhang, Z., Ni, A. & Dzau, V. J. Paracrine mechanisms in adult stem cell signaling and therapy. *Circ. Res.* **103**, 1204–1219 (2008).

84. Bellamy, V. *et al.* Long-term functional benefits of human embryonic stem cell-derived cardiac progenitors embedded into a fibrin scaffold. *J. Heart Lung Transplant. Off. Publ. Int. Soc. Heart Transplant.* **34**, 1198–1207 (2015).
85. Gnecchi, M. *et al.* Paracrine action accounts for marked protection of ischemic heart by Akt-modified mesenchymal stem cells. *Nat. Med.* **11**, 367–368 (2005).
86. Takahashi, M. *et al.* Cytokines produced by bone marrow cells can contribute to functional improvement of the infarcted heart by protecting cardiomyocytes from ischemic injury. *Am. J. Physiol. Heart Circ. Physiol.* **291**, H886-893 (2006).
87. Stewart, D. J. *et al.* VEGF gene therapy fails to improve perfusion of ischemic myocardium in patients with advanced coronary disease: results of the NORTHERN trial. *Mol. Ther. J. Am. Soc. Gene Ther.* **17**, 1109–1115 (2009).
88. Engelmann, M. G. *et al.* Autologous bone marrow stem cell mobilization induced by granulocyte colony-stimulating factor after subacute ST-segment elevation myocardial infarction undergoing late revascularization: final results from the G-CSF-STEMI (Granulocyte Colony-Stimulating Factor ST-Segment Elevation Myocardial Infarction) trial. *J. Am. Coll. Cardiol.* **48**, 1712–1721 (2006).
89. van Rooij, E. & Olson, E. N. MicroRNA therapeutics for cardiovascular disease: opportunities and obstacles. *Nat. Rev. Drug Discov.* **11**, 860–872 (2012).
90. Zangi, L. & Hajjar, R. J. Synthetic MicroRNAs Stimulate Cardiac Repair. *Circ. Res.* **120**, 1222–1223 (2017).
91. Borden, A. *et al.* Transient Introduction of miR-294 in the Heart Promotes Cardiomyocyte Cell Cycle Reentry After Injury. *Circ. Res.* **125**, 14–25 (2019).
92. Adamiak, M. *et al.* Induced Pluripotent Stem Cell (iPSC)-Derived Extracellular Vesicles Are Safer and More Effective for Cardiac Repair Than iPSCs. *Circ. Res.* **122**, 296–309 (2018).

93. Barile, L., Milano, G. & Vassalli, G. Beneficial effects of exosomes secreted by cardiac-derived progenitor cells and other cell types in myocardial ischemia. *Stem Cell Investig.* **4**, (2017).

94. Chen, L. *et al.* Cardiac progenitor-derived exosomes protect ischemic myocardium from acute ischemia/reperfusion injury. *Biochem. Biophys. Res. Commun.* **431**, 566–571 (2013).

95. Farber, D. B. & Katsman, D. Embryonic Stem Cell-Derived Microvesicles: Could They be Used for Retinal Regeneration? *Adv. Exp. Med. Biol.* **854**, 563–569 (2016).

96. Vella, L. J., Hill, A. F. & Cheng, L. Focus on Extracellular Vesicles: Exosomes and Their Role in Protein Trafficking and Biomarker Potential in Alzheimer's and Parkinson's Disease. *Int. J. Mol. Sci.* **17**, 173 (2016).

97. Escudier, B. *et al.* Vaccination of metastatic melanoma patients with autologous dendritic cell (DC) derived-exosomes: results of thefirst phase I clinical trial. *J. Transl. Med.* **3**, 10 (2005).

98. Andre, F. *et al.* Malignant effusions and immunogenic tumour-derived exosomes. *Lancet Lond. Engl.* **360**, 295–305 (2002).

99. Pan, B. T. & Johnstone, R. M. Fate of the transferrin receptor during maturation of sheep reticulocytes in vitro: selective externalization of the receptor. *Cell* **33**, 967–978 (1983).

100. Regev-Rudzki, N. *et al.* Cell-cell communication between malaria-infected red blood cells via exosome-like vesicles. *Cell* **153**, 1120–1133 (2013).

101. Frühbeis, C., Fröhlich, D. & Krämer-Albers, E.-M. Emerging Roles of Exosomes in Neuron–Glia Communication. *Front. Physiol.* **3**, (2012).

102. Luga, V. *et al.* Exosomes mediate stromal mobilization of autocrine Wnt-PCP signaling in breast cancer cell migration. *Cell* **151**, 1542–1556 (2012).

103. Marcilla, A. *et al.* Extracellular vesicles from parasitic helminths contain specific excretory/secretory proteins and are internalized in intestinal host cells. *PloS One* **7**, e45974 (2012).

104. Barteneva, N. S., Maltsev, N. & Vorobjev, I. A. Microvesicles and intercellular communication in the context of parasitism. *Front. Cell. Infect. Microbiol.* **3**, 49 (2013).

105. Akers, J. C., Gonda, D., Kim, R., Carter, B. S. & Chen, C. C. Biogenesis of extracellular vesicles (EV): exosomes, microvesicles, retrovirus-like vesicles, and apoptotic bodies. *J. Neurooncol.* **113**, 1–11 (2013).

106. Colombo, M., Raposo, G. & Théry, C. Biogenesis, secretion, and intercellular interactions of exosomes and other extracellular vesicles. *Annu. Rev. Cell Dev. Biol.* **30**, 255–289 (2014).

107. Minciacchi, V. R., Freeman, M. R. & Di Vizio, D. Extracellular vesicles in cancer: exosomes, microvesicles and the emerging role of large oncosomes. *Semin. Cell Dev. Biol.* **40**, 41–51 (2015).

108. Denzer, K., Kleijmeer, M. J., Heijnen, H. F., Stoorvogel, W. & Geuze, H. J. Exosome: from internal vesicle of the multivesicular body to intercellular signaling device. *J. Cell Sci.* **113 Pt 19**, 3365–3374 (2000).

109. Théry, C., Ostrowski, M. & Segura, E. Membrane vesicles as conveyors of immune responses. *Nat. Rev. Immunol.* **9**, 581–593 (2009).

110. Brennan, K. *et al.* A comparison of methods for the isolation and separation of extracellular vesicles from protein and lipid particles in human serum. *Sci. Rep.* **10**, 1–13 (2020).

111. Gould, S. J. & Raposo, G. As we wait: coping with an imperfect nomenclature for extracellular vesicles. *J. Extracell. Vesicles* **2**, (2013).

112. Witwer, K. W. *et al.* Standardization of sample collection, isolation and analysis methods in extracellular vesicle research. *J. Extracell. Vesicles* **2**, (2013).

113. Théry, C. *et al.* Minimal information for studies of extracellular vesicles 2018 (MISEV2018): a position statement of the International Society for Extracellular Vesicles and update of the MISEV2014 guidelines. *J. Extracell. Vesicles* **7**, 1535750 (2018).

114. Yáñez-Mó, M. *et al.* Biological properties of extracellular vesicles and their physiological functions. *J. Extracell. Vesicles* **4**, 27066 (2015).

115. Grant, B. D. & Donaldson, J. G. Pathways and mechanisms of endocytic recycling. *Nat. Rev. Mol. Cell Biol.* **10**, 597–608 (2009).

116. Morelli, A. E. *et al.* Endocytosis, intracellular sorting, and processing of exosomes by dendritic cells. *Blood* **104**, 3257–3266 (2004).

117. Stoorvogel, W., Strous, G. J., Geuze, H. J., Oorschot, V. & Schwartz, A. L. Late endosomes derive from early endosomes by maturation. *Cell* **65**, 417–427 (1991).

118. Kowal, J. *et al.* Proteomic comparison defines novel markers to characterize heterogeneous populations of extracellular vesicle subtypes. *Proc. Natl. Acad. Sci. U. S. A.* **113**, E968-977 (2016).

119. Colombo, M. *et al.* Analysis of ESCRT functions in exosome biogenesis, composition and secretion highlights the heterogeneity of extracellular vesicles. *J. Cell Sci.* **126**, 5553–5565 (2013).

120. Henne, W. M., Buchkovich, N. J. & Emr, S. D. The ESCRT pathway. *Dev. Cell* **21**, 77–91 (2011).

121. Raiborg, C. & Stenmark, H. The ESCRT machinery in endosomal sorting of ubiquitylated membrane proteins. *Nature* **458**, 445–452 (2009).

122. Babst, M., Katzmann, D. J., Estepa-Sabal, E. J., Meerloo, T. & Emr, S. D. Escrt-III: an endosome-associated heterooligomeric protein complex required for mvb sorting. *Dev. Cell* **3**, 271–282 (2002).

123. Muralidharan-Chari, V. *et al.* ARF6-regulated shedding of tumor cell-derived plasma membrane microvesicles. *Curr. Biol. CB* **19**, 1875–1885 (2009).

124. Bucki, R., Bachelot-Loza, C., Zachowski, A., Giraud, F. & Sulpice, J. C. Calcium induces phospholipid redistribution and microvesicle release in human erythrocyte membranes by independent pathways. *Biochemistry* **37**, 15383–15391 (1998).

125. Pasquet, J. M., Dachary-Prigent, J. & Nurden, A. T. Calcium influx is a determining factor of calpain activation and microparticle formation in platelets. *Eur. J. Biochem.* **239**, 647–654 (1996).

126. Wang, T. *et al.* Hypoxia-inducible factors and RAB22A mediate formation of microvesicles that stimulate breast cancer invasion and metastasis. *Proc. Natl. Acad. Sci. U. S. A.* **111**, E3234-3242 (2014).

127. Kerr, J. F., Wyllie, A. H. & Currie, A. R. Apoptosis: a basic biological phenomenon with wide-ranging implications in tissue kinetics. *Br. J. Cancer* **26**, 239–257 (1972).

128. Hristov, M., Erl, W., Linder, S. & Weber, P. C. Apoptotic bodies from endothelial cells enhance the number and initiate the differentiation of human endothelial progenitor cells in vitro. *Blood* **104**, 2761–2766 (2004).

129. Ihara, T., Yamamoto, T., Sugamata, M., Okumura, H. & Ueno, Y. The process of ultrastructural changes from nuclei to apoptotic body. *Virchows Arch. Int. J. Pathol.* **433**, 443–447 (1998).

130. Takizawa, F., Tsuji, S. & Nagasawa, S. Enhancement of macrophage phagocytosis upon iC3b deposition on apoptotic cells. *FEBS Lett.* **397**, 269–272 (1996).

131. Vandivier, R. W. *et al.* Role of surfactant proteins A, D, and C1q in the clearance of apoptotic cells in vivo and in vitro: calreticulin and CD91 as a common collectin receptor complex. *J. Immunol. Baltim. Md 1950* **169**, 3978–3986 (2002).

132. Friedl, P., Vischer, P. & Freyberg, M. A. The role of thrombospondin-1 in apoptosis. *Cell. Mol. Life Sci. CMLS* **59**, 1347–1357 (2002).

133. Conde-Vancells, J. *et al.* Characterization and comprehensive proteome profiling of exosomes secreted by hepatocytes. *J. Proteome Res.* **7**, 5157–5166 (2008).

134. Théry, C. *et al.* Proteomic analysis of dendritic cell-derived exosomes: a secreted subcellular compartment distinct from apoptotic vesicles. *J. Immunol. Baltim. Md 1950* **166**, 7309–7318 (2001).

135. Turiák, L. *et al.* Proteomic characterization of thymocyte-derived microvesicles and apoptotic bodies in BALB/c mice. *J. Proteomics* **74**, 2025–2033 (2011).

136. Durcin, M. *et al.* Characterisation of adipocyte-derived extracellular vesicle subtypes identifies distinct protein and lipid signatures for large and small extracellular vesicles. *J. Extracell. Vesicles* **6**, 1305677 (2017).

137. H, K. *et al.* Vesiclepedia: a compendium for extracellular vesicles with continuous community annotation. *Plos Biol.* **10**, e1001450–e1001450 (2012).

138. Urbanelli, L. *et al.* Signaling pathways in exosomes biogenesis, secretion and fate. *Genes* **4**, 152–170 (2013).

139. Meckes, D. G. & Raab-Traub, N. Microvesicles and Viral Infection. *J. Virol.* **85**, 12844–12854 (2011).

140. Llorente, A. *et al.* Molecular lipidomics of exosomes released by PC-3 prostate cancer cells. *Biochim. Biophys. Acta* **1831**, 1302–1309 (2013).

141. Carayon, K. *et al.* Proteolipidic composition of exosomes changes during reticulocyte maturation. *J. Biol. Chem.* **286**, 34426–34439 (2011).

142. Subra, C., Laulagnier, K., Perret, B. & Record, M. Exosome lipidomics unravels lipid sorting at the level of multivesicular bodies. *Biochimie* **89**, 205–212 (2007).

143. Fitzner, D. *et al.* Selective transfer of exosomes from oligodendrocytes to microglia by macropinocytosis. *J. Cell Sci.* **124**, 447–458 (2011).

144. Bicalho, B., Holovati, Jelena L. & Acker, J. P. Phospholipidomics reveals differences in glycerophosphoserine profiles of hypothermically stored red blood cells and microvesicles. *Biochim. Biophys. Acta BBA - Biomembr.* **1828**, 317–326 (2013).

145. Zaborowski, M. P., Balaj, L., Breakefield, X. O. & Lai, C. P. Extracellular Vesicles: Composition, Biological Relevance, and Methods of Study. *Bioscience* **65**, 783–797 (2015).

146. Guescini, M., Genedani, S., Stocchi, V. & Agnati, L. F. Astrocytes and Glioblastoma cells release exosomes carrying mtDNA. *J. Neural Transm. Vienna Austria 1996* **117**, 1–4 (2010).

147. Waldenström, A., Gennebäck, N., Hellman, U. & Ronquist, G. Cardiomyocyte microvesicles contain DNA/RNA and convey biological messages to target cells. *PloS One* **7**, e34653 (2012).

148. Balaj, L. *et al.* Tumour microvesicles contain retrotransposon elements and amplified oncogene sequences. *Nat. Commun.* **2**, 180 (2011).

149. Ogawa, Y., Taketomi, Y., Murakami, M., Tsujimoto, M. & Yanoshita, R. Small RNA transcriptomes of two types of exosomes in human whole saliva determined by next generation sequencing. *Biol. Pharm. Bull.* **36**, 66–75 (2013).

150. Li, C. C. Y. *et al.* Glioma microvesicles carry selectively packaged coding and non-coding RNAs which alter gene expression in recipient cells. *RNA Biol.* **10**, 1333–1344 (2013).

151. Cheng, L., Sun, X., Scicluna, B. J., Coleman, B. M. & Hill, A. F. Characterization and deep sequencing analysis of exosomal and non-exosomal miRNA in human urine. *Kidney Int.* **86**, 433–444 (2014).

152. Valadi, H. *et al.* Exosome-mediated transfer of mRNAs and microRNAs is a novel mechanism of genetic exchange between cells. *Nat. Cell Biol.* **9**, 654–659 (2007).

153. Cantaluppi, V. *et al.* Microvesicles derived from endothelial progenitor cells protect the kidney from ischemia-reperfusion injury by microRNA-dependent reprogramming of resident renal cells. *Kidney Int.* **82**, 412–427 (2012).

154. EL Andaloussi, S., Mäger, I., Breakefield, X. O. & Wood, M. J. A. Extracellular vesicles: biology and emerging therapeutic opportunities. *Nat. Rev. Drug Discov.* **12**, 347–357 (2013).

155. Yang, M. *et al.* Microvesicles secreted by macrophages shuttle invasion-potentiating microRNAs into breast cancer cells. *Mol. Cancer* **10**, 117 (2011).

156. Piffoux, M., Silva, A. K. A., Wilhelm, C., Gazeau, F. & Tareste, D. Modification of Extracellular Vesicles by Fusion with Liposomes for the Design of Personalized Biogenic Drug Delivery Systems. *ACS Nano* **12**, 6830–6842 (2018).

157. Kervadec, A. *et al.* Cardiovascular progenitor-derived extracellular vesicles recapitulate the beneficial effects of their parent cells in the treatment of chronic heart failure. *J. Heart Lung Transplant.* **35**, 795–807 (2016).

158. Writing Group Members *et al.* Executive Summary: Heart Disease and Stroke Statistics--2016 Update: A Report From the American Heart Association. *Circulation* **133**, 447–454 (2016).

159. Hong, K. U. *et al.* c-kit+ Cardiac stem cells alleviate post-myocardial infarction left ventricular dysfunction despite poor engraftment and negligible retention in the recipient heart. *PloS One* **9**, e96725 (2014).

160. Kamata, S. *et al.* Improvement of cardiac stem cell sheet therapy for chronic ischemic injury by adding endothelial progenitor cell transplantation: analysis of layer-specific regional cardiac function. *Cell Transplant.* **23**, 1305–1319 (2014).

161. Vlassov, A. V., Magdaleno, S., Setterquist, R. & Conrad, R. Exosomes: current knowledge of their composition, biological functions, and diagnostic and therapeutic potentials. *Biochim. Biophys. Acta* **1820**, 940–948 (2012).

162. Xin, H. *et al.* Systemic administration of exosomes released from mesenchymal stromal cells promote functional recovery and neurovascular plasticity after stroke in rats. *J. Cereb. Blood Flow Metab.* **33**, 1711–1715 (2013).

163. Cosenza, S., Ruiz, M., Maumus, M., Jorgensen, C. & Noël, D. Pathogenic or Therapeutic Extracellular Vesicles in Rheumatic Diseases: Role of Mesenchymal Stem Cell-Derived Vesicles. *Int. J. Mol. Sci.* **18**, 889 (2017).

164. Bruno, S., Porta, S. & Bussolati, B. Extracellular vesicles in renal tissue damage and regeneration. *Eur. J. Pharmacol.* Jul 1. pii: S0014-2999(16)30427-7. doi:10.1016/j.ejphar.2016.06.058. [Epub ahead of print] (2016) doi:10.1016/j.ejphar.2016.06.058.

165. Lai, R. C. *et al.* Exosome secreted by MSC reduces myocardial ischemia/reperfusion injury. *Stem Cell Res.* **4**, 214–222 (2010).

166. Arslan, F. *et al.* Mesenchymal stem cell-derived exosomes increase ATP levels, decrease oxidative stress and activate PI3K/Akt pathway to enhance myocardial viability and prevent adverse remodeling after myocardial ischemia/reperfusion injury. *Stem Cell Res.* **10**, 301–312 (2013).

167. Barile, L. *et al.* Extracellular vesicles from human cardiac progenitor cells inhibit cardiomyocyte apoptosis and improve cardiac function after myocardial infarction. *Cardiovasc. Res.* **103**, 530–541 (2014).

168. Khan, M. *et al.* Embryonic stem cell-derived exosomes promote endogenous repair mechanisms and enhance cardiac function following myocardial infarction. *Circ. Res.* **117**, 52–64 (2015).

169. Gallet, R. *et al.* Exosomes secreted by cardiosphere-derived cells reduce scarring, attenuate adverse remodelling, and improve function in acute and chronic porcine myocardial infarction. *Eur. Heart J.* Sep 27. pii: ehw240. [Epub ahead of print] (2016) doi:10.1093/eurheartj/ehw240.

170. Hu, G. *et al.* Exosomes secreted by human-induced pluripotent stem cell-derived mesenchymal stem cells attenuate limb ischemia by promoting angiogenesis in mice. *Stem Cell Res. Ther.* **6**, 10. doi: 10.1186/scrt546 (2015).

171. Menasché, P. Stem cell–derived exosomes and the failing heart: Small cause, big effect. *J. Thorac. Cardiovasc. Surg.* **156**, 1089–1092 (2018).

172. Sharma, S. *et al.* A Deep Proteome Analysis Identifies the Complete Secretome as the Functional Unit of Human Cardiac Progenitor Cells. *Circ. Res.* **120**, 816–834 (2017).

173. El Harane, N. *et al.* Acellular therapeutic approach for heart failure: in vitro production of extracellular vesicles from human cardiovascular progenitors. *Eur. Heart J.* **39**, 1835–1847 (2018).

174. Halade, G. V. Targeting Resolution of Inflammation Following Myocardial Infarction. *J. Cardiol. Clin. Res.*

175. Nahrendorf, M. *et al.* The healing myocardium sequentially mobilizes two monocyte subsets with divergent and complementary functions. *J. Exp. Med.* **204**, 3037–3047 (2007).

176. Ma, Y., Yabluchanskiy, A. & Lindsey, M. L. Neutrophil roles in left ventricular remodeling following myocardial infarction. *Fibrogenesis Tissue Repair* **6**, 11 (2013).

177. High dose aspirin and left ventricular remodeling after myocardial infarction | SpringerLink. https://link.springer.com/article/10.1007/s00395-007-0647-2.

178. Lima Correa, B. *et al.* Extracellular vesicles from human cardiovascular progenitors trigger a reparative immune response in infarcted hearts. *Cardiovasc. Res.* doi:10.1093/cvr/cvaa028.

179. Barile, L. *et al.* Cardioprotection by cardiac progenitor cell-secreted exosomes: role of pregnancy-associated plasma protein-A. *Cardiovasc. Res.* **114**, 992–1005 (2018).

180. Torán, J. L. *et al.* Definition of a cell surface signature for human cardiac progenitor cells after comprehensive comparative transcriptomic and proteomic characterization. *Sci. Rep.* **9**, 4647 (2019).

181. Davidson, S. M. & Yellon, D. M. Exosomes and cardioprotection - A critical analysis. *Mol. Aspects Med.* **60**, 104–114 (2018).

182. Nikolaeva, L. L. *et al.* Lyophilization as a Method for Stabilizing Pharmaceuticals. *Pharm. Chem. J.* **51**, 307–311 (2017).

183. Hamada, T. *et al.* In vitro controlled release of extracellular vesicles for cardiac repair from poly(glycerol sebacate) acrylate-based polymers. *Acta Biomater.* **115**, 92–103 (2020).

184. efficacy. *The Free Dictionary*.

185. Abdullah, C. S. *et al.* Doxorubicin-induced cardiomyopathy associated with inhibition of autophagic degradation process and defects in mitochondrial respiration. *Sci. Rep.* **9**, 2002 (2019).

186. Chatterjee, K., Zhang, J., Honbo, N. & Karliner, J. S. Doxorubicin Cardiomyopathy. *Cardiology* **115**, 155–162 (2010).

187. Adamcova, M., Skarkova, V., Seifertova, J. & Rudolf, E. Cardiac Troponins are Among Targets of Doxorubicin-Induced Cardiotoxicity in hiPCS-CMs. *Int. J. Mol. Sci.* **20**, (2019).

188. Follath, F. Ischemic versus non-ischemic heart failure: should the etiology be determined? *Heart Fail. Monit.* **1**, 122–125 (2001).

189. Zhao, L. & Zhang, B. Doxorubicin induces cardiotoxicity through upregulation of death receptors mediated apoptosis in cardiomyocytes. *Sci. Rep.* **7**, (2017).

190. Keefe, D. L. Anthracycline-induced cardiomyopathy. *Semin. Oncol.* **28**, 2–7 (2001).

191. Tang, X.-L. *et al.* Repeated Administrations of Cardiac Progenitor Cells Are Superior to a Single Administration of an Equivalent Cumulative Dose. *J. Am. Heart Assoc.* **7**, (2018).

192. Reich, H. *et al.* Repeated transplantation of allogeneic cardiosphere-derived cells boosts therapeutic benefits without immune sensitization in a rat model of myocardial infarction. *J. Heart Lung Transplant.* **35**, 1348–1357 (2016).

193. Wysoczynki, M., Khan, A. & Bolli, R. New Paradigms in Cell Therapy: Repeated Dosing, Intravenous Delivery, Immunomodulatory Actions, and New Cell Types. *Circ. Res.* **123**, 138–158 (2018).

194. Bartolucci, J. *et al.* Safety and Efficacy of the Intravenous Infusion of Umbilical Cord Mesenchymal Stem Cells in Patients With Heart Failure: A Phase 1/2 Randomized Controlled Trial (RIMECARD Trial [Randomized Clinical Trial of Intravenous Infusion Umbilical Cord Mesenchymal Stem Cells on Cardiopathy]). *Circ. Res.* **121**, 1192–1204 (2017).

195. Yang, L. *et al.* Stem cell-derived extracellular vesicles for myocardial infarction: a meta-analysis of controlled animal studies. *Aging* **11**, 1129–1150 (2019).

196. Sun, X., Shan, A., Wei, Z. & Xu, B. Intravenous mesenchymal stem cell-derived exosomes ameliorate myocardial inflammation in the dilated cardiomyopathy. *Biochem. Biophys. Res. Commun.* **503**, 2611–2618 (2018).

197. Milano, G. *et al.* Intravenous administration of cardiac progenitor cell-derived exosomes protects against doxorubicin/trastuzumab-induced cardiac toxicity. *Cardiovasc. Res.* (2019) doi:10.1093/cvr/cvz108.

198. Vandergriff, A. C. *et al.* Intravenous Cardiac Stem Cell-Derived Exosomes Ameliorate Cardiac Dysfunction in Doxorubicin Induced Dilated Cardiomyopathy. *Stem Cells Int.* **2015**, 960926 (2015).

199. Webb, R. L. *et al.* Human Neural Stem Cell Extracellular Vesicles Improve Tissue and Functional Recovery in the Murine Thromboembolic Stroke Model. *Transl. Stroke Res.* **9**, 530–539 (2018).

200. Willis, G. R. *et al.* Mesenchymal Stromal Cell Exosomes Ameliorate Experimental Bronchopulmonary Dysplasia and Restore Lung Function through Macrophage Immunomodulation. *Am. J. Respir. Crit. Care Med.* **197**, 104–116 (2017).

201. Rong, Y. *et al.* Neural stem cell-derived small extracellular vesicles attenuate apoptosis and neuroinflammation after traumatic spinal cord injury by activating autophagy. *Cell Death Dis.* **10**, 1–18 (2019).

202. Cheng, M. *et al.* Circulating myocardial microRNAs from infarcted hearts are carried in exosomes and mobilise bone marrow progenitor cells. *Nat. Commun.* **10**, 959 (2019).

203. Murphy, D. E. *et al.* Extracellular vesicle-based therapeutics: natural versus engineered targeting and trafficking. *Exp. Mol. Med.* **51**, (2019).

204. Ciullo, A. *et al.* Exosomal Expression of CXCR4 Targets Cardioprotective Vesicles to Myocardial Infarction and Improves Outcome after Systemic Administration. *Int. J. Mol. Sci.* **20**, 468 (2019).

205. Pezzana, C., Agnely, F., Bochot, A., Siepmann, J. & Menasché, P. Extracellular Vesicles and Biomaterial Design: New Therapies for Cardiac Repair. *Trends Mol. Med.* (2020) doi:10.1016/j.molmed.2020.10.006.